

Development of Novel Aptasensing Techniques for Detection of Mycotoxins and Antibiotic Residues in Food and Beverages

THESIS

Submitted in partial fulfilment
of the requirements for the degree of
DOCTOR OF PHILOSOPHY

by

ATUL SHARMA

Under the Supervision of

Prof. Sunil Bhand

and

Co-supervision of

Prof. Jean Louis MARTY



BITS Pilani
Pilani | Dubai | Goa | Hyderabad

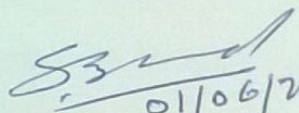
**BIRLA INSTITUTE OF TECHNOLOGY AND SCIENCE
PILANI (RAJASTHAN) INDIA**

2017

**BIRLA INSTITUTE OF TECHNOLOGY AND SCIENCE
PILANI (RAJASTHAN)**

CERTIFICATE

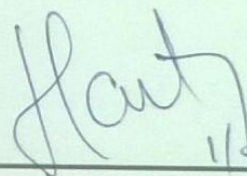
This is to certify that the thesis entitled “DEVELOPMENT OF NOVEL APTASENSING TECHNIQUES FOR DETECTION OF MYCOTOXINS AND ANTIBIOTIC RESIDUES IN FOOD AND BEVERAGES”, which is submitted by ATUL SHARMA ID No 2012PHXF0407G for award of Ph.D. degree of the Institute embodies original work done by him under my supervision/ co-supervision.


01/06/2018

Signature of the Supervisor

Name: **Prof. Sunil Bhand**

Designation: Professor,
Department of Chemistry
Dean, Sponsored Research and
Consulting Division
(University Wide)
BITS Pilani- K K Birla Goa Campus
Goa, India


1/06/2018

Signature of the Co-Supervisor

Prof. Jean Louis MARTY

Professor,
“Classe exceptionnelle” in
Biotechnology,
BAE-LBBM
Université de Perpignan Via
Domitia (UPVD), Perpignan
CEDEX, France

Date: 01.06.2018

ABSTRACT

Dietary habits of people throughout the world are different depending upon the availability, ethnicity, cultural influences, preparation and preferences for food. Apart from beneficial constituents, food products also contain contaminants that are toxic in nature and can cause infection and severe illness. The excessive contamination in food, dairy and agriculture lead to pollution of the food products, which ultimately enters the food chain and reaches into the human and animal bodies. Thus, access to the high quality and safe food is a basic need in our community. Defining human exposure to various contaminants like mycotoxins and antimicrobial (antibiotics) is an enormous task. The quality and nutritional value of food products are on high risk due to increased consumption and accumulation of toxic chemicals and fungal toxins. The main classes of food contaminants that pose the serious problems are mycotoxins (ochratoxins and aflatoxins) and antimicrobial (aminoglycosides and tetracyclines). While these contaminants are associated with many adverse health effects, there is a lack of their continuous and on-line monitoring. Conventional techniques are effective for analysis of food contaminants but not capable of providing high-throughput and sensitive detection especially in unprocessed (untreated) food products (milk) and beverages (alcoholic beverages). Hence, for continuous screening, quantitation and facilitating the early alarming systems for contaminated food and beverages samples, biosensor has emerged out as choice of analytical methods providing rapid, highly specific, selective, reliable and cost effective analysis (Chapter 1).

Since the outbreaks of mycotoxin contamination (ochratoxins and aflatoxins) in milk and alcoholic beverages (beer and wine), the analysis of these fungal toxins in food and beverages has become primary interest of researchers. Meanwhile, the residual presence of antibiotics in food and food products has also been reported. Contamination of milk and beverages is hazardous and causing the serious toxic effects on human and veterinary animal health. Various international and national regulatory authorities have mandated several maximum residual levels (MRLs) and maximum permissible limits (MPLs) for these contaminants in food and beverages. Among the various reported biosensor techniques, the aptasensor has gained tremendous attention as an alternative method owing to their high specificity, selectivity, sensitivity and long-term stability. The availability of SELEX process and implication of in-vivo modifications combines with the ease of modification and facile labelling, greater selectivity make it possible to develop aptasensing platform utilizing various transducer such as optical, electrochemical and piezoelectric. Due to need of rapid

screening process, the development of biosensing platform for milk and alcoholic beverages analysis without much matrix treatment is paramount interest. Recently, the principle of structure switching aptasensors, which pave a new era to aptasensor development attained significant attention. However, the structure signalling aptaswitches platforms have not been explored much till date. In present thesis work, designing the signalling aptaswitches were prime focus for further integration and development. Herein, the special attention was paid to analysis of sample (milk, beer and wine) taking aspects of pre-treatment, matrix matching and validation of biosensor development into consideration (Chapter 1).

Chapter 2 of the present thesis represents the development of fluorescence quenching based aptamer assay platform for OTA analysis in beer and wine. Herein, the two different approaches, firstly a fluorescence quenching based aptasensing platform utilizing fluorescently labelled aptamer (labelled technique) and second a non-labelled technique utilizing a non-labelled anti-OTA aptamer were designed. In first approach, a fluorescence quenching based aptasensing platform has been developed using fluorescently labelled aptamer (labelled technique) and TiO₂-NPs as fluorescence quencher. In the second part, a non-labelled technique was developed using non-labelled anti-OTA aptamer, which capitalizes on the concept of aptamer assisted stability of TiO₂-NPs and carboxylate modified microsphere nanoparticles as fluorescent probe. Post characterization and optimization of parameters, the OTA analysis was based on the fluorescence recovery response resulting from the binding interaction of the anti-OTA aptamer with OTA present in the sample. The analytical parameters of both aptasensing platforms compared. The developed platform can analysed OTA down to 1.5 nM with linearity of 1.5 nM- 1.0 μM (labelled technique) and 1.35 nM with linearity of 17 nM- 5.0 μM (non-labelled technique) in beer and wine samples meeting the regulatory standards i.e. 2.0 μg kg⁻¹ (0.22 μM). Recoveries were obtained in the range 94.30-102.68 % for triplicate measurements in beer and wine samples. The developed platforms showed very good precision with reproducibility of % R.S.D. 2.89 (n=3) and % R.S.D. 5.04 (n=3) for intraday analysis against methodology 1 and 2, respectively. Validation of present platform was carried against HPLC method. This proves its capability to implement in the beverages industries for OTA monitoring.

Chapter 3 of the present thesis represents the development of the structure switching aptamer assay for aflatoxin M1 (AFM1) in milk. Milk is considered as a balance diet and complete food for adults and infants due to high nutritional values. The presence and increase contamination of AFM1 in milk causes the serious toxicity and illness to human such as

hepatotoxicity; nephrotoxicity etc. The recommended MRLs of AFM1 in milk has been mandated to 50 ng kg⁻¹ (for adults) and 25 ng kg⁻¹ (for infants). In earlier reported methods, the matrix matching or sample pre-treatment protocols are a major issue. In order to eliminate and improve feasibility of assay platform for field analysis, the practical utility of developed assay platform was verified in untreated milk samples. AFM1 measurements in milk depends upon the fluorescence recovery response obtained from the structure switching of fluorescein labelled anti-AFM1 aptamer upon binding with AFM1 in presence of quencher labelled (TAMRA labelled) complementary aptamer sequences. The developed aptamer assay showed the excellent precision with dynamic range 1-2000 ng kg⁻¹ AFM1 and good linearity with a LOD of 1 ng kg⁻¹ AFM1 in milk. Excellent recoveries were obtained in the range from 94.40-95.28 % in the AFM1 spiked milk samples. The observed recoveries were in good agreement with the recoveries from commercial ELISA kit available for AFM1 analysis.

The increasing incidences and occurrence of antibiotic residual contamination in milk samples has also attracted significant attention due to the increased risk of microbial resistance and transferring the resistance to genes to human pathogens. The antibiotic abuse resulted in the sustainable side effects to human health and increased mortality rates. Thus, the continuous monitoring of antibiotic contamination in milk considering milk as a balance diet has become scientific and social interest. Several regulatory agencies such as Food Safety and Standard Authority of India (FSSAI), United States Food and Drug Administration (USFDA), Codex Alimentous Commission (CODEX) have mandated the limits of antibiotics in milk and milk based products i.e. 100-200 µg kg⁻¹ for kanamycin (KANA) and 100-300 µg kg⁻¹ for tetracycline (TET). Chapter 4 of the present thesis represents the development of EIS based label-free and disposable aptasensor for kanamycin determination in milk sample. In this design, the focus was on the development of a portable and disposable aptasensor, thus the screen printing technology was integrated. The utilization of SPCEs technology and diazonium coupling mechanism used for immobilization of aptamer provided the improved stability and sensitivity to aptasensor. The aptasensor was characterized using surface morphology and electrochemical techniques. Sensitivity and selectivity of developed aptasensor were evaluated by monitoring the change in impedimetric response (R_{ct} value) on aptasensor surface after incubation with kanamycin on transducer surface. The devised aptasensor exhibited a dynamic detection range of 1.20-600 ng mL⁻¹ with detection limit of 0.11 ng mL⁻¹ KANA in milk with an analysis time of less than 3 min and recovery percentage 96.88-100.5% in KANA spiked milk samples.

Chapter 5 of the present thesis represents the development of μ FIA-EQCN aptasensor for analysis of tetracycline (TET) residue in milk. Here, the principle of microfluidic flow injection analysis (μ FIA) integrated with electrochemical quartz crystal nanobalance (EQCN) was developed for determination of residual TET contamination in milk. The ssDNA TET-aptamer was immobilized on the gold quartz crystal surface using coupling chemistry. The surface morphology of devised aptasensor was characterized utilizing Fourier transform infra-red spectroscopy (FT-IR), scanning electron microscopy (SEM) and atomic force microscopy (AFM). The developed μ FIA-EQCN aptasensor was successfully employed for TET analysis in various milk samples. The aptasensor showed the dynamic detection range 1.562-2000 ng mL⁻¹ TET meeting the requirement of regulatory standards (i.e. 100-300 μ g kg⁻¹). The devised μ FIA-EQCN TET aptasensor can detect down to the 0.531 ng mL⁻¹ TET in milk sample. The developed aptasensor platform exhibiting promising results thus could be employed for on-line determination of TET in milk sample. In validation of presented aptasensor against commercial ELISA kit, the developed μ FIA-EQCN aptasensor showed comparative and sensitive detection of TET in real time mode. The recoveries were calculated in the range of 97.43-102.60 % with high precision and accuracy over ELISA kit (97.95-100.18 %).

In brief, aptasensing platforms for analysis of mycotoxins (OTA, AFM1) and antibiotics (kanamycin and tetracycline) in food (milk) and alcoholic beverages (beer and wine) have been developed. The major highlights of the present thesis work include the development of

1. Fluorescence quenching based aptasensing platforms (labelled and label-free) has been developed for mycotoxin analysis in alcoholic beverages (beer and wine) utilizing titanium dioxide nanoparticles (TiO₂-NPs) as fluorescence quencher.
2. Validation of developed platforms with conventional HPLC method in beer and wine samples and its application to beverages industries.
3. Structure switching aptamer assay for analysis of AFM1 in milk sample provided no complex matrix treatment and high throughput.
4. Label-free and disposable impedimetric aptasensor integrated on SPCEs for rapid measurements of kanamycin in milk sample and high specificity of aptasensor.
5. μ FIA-EQCN aptasensor technology for on-line and real time analysis of tetracycline in milk sample, validation of developed aptasensor and its application to dairy industries.

Declaration of Academic Integrity

I, **Atul Sharma** s/o Mr. Devender Kumar Sharma, declare that this written submission represents my ideas in my own words and where others ideas or words have been included. I have adequately cited and referenced the original sources. I also declare that I have adhered to all principles of academic honesty and integrity and have not misrepresented or fabricated or falsified any idea/data/fact/source in my submission. I understand that any violation of the above will be cause for disciplinary action as per rules and regulations of the institute.



Atul Sharma

(ID No. 2012PHXF0407G)

ACKNOWLEDGEMENTS

In our Vedic culture Guru (Teacher) holds a supreme purpose in shaping student's life and relations between a teacher and student is a reflection of purity, understanding, respect and undefined. It is my privilege to take this opportunity to express my earnest gratitude to my supervisor, Prof. Sunil Bhand for his constant encouragement and invaluable guidance throughout my thesis work. During my research work, he has provided me the high flexibility in various scientific research and creative thinking. From you, I have learned so much, not only the bare scientific facts but the thinking and meaning of science. He has paid attention to my weakness and pushed me hard to bring out the best what I can.

I am honoured to say thank to my Co-supervisor Prof. Jean Louis MARTY for his groundbreaking ideas and firm supports around my doctoral work. He has provided the opportunities to work with his group (BAE Laboratory, Université de Perpignan Via Domitia, Perpignan, France) and make my visit highly interactive and productive. The scientific work carried out in France helped me to improve my scientific skills and strengthen my career providing value addition to the thesis work.

I would like to thank my supervisor's to provide me the opportunities to take part in the various international/national conferences and workshop. These opportunities have broadened my experience and knowledge in the field of science and technology.

I am extremely grateful to Prof. Souvik Bhattacharyya (Vice Chancellor, BITS Pilani), Prof. Raghurama G (Director, BITS Pilani K K Birla Goa Campus), Prof. S. K. Verma (Dean, Academic Research, Ph. D. Programme, BITS Pilani), Prof. Sunil Bhand (Dean, Sponsored Research and Consulting Division, BITS Pilani-University Wide), and Prof. P. K. Das (Associate Dean, Academic Research, BITS Pilani K K Birla Goa Campus) for providing me the Institutional financial support and facilities to conduct my research work at BITS Pilani K K Birla Goa Campus.

I express my sincere gratitude to the members of the Doctoral Advisory Committee (DAC Members), Prof. Aditya P. Koley and Prof. N. N. Ghosh, Department of Chemistry for their guidance and co-operation. I also express my sincere thanks to Prof. Anjan Chattopadhyay, Head, Department of Chemistry, BITS Pilani K K Birla Goa Campus. I would also like to thank to Prof. R. N. Behera, Convener, Departmental Research Committee (DRC), and members Prof. Bhavana P., Prof. Halan Prakash, and Dr. Amrita Chatterjee for their valuable support.

I extend my sincere thanks to Prof. A. P. Koley (Professor and Associate Dean, Instruction Division) for his valuable advice, motivation, and support at various academic phases. I would also like to extend my special gratitude to Prof. Bengt Danielsson, Acromed Invest Lund, Sweden, Prof. Sudhir Chandra, CARE, IIT Delhi and Dr. S. F. D'Souza, Nuclear Agriculture and Biotechnology Division BARC, Mumbai, for scientific interaction and fruitful discussions.

I am very thankful to my collaborators from BAE Laboratory, France Dr. Gaelle Catanante, Dr. Akhtar Hayat, Dr. Rupesh K. Mishra and Dr. George Instanboulie for their active collaboration, constant support, and fruitful scientific discussions. I would like to thank my other lab members within Biosensor laboratory Dr. Kanchanmala Deshpande, Dr. Gautam Bacher, Dr. Souvik Pal, Dr. Lizy Kanungo, Ms. Aruna Chandra Singh, Mr. Arun Prusty and from BAE laboratory Mr. Yugender Kotagiri. I would like to give special thanks to Dr. Diana Bruno from BAE Laboratory, France for helping in working on her customized fluorescence imaging system. I extend sincere thank to Mr. Rehan Deshmukh (Department of Biological Sciences) for helping me with RT-qPCR instrument in scientific work and I am thankful to other department colleagues also for their kind help and support.

I am very thankful for EUPHRATES Program for providing me the Erasmus Mundus Doctoral Fellowship (2014-15) for 1-year research work. I also express my sincere thanks to Prof. Thierry Noguer, Director, BAE Laboratory, Perpignan, France to make me part of the lab and Ms. Simona Brajou (Project Manager, Erasmus Mundus Program), UPVD, Perpignan, France for their help and make my stay fruitful.

I must say without financial support, it would not be possible for me to carry out my research study. Therefore, I take this opportunity to thank BITS Pilani K K Birla Goa Campus (Institute Research Fellow) from November, 2015 (ongoing); EUPHRATES Program (Erasmus Mundus Fellow), November 2014-October 2015; NFBSFARA-ICAR Project (Senior Research Fellowship), January 2014-October 2014; National Agricultural Innovation Project (Senior Research Fellowship), June 2013-December 2013; BITS Pilani K K Birla Goa Campus (January 2013-June 2013) and NATO SfP- Bio-Optical Sensors, Project for their financial support.

I would also express my sincere gratitude to PROMES Laboratory (Perpignan, France) to provide us the nanomaterial (as prepared) for scientific work (detailed in chapter 2) and Base Pair Biotechnologies (Texas, USA) for aptamer synthesis and supply (detailed in chapter 5).

No words can express my gratefulness towards my grandparents Late Shri Jaipal Sharma and Late Smt. Rammurti Sharma, my parents Shri Devinder Kumar Sharma and Late Smt. Rajbala Sharma, my brother Mr. Banty Sharma and sister-in-law Smt. Ila Sharma, my brother Mr. Ashu Sharma and sister-in-law Smt. Priya Sharma and last but not the least my niece's Ms. Gunita Sharma, Ms. Avika Sharma and my nephew Mr. Aditya Sharma for their constant support and motivations throughout my doctoral work and their endless love and patience kept me focused and always steered me in the right direction.

I would like to thank the Almighty Lord for all the wonderful things and surrounding life he is giving to me every moment and hope his blessing will be continuing on my journey.

Atul Sharma

CONTENTS

Description	Page No.
Abstract	iii-vi
Declaration	vii
Acknowledgment	viii-ix
Table of content of chapters	xi-xviii
List of Tables	xix-xxi
List of Figures	xxii-xxix
List of Schemes	xxix
List of Abbreviations and symbols	xxx-xxxiii
List of Keywords	xxxiv
Chapter 1	1-31
Chapter 2	32-70
Chapter 3	71-98
Chapter 4	99-129
Chapter 5	130-161
Chapter 6 (Conclusion, Summary and Future outlook)	162-165
References	166-190
List of Publications	Appendix i
Brief Biography of Candidate	Appendix ii
Brief Biography of Supervisor	Appendix iii
Brief Biography of Co-supervisor	Appendix iv
Reprint of Publications (Front page of each publication)	Appendix v

Table of Content for Chapters

Chapters	Page No.
CHAPTER 1: INTRODUCTION	
1.1 Background of research	2
1.2 Motivation in research	2
1.3 Biosensor	3
1.3.1 Recognition elements	5
1.3.1.1 Catalytic biosensor	5
1.3.1.2 Affinity biosensor	5
1.3.2 Transducers	8
1.3.2.1 Optical biosensor	8
1.3.2.2 Electrochemical biosensor	8
1.3.2.3 Thermal biosensor	8
1.3.2.4 Piezoelectric biosensor	8
1.4 Generation of biosensors	8
1.5 (Bio)receptors used in the present thesis for biosensor development	9
1.5.1 Aptamer and SELEX	9
1.5.2 MIP	11
1.6 Transducers used in the present thesis for biosensors development	13
1.6.1 Optical transducer	14
1.6.2 Electrochemical (impedimetric) transducer	15
1.6.3 Piezoelectric (mass-sensitive) transducer	16
1.7 Performance criteria of biosensor and analytical figures of merits	17
1.7.1 Performance criteria of biosensor	17
1.7.2 Analytical figures of merits	19
1.8 State of art for mycotoxin and antibiotic residue analysis	20
1.8.1 Aptasensors or aptamer assays for mycotoxin analysis	20
1.8.2 Aptasensors for antimicrobial (antibiotics) determination	24

2.2.3.4 Preparation of OTA and interferents standard solutions	43
2.2.3.5 Preparation of spiked real sample for OTA analysis	43
2.2.3.5.1 OTA analysis using spiked beer samples	43
2.2.3.5.2 OTA analysis using spiked wine samples	43
2.2.4 Quenching measurement using TiO ₂ -NPs	44
2.2.4.1 Quenching measurements against FAM-OTA aptamer	44
2.2.4.2 Quenching measurements against fluorescent probe (FCM)	44
2.2.5 OTA detection based on fluorescence quenching	44
2.2.5.1 Labelled technique (OTA detection using fluorescently labelled aptamer)	44
2.2.5.2 Non-labelled technique (OTA detection using non-fluorescent labelled aptamer)	45
2.3 Result and Discussions	45
2.3.1 Labelled technique (OTA detection using fluorescently labelled aptamer)	45
2.3.1.1 UV-Vis spectroscopic analysis	45
2.3.1.2 Fluorescence imaging study	46
2.3.1.3 Optimization of experimental variables	48
2.3.1.3.1 FAM-OTA aptamer concentration	48
2.3.1.3.2 TiO ₂ -NPs concentration	48
2.3.1.3.3 Selection of buffer, pH and ionic strength	49
2.3.1.4 Aptamer assay for OTA detection	51
2.3.1.5 Selectivity and specificity of aptamer assay	52
2.3.1.6 Analytical performance of developed aptamer assay for OTA analysis	53
2.3.1.7 Feasibility of developed aptamer assay for OTA analysis in spiked beer and wine samples	54
2.3.2 Non-labelled technique (OTA detection using non-fluorescent labelled aptamer)	55
2.3.2.1 UV characterization of aptamer stabilized TiO ₂ -NPs	55
2.3.2.2 Fluorescence imaging study	57
2.3.2.3 SEM characterization of bare and aptamer stabilised TiO ₂ -NPs	58

2.3.2.4 Optimization of experimental parameters using non-labelled technique	59
2.3.2.4.1 TiO ₂ -NPs concentration	59
2.3.2.4.2 Aptamer concentration	59
2.3.2.4.3 Optimization of buffer, pH and salt concentrations	60
2.3.2.5 OTA detection using label-free platform (FCM probe)	62
2.3.2.6 Selectivity and Specificity of aptamer Assay	63
2.3.2.7 Analytical performance of developed platform for OTA detection	66
2.3.2.8 Analysis of OTA spiked beer and wine samples	66
2.3.3 Validation using HPLC method	67
2.3.4 Analytical performance comparison of developed assay protocols	69
2.4 Conclusion	70

CHAPTER 3: STRUCTURE SWITCHING APTAMER ASSAY FOR AFLATOXIN M1 (AFM1) ANALYSIS IN MILK SAMPLE

3.1 Background	72
3.1.1 Regulatory legislation for AFM1 detection in milk samples	73
3.1.2 State of art for analysis of AFM1 in milk	73
3.1.3 Aptasensing platforms for AFM1 analysis in milk	75
3.1.3.1 Structure switching signalling aptasensing platform	76
3.1.3.2 Advantages of structure signalling aptaswitches	78
3.1.4 Objective	78
3.1.5 Methodology	78
3.2. Experimental Section	79
3.2.1 Biochemicals and chemicals	79
3.2.2 Instrumentation	80
3.2.3 Solution preparation	80
3.2.3.1 Preparation of binding buffer	80
3.2.3.2 Preparation of AFM1 standard solutions	81
3.2.3.3 Preparation of AFM1 aptamer solutions	81

3.2.3.4 Preparation of milk sample for AFM analysis	81
3.2.4 UV characterization	82
3.2.5 Fluorescence measurements	82
3.3 Result and Discussion	82
3.3.1 Optimization of experimental parameters	82
3.3.1.1 Optimization of F-aptamer (fluorescein labelled anti-AFM1 aptamer)	83
3.3.1.2 Optimization of aptamer-quencher ratio	83
3.3.1.3 Effect of buffer, ionic strength and pH	84
3.3.1.4 Temperature-changing profile studies	86
3.3.2 Evidences of structure switching mechanism	87
3.3.2.1 UV Characterization	87
3.3.2.2 Response optimization	89
3.3.2.3 Fluorimetric measurements	90
3.3.3 Calibration curve for AFM1 detection	90
3.3.4 Specificity and selectivity of aptamer assay	92
3.3.5 Milk sample analysis	93
3.3.6 Precision of developed assay	94
3.3.7 Cross-validation of developed aptamer assay with AFM1 ELISA Kit	95
3.4 Conclusions	97

**CHAPTER 4: DEVELOPMENT OF LABEL-FREE AND DISPOSABLE
IMPEDIMETRIC APTASENSOR FOR DETECTION OF KANAMYCIN IN MILK
SAMPLE**

4.1 Background	100
4.1.1 Regulation for kanamycin contamination in milk samples	101
4.1.2 State of art of KANA detection	101
4.1.3 Electrochemical aptasensor for KANA detection	102
4.1.3.1 Screen printed technology	103
4.1.3.2 Self assembled monolayer	104

4.1.4 Research gap identified	105
4.1.5 Objective	105
4.2. Experimental Section	105
4.2.1 Biochemicals and reagents	105
4.2.2 Instrumentation	106
4.2.3 Solution preparation	106
4.2.3.1 Preparation of binding buffer solution	106
4.2.3.2 Preparation of aptamer solutions	106
4.2.3.3 Preparation of kanamycin stock and working dilutions	107
4.2.3.4 Matrix matching (milk sample preparation)	107
4.2.4 Fabrication of KANA-aptasensor on diazotized SPCEs	107
4.2.4.1 SPCE surface cleaning	107
4.2.4.2 Surface modification and end group activation	108
4.2.4.3 Aptamer immobilization and blocking	110
4.2.5 Impedimetric measurements	110
4.3 Result and discussions	111
4.3.1 Surface characterization of KANA-aptasensor	111
4.3.1.1 Infrared spectroscopy (FT-IR)	111
4.3.1.2 Scanning electron microscopy	113
4.3.1.3 Atomic force microscopy (AFM)	113
4.3.2 Electrochemical characterization of KANA-aptasensor	115
4.3.2.1 Cyclic voltammetry (CV)	116
4.3.2.2 Electrochemical impedance spectroscopy (EIS)	117
4.3.3 Equivalent circuit analysis and validation	119
4.3.4 Optimization parameters for experimental conditions	120
4.3.4.1 Influence of anti-KANA aptamer concentration	120
4.3.4.2 Influence of incubation time	121
4.3.4.3 Influence of pH	121
4.3.5 Sensitivity measurements for KANA detection (calibration curve)	122

4.3.6 Selectivity performance of KANA-aptasensor	125
4.3.7 Application in milk sample	127
4.3.8 Analytical performance of KANA-aptasensor	128
4.4 Conclusion	129

CHAPTER 5: DEVELOPMENT OF μ FIA-EQCN APTASENSOR FOR ANALYSIS OF TETRACYCLINE RESIDUE IN MILK SAMPLE

5.1 Background	131
5.1.1 Occurrence of antibiotic contamination in milk	131
5.1.2 State of art for TET analysis on in milk	132
5.1.3 Aptasensors for TET determination	133
5.1.4 Flow injection analysis (μ FIA)	134
5.1.5 Working principle of EQCN	135
5.1.6 Research gap identified	136
5.1.7 Objective	137
5.2. Experimental Section	137
5.2.1 Biochemicals and reagents	137
5.2.2 Instrumentation	137
5.2.3 Solution preparation	138
5.2.3.1 Preparation of buffers	138
5.2.3.2 Preparation of TET standards	138
5.2.3.3 Aptamer preparation	138
5.2.3.4 Matrix matching	139
5.2.4 Methodology for aptasensor construction	139
5.2.5 Design of flow cell (microfluidic system)	140
5.2.6 Binding assay of anti-TET aptamer	141
5.3 Result and discussions	142
5.3.1 Kinetics parameters for binding assay	142
5.3.2 Optimization of experimental parameters	143

5.3.2.1 Influence of self assembled monolayer's (SAMs)	143
5.3.2.2 Influence of aptamer concentration	144
5.3.2.3 Influence of buffer, ionic strength, pH and flow rate	145
5.3.3 Characterization of TET-aptasensor on transducer surface	146
5.3.3.1 Attenuated total reflection FT-IR (ATR-FTIR)	146
5.3.3.2 Surface topography (using AFM analysis)	148
5.3.3.3 SEM analysis	151
5.3.4 Aptasensor performance for detection of TET (calibration curve)	153
5.3.5 Specificity performance of μ FIA-EQCN aptasensor	155
5.3.6 Recovery studies for TET spiked milk samples	156
5.3.7 Cross validation and comparison	157
5.3.8 Precision and analytical performance of μ FIA-EQCN aptasensor	159
5.4 Conclusion	160
CHAPTER 6: CONCLUSION AND FUTURE SCOPE OF WORK	162-165

List of Tables

S. No.	Description	Page No.
1.1	Characteristics comparison of biosensor receptor	6
1.2	Comparison of properties and advantages of aptamer over antibodies	10
1.3	Analytical merit of figure for a biosensor and aptasensor	19
1.4	Reported aptasensing platforms for mycotoxins (other than OTA) analysis in food and beverages	22
1.5	Reported aptasensing platforms for OTA analysis in food and beverages	23
1.6	Reported aptasensors for antibiotics determination food and animal samples	26
2.1	Reported regulatory maximum residue limits for OTA in beer and wine	34
2.2	Summary of reported aptasensors for OTA determination using optical transducers	36
2.3	Summary of reported aptaswitches for analysis of OTA in alcoholic beverages	36
2.4	UV-Vis absorption characterization of aptamer assay in HBB (pH 7.4)	46
2.5	Fluorescence magnitude value of blue components	47
2.6	Selectivity and specificity performance of assay platform for OTA detection	53
2.7	Precision performance of developed assay for OTA analysis	54
2.8	Recovery performance of labelled assay platform for OTA determination in spiked beer and wine samples	55
2.9	UV-Vis absorption characterization of aptamer assay in HBB (pH 7.4)	56
2.10	Fluorescence magnitude value of blue components	57
2.11	Selectivity and specificity performance of assay platform for OTA detection	65

2.12	Analytical precision performance of developed aptaswitch	66
2.13	Recovery performance of label-free platform for OTA spiked beer and wine samples	67
2.14	Recovery performance of cross validation with HPLC method	69
2.15	Comparative analytical figures of merits of developed protocols	69
3.1	Reported regulatory maximum residue limits for AFM1 in milk and infant formula	73
3.2	Summary of reported immunosensor for analysis of AFM1	75
3.3	Summary of reported aptasensors for analysis of AFM1 in milk samples	76
3.4	Description of anti-AFM1 aptamer and complementary aptamer sequences used	80
3.5	UV absorption results for structure switching mechanism	89
3.6	Selectivity performance of aptamer assay for AFM 1 detection	93
3.7	Recovery performance of aptamer assay for detection of AFM1 in spiked milk sample	94
3.8	Precision performance of developed assay for detection of AFM1	95
3.9	Recovery studies of AFM1 in milk sample from aptamer AFM1 assay and commercial ELISA kit	96
3.10	Comparison of analytical merits of figures of aptamer assay and ELISA kit	97
4.1	Maximum residue limits of KANA residue in milk and milk products	101
4.2	Reported electrochemical based aptasensor for detection of KANA in milk samples	103
4.3	AFM topological parameters before and after modification for the screen printed carbon electrode, aptasensor and aptasensor incubated with analyte.	115
4.4	Stimulated values of all elements in the equivalent electric circuit	119

	(Randles Circuit) for the various steps of the aptasensor fabrication and performance.	
4.5	Specificity and selectivity performance of KANA-aptasensor	126
4.6	Recovery calculation of KANA-aptasensor for KANA spiked milk samples.	128
4.7	Precision performance of aptasensor for detection of KANA in milk sample	128
4.8	Analytical merit of figures for devised KANA-aptasensor	129
5.1	Recommended MRLs for TET in milk and milk based products	132
5.2	Summary of reported aptasensors for detection of TET in the milk samples	134
5.3	Cross-reactivity studies of TET against structural and non-structural analogues in milk sample	156
5.4	Recovery studies of TET spiked milk samples using μ FIA-EQCN aptasensor	157
5.5	Recovery performance of μ FIA-EQCN aptasensor and ELISA Kit for TET analysis	158
5.6	Precision and reproducibility studies of μ FIA-EQCN aptasensor for TET	159
5.7	Analytical figures of merit for devised μ FIA-EQCN TET-aptasensor	160

List of Figures and Schemes

S. No.	Description	Page No.
1.1	Schematic representation of biosensor components	4
1.2	Recognition elements in biosensor (a) antibody; (b) nucleotides; (c) fluorescein labelled (F) aptamer; (d) Dual labelled (fluorophore and quencher; F and Q) aptamer helical structure; (e) Functionally (amine) modified aptamer; (f) Molecularly imprinted polymer (MIP)	7
1.3	Generation of biosensors	9
1.4	Schematic representation of the SELEX Process (demonstrating all main 5 steps): Steps in solid arrow line are specific for ssDNA aptamer selection and steps in dotted arrow line are specific for RNA aptamer selection	12
1.5	Schematic representation for the preparation of molecularly imprinted polymer	13
1.6	Schematic representation of fluorescence quenching based aptaswitches for biosensor development	15
1.7	Designed of a screen printed carbon electrode (used in the present work)	16
1.8	Different transduction principles used for biosensor development	17
1.9	A calibration curve plot showing performance criteria for biosensor	18
1.10	Structure of commonly found mycotoxin in milk and beverages	21
1.11	Structure of commonly found antibiotics in milk and food commodities	25
1.12	Flowchart detailing the different stages of the thesis works	29
2.1	Source and toxic effect of OTA on human health	33
2.2	A portable and customized fluorescence imaging system (a) camera; (b) stage; (c) cuvette; (d) wire interface connection; (e) computer; (f) RGB component analysis.	41
2.3	UV-Vis absorption analysis of aptamer-TiO ₂ -NPs complex for	46

	structure switching elucidation in HBB (pH 7.4)	
2.4	Fluorescence imaging of (a) FAM-OTA aptamer, (b) FAM-OTA aptamer+ TiO ₂ -NPs, (c) FAM-OTA+ OTA+ TiO ₂ -NPs in HBB (pH 7.4)	47
2.5	Fluorescence response of FAM-OTA aptamer with increasing concentration 0.062-5.0 μM (optimized concentration for further experimentation encircled with blue).	48
2.6	Quenching performance of TiO ₂ -NPs (2.5-300 μg mL ⁻¹) on fluorescence intensity of FAM-OTA aptamer (2.0 μM) in HBB (pH 7.4) (n=3).	49
2.7	(a) Effect of HBB and PBB on quenching efficiency of TiO ₂ -NPs (150 μg mL ⁻¹). (b) Effect of pH (6.8-8.2) of HBB on quenching performance of TiO ₂ -NPs.	50
2.8	(a) Effect of various concentration of NaCl (30, 60, 90, 120 mM) on quenching efficiency of TiO ₂ -NPs in HBB (pH 7.4) (n=5); (b) Effect of various concentration of MgCl ₂ (1, 2.5, 5 and 7.5 mM) on quenching efficiency of TiO ₂ -NPs in HBB (pH 7.4) (n=5); (c) Effect of various concentration of CaCl ₂ (1, 5, 10, 20, 30 and 40 mM) on quenching efficiency of TiO ₂ -NPs in HBB (pH 7.4) (n=5).	51
2.9	Calibration curve obtained for OTA (0.0015, 0.0031, 0.015, 0.062, 0.125, 0.25, 1.0, 5.0, 10.0, 20.0 μM) in HBB at pH 7.4 (Inset shows the logarithmic linear fit graph from 1.5 nM to 1.0 μM OTA).	52
2.10	Bar graph representation of specificity studies of aptamer assay with structural (OTB) (n=3) at various concentrations (0.0031, 0.25 and 10.0 μM).	53
2.11	UV-Vis spectrum analysis of TiO ₂ -NPs before and after stabilization with aptamer in HBB (pH 7.4)	56
2.12	Fluorescence imaging of (a) OTA, (b) FCM, (c) FCM + TiO ₂ -NPs, (d) FCM + anti-OTA aptamer-TiO ₂ -NPs, (e) FCM + anti-OTA aptamer-TiO ₂ -NPs + OTA in HBB (pH 7.4)	57

2.13	Scanning electron micrograph (a) bare TiO ₂ -NPs; (b) anti-OTA aptamer stabilized TiO ₂ -NPs	58
2.14	Optimization of TiO ₂ -NPs concentration (2.5 to 1000 µg mL ⁻¹) against FCM probe (10 µL of 100 µg mL ⁻¹ FCM in microwell) for structure switching aptaswitch	59
2.15	Effect of aptamer concentration on structure switching aptasensing platform.	60
2.16	(a) Optimization of buffer pH (6.8-8.2) for development of structure signalling aptaswitch platform in HBB (n=3); (b) Effect of pH on quenching efficiency of anti-OTA aptamer stabilized TiO ₂ -NPs (aptamer- TiO ₂ -NPs complex) (n=3).	61
2.17	Effect of (a) NaCl concentration on quenching efficiency of anti-OTA aptamer stabilized TiO ₂ -NPs at optimized concentration; (b) MgCl ₂ concentration on quenching efficiency of anti-OTA aptamer stabilized TiO ₂ -NPs at optimized concentration; (c) dilution or assay volume on assay performance. All measurements were performed in three parallel experiments (n=3).	62
2.18	Calibration curve obtained for OTA (0.017-5.0 µM) in HBB (pH 7.0, n=3).	63
2.19	Bar graph representation of specificity studies of developed aptaswitch for OTA detection with structural and non-structural analogues (n=3) at various concentrations (0.0031, 0.25 and 10.0 µM).	64
2.20	HPLC chromatograph for blank (a) 0 ng mL ⁻¹ OTA; (b) OTA (2 ng mL ⁻¹); (c) OTA (5 ng mL ⁻¹) spiked in wine.	68
3.1	Source of AFM1 in milk and its toxic effect	72
3.2	Schematic representation of (a) direct ELISA; (b) indirect ELISA; (c) sandwich ELISA; (d) Competitive ELISA	74
3.3	Schematic representation of structure signalling aptaswitches approaches (a) monochromatic approach, (b) bischromophoric approach.	77

3.4	Principle of structure switching signalling aptamer assay for AFM1 detection	79
3.5	Fluorescence intensity response of different aptamer concentration in HBB (50 mM, pH 7.0)	83
3.6	Optimization of F-aptamer: Q-aptamer ratio with two different quencher base complementary sequences (7 and 9 Bases)	84
3.7	Effect of (a) Buffers (PBB and HBB); (b) ionic strength of HBB; (c) Effect of pH; (d) solvent percentage on quenching efficiency	85
3.8	Temperature mismatch profile studies of structure switching of aptamer duplex against quencher (a) 7 Bases and (b) 9 Bases	87
3.9	UV absorption characterizations for evidence of structure switching mechanism	88
3.10	Fluorescence response studies of aptasensing platform with 7 and 9 based on Q-aptamer	89
3.11	Fluorescence spectrum of structure switching aptaswitches for various concentration of AFM1 (50, 500, 1000 ng kg ⁻¹)	90
3.12	Calibration curve obtained for AFM1 in HBB at pH 7.4 with 7 Base quencher sequences (Inset show the linear fit graph)	91
3.13	Calibration curve obtained for AFM1 in HBB at pH 7.4 with 9 Base quencher sequences (Inset show the linear fit graph)	92
3.14	Specificity studies of aptamer assay with structural (AFB1) and non structural analogue (OTA) at 50 and 500 ng kg ⁻¹	93
4.1	Structure (3D) and toxic effect of kanamycin in human	100
4.2	Customized screen printed carbon electrode (used in the present work)	104
4.3	Cyclic voltammogram of bare SPCE during cleaning from 1.0 to -1.5 V vs. pseudo Ag/AgCl reference electrode in 0.5 M H ₂ SO ₄ containing 0.1 M KCl.	108
4.4	Electrografting of in-situ generated diazonium salt on SPCEs surface	109

	using linear sweep voltammogram (LSV)	
4.5	Linear sweep voltammogram (LSV) of bare SPCE electrode in the aqueous diazonium salt solution (NaNO ₂ and 4-aminobenzoic acid 2 mM in 0.5 M HCl) in the potential range 0.6 to -0.8 V vs. Ag/AgCl. Inset showing the two consecutive cycles on same electrode	109
4.6	Immobilization of aptamer on diazotized electrode surface followed by blocking	110
4.7	Design of a simple Randles Equivalent Circuit	111
4.8	FT-IR spectrum (a) 4-CP/SPCE modified; (b) 4-CP/SPCE/ activated/ Apta; (c) 4-CP/SPCE/activated/Apta/KANA incubated electrodes recorded at 128 scans at 64 cm ⁻¹ resolution	112
4.9	SEM images of (a) Bare SPCE; (b) 4-CP/SPCE/activated/ Apta immobilized; (c) 4-CP/SPCE/activated/Apta/KANA incubated electrode; AFM images (a) Bare SPCE; (b) 4-CP/SPCE/activated/ Apta; (c) 4-CP/SPCE/activated/ Apta/KANA incubated electrode in semicontact tapping mode	114
4.10	Cyclic voltammograms (a) bare SPCE; (b) 4-CP/SPCE; (c) 4-CP/SPCE/ activated; (d) 4-CP/SPCE/activated/Apta; (e) 4-CP/SPCE/activated/Apta/KANA incubated electrodes in 1 mM [Fe(CN) ₆] ^{4-/3-} (prepared in PBB, pH 7.0) at scan rate of 100 mV/s	117
4.11	Nyquist plots (a) bare SPCE; (b) 4-CP/SPCE modified electrode; (c) 4-CP/ SPCE/activated electrode; (d) 4-CP/SPCE/activated/Apta; (e) 4-CP/SPCE/activated/Apta/ KANA incubated electrodes obtained in 1 mM [Fe(CN) ₆] ^{4-/3-} (prepared in PBB, pH 7.0) at an applied potential of 100 mV (vs. Ag/AgCl reference electrode) using a frequency range of 10 KHz to 0.5 Hz with an AC amplitude of 5 mV	118
4.12	Fitting curve of impedance spectrum and phase at ac applied potential: 0.1V; frequency range: 0.1 Hz to 1 KHz	120
4.13	Influence of experimental variables (a) aptamer concentrations (0.125 to 4 μM); (b) incubation time; (c) pH on aptasensor performance at	122

	37.5 ng mL ⁻¹ KANA in 1 mM [Fe(CN) ₆] ^{4-/3-} (prepared in PBB)	
4.14	Binding and recognition of KANA molecule by ssDNA anti-KANA aptamer on aptasensor surface in PBB (10 mM, pH 7.0)	123
4.15	Nyquist plots of KANA aptasensor against different concentrations of KANA (a) 1.20, (b) 2.40, (c) 4.75, (d) 9.50, (e) 19.0, (f) 37.5, (g) 75.0, (h) 150, (i) 300 and (j) 600 ng mL ⁻¹ (vs. Ag/AgCl reference electrode) spiked in buffer with the fitted theoretical data obtained 1 mM [Fe(CN) ₆] ^{4-/3-} (prepared in PBB, pH 7.0)	124
4.16	Calibration curve showing change in the Δ ratio vs KANA concentration (1.2-600 ng mL ⁻¹) in PBB (10 mM, pH 7.0). Inset represents the linear curve from 1.2-7.5 ng mL ⁻¹ (n=4)	124
4.17	Calibration curve in milk showing the change in the Δ ratio vs various concentrations of KANA (1.2- 600 ng mL ⁻¹). Inset represents the linear curve from 1.2-7.5 ng mL ⁻¹ (n=3)	125
4.18	Impedimetric responses (Δ ratio) of fabricated aptamer for KANA, SRT and GENTA at concentration level 9.5 and 37.5 ng mL ⁻¹ (n=3)	126
4.19	Nyquist plots of anti-KANA-aptamer modified SPCEs with different concentrations of KANA spiked in the milk sample (ng mL ⁻¹); (a) 4.75, (b) 9.50, (c) 37.50 and (d) 150 obtained 1 mM [Fe(CN) ₆] ^{4-/3-} (prepared in PBB, pH 7.0) fitted theoretical data	127
5.1	Toxicity effect of TET contamination on human health	132
5.2	Flow diagram for the development of μ FIA-EQCN biosensor	135
5.3	Schematic for fabrication of μ FIA-EQCN TET-aptasensor for TET analysis	140
5.4	Design of microfluidic platform of μ FIA-EQCN aptasensor	141
5.5	A real time sensogram of μ FIA-EQCN aptasensor for binding and regeneration of TET on aptasensor surface in binding buffer (10 mM, pH 7.0)	141
5.6	Binding affinity curves obtained using mass binding of TET (25 ng	142

	mL ⁻¹) with various concentrations of ssDNA anti-TET aptamer	
5.7	Optimization of binding response of aptasensor using different SAMs over gold surface curve at fixed concentration of TET (25 ng mL ⁻¹) in binding buffer (10 mM, pH 7.0). Inset showing the real time binding response for each SAMs	143
5.8	Binding response for ssDNA anti-TET aptamer (0.125-2.0 μM) in HBB (10 mM, pH 7.4) at 25 ng mL ⁻¹ TET. Inset showing mass change for different aptamer concentration	144
5.9	Optimization of various experimental variables (a) buffer; (b) ionic strength; (c) pH; (d) flow rate on binding performance of anti-TET aptamer to TET (25 ng mL ⁻¹)	145
5.10	FT-IR spectra of (a) bare and 11-MUA modified gold surface; (b) ssDNA anti-TET aptamer immobilized over modified gold surface; (c) ssDNA anti-TET aptamer incubated with TET in ATR mode with 128 scans at 64 cm ⁻¹ resolution under vacuum	147
5.11	AFM micrographs of (a) bare gold quartz crystal surface (3D) micrograph; (b) different surface parameters calculated for bare quartz crystal; (c) histogram of bare gold quartz crystal surface; (d) 11-MUA modified gold quartz crystal surface (3D) micrograph; (e) different surface parameters calculated for 11-MUA modified gold quartz crystal surface (f) histogram of 11-MUA modified gold quartz crystal surface	149
5.12	AFM micrographs of (a) anti-TET aptamer immobilized on 11-MUA modified gold quartz crystal surface (3D) micrograph; (b) different surface parameters calculated for 11-MUA coupled gold quartz crystal surface; (c) histogram of anti-TET aptamer immobilized on 11-MUA coupled gold quartz crystal surface; (d) anti-TET aptasensor incubated with TET (25 ng mL ⁻¹) (3D) micrograph; (e) different surface parameters calculated for anti-TET aptasensor incubated with TET (25 ng mL ⁻¹); (f) histogram of anti-TET aptasensor incubated with TET (25 ng mL ⁻¹)	150

5.13	Scanning electron micrographs of (a) bare gold quartz crystal surface at scale of 1.0 μm ; (b) 11-MUA coupled (SAMs formation) on the surface of bare gold quartz crystal surface; (c) anti-TET aptamer immobilized on 11-MUA coupled gold surface	152
5.14	Calibration graph for analysis of TET ($1.5\text{-}2000\text{ ng ml}^{-1}$) in HBB (10 mM, pH 7.4) at 0.1 ml min^{-1} flow arte. Inset showing the linear fit data for TET analysis in HBB	153
5.15	Calibration graph for analysis of TET in milk (spiked with $1.5\text{-}2000\text{ ng ml}^{-1}$ TET) at 0.1 ml min^{-1} flow arte. Inset showing the linear fit data for TET analysis in milk	154
5.16	Cross-reactivity responses of developed $\mu\text{FIA-EQCN}$ TET-aptasensor for different analogues at 25 ng mL^{-1} ($n=3$) in spiked milk samples	155
5.17	(a) Validation responses from $\mu\text{FIA-EQCN}$ TET-aptasensor and commercial ELISA Kit of TET analysis ($1.562\text{-}300\text{ ng mL}^{-1}$); (b) Correlation data between both techniques and inset showing the sample image in ELISA test	158

List of Schemes

S. No.	Description	Page No.
1.	Principle of $\text{TiO}_2\text{-NPs}$ fluorescence quenching based aptaswitch platform for OTA detection (a) in the absence of OTA, adsorption of FAM-OTA aptamer on $\text{TiO}_2\text{-NPs}$ surface led to fluorescence quenching; (b) In the presence of OTA, the anti-parallel G-quadruplex structure form and fluorescence recovered.	38
2.	Structure switching signalling aptaswitch based on fluorescence quenching principle for detection of OTA (a) bare $\text{TiO}_2\text{-NPs}$ quench the fluorescence of FCM particles, (b) in the absence of OTA, the aptamer stabilized $\text{TiO}_2\text{-NPs}$ showed increased quenching and in the presence of OTA, increased fluorescence due to formation of anti-OTA-G-quadruplex aptamer complex.	39

List of Abbreviations

Abbreviations	Description
11-MUA	11-mercaptoundecanoic acid
4-ABA	4-aminobenzoic acid
4-ATP	4-aminothiophenol
4-CP	4-Carboxy phenyl
ACN	Acetonitrile
AFB1	Aflatoxin B1
AFB2	Aflatoxin B2
AFM1	Aflatoxin M1
AFM2	Aflatoxin M2
AFs	Aflatoxins
Apta	Aptamer
ATR	Attenuated total reflectance
CAP	Chloramphenicol
CCDs	Charge-coupled devices
CODEX	Codex Alimentous Commission
CV	Cyclic voltammetry
DNA	Deoxyribonucleic acid
DOXY	Doxycycline
DPV	Differential pulse voltammetry
EDC	<i>N</i> -(3-dimethylaminopropyl)- <i>N</i> -ethyl-carbodiimide hydrochloride
EIS	Electrochemical impedance spectroscopy
ELAAAs	Enzyme linked aptamer assays
ELISA	Enzyme linked immunosorbent assay
EQCN	Electrochemical quartz crystal nanobalance
EU	European Union
F	Fluorescence intensity in the presence of target
FAM	Fluorescein
F-aptamer	Fluorescein labelled aptamer
FCM	Fluorophore carboxylate modified nanoparticles
FD	Fluorescence detection
μFIA	Microfluidic flow injection analysis
FI-IA	Flow injection immunoassay
F ₀	Fluorescence intensity in the absence of target
FRA	Frequency resonance analyzer
FRET	Fluorescence resonance energy transfer

FSSAI	Food Safety and Standard Authority of India
FT-IR	Fourier Transform Infra-Red
GC	Gas chromatography
GENTA	Gentamicin
HBB	HEPES binding buffer
HPLC	High performance liquid chromatography
IAC	Immunoaffinity columns
IARC	International Agency for Research on Cancer
IPUAC	International Union of Pure and Applied Chemistry
KANA	Kanamycin
LOD	Limit of detection
LOL	Limit of linearity
LOQ	Limit of quantification
LRET	Luminescence resonance energy transfer
LSPR	Localised surface plasmon resonance
LSV	Linear sweep voltammetry
MeOH	Methanol
MES	2-(<i>N</i> -morpholino)ethanesulphonic acid buffer
MINO	Minocycline
MIP	Molecularly imprinted polymer
MIPSE	Molecularly imprinted polymer solid phase extraction columns
MRLs	Maximum residual limits
MS	Mass chromatography
NAP	<i>N</i> -acetyl- <i>L</i> -phenylalanine
NHS	<i>N</i> -hydroxysuccinimide
OAs	Ochratoxins
OTA	Ochratoxin A
OTB	Ochratoxin B
OTC	Oxytetracycline
PBB	Phosphate binding buffer
PCR	Polymerase chain reaction
PMTs	Photomultiplier tubes
PSA	Particle size analyzer
PVP	Polyvinyl polymer
Q-aptamer	Quencher labelled aptamer
TAMRA	Carboxytetramethylrhodamine
QCM	Quartz crystal microbalance
R.E.	Relative error
R _a	Average roughness

R_{ct}	Charge transfer resistance between solution and the electrode surface
C_{dl}	Double layer capacitance
Ref. index	Refractive index
RGB	Red green and blue component
R_{ku}	Fractal value
RMS	Root mean square roughness
RNA	Ribonucleic acid
R_q	Root mean square roughness
RSD	Relative standard deviation
R_{sol}	Solution resistance
RT-PCR	Reverse transcription polymerase chain reaction
S.D.	Standard deviation
SELEX	Systemic Evolution of Ligand Exponential Enrichment
SEM	Scanning electron microscope
SERS	Surface-enhanced Raman Spectroscopy
SFZ	Sulphathiazole
SPCE	Screen printed carbon electrode
SPR	Surface plasmon resonance
ss	Single stranded
STR	Streptomycin
SWCNHs	Single walled carbon nanohorns
SWNTs	Single walled carbon nanotubes
SWV	Square wave voltammetry
TET	Tetracycline
TiO ₂ -NPs	Titanium dioxide nanoparticles
TLC	Thin layer chromatography
USFDA	United States Food and Drug Administration
UV	Ultra-violet
W	Warburg impedance corresponds to the diffusion of the redox probe
XNA	Xenonucleic acid

List of Symbols

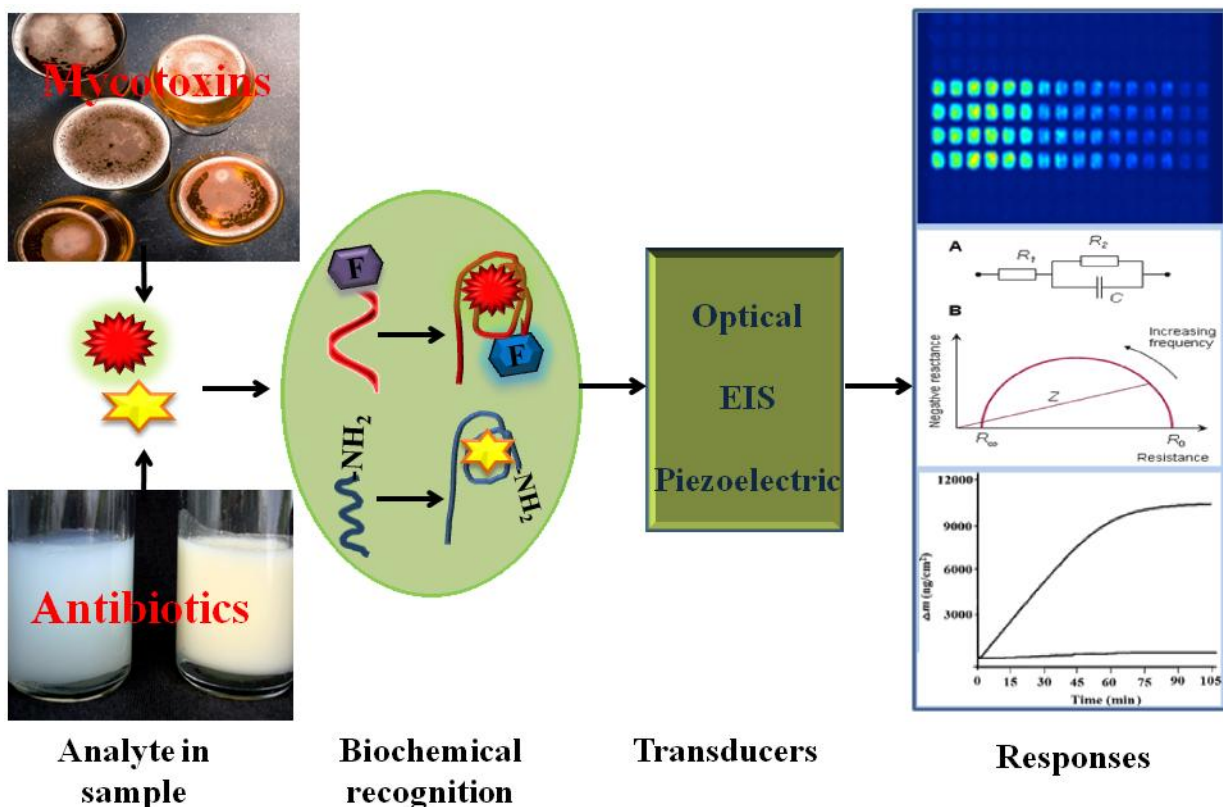
Symbols	Description
Z'	Absolute impedance
Z''	Imaginary impedance
$ Z $	Absolute impedance
μg	Microgram
μL	Micro litre
μM	Micro molar
μm	Micrometer
A	Active surface area
C_f	Resonance frequency of crystal
h	Hour
Hz	Hertz
K_a	Association constant
K_d	Dissociation constant
Kg	Kilogram
KHz	Kilo Hertz
L	Litre
mL	Millilitre
mV	Millivolt
ng	Nanogram
nm	Nano meter
nM	Nanomolar
n_p	Number of moles of products
$^{\circ}\text{C}$	Degree centigrade
pg	Picogram
pH	Potential of hydrogen
pmol	Pico mole
Q	Total heat
Q%	Quenching percentage
RT	Room temperature
S/N	Signal to noise ratio
Δf	Change in frequency
ΔH	Molar enthalpy change
Δm	Change in mass per unit area
λ_{max}	Absorption maxima

List of Keywords

- 1. Aptamer**
- 2. Structure Switching concept**
- 3. Aptamer assay**
- 4. Fluorescence Quenching-dequenching**
- 5. Labelled and non-labelled**
- 6. Mycotoxins**
- 7. Ochratoxin A**
- 8. Aflatoxin M1**
- 9. Antibiotic**
- 10. Kanamycin**
- 11. Tetracycline**
- 12. Beer and Wine**
- 13. Milk sample**
- 14. SELEX (Systemic Evolution of Ligands by Exponential Enrichment)**
- 15. Impedance**
- 16. Electrochemical Quartz Cristal Nanobalance**
- 17. Sensitivity and precision**
- 18. Food and Beverages**
- 19. Flow injection analysis**
- 20. Fluorescence imaging**

CHAPTER 1: INTRODUCTION

Thesis overview: Monitoring of the bio-molecular interaction has become an important element of various sensing applications. The present thesis deals with the latest advancements in the field of aptamer-based sensing platform for detection of food and environmental contaminants (mycotoxins and antibiotics). In this work, the microwell plate-based assays have been developed utilizing aptamer (as recognition element) and titanium dioxide nanoparticles (as a fluorescence quencher). We have used the functionally modified single stranded (ss) DNA-aptamer sequences, which are more stable during modifications and having higher sensitivity, stability and shelf life. By using the highly specific ssDNA aptamer sequences, we have developed aptasensor based on electrochemical impedance and piezoelectric transducer and focus on practical application in unprocessed real samples.



Graphical abstract of the thesis contents

1.1 Background of research

With increased globalization of the food supply, the increasing prevalence and incidence of food contamination around the world has stipulated the both opportunity and challenges in food safety. The foodborne illnesses are usually infectious or toxic in nature and caused by toxins (mycotoxins), pharmaceuticals (antibiotics, anti-infective agents), chemical substances (heavy metals, dyes), microbes (bacteria, virus), which is a potential threat to human health and the environment (Rasooly and Herold, 2006; Kantiani et al., 2010). The widespread use and proliferation of food pathogens have been affecting human and eco-system. The presence of mycotoxins contamination at both pre- and post harvesting level is always remain a challenge to food and beverage industries (Marin et al., 2013). The emergence of microorganisms resistant and incidences of “suprainfection and cocktail effect” caused due to the secondary effects of antibiotics results in consistently high mortality and morbidity rates (Megoules and Koupparis, 2005). The outbreaks of food contamination can be traced as far as the ‘Stone Age’. The only difference between now and then is that, now, the causes of illness are identifiable and the knowledge of how to protect and prevent against illness has been acquired. However, the science and methodologies for continually improving the sanitation, identifying and controlling outbreaks, ensuring food safety and quality are of immense societal and economic value.

1.2 Motivation in research

Identification and detection of food contaminants from single molecule to whole cells, continues the challenge to scientists and researchers worldwide. In the last decades, the increased incidences of small molecule contamination such as mycotoxins with low molecular weight toxins have gained significant attention. These biological toxins are mainly responsible for food poisoning and have the potential to be used as biological warfare agents at the toxic dose. Due to the poisonous nature of mycotoxins, effective analysis techniques for quantifying their toxicity are indispensable. In the mean time, the emergence and prevalence of increasing irrational use of antibiotics and bacterial resistance against majority of antibiotics has resulted in sustainable side effects on human health and high mortality rates (Thakur et al., 2013). “Suprainfection and increased bacterial resistance” has alarmed the situation for early detection of these molecules for human and environmental safety (Sarmah et al., 2006; Naik et al., 2015).

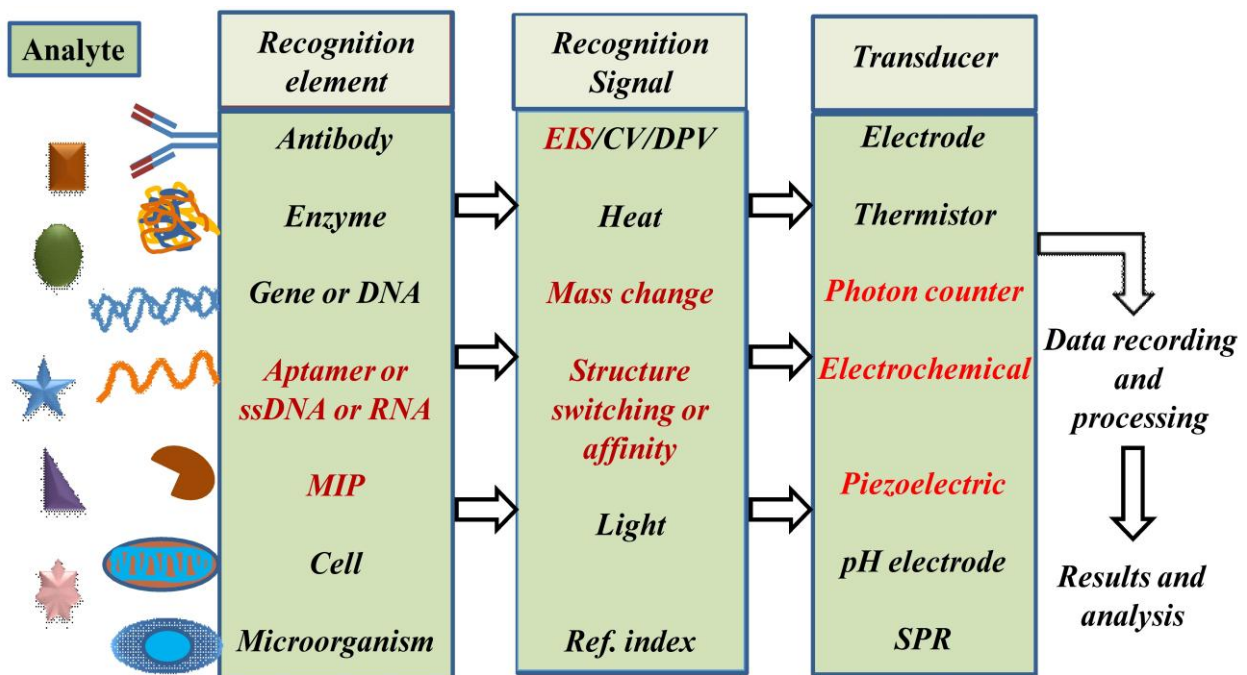
The discovery of a novel, innovative, fast and cost effective method to detect analyte of interest at low levels will have the high impact in food safety, healthcare and environmental science. For early detection of these contaminants, biosensors have been emerged as a powerful tool to monitors toxins at extremely low level.

In this context, the bio-analytical methods i.e. Biosensors, with focus on the involvements of newly synthesized recognition elements (aptamers, molecularly imprinted polymers, recombinant antibodies) are of current interest. Biosensors being able to detect the food contaminants or adulterants in real food sample, food stuffs and beverages would enable the physician to accurately diagnose patients and industrialist without having a much wait for samples to be analysed in a central accredited laboratory. Whereas, the detection of contaminants in food and beverages would enable the regulatory agencies to quickly analyze the sample and take decision. However, it is not an easy task to develop the biosensing platforms, since the sensitivity, specificity, selectivity, accuracy and precision is the crucial factor for the reliability of a biosensor. Owing to the advancements in the analytical methods, the biosensor application in the analysis of food and environmental contaminants is a growing field with increasing demand for reliable biosensors (Bhand et al., 2010). In the present thesis work, we will discussed the development of reliable, sensitive and cost effective aptamer assay and aptasensors for detection of commonly found mycotoxin i.e. ochratoxin A, aflatoxin M1 (in milk and alcoholic beverages) and antibiotic residues i.e. kanamycin and tetracycline (in milk).

1.3 Biosensors

As advancements in sensor technology, biosensors are becoming more and more indispensable tools in food safety, environmental monitoring, clinical diagnostic and many more. With rapid proliferation of biosensors and their diversity led to a lack of rigour in defining their performance criteria. Whereas, each biosensor can be evaluated for specific application, however, it is still important to examine how standard protocols for biosensor performance criteria may be defined in accordance with the International Union of Pure and Applied Chemistry (IUPAC) guidelines. In accordance with the IUPAC definition “biosensor is a device that uses specific biochemical reactions mediated by isolated enzymes, immunosystems, tissues, organelles or whole cells to detect chemical compounds usually by electrical, thermal or optical signals (Compendium of Chemical Terminology, 2nd edition (the "Gold Book"))”. In a typical design of biosensor, transducer converts the signal of

specific biochemical reaction into a quantifiable and measurable signal, which is proportional to the concentration of cognate molecule or group of analyte present. Biosensors are characterized by a high level of specificity and selectivity of bio-recognition elements, which specifically reacts with a given target molecule. The different components of biosensor have been shown in Fig. 1.1. The combination of this specificity and sensitive transducer ensure the unique and unrivalled characteristics of biosensors to detect the variety of analytes, even when they are present in complex matrices. Even though the biosensor, primarily immunosensors have been successfully implemented in a number of analytical/ diagnostic laboratories. Moreover, the overall commercialization of biosensor technology has lagged behind research output assessed by the sheer number of publications and patent filings (Luong et al., 2008). This commercialization lag is could be attributed to the high development costs and technical barriers involved. In the last decades, the field of analytical chemistry has grown enough and focus shifted towards miniaturization, high throughput and automation of process control. These requirements impose a greater challenge in biosensors, which is usually design to detect a specific target molecule.



*EIS: Electrochemical Impedance Spectroscopy; CV: Cyclic Voltammetry; DPV: Differential Pulse Voltammetry; Ref. index: Refractive Index; SPR: Surface Plasmon Resonance; MIP: Molecularly imprinted polymer

Figure 1.1: Schematic representation of biosensor components.

1.3.1 Recognition elements

Molecular recognition element is a central key in the design of a biosensor. The bio-recognition elements/receptors essentially required to be highly selective and specific towards the cognate target avoiding the interference with analogues and non-analogues molecules. Biosensors can be further classified based on the recognition component:

1.3.1.1 Catalytic biosensor

- ❖ **Enzyme based biosensors (Biocatalysis-Biosensors):** These biosensors depend universally on the use of enzymes as bio-recognition element. The working principle of this biosensor is based on the catalytic or inhibition properties of enzyme.
- ❖ **Whole cell/ Microbes Biosensor:** These biosensors utilize microorganisms as their biosensing element to respond the environmental cues and chemicals.

1.3.1.2 Affinity biosensor

- ❖ **Antibody based biosensor (Immunosensors):** These biosensors depend on the use of biomolecule i.e. antibody (monoclonal and polyclonal). The principle of this biosensor is mainly depending upon the affinity of antigen-antibody interaction.
- ❖ **Aptamer based biosensor (Aptasensors):** They used aptamers/oligonucleotides (DNA/RNA)/ peptides as bio-recognition element. The sensing mechanism is based on specific binding of biomolecule to the non-nucleotide target molecules such as pathogen, proteins etc.
- ❖ **Molecularly imprinted polymer (MIP) based sensor:** MIP is a designed polymer with a memory of the shape and functional groups with an affinity against a selected template molecule.

Table 1.1: Characteristics comparison of biosensor receptor (Shruthi et al., 2014; Bhalla et al., 2016)

Receptor	Merits	Demerits
Enzyme	<ol style="list-style-type: none"> 1. Highly selective and fast acting 2. Have catalytic activity, thus improving sensitivity 	<ol style="list-style-type: none"> 1. Expensive (cost of source, isolation and purification) 2. Loss on activity on immobilization 3. Loss of activity over the time unless stored under appropriate condition.
Whole cell/ Microbes	<ol style="list-style-type: none"> 1. Cheaper source of enzymes than isolated enzymes 2. Less sensitive to inhibition by solutes. Tolerance to pH & temperature changes that leads to longer lifetimes 	<ol style="list-style-type: none"> 1. Longer response and regeneration time due to diffusion of substrate through/be transported into cytoplasm; 2. Less selective (contain many enzymes like tissues)
Antibody	<ol style="list-style-type: none"> 1. Very selective 2. Ultra-sensitive 3. High binding ($K_a = 10^6$) 	<ol style="list-style-type: none"> 1. No catalytic effect 2. Due to high binding, very strong & harsh conditions needed to reverse the reaction.
Aptamer	<ol style="list-style-type: none"> 1. High stability and specificity 2. High selectivity and sensitivity 3. No immunogenicity 	<ol style="list-style-type: none"> 1. Need time to optimized in-vitro process. But once optimized, ease for modification with improved stability and shelf life

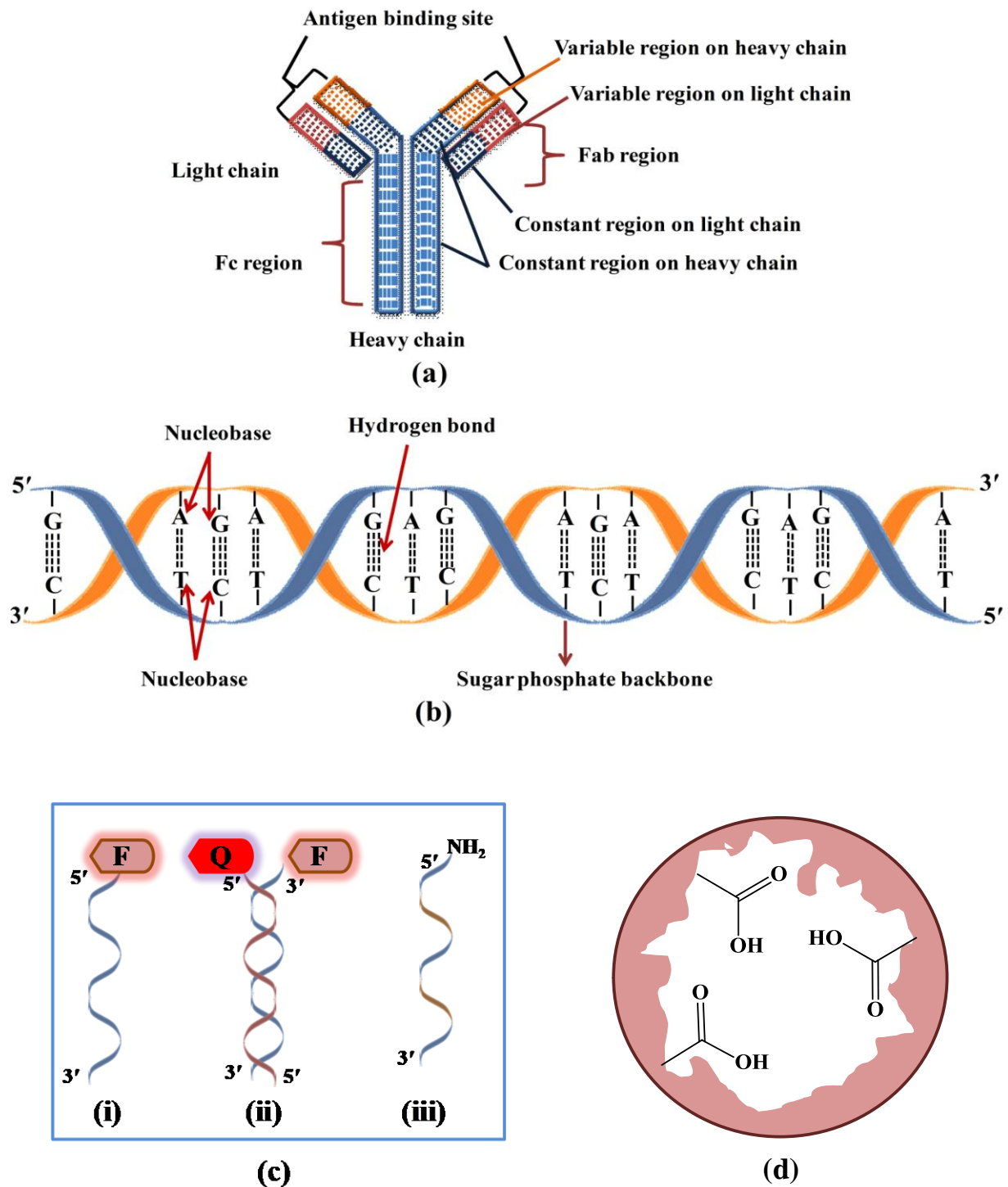


Figure 1.2: Recognition elements in biosensor (a) antibody; (b) nucleotides; (c) (i) fluorophore labelled (F) ss-aptamer; (ii) dual labelled, fluorophore (F) and quencher (Q) aptamer helical structure; (iii) functionally (amine, -NH₂) modified ss-aptamer; (d) molecularly imprinted polymer (MIP).

1.3.2 Transducers

1.3.2.1 Optical biosensors: The optical biosensor is a device, which works on the principle of optical measurements like fluorescence, absorbance, electroluminescence etc. They are used in fibre optics and optoelectronic transducers. Mainly two modes of measurements are used as colorimetric (change in light absorption) and photometric for light intensity (photon count for fluorescent or luminescence process).

1.3.2.2 Electrochemical biosensor: The electrochemical biosensor is a simple device, which measure the biochemical reaction between target and receptor that produces or consume ions/ electrons. It measures the change in electronic current, ionic or conductance changes carried by bio-electrodes.

1.3.2.3 Thermal or thermometric biosensor: This biosensor work on the measurement of change in absorption or production of heat during a biochemical reaction. The total heat produced or consume is equal to molar enthalpy changed and total no of molecules produced in reaction.

$$Q = -n_p (\Delta H) \quad (1.1)$$

Where, Q- total heat; n_p - number of moles of product; and ΔH - molar enthalpy change.

1.3.2.4 Resonant biosensor/Piezoelectric biosensor: The principle of piezoelectric/resonant biosensor is based on the change in frequency occurred or change in the mass of absorbed products. The basics of the piezoelectric crystals and its characteristic frequencies are trembling with the charge on crystal. Change in vibrational frequency of crystal becomes the basis of measurements.

$$\Delta f = (C_f/A) \Delta m \quad (1.2)$$

Where, Δf - change in frequency; C_f - resonant of frequency of crystal; A- active surface area of electrode; Δm - change in mass per unit area.

1.4 Generation of biosensors

Biosensors can be further classified into three generations according to the degree of integration of the recognition element (bioreceptor) with the base indicator (transducer) element (Fig. 1.3) (Murugaiyan et al., 2014). In the first generation, the bioreceptor molecule is retained in the vicinity of the base sensor behind a dialysis membrane, thus the reaction

product diffuses to the transducer and generate signals. In the next generations, the immobilization is achieved via cross-linking reagents or bi-functional reagents at a suitably modified transducer interface/ incorporation into a polymer matrix at the transduction surface. In the third generation, the individual components remain essentially distinct and generation of the signal depends upon the use of mediators between reaction surface and transducer. In this generation, the recognition element is in the close vicinity or an integral part of the base sensing element. Where, the reaction itself is enough to generate a response. As the literature suggest, there have been immense research efforts made for advancement in the instrumentation as well as the designing of biosensing platforms keeping the common goal of progressing towards the application in real-world sensing (Kim et al., 2017).

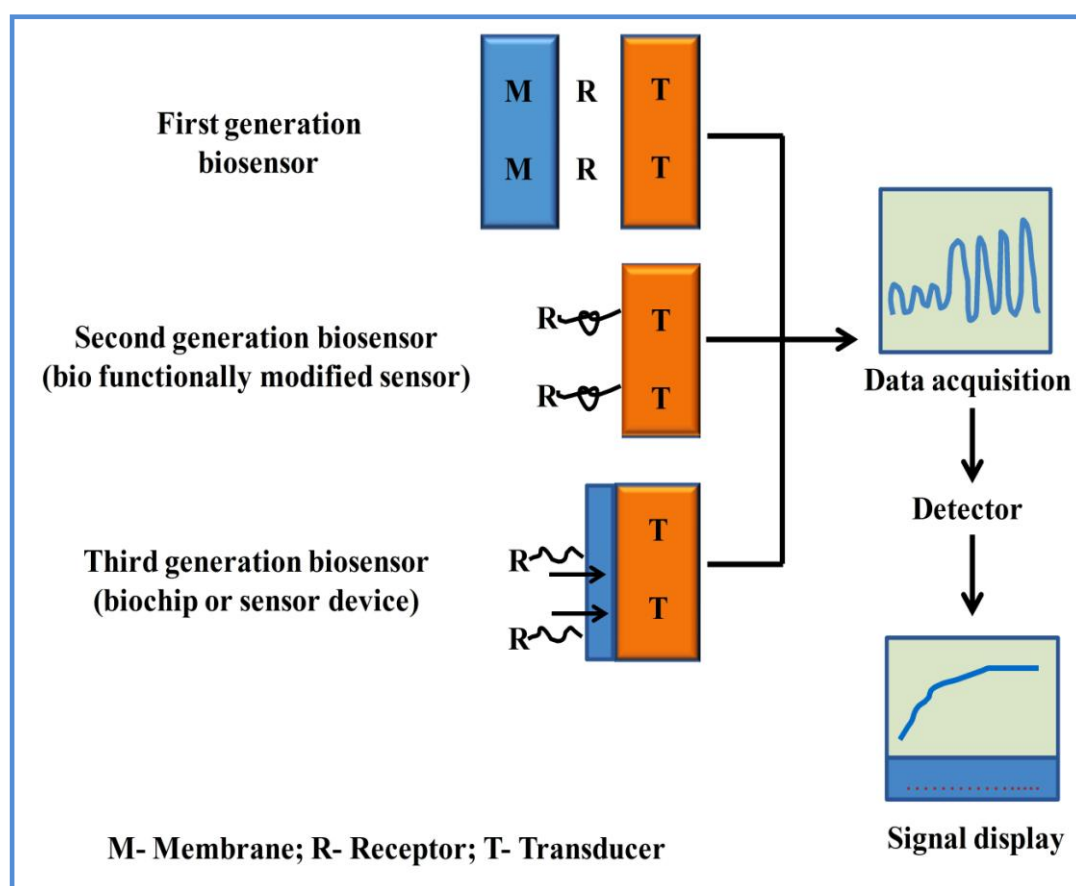


Figure 1.3: Generation of biosensors.

1.5 (Bio) receptors used in the present thesis for biosensor development

1.5.1 Aptamer and SELEX

Since the discovery of aptamers in early 1990s, aptamer has gathered tremendous interest in therapeutics and bio-analytical application (Gold et al., 2012). Aptamers are the synthetic

short sequences (30-100 nucleotides) of single-stranded (ss) oligonucleotides (DNA/RNA/XNA) or peptides obtained from an *in-vitro* process as a Systemic Evolution of Ligands by Exponential Enrichment (SELEX). From SELEX, an aptamer sequence is selected from a very large and the random pool of nucleic acid libraries and amplified (Song et al., 2008; Cox and Ellington, 2001). As recognition mechanism, upon target binding, the target specific aptamer folds into a specific G-quadruplex aptamer-target complex structure. The RNA aptamers are unstable and have a shorter life span in biological fluids or real sample analysis due to the presence of nucleases. On the other side, the ssDNA aptamer exhibits the inherent stability and resistance to degradation, which makes them an ideal candidate for biosensing application (Swenson et al., 2009). Aptamers possess the high affinity and specificity towards their cognate targets, providing greater selectivity, ease of modification, facile labelling and long term stability over the natural receptor i.e. antibodies or enzymes (Jayasena, 1999). The high target specificity that aptamers exhibit, make aptasensors suited for bio-analytical applications. The comparative characteristic features of aptamer over antibodies have been summarized in Table 1.2 (Jayasena, 1999; Toh et al., 2015).

Table 1.2: Comparison of properties and advantages of aptamer over antibodies

Aptamer	Antibody
Identified through <i>in-vitro</i> process (SELEX)	Requires the use of animal (Immunization)
Toxins as well as small molecules that do not elicit good immune response can be utilized to generate high affinity aptamers	Limitations against target representing constituent of the body and toxic substances
Long term inherent stability	Limited shelf life (prone to thermal degradation)
Ambient temperature handling	Sensitive to temperature
Denatured aptamers can be regenerated within minutes	May undergo denaturation
Little or no batch to batch variation due to use of an <i>in-vitro</i> chemical process	High batch to batch variation due to different immunity of immunized animal
Ease of labelling or modification without affecting binding motif.	Labelling of antibodies can cause loss in affinity or reduced activity
Multiple labeling possible	Multiple labelling not possible
No negative immune system activation	Activation of immune system because antibody recognized by body immune system

Development of the *in-vitro* SELEX process provides a platform to isolate the oligonucleotides sequences with the capacity to recognize various target molecules with high affinity and specificity. The five basic steps i.e. binding, partitioning, elution, amplification and conditioning that comprise a SELEX process are outlined (Fig. 1.4). Initially, the synthetic oligonucleotides (ssDNA/ ssRNA) sequence library from some hundreds to thousands is randomized under a specific set of experimental conditions (James, 2006; Stoltenburg et al., 2007). Before binding, a pre-treatment step is usually performed where the oligonucleotides (ssDNA or ssRNA) library is incubated with target-free selection matrix (negative SELEX) to remove any non-specific binding sequences. The first step of the SELEX cycle is the binding, where the randomized oligonucleotides sequences are incubated with the specific target analyte of interest. Secondly, the most important step is to separate the target bound sequences from unbound or weakly bound oligonucleotides utilizing different separation techniques (chromatographic, flow cytometry, electrophoresis etc.) (Musheev and Krylov, 2006). Then, the bound sequences are eluted and further amplified by PCR (DNA SELEX) or RT-PCR (RNA SELEX). The enriched oligonucleotides pool is the re-introduced into the next SELEX cycle. Iterative selection and amplification rounds in each cycle reduce the nucleotides pool to lower number consisting of sequences with the highest affinity and specificity to cognate molecules. The total number of SELEX cycles performed is highly variable from experiment to experiment and a number of parameters such as target molecule structure, selection conditions (such pH, buffer strength, temperature etc.), partition step efficiency. However, it requires time to optimize SELEX parameters, but once optimized it reflects the high efficiency conditions of aptamer towards target.

The event of aptasensor recognition and binding to their cognate molecules is characterized by molecular shape conformational, electrostatic/ van der Waals and hydrogen bonding interactions and stacking of aromatic rings. Aptasensors offers the merits of high selectivity, specificity, rapidity, stability, applicability of diverse measurements methods for wide range of analyte. The aptasensor application in the analysis of contaminants present in food and beverages is of paramount interest of researchers to develop reliable and affordable techniques with less or minimal sample preparation.

1.5.2 MIP

Molecularly imprinted polymers (MIPs) are chemically synthesized possible mimics of natural receptors with predetermined selectivity and recognition towards its template

molecule (Fig. 1.5). They imitate the natural recognition possessing high selectivity, thermal and chemical stabilities, ease of preparation, applicability for a wide range of operating conditions and applications (Mosbach and Ramstrom, 1996; Vasapollo et al., 2011). The

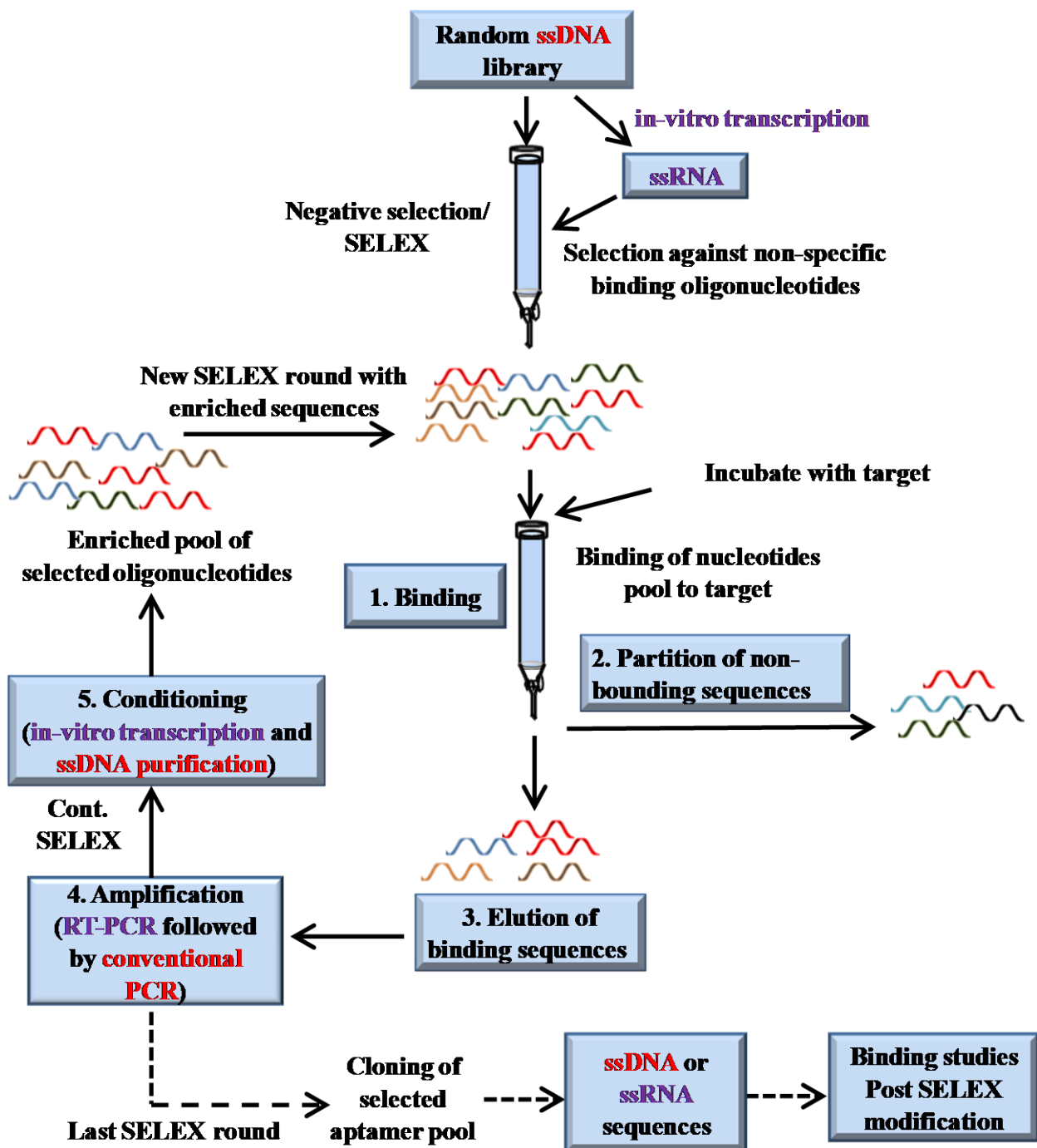


Figure 1.4: Schematic representation of the SELEX Process (demonstrating all main 5 steps): Steps in solid arrow line are specific for ssDNA aptamer selection and steps in dotted arrow line are specific for RNA aptamer selection.

commonly used approach to prepare an imprinted polymer involves interactive pre-organization (pre-polymerization) between the ‘functional monomers’ and ‘template’ molecules, followed by complete polymerization in the presence of a large excess of cross-linking agents using initiator or not. Based on high mechanical strength and thermal stability, they can be repeatedly used over conventional immunosorbent. MIP based sensors can be categorised based on their polymerization and application (Benito-Pena, et al., 2009; Wackerlig and Schirhagl, 2016). Meanwhile, the application of label-free optical sensing platforms simplifies the assays and enables time-resolved process to study the molecular interactions.

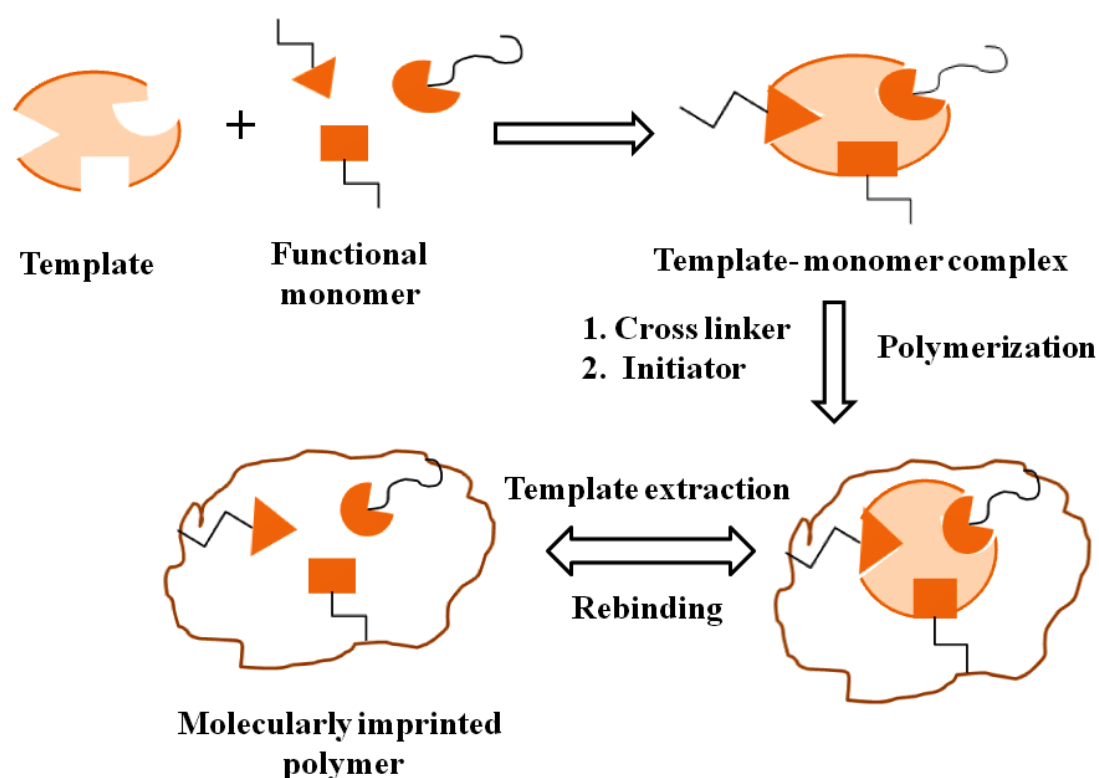


Figure 1.5: Schematic representation for the preparation of molecularly imprinted polymer.

1.6 Transducers used in the present thesis for biosensors development

Biosensors can also be classified according to their signal transduction principles (section 1.3.2). The transducer is an important component in a biosensor, through which the measurement of the target analyte is achieved by selective interaction of a biomolecule and analyte into a quantifiable signal. In the present thesis, we have been focused on the three transducers; those have been discussed in details:

1.6.1 Optical transducer

Optical transducer measures the change in an optical signal (light rays) in the form of electric signal. It does this by generating an electrical current proportional to the intensity of incident radiation. The transduction process induces a change in the fluorescence, absorption, luminescence, polarization, surface plasmon resonance (SPR) and amplitude of the input light. These changes are due to the physical and chemical change produced by the bio-recognition process. Optical transducer represents the largest and fastest growing area in biosensor technology. Photomultiplier tubes (PMTs) and charge-coupled devices (CCDs) are among the most extensively reported transducers for optical biosensors (Narsaiah et al., 2012). PMTs are extremely sensitive detector for measurements of light in the ultraviolet, visible and near-infrared region of the electromagnetic spectrum. Numerous literatures have been reported for the aptamer based biosensor using optical transducer for food and environmental applications (Wang et al., 2011; Van Dorst et al., 2010; Amaya-González et al., 2013; Goud et al., 2016). Among the various reported optical techniques, fluorescence is commonly employed technique with improved and high sensitivity. Fluorescence phenomenon occurs when molecule absorb light at one wavelength and emit corresponding at a longer wavelength. Since, the excitation and emission occurs at distinct energy levels, each fluorescent molecule possess a unique spectral fingerprint, which is an important parameter for the optical biosensing applications (Lechuga, 2005). Fluorescence based biosensors offers the advantages of high selectivity, sensitivity, high throughput, ease of miniaturization, immunity to electromagnetic interference and applicability of diverse measurement methods with a single control instrument (Damborsky et al., 2016).

In this thesis, we have adopted fluorescence quenching based techniques using labelled and non-labelled aptamer sequences to design the structure switching aptaswitches for mycotoxin analysis. In a typical design of fluorescence quenching based aptaswitches, the universal capability of aptamer to switch structure between designed to G-quadruplex aptamer-target complex results in generation of signal. For example, in the absence of target molecule the fluorophore is in the close proximity to the quencher result decrease in fluorescence signal, either signal off or decrease signal intensity. Upon target recognition, the structural conformation of aptamer-target complex obstructs the quenching phenomenon, which causes signal on/ increase. Many researchers have reviewed the principle of fluorescence quenching or FRET phenomenon and their applications in aptamer based

biosensors (Wang et al., 2011; Shi et al., 2015; Sabet et al., 2017). Principle of fluorescence quenching based aptaswitches strategies has been shown (Fig. 1.6).

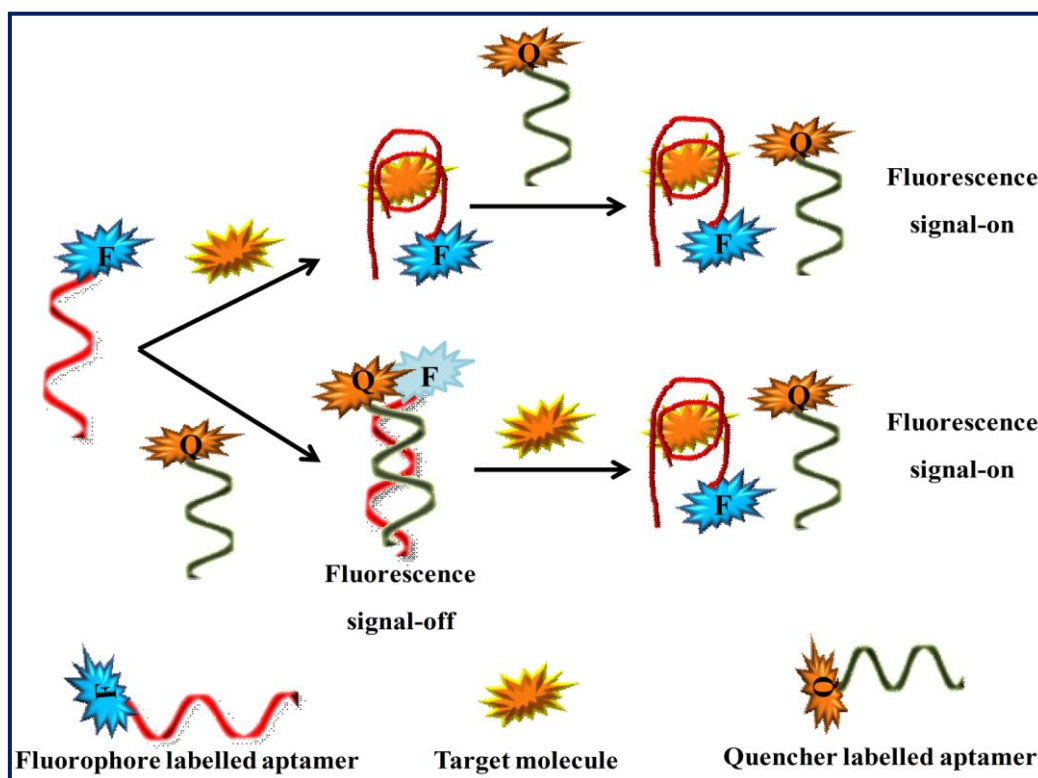


Figure 1.6: Schematic representation of fluorescence quenching based aptaswitches for biosensor development.

1.6.2 Electrochemical (impedimetric) transducer

The basic principle of electrochemical transduction is based on the bio-chemical reaction between immobilized biomolecule and target analyte produce or consumes ions/electrons, which affects the measurable electrical properties of the solution like electric current, resistance, potential etc (Thevenot et al., 1999; Joshi et al., 2005). Recently, the electrochemical impedance spectroscopy (EIS) has been emerged out as sensitive technique in the field of biosensor development (Grieshaber et al., 2008). EIS based biosensor shows the multiple advantages as fast response, low cost, portable and capability of miniaturization. EIS sensors are attractive to researchers since they allow label-free detection with high sensitivity even at trace level. Traditionally, the EIS sensors used the macro sized metal rods or wires electrodes immersed in the solution to measure the impedance and it is suitable to analyze the electrical properties of the modified electrodes. Moreover, it is cumbersome to use conventional (rod type) electrodes in electrochemical biosensors due to need of several

optimization and many point calibration steps during fabrication. In the mean time, the integration of SPCEs technology (screen printed carbon electrodes) with electrochemical biosensor offers the advantages of disposability, portability and feasibility for the on-site application over the conventional electrochemical biosensor has garnered the significant potential (Lee et al., 2017). Due to the simple, cost effective and versatility of SPCEs mass production, it is easy to increase production and miniaturized SPCEs based electrochemical biosensor for on-site analysis in real sample (Hayat and Marty, 2014). In the present thesis, we have used the SPCEs technology to develop impedimetric aptasensor for kanamycin detection (Fig. 1.7).

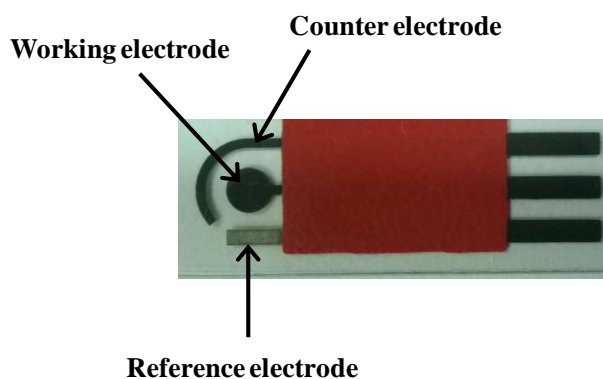


Figure 1.7: Design of a customized SPCE (used in the present work).

1.6.3 Piezoelectric (mass-sensitive) transducer

The piezoelectric transducer working is based on the principle of piezoelectric effect. These biosensors are based on the coupling of the bio-recognition element on piezoelectric component, usually a quartz-crystal coated with gold electrodes. Piezoelectric effect states that when a biochemical interaction occurs on the quartz crystal surface, the crystal vibrate at a specific frequency with the application of an electrical signal at a specified frequency. Based on this, the vibrational frequency of crystal is dependent on the electrical frequency applied or the change in the mass on quartz crystal surface. With the change in crystal mass upon target binding, the crystal vibrational frequency changed that corresponding change is used to determine the additional mass (both decrease or increase in mass) on the crystal surface (mass-sensitive techniques) (O'Sullivan and Guilbault, 1999). The relation obeying the change in frequency and mass is shown in the Equation 2. There is a high interest in the application of piezoelectric sensors, since it was realized that several possibilities for molecular sensing might be opened up by coupling the suitable recognition layer on crystal surface. Presently, the piezoelectric (mass sensitive) biosensor is thought to be one of the most sensitive analytical techniques till date being capable of detecting analyte of interest in

the picogram range. Piezoelectric biosensors possess the inherent ability of label-free detection of molecule, durability, chemical inertness, real time analysis, applicability to measure dynamic process and integration with flow injection analysis (Janshoff et al., 2000; Gautschi, 2002). Initially, these sensors were believed to have the potential to detect antigens in the gas or liquid phase. However, the piezoelectric biosensor showed potential applications in food, environmental and clinical analysis (Skladal et al., 2004; Tombelli et al. 2005). The piezoelectric biosensor opens the new platform for the direct and real time detection of different analytes such as food and environmental contaminants. In the present work, the piezoelectric aptasensor is developed for tetracycline detection (as discussed in chapter 5).

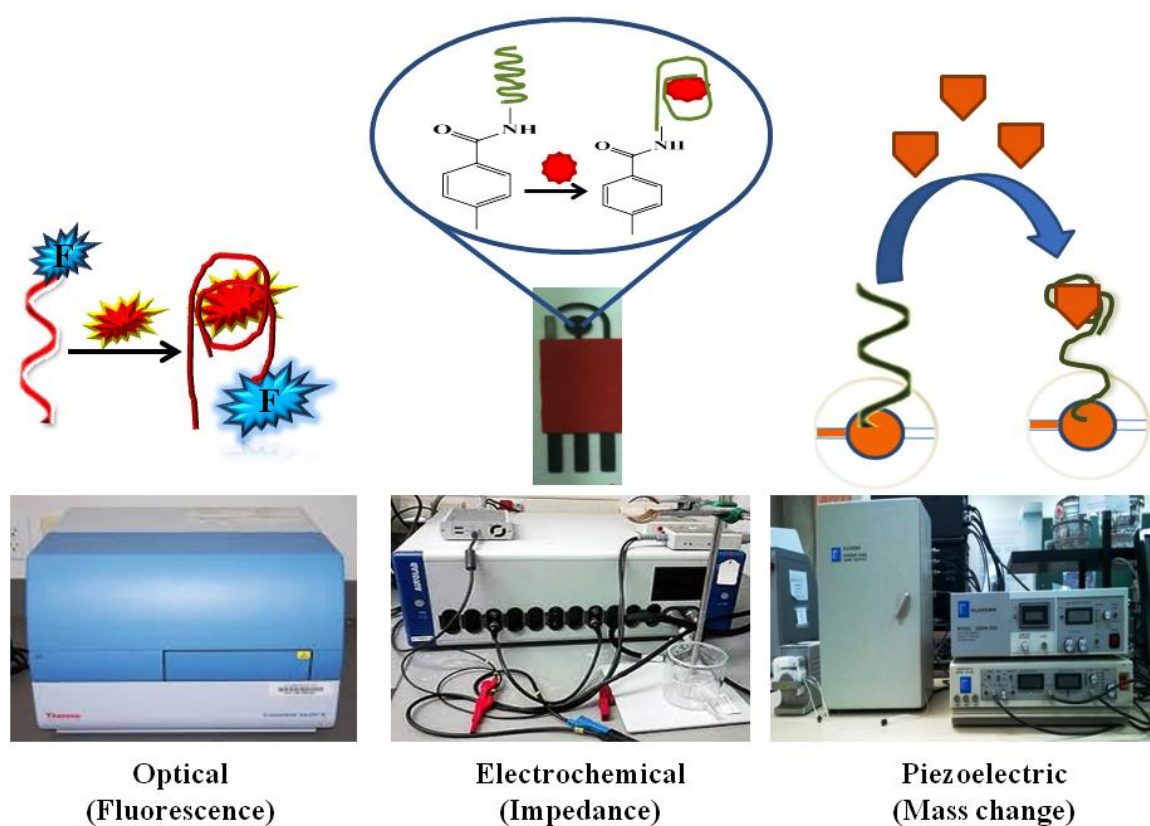


Figure 1.8: Different transduction principles used for biosensor development.

1.7 Performance criteria of biosensor and analytical figures of merits

1.7.1 Performance criteria of biosensor

The biosensor performance can be evaluated on the basis of various parameters. Parameters significant in evaluating biosensor performance are listed below:

1. Specificity: Ability of a biosensor to detect one analyte in the presence of another.

2. **Selectivity:** Ability of biosensor to distinguish the response of two nearly close signal in presence of interference molecule.
3. **Sensitivity:** It is obtained from the slope of the calibration curve. If the curve is in fact a 'curve', rather than a straight line, then sensitivity will be a function of analyte concentration.
4. **Stability:** Operational stability of a biosensor may vary according to the sensor design, method of preparation, as well as on the method of application. The produce signal must be stable over a period of time under optimum conditions. This gives an idea of the durability of biosensor.
5. **Precision:** It is the measurement of the instrument reproducibility, which defines the ability to obtain the same value with repeated measurements of a process variable.
6. **Low background noise:** It must produce less background signal or efficient to distinguish between background and analyte response.
7. **Response time:** It is the time required for the detector output to go from the initial value to a percentage (e.g. 99%) of the final value.
8. **Sample throughput:** The number of results that is produced by an instrument divided by time of operation in a given reaction time.

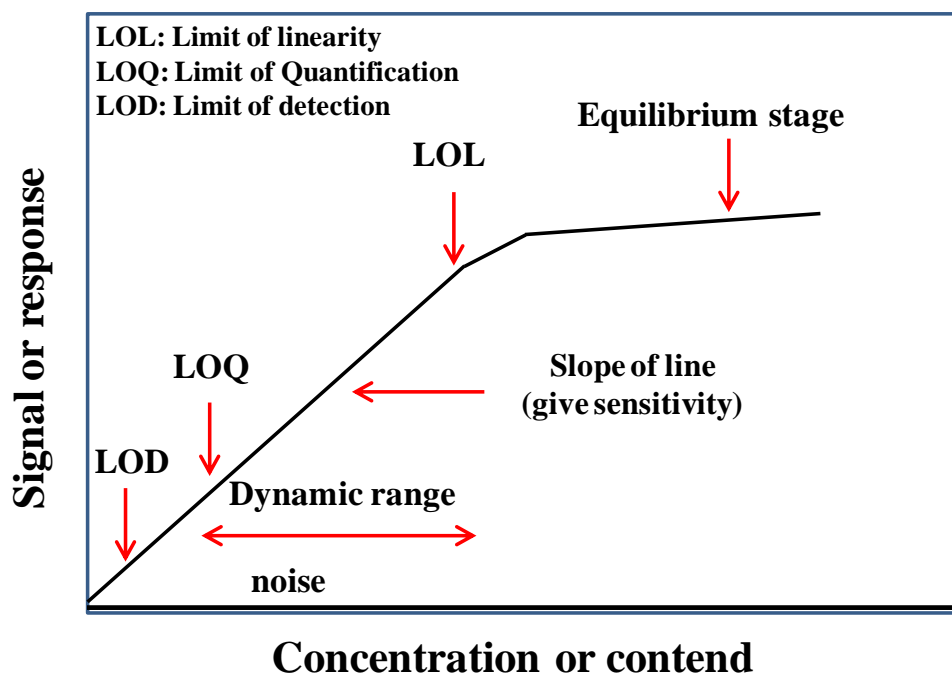


Figure 1.9: A calibration curve showing performance criteria for biosensor.

1.7.2 Analytical figures of merits

The performance of any biosensing technique is generally determined based on the analytical figures of the merits of a biosensor, which are listed below in Table 1.3

Table 1.3: Analytical merit of figure for a biosensor and aptasensor

Parameters	Biosensor Performance	Aptasensors performance
Dynamic range	The concentration range over which signal varies in a monotonic manner with analyte concentration	It must cover the limit of quantitation (LOQ) to the limit of linearity (LOL)
Linearity	The relationship of signal to amount of analyte over a range of concentration of analyte with a constant proportionality factor	Must fall within range of 0 to 80 %
Limit of detection (LOD)*	The lowest concentration of the analyte which can be measured at a specific confidence level	Preferably, the response must be blank plus three time the standard deviation of blank ($S/N = 3$)
Limit of quantification (LOQ)*	The lowest concentration level at which a measurement is quantitatively meaningful. Normally LOQ is more than LOD	Preferably, the response must be blank plus ten times the standard deviation of blank ($S/N = 10$)
Limit of linearity	This is an upper limit of quantification, where calibration curve tends to become non-linear	Usually upto 80 % but could 100% also. It depends upon the technique or transducer employed and signal correlation
Reaction time	The period of time that elapses between the start of the reaction and the attainment of a given extent of a reaction	Total time for aptamer-target complex recognition and generation of response or signal

* **LOD and LOQ calculation** may be different depending upon the transduction principle and strategy employed in the construction of biosensor.

1.8 State of art for mycotoxin and antibiotic residue analysis

1.8.1 Aptasensors or aptamer assays for mycotoxin analysis

Mycotoxin analysis in food and beverages is an important practice to ensure their quality and to eliminate the risk of consuming contaminated foods. Mycotoxins are the toxic secondary metabolites produced by the fungi (micromycetes and macromycetes) under specific conditions of temperature and pressure (Boonen et al., 2012). Structure of commonly found mycotoxin in food commodities has been shown in Fig. 1.10. Toxicities and prevalence of mycotoxins i.e. aflatoxin M1, B1, fumonisin B1 (FB1), deoxynivalenol (DON) and zearalenone (ZEN) and ochratoxin A (OTA) in food commodities (especially milk) and beverages (alcoholic beverages) has necessitated the development of rapid and highly sensitive methods in order to ensure the quality of human food and animal feed supplies (Maragos, 2009). Hence, being able to analyse and detect mycotoxins in foods and beverages gathered priority to comply with the legislative limits (maximum residue limit i.e. MRL) set by regulatory authorities worldwide.

Mostly, the analysis of these toxins is performed by classical conventional techniques such as high performance liquid chromatography (HPLC), gas chromatography/mass spectroscopy (GC/MS), liquid chromatography coupled with mass chromatography (LC-MS), enzyme linked immuno-sorbent assay (ELISA) etc. (Rodriguez Velasco et al., 2003; Sieber et al., 2009; Iha et al., 2011; Prella et al., 2013; Al-Taher et al., 2013). Till date, various emerging and innovative technologies being developed for mycotoxins analysis and these can range from minimally invasive, invasive to non-invasive technologies. However, the inherent properties involved, such as long and complicated sample preparation process, time and expensive instrumentation are the main impediment for their applications on a regular basis and on-site analysis. This necessitates the need of fast, simple and reliable analytical methods for determination of mycotoxin from the complex matrices such as milk and alcoholic beverages. Biosensors have proved to be able to provide the rapid, sensitive and robust quantitative methods for on-site analysis (Rasooly and Herold, 2006). Whereas, the advents of aptasensor technology as bio-recognition element have been emerged out as an alternative potential for analysis of food contaminants and environmental pollutants. On the other side, with the advancements in nanotechnology and its integration with biosensors, mycotoxins analysis has been benefitted by applying nanomaterials for development of ultrasensitive detection methods (Tohill, 2011).

In the last decades, numerous aptasensing platforms have been reported for the analysis of mycotoxins (other than OTA) and OTA in food and beverages, which are listed in Table 1.4 and 1.5, respectively. Based on our literature survey, there is still potential and need to explore novel sensing platform for detection of mycotoxin contamination. In the present thesis work, we will use labelled and non-labelled aptamer as recognition element and will discuss the development of aptasensing platforms for mycotoxin detection in details (Chapter 2 and 3).

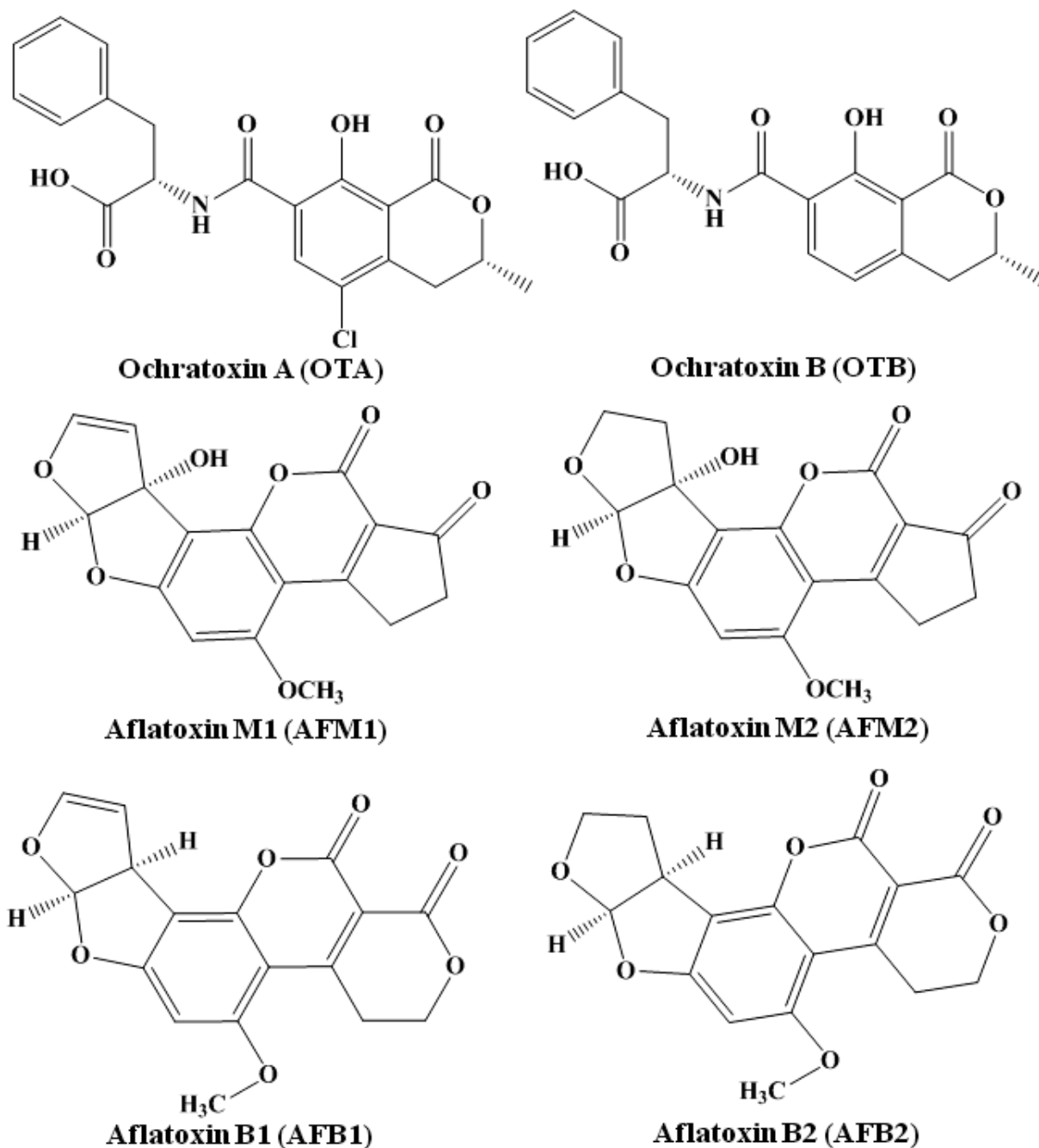


Figure 1.10: Structure of commonly found mycotoxin in milk and beverages

Table 1.4: Reported aptasensing platforms for mycotoxins (other than OTA) analysis in food and beverages

Analyte	Transducer	Principle/ mechanism	Matrix	Ref
AFM1	Electrochemical	Amperometric (signal generation due to DNA hybridization)	Milk	Siontorou et al., 1998
AFM1	Electrochemical	Impedimetric	Milk	Dinckaya et al., 2011
AFM1	Electrochemical	Cyclic (CV) and square wave voltammetry (SWV)	Milk	Nguyen et al., 2013
AFM1	Optical	Real time polymerase chain reaction (RT-qPCR)	Rice cereal and infant milk powder	Guo et al., 2016
AFM1	Electrochemical	Impedimetric	Milk	Istamboulie et al., 2016
AFM1	Resonator-Based aptasensor	Resonance	Buffer	Chalyan et al., 2017
AFB1	Optical	FRET	Beer and Wine	Goud et al., 2016
AFB1	Colorimetric	Sandwich ELISA	Food sample	Aswani Kumar et al., 2018
AFB1	Optical	Fluorescent bioassay	Peanut	Ma et al., 2014
AFB1	Optical	Chemiluminescence (aptamer assay)	Corn	Shim et al., 2014
AFB1	Electrochemical	CV and Electrochemical impedance spectroscopy (EIS)	Peanut	Castillo et al., 2015
AFB1	Optical (Colorimetric)	Structure switching aptamer assay	Ground corn samples	Seok et al., 2015
AFB1	Electrochemical	SWV	Corn	Zheng et al., 2016
FB1	Optical	Fluorescence	Corn	Thompson and Maragos, 1996
DON and ZEN	Optical	Fluorescence	Corn	Ji et al., 2016

Table 1.5: Reported aptasensing platforms for OTA analysis in food and beverages

Matrix	Transducer	Principle/ mechanism	Ref
Wine	Electrochemical aptasensor	Signal on-off aptamer assay (displacement assay)	Kuang et al., 2010
	Optical (Colorimetric)	Enzyme linked aptamer assay (ELAAs)	Barthelmebs et al., 2011a
	Electrochemical and optical	Indirect and direct competition assays	Barthelmebs et al., 2011b
	Electrochemical aptasensor	Folding based aptasensor	Wu et al., 2012
	Optical	Colorimetric (hybridization chain reaction)	Wang et al., 2015
	Electrochemical	Impedimetric	Mejri-Omrani et al., 2016
Beer	Electrochemical aptasensor	Indirect assay using flow injection analysis	Rhouati et al., 2013
	Electrochemical aptasensor	Impedimetric	Hayat et al., 2013
	Optical	Luminescence resonance energy transfer (LRET)	Dai, et al., 2016
Maize	Optical	Luminescence	Wu et al., 2011
	Optical	Fluorescence resonance energy transfer (FRET)	Duan et al., 2012
	Optical	Multiplex FRET aptamer assay	Wu et al., 2012
Wheat	Optical	Fluorescent based structure switching signal on aptasensor	Chen et al., 2014
Corn powder	Optical	Localised surface plasmon resonance (LSPR)	Park et al., 2014
Oat	Optical	Evanescence	Wang et al., 2015
Cocoa beans	Electrochemical	Differential pulse voltammetry (DPV)	Mishra et al., 2016

1.8.2 Aptasensors for antimicrobial (antibiotics) determination

Antimicrobial agents (antibiotics) are medicines leading asset for treatment and prevention of bacterial infection, which is one of the leading causes of increased mortality worldwide. However, the misuse or indiscriminate use of antibiotic results in the serious clinical infections, rapid growth in the antibiotic resistance among bacteria and the development of multiple resistant pathogens (Virolainen and Karp, 2014). The structure of commonly notified antibiotics in food commodities has been shown (Fig. 1.11). Despite of these, the “suprainfection and cocktail effect” of antibiotics therapy is also a major concern. Due to increased use of antibiotics in food, dairy and agriculture industry, it is critically important to limit or ensure the use of antibiotics to avoid transfer of bacterial resistance from animal to human (Megoulas and Koupparis, 2005). The use of antibiotics in food production and dairy industry is strictly controlled by the legislative authorities such as European Union (EU), Food Safety and Standard Authority of India (FSSAI), United States Food and Drug Administration (USFDA) and Codex Alimentous Commission (CAC). Very stringent maximum residue limits (MRLs) of around 5 to 300 $\mu\text{g kg}^{-1}$ in milk and milk products has been mandated depending upon the group of antibiotics (CAC, 2003; Suarez et al., 2009; Food Safety and Standard Authority of India, 2012).

Various classical analytical methods have been reported for determination of antibiotics in various food matrices. These includes high performance liquid chromatography coupled with ultraviolet (HPLC-UV) and fluorescence detection (HPLC-FD), LC-MS, surface-enhanced raman spectroscopy (SERS), ELISA, immunosensor etc (Mesgari Abbasi et al., 2011; Cordewener et al., 2009; Craig et al., 2013; Adrian et al., 2008; Ricci et al., 2007). Among them, the microbiological growth inhibition assay and ELISA found with the lowest limit of detection with 0.1 ng mL^{-1} with fluorescence based detection. These methods are sensitive, high throughput and specific but the experimental procedures such as preparation of antigen or antibody conjugate, complicated enzymatic reaction and susceptibility to interferents are tedious and time consuming. These necessitate the choice of alternative methods, where biosensors have gathered notable success in analysis of contaminants in food and food commodities. In the last decades, various aptasensor has been reported for detection of antibiotics in food especially milk, serum and other clinical sample. However, they have not yet reached their full potential and new products are being under development stage. The aptasensors reported for the analysis of antibiotics in real samples have been listed in Table 1.5. In the present thesis, we will discuss the development of label-free (impedimetric) and

real time aptasensor (flow injection analysis) for detection of antibiotic residue (discussed in detail in the chapter 4 and 5).

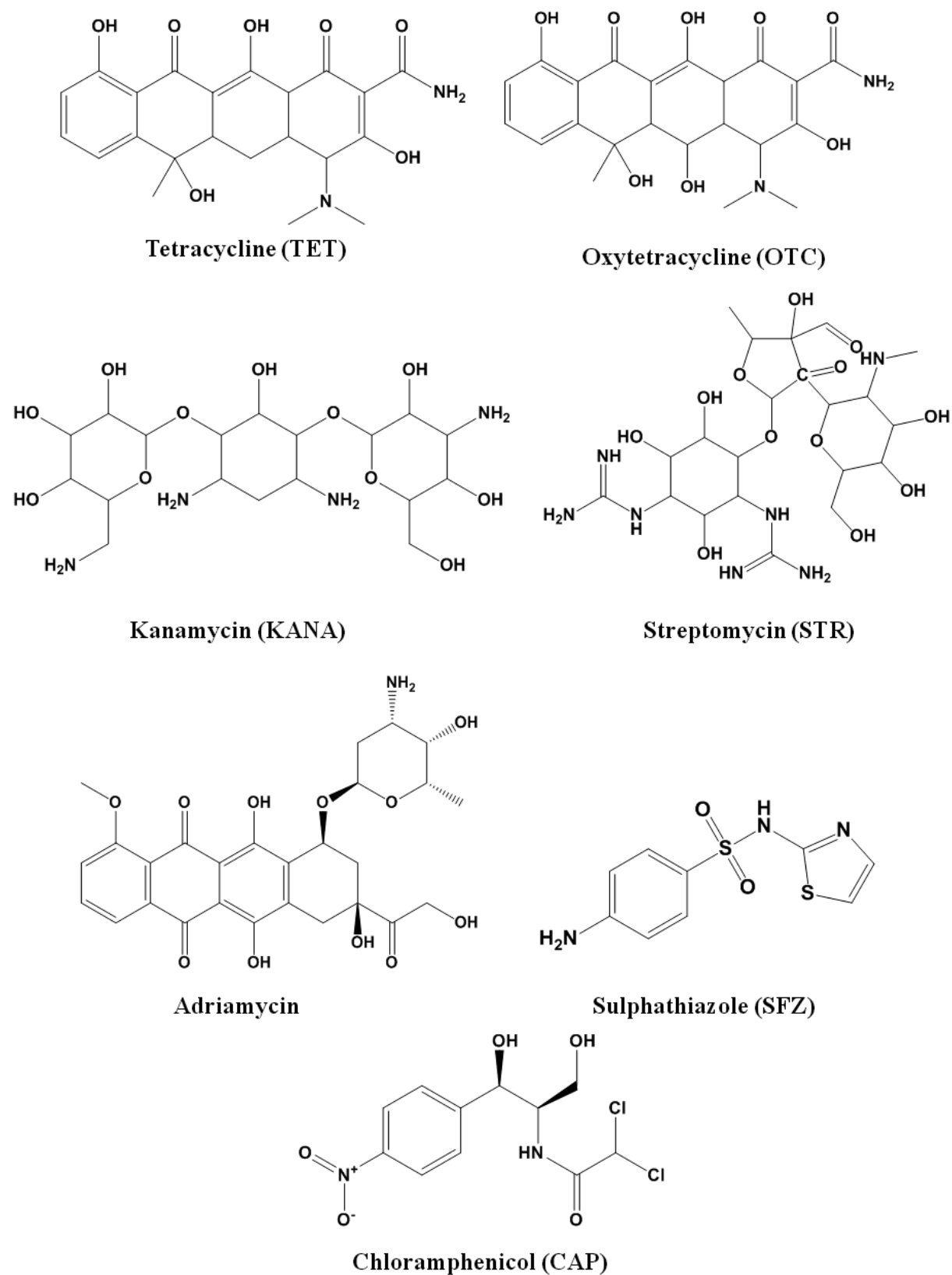


Figure 1.11: Structure of commonly found antibiotics in milk and food commodities.

Table 1.6: Reported aptasensors for antibiotics determination food and animal samples

Analyte	Transducer	Principle/ mechanism	Matrix	Ref
Tobramycin	Electrochemical	Impedimetric	Milk	Gonzalez-Fernandez et al., 2011
TET	Electrochemical	DPV	Milk	Zhou et al., 2012
Ampicillin	Optical	Dual fluorescence and colorimetric method	Milk and animal tissues	Song et al., 2012a
Sulfadimethoxine	Optical	Nanoparticles based Fluorescence quenching aptamer assay	Milk	Song et al., 2012b
Ampicillin and KANA A	Electrochemical	Impedimetric	Milk	Dapra et al., 2013
KANA	Optical	Luminescence based structure switching assay	Aqueous solution and Fish	Leung et al., 2013
OTC	Optical	Enzyme linked aptamer assay (ELAAa)	Milk	Kim et al., 2014
TET	Electrochemical	Impedimetric	Milk	Chen et al., 2014
KANA	UV spectrophotometer	UV absorption	Milk	Zhou et al., 2014
KANA	Electrochemical	DPV	Milk	Qin et al., 2015
TET	Optical	Colorimetric aptasensor	Milk	Luo et al., 2015
Streptomycin	Optical	Colorimetric and Fluorescence Quenching	Milk and blood Serum	Emrani et al., 2016
OTC and Chloramphenicol	Electrochemical	SWV	Milk	Yan et al., 2016
TET	Electrochemical	CV	Milk and serum samples	Taghdisi et al., 2016

1.9 Integration of nanomaterials in biosensors (aptasensors)

With the advancement in nanotechnology, the new and emerging nanomaterials having a high impact in developing biosensors/aptasensors with new capabilities that can be further explored for analysis of food contaminants. Moreover, the technology is still in developing stage, which needs to be further explored before real commercial products are widespread on the market. Focus in nanotechnology relies on the new properties that materials exhibit when reduced to the nanometre scale compares to the bulk materials. Nanomaterial has the significant potential to improve quality and safety of food commodities through the use of advanced micro and nano-sensors tracking systems. Nanotechnology is the inter-discipline research focused at the interface between chemistry, biology and material science, where the ultra precision can be combined with the surface activity or manipulation to develop sensitive assays. To date many review articles have been published in this area (Pérez-López and Merkoçi, 2011; Durán and Marcato, 2013; Sharma et al., 2015). Currently, the development of nanomaterials based aptasensing platforms based on fluorescence and FRET mechanism is growing field (Vinayaka and Thakur, 2011; Thakur and Ragavan, 2013; Malhotra et al., 2014). These platforms utilize the new and novel biorecognition materials being developed those are capable for sensor development (Su et al., 2012). These methods imply on principle of fluorescence quenching, which involves the conjugation of biomolecule with fluorophore (Bamrungsap et al., 2012). Nanomaterials have been widely employed in sensor development due to the excellent advantages of signal enhancement, high surface area-volume impact ratio, miniaturization, immobilization support etc. Still, the nanomaterial has enough potential to be explored further for biosensor applications.

1.10 Gaps in existing research

Plethora of literature is available in the field of biosensors for mycotoxin and residual antibiotic contamination. However, there are some areas that still need to explore further. The areas, which need special and immediate attentions, are as follows:

1.10.1 Need for sensitive and high throughput techniques for mycotoxin analysis: From the existing survey of literature, it is evident that the mycotoxins (OTA and AFM1) even present at ultra low (ng mL^{-1} or pg mL^{-1}) level are highly toxic in nature. Their presence in milk and alcoholic beverages is of primary concern. Due to the involvement of complex matrix matching procedures, the reported biosensor techniques do not meet the standards for their monitoring in milk and other food matrices. According to European Union (EU), the

maximum residual limits (MRLs) for AFM1 in milk 50 ng kg⁻¹ for adult and 25 ng kg⁻¹ for baby foods) and OTA in alcoholic beverages (2 µg kg⁻¹) have been already mandated by regulatory authorities. The AFM1 and OTA levels tend to increase with our daily food habits and common constituent of dietary habits. Development of highly sensitive yet with stable and continues monitoring biosensors with minimal sample treatment requirement are needed for AFM1 and OTA in analysis in milk and alcoholic beverages (beer and wine).

1.10.2 Development of biosensors for residual antibiotics analysis: It is evident from the existing literature that even the presence of nano or sub-pico concentration of residual antibiotic (kanamycin and tetracyclines) can also trigger the potential health hazards, suprainfection (or secondary residual cocktail effect) and increase in microbial resistance. The existing methods involve the complex matrix treatment steps thus incur with long analysis time. Development of biosensor with an ability to detect residual antibiotic contamination can save time, sample quantity and the minimal/ no sample processing steps will reduce analysis time and cost of analysis and increase the affordability of system.

1.10.3 Development of label-free and online platform for residual antibiotics determination in milk: The antibiotic-resistant superbugs are an alarming situation to world because of their increased consumption in agriculture and dairy industry. Online monitoring system such as label-free and fast screening methods in food and dairy industry are required for routine control and right measures. Influence of matrix and cross-contamination has significant effect on detection system thus the selectivity and sensitivity of developed biosensor without complex matrix preparation steps and significance interference is of paramount interest.

1.11 Objective in the present research: The present research work aims at:

1. Development of **novel aptasensing techniques** for analysis of **mycotoxins in milk and alcoholic beverages (Gap 1.10.1)**.
2. Development of **label-free aptasensing platforms** for detection of **antibiotic residue** in milk (**Gap 1.10.2**).
3. Development of flow injection analysis (µFIA) mode aptasensors for on-line monitoring of the **antibiotic residue** in milk (**Gap 1.10.3**).

1.12 Thesis structure:

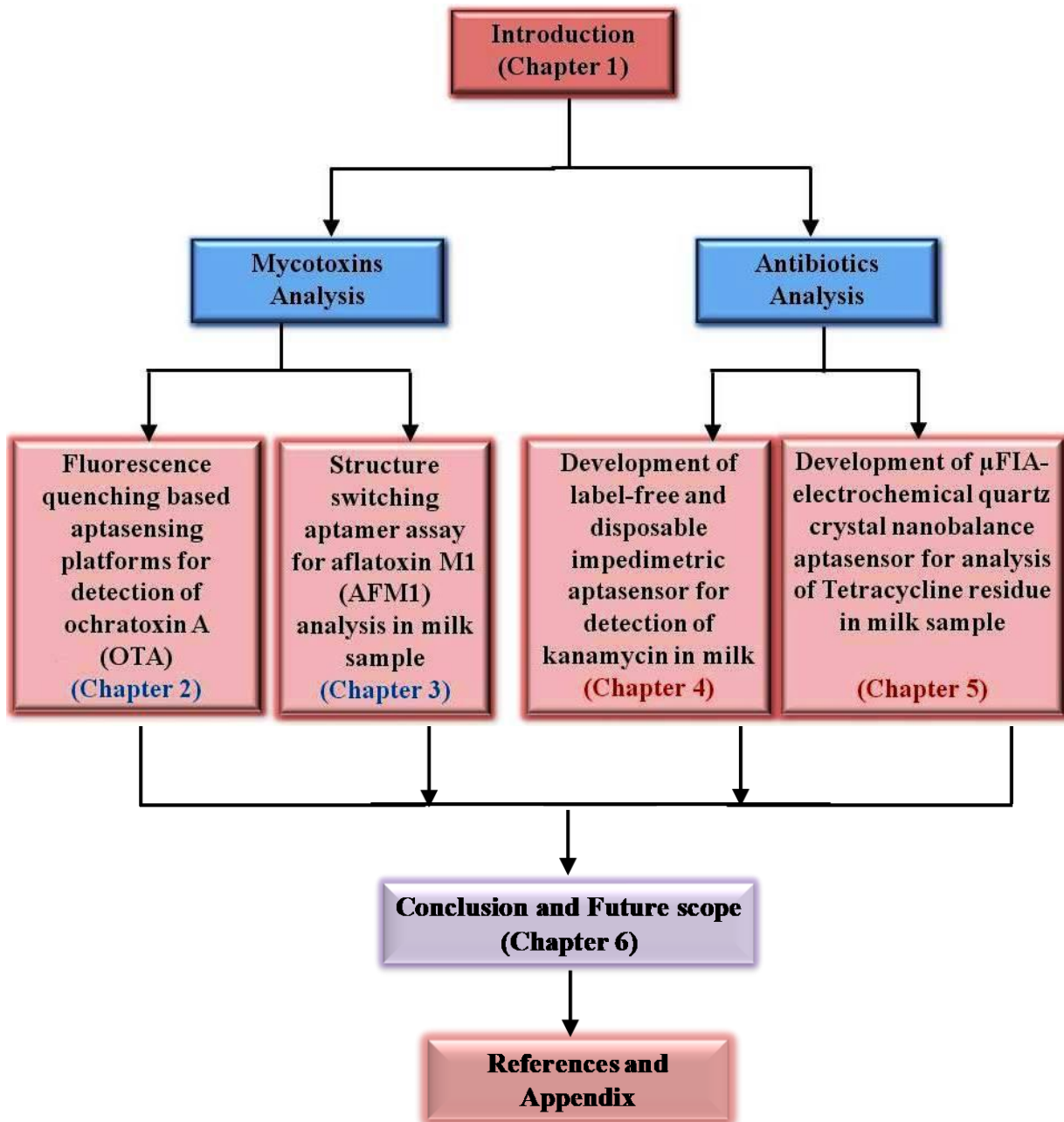


Figure 1.12: Flowchart detailing the different stages of the thesis works.

This thesis comprises six chapters and brief summary of each chapter has been described below:

1.12.1 Chapter 1: Introduction

The present chapter gives a description of biosensors, classification, recognition elements used in the biosensor (introduction to SELEX and MIPs preparation), transducers, various aspects of biosensors, analytical characteristics of biosensors, state of art of mycotoxins and antibiotics analysis and a brief introduction of nanotechnology in biosensor applications. The present chapter also discussed about the gaps in the existing research and objective of proposed doctoral thesis work and finally the thesis structure.

1.12.2 Chapter 2: Fluorescence quenching based aptasensing platforms for detection of ochratoxin A (OTA)

This chapter gives detailed account for the development of fluorescence quenching based aptamer assay platform for mycotoxin analysis in alcoholic beverages (wine and beer) using titanium dioxide nanoparticles (TiO₂-NPs) and fluorescent probe. This chapter is divided into two parts; in first methodology a fluorescence quenching based aptasensing platform has been developed using fluorescently labelled aptamer (labelled technique). In the second part, a non-labelled technique was developed using non-labelled ant-OTA aptamer, which based on the capitalization of the concept of aptamer assisted stability of TiO₂-NPs. The chapter include detailed account on characterization of aptamer and TiO₂-NPs interaction, optimization of experimental parameters such as aptamer preparation, concentration of aptamer and TiO₂-NPs, binding buffer, pH, ionic strength of buffer, assay volume, sample preparation and other parameters have been described in detail. Measurements of OTA spiked beer and wine samples and recoveries studies have also been discussed. The developed technique has potential for OTA detection in spiked samples (beer and wine). The results have been validated against HPLC method.

1.12.3 Chapter 3: Structure switching aptamer assay for aflatoxin M1 (AFM1) analysis in milk sample

This chapter gives a detailed account of selection of various aptamer sequences for biosensing application based on rational design of structure switching aptamer assay. A novel structure switching signalling aptamer assay was developed for using fluorescence quenching mechanism for AFM1 analysis in milk sample (no complex matrix matching). The specific

aptamer sequence to AFM1 provides the improved stability and sensitivity to the system. The developed user friendly methods provide broad detection range within a short analysis time compare to commercial ELISA kit technique for AFM1 analysis in milk samples.

1.12.4 Chapter 4: Development of label-free and disposable impedimetric aptasensor for detection of kanamycin in milk sample

This chapter start with the transition from optical to electrochemical transduction in present work. It describes the development of label-free and disposable impedimetric aptasensor for kanamycin detection in milk sample. For fabrication of aptasensor, the SPCEs were used as transducer surface. Aptasensor fabrication was characterized using surface morphology and electrochemical techniques. The aptasensor fabrication was carried out using immobilization of aptamer via diazonium coupling. The diazotized surface immobilization provides stability and no leakage of aptamer on storage. The developed aptasensor is rapid, stable and capable of detecting kanamycin directly in milk sample.

1.12.5 Chapter 5: Development of μ FIA-EQCN aptasensor for analysis of tetracycline residue in milk sample

The present chapter describe about the development of μ FIA-EQCN aptasensor for tetracycline analysis in milk samples. This chapter describes about the immobilization of aptamer on the crystal surface in a semi-automated mode and optimization of μ FIA system including matrix matching for milk sample analysis. The selection of aptamer sequence, surface modification, immobilization of aptamer on crystal surface, calculation of K_d value and characterization of aptasensor surface has been discussed in detail. For aptasensors development all the necessary experimental parameters such as aptamer concentration, selection of binding buffer, pH, ionic strength and flow rates were optimized and discussed. The practical utility of developed aptasensor was verified in milk. The obtained results indicate the applicability of developed platform in dairy industries. Additionally, the developed aptasensor is free from complex sample preparation steps. Aptasensor performance has been cross validated with commercial ELISA kit describing the precision and reproducibility of the μ FIA-EQCN aptasensor.

1.12.6 Brief summary of Chapter 6: Conclusion and future scope of work

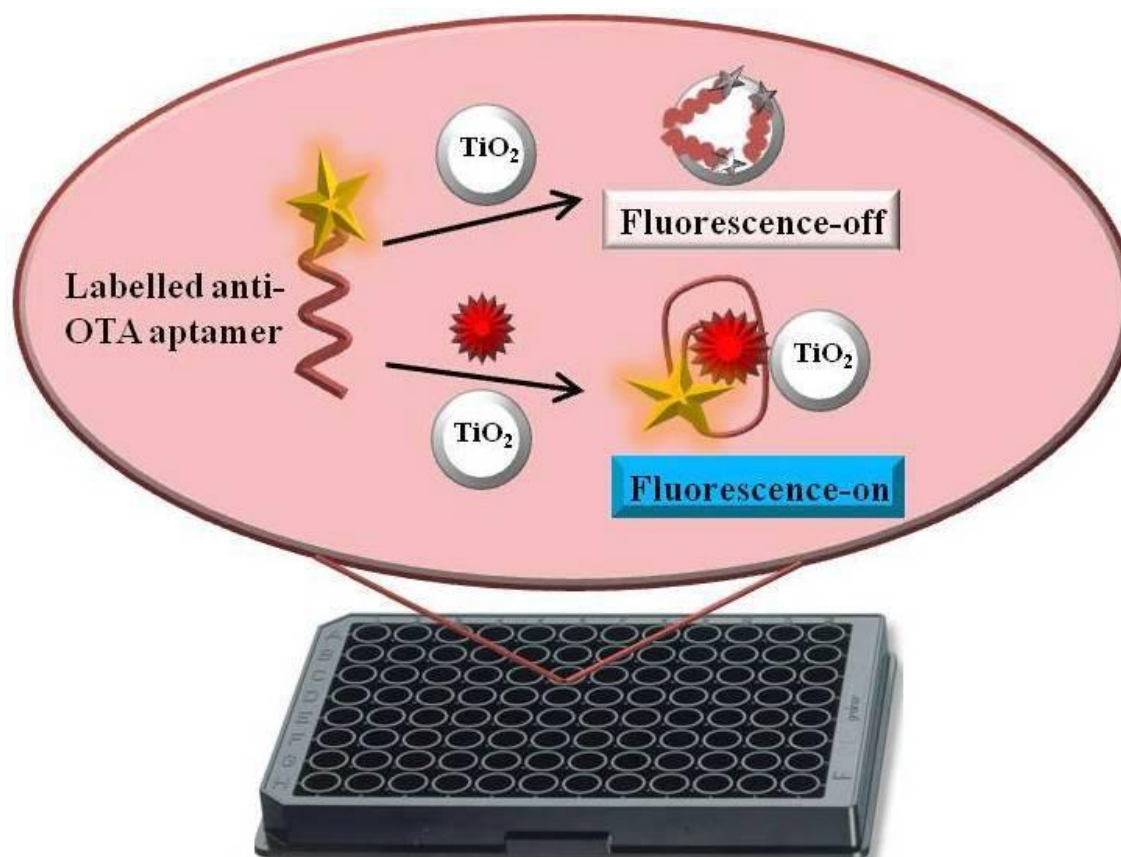
This chapter has drawn the conclusion on the basis of review of all the six chapters and proposed the future scope of work followed by references and appendix.

CHAPTER 2

Fluorescence quenching based aptasensing platforms for detection of ochratoxin A (OTA)

Novelty Statement:

- Structure switching aptaswitches utilizing titanium dioxide nanoparticles (TiO_2 -NPs) as fluorescence quencher were successfully demonstrated for OTA analysis.
- Design and evaluation of TiO_2 -NPs quenching based aptasensing platform against labelled and non-labelled anti-OTA aptamer sequence.
- Designed strategies exhibited the detection limit of 1.5 and 1.35 nM OTA in real sample.
- Applicability of developed platforms for detection of various analyte of interest.



Graphical abstract for chapter content

2.1 Background

The presence of toxins producing molds or fungal species in cereals used for the production of alcoholic beverages such as beer, wine and spirits (or distilled beverage) has attracted significant attention, as alcoholic beverages gathered a key role in the social life of many contemporary societies (Bellver Soto et al., 2014). Besides the known toxicological effects of alcohol (drowsiness, liver toxicity etc.), these beverages could be the potential source of several toxins transmitted from grains and cereals used in the brewing process. The cereals such as wheat, barley, maize, fruits, which are mainly used for the production of alcoholic beverages have found to be contaminated by various fungal toxins as ochratoxins (OAs), aflatoxins (AFs), fumonisins (Hwang et al., 2006; Mateo et al., 2007; Piacentini et al., 2015). Among all, ochratoxin A (OTA) is the most important and commonly found mycotoxin in several food commodities (Monaci and Palmisano, 2014) (Fig. 2.1). Presence of OTA has already been reported in the varieties of beverages such as beer, wine, grape juice and other foodstuffs such as wheat, barley, maize, coffee beans (Kumar et al., 2008). In recent years, the OTA contamination in alcoholic beverages has also been witnessed the increased risk to human health such as nephrotoxicity, hepatotoxicity, carcinogenicity, teratogenicity and immunotoxicity. The International Agency for Research on Cancer (IARC) has classified OTA as a possible human carcinogen in Group 2B (IARC Monograph, 1993). Owing to high toxicity and persistence of OTA, the regular monitoring of OTA contamination in these beverages is highly recommended.

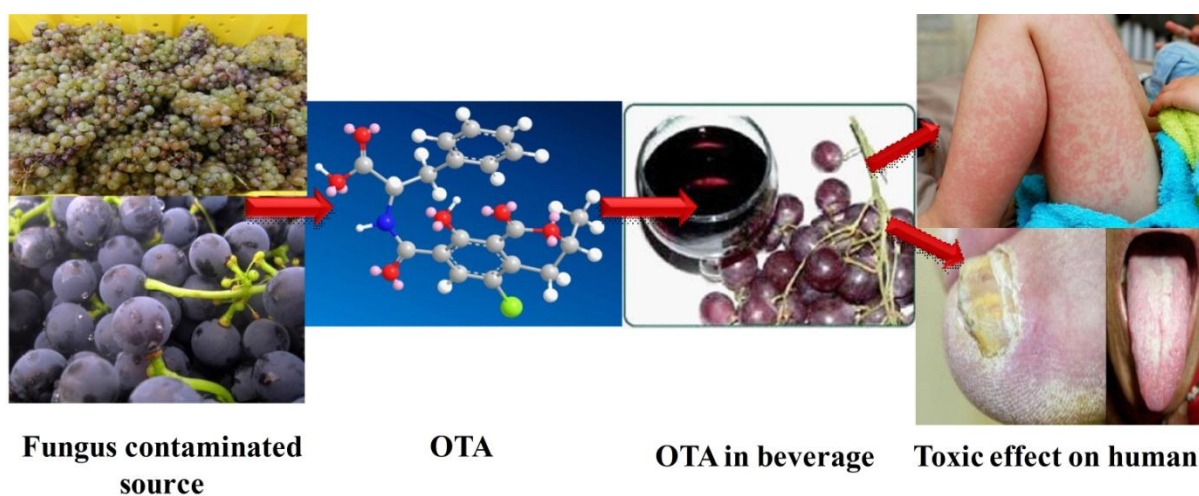


Figure 2.1: Sources and toxic effect of OTA on human health.

2.1.1 Regulatory legislation for OTA in alcoholic beverages (beer and wine)

Considering their toxicity and high consumption of contaminated beverages, the European Union (EU) Commission has established the legislation for the maximum residual levels (MRLs) of OTA in wine as $2 \mu\text{g kg}^{-1}$, whereas EU has not mandated any MRLs for OTA in beer (Duarte et al., 2010; EU Commission regulation, 2005). However, the MRLs of OTA in beer have been mandated by some countries based on the high consumption of beer, for example, the Netherlands ($0.3 \mu\text{g kg}^{-1}$), Finland ($0.5 \mu\text{g kg}^{-1}$) and Italy ($0.2 \mu\text{g kg}^{-1}$). In research studies, several authors have assumed a maximum tolerable limit of 0.2 ng mL^{-1} OTA in beer based on the various regulation of OTA levels in the source material used for the preparation of beer, specifically in malt (EU Commission regulation, 2002; Bellver Soto et al., 2014).

Table 2.1: Reported regulatory maximum residue limits for OTA in beer and wine (Anli and Alkis, 2010)

Sample	MRLs				
	EU	CODEX	Netherland	Finland	Italy
Beer	$3 \mu\text{g kg}^{-1}$ (malt)	$3 \mu\text{g kg}^{-1}$ (malt)	$0.3 \mu\text{g kg}^{-1}$	$0.5 \mu\text{g kg}^{-1}$	$0.2 \mu\text{g kg}^{-1}$
Wine	$2 \mu\text{g kg}^{-1}$	$2 \mu\text{g kg}^{-1}$	-	-	-

2.1.2 State of art for OTA detection in alcoholic beverages

Alcoholic beverages are considered as powerful and versatile symbolic tools to stipulate and manipulate the social world (Barefoot et al., 2002). Due to the severity of incidences around the world (especially in European continent), the OTA contamination in alcoholic beverages causes an alarming situation to the beverages industries (Murphy et al., 2006). Since the first report of OTA incident on endemic nephropathy and presence in wine (Zimmerli and Dick, 1995), various methods has been reported for OTA determination in alcoholic beverages. To ensure the safety and avoiding the risk of OTA contamination, it is of great interest to develop rapid and sensitive analytical methods for OTA monitoring in beer and wine. Traditionally, the OTA was mainly determined by an immunochemical method as ELISA

(Yu et al., 2005), however, the false positive performance and cross-reactivity limit their wider utility. In the last decade, several techniques has been identified and reported for OTA detection such as thin layer chromatography (TLC) (Songsermsakul et al., 2008), gas chromatography coupled with mass spectroscopy (GC-MS) (Sieber et al., 2009), high-performance liquid chromatography (HPLC) (Prelle et al., 2013), inductive coupled plasma and liquid chromatography coupled with MS (LC-MS) (Giesen et al., 2010; Al-TaHER et al., 2013). Although, the most commonly used technique is the LC coupled with fluorimetric and mass detectors for high sensitive detection signal ($\mu\text{g kg}^{-1}$). In chromatographic techniques, the sample preparation requires pre-treatment of a matrix, which implies the process of extraction, purification and concentration to reach the concentrations that have been established by legislation. Matrix matching is necessary to remove the components that are usually present in the real sample and can interfere, which decreases the sensitivity of the detection method. Isolation of OTA from the real matrix is usually performed by solid phase extraction using immobilized antibodies (immunoaffinity columns, IAC), C_{18} cartridges, molecularly imprinted polymer solid phase extraction columns (MIPSE) (Rhouati, et al., 2013a and 2013b). Above mentioned procedures encounter with several problems such as high cost, cross-reactivity, limited shelf life, sophisticated equipment, use large organic solvents, decrease in the column performance and carry-over effect (Prelle et al., 2013). Thus, the application of these methods for OTA analysis has remained as an analytical challenge.

2.1.3 Nanomaterial based aptasensing platform for OTA detection

In recent years, the development of nanomaterial integrated aptasensing platform has gathered promising attention. Since the discoveries of DNA-functionalized gold nanoparticles, many nanomaterials have been deployed in designing the DNA/ aptamer-based switchable nanosensors and aptaswitches (Alivisatos et al., 1996; Liu and Lu, 2005; Bamrungsap, et al., 2012). In the interim, the evolution of bifunctionally modified or conjugated nanomaterial has provided notable transaction of biochemistry or biology knowledge into bioanalytical applications (Cui et al., 2001; Liu et al., 2012). The intelligent use of nanomaterial led to the enhancement in performances with improved sensitivities and higher detection limits. Various nanomaterial-based aptasensing strategies have been reported for OTA detection (Table 2.2). Among them, the fluorescence signalling based aptaswitches received promising attention due to their simplicity, high-throughput and availability of

different methods replacing the conventional structure signalling aptaswitches (Lakowicz, 1999; Lv et al., 2014). In principle, the uniform colloidal dispersion of the nanoparticles exhibits well-defined surface activities, whereas the aggregation phenomenon results in negligible surface activities. The concept of ssDNA/ aptamer stabilization nanostructures with enhanced surface reactivity was reported (Zheng et al., 2003). Encouragingly, in the present thesis, the novel aptaswitches capitalized on the surface chemistry of TiO₂-NPs have been developed for determination of OTA in beer and wine. Recently reported aptaswitches for OTA determination in beer and wine has been tabulated in Table 2.3.

Table 2.2: Summary of reported aptasensors for OTA determination using optical transducers

S. No.	Materials	Methods	Linearity	LOD	Ref.
1.	Gold nanoparticles	Colorimetric	20-625 nM	20.0 nM	Yang et al., 2011
2.	Terbium (Tb ³⁺)	Fluorescence	0.1–1 ng/mL	20.0 pg/mL	Zhang et al., 2013
3.	Gold nanoparticles	Colorimetric	12 nM – 0.12 μM	22.0 nM	Luan et al., 2015
4.	Quantum-dots	Fluorescence	0-24.7 nM	4.7 nM	Wang et al., 2011

Table 2.3: Summary of reported aptaswitches for analysis of OTA in alcoholic beverages

S. No.	Materials	Methods	Linearity	LOD	Ref.
1.	Graphene oxide (a) Bare graphene (b) PVP coated graphene oxide	Fluorescence	2-35 μM 50-500 nM	1.9 μM 21.8 nM	Sheng et al., 2011
2.	Single walled carbon nanotubes (SWNTs)	Fluorescence	25-200 nM	24.1 nM	Guo et al., 2011
3.	Nanographite (a) Bare nanographite	Fluorescence	2-50 μM	2.0 μM	Wei et al.,

	(b) DNase catalyzed amplification		20-400 nM	20.0 nM	2015
4.	Single-walled carbon nanohorn (SWCNHs)	Fluorescence	20-500 nM	17.2 nM	Lv et al., 2016
5.	Ferrite upconversion nanoparticles	Luminescence resonance energy transfer (LRET)	2.48 to 619 nM	2.48 nM	Dai et al., 2017

2.1.4 Objective

The objective of present work was to develop the fluorescence quenching based aptasensing platforms for detection of ochratoxin A (OTA) in alcoholic beverages (beer and wine).

2.1.5 Methodology

In this part of the work, two different strategies were designed for the development of fluorescence quenching based aptaswitches utilizing TiO₂-NPs for OTA detection.

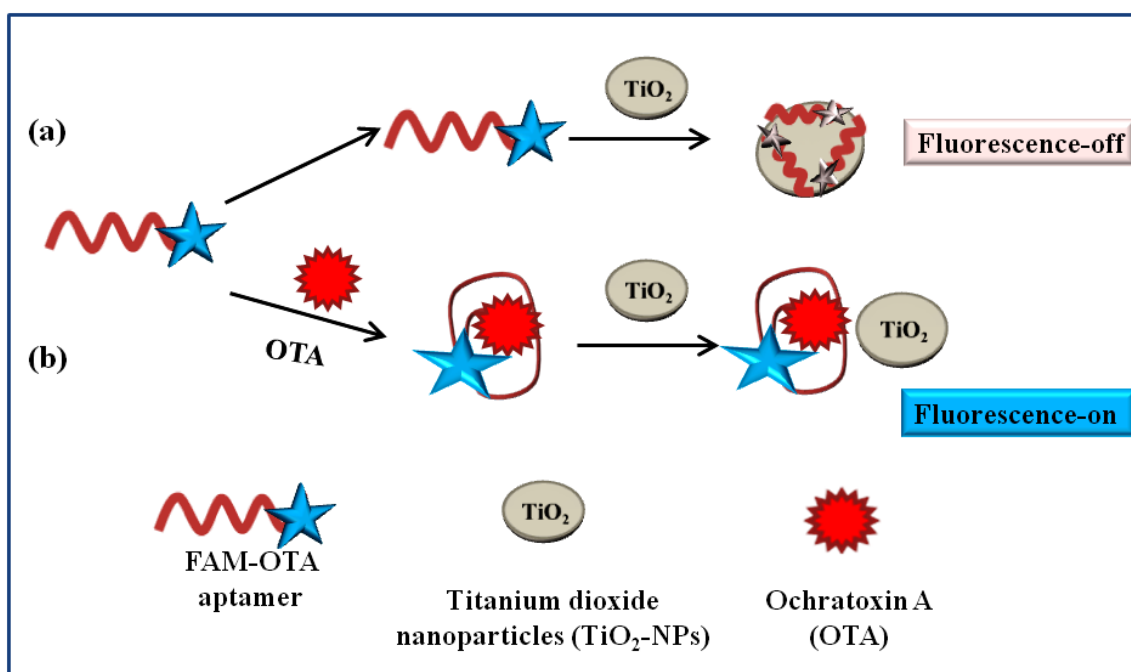
2.1.5.1 Labelled technique (OTA detection using fluorescently labelled aptamer)

In this strategy, a fluorescence quenching based aptaswitches utilizing the fluorescein labelled anti-OTA aptamer (FAM-OTA aptamer) and TiO₂-NPs was developed for OTA detection (Scheme-1). The configuration chosen for this experiment was based on the universal capability of aptamer sequence to form an antiparallel-G-quadruplex aptamer-target structural conformation on target recognition. In the absence of OTA, the interaction of FAM-OTA aptamer and TiO₂-NPs results in the fluorescence quenching of FAM-OTA aptamer fluorescence. The quenching mechanism was attributed to the large band gap semiconductor behaviour of TiO₂-NPs and the electrostatic interaction involving Ti-O bond between TiO₂-NPs and FAM-OTA aptamer molecules. This results in the fluorescence quenching through the acceptance of electrons from excited FAM molecules (Moser and Graetzel, 1984; Wang et al., 1998; Wu et al., 2007). In the presence of OTA, the OTA induced conformational change in the aptamer structure led to the formation of anti-OTA-G-quadruplex aptamer complex. These conformational changes causes decrease in interaction between TiO₂-NPs and FAM-OTA aptamer, which weakens the quenching ability and

quench fluorescence recovered. The recovered fluorescence corresponds to the concentration of OTA present. Quenching efficiency (Q %) was calculated using the following equation:

$$Q (\%) = [1 - F_0/F] \quad (2.1)$$

where, Q (%) is the quenching percentage, F_0 and F were the fluorescence intensity in the absence and presence of OTA, respectively (Balcioglu et al., 2014).

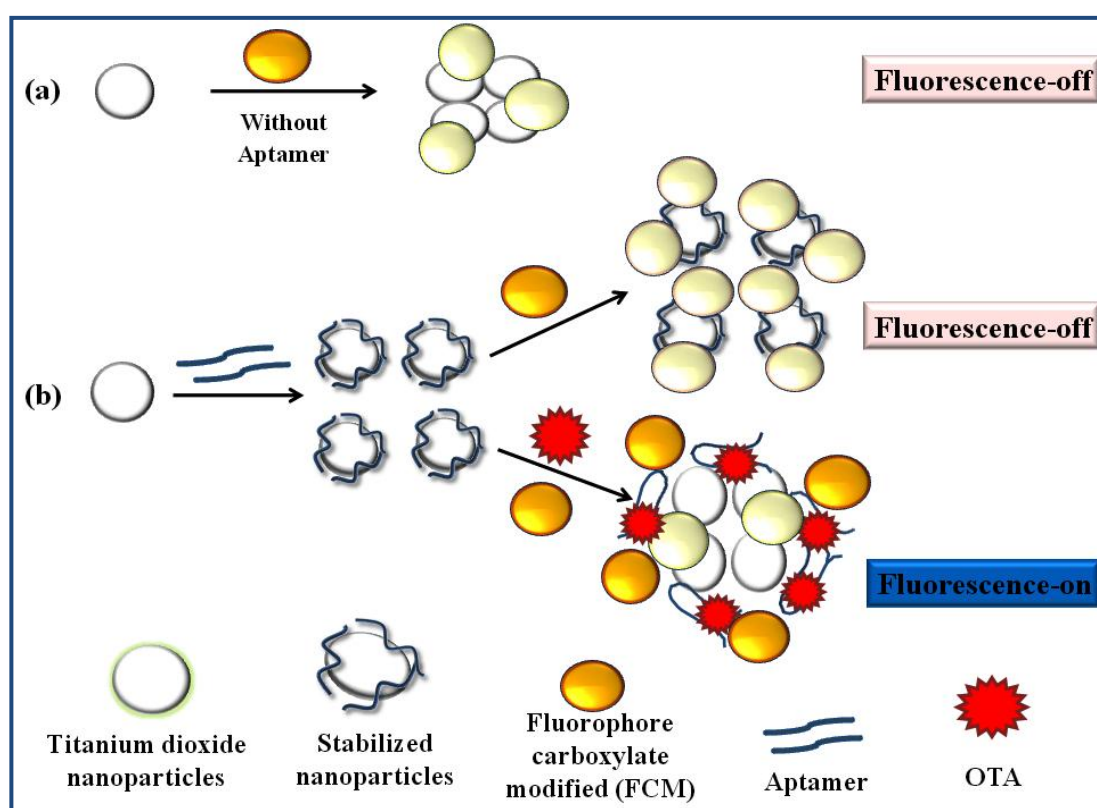


Scheme 1: Principle of TiO₂-NPs fluorescence quenching based aptaswitch platform for OTA detection (a) in the absence of OTA, adsorption of FAM-OTA aptamer on TiO₂-NPs surface led to fluorescence quenching; (b) in the presence of OTA, the anti-parallel G-quadruplex structure form and fluorescence recovered.

2.1.5.2 Non-labelled technique (OTA detection using non-fluorescent labelled aptamer)

The strategy designed for the development of an aptaswitch that capitalizes on the surface chemistry of TiO₂-NPs, which quench the fluorescence of fluorescent particles and eliminate the need of fluorophore conjugated aptamer (Scheme-2). In this strategy, fluorescence quenching potential of bare TiO₂-NPs and aptamer stabilized TiO₂-NPs was evaluated against the fluorescence emission intensity of fluorophore carboxylate modified nanoparticles (FCM). The high fluorescence intensity of FCM nanoparticles is quenched by TiO₂-NPs as depicted (Scheme 2a), which is due to the electrostatic interaction of Ti-O bond between

TiO₂-NPs and fluorescent probe (FCM). This results in fluorescence quenching due to acceptance of electrons from FCM probe (Wang et al., 1998; Wu et al., 2007). Adsorption of anti-OTA aptamer on TiO₂-NPs surface stabilizes and uniformly disperses the TiO₂-NPs. The stabilized TiO₂-NPs showed an increase in the quenching efficiency due to the enhancement in surface activity (Scheme 2b). On addition of OTA, the OTA induced conformational change in aptamer assembly resulting in desorption of the OTA-aptamer complex from the TiO₂-NPs surface. This causes the subsequent recovery of quenched fluorescence, which corresponds to the concentration of OTA present.



Scheme 2: Structure switching signalling aptaswitch based on fluorescence quenching principle for detection of OTA (a) bare TiO₂-NPs quench the fluorescence of FCM particles, (b) in the absence of OTA, the aptamer stabilized TiO₂-NPs showed increased quenching and in the presence of OTA, increased fluorescence due to formation of anti-OTA-G-quadruplex aptamer complex.

2.2. Experimental

2.2.1 Biochemicals and chemicals

The aptamer sequence highly specific to OTA, which form the anti-OTA-G-quadruplex structure upon OTA binding was selected as reported in literature (Cruz-Aguado and Pennar, 2008). The fluorescein labelled anti-OTA aptamer at 3' end (3'FAM-OTA aptamer) with 36 base sequences was synthesized and purified by Microsynth (Switzerland). The non-labelled anti-OTA aptamer was synthesized and purified by Eurogentec (France). Two different forms of anti-OTA aptamer used were as follows:

3'FAM-OTA aptamer (36 base sequences): Fluorescein (FAM) labelled aptamer sequence

5'-GATCGGGTGTGGGTGGCGTAAAGGGAGCATCGGACA-FAM-3'

anti-OTA aptamer (36 base sequences): Non-labelled aptamer sequence

5'-GATCGGGTGTGGGTGGCGTAAAGGGAGCATCGGACA-3'

TiO₂-NPs with a size of approx. 25 nm were synthesized and received as prepared material from PROMES Laboratory, UPVD-Perpignan, France. Fluorophore carboxylate modified particles (FCM) 0.1 μm (excitation 350 nm and emission 440 nm) were procured from Life Technologies (USA). HEPES sodium salt was purchased from Fisher Scientific (New Jersey, USA). All other chemical sodium phosphate dibasic (Na₂HPO₄), potassium phosphate monobasic (KH₂PO₄), calcium chloride (CaCl₂), potassium chloride (KCl), magnesium chloride (MgCl₂) and sodium chloride (NaCl) of analytical grade were procured from Sigma-Aldrich (St. Quentin Fallavier Cedex, France). OTA, derived from (*Aspergillus ochraceus*) was purchased from Sigma Aldrich (France). Ochratoxin B (OTB), derived from (*Aspergillus ochraceus*) was procured from Santa Cruz Biotechnology (Heidelberg, Germany). For cross-reactivity studies, *N*-acetyl-L-phenylalanine (NAP) and warfarin was obtained from Sigma-Aldrich (USA). Deionized Milli-Q water (Millipore, Bedford, MA, USA) was used for preparation of reagents throughout the experiments. Beer (brand name Heineken from Netherlands) and wine (brand name Blanc from Bordeaux, France) samples were purchased from local market of Perpignan, France.

2.2.2 Instrumentation

A customized fluorescence imaging system (built in-house) consisting of ultraviolet light source coupled with a light excluding compartment, a lens, digital camera and computer was used for elucidation of principle reaction (Bueno et al., 2016). Each individual image was decomposed into its red, green and blue component (RGB components) and analyzed using a designed MET-Lab interface on computer (Fig. 2.2). The fluorimetric measurements (excitation 355 nm; emission 460 nm) were carried out using Fluoroskan Ascent FL 2.6 (Thermo Scientific-Finland) equipped with Ascent software version 2.6. The UV-visible spectral measurements were carried out on UV- spectrophotometer (UV-1800, USA) equipped with TCC controller (TCC 240 A) to measure the surface adsorption characteristics of aptamer-TiO₂ complex. All fluorimetric measurements were performed in standard 96 black microwell plates obtained from Thermo Fisher Scientific (Roskilde, Denmark). The aptamer sequences were pre-treated in PCR thermocycler (Eppendorf, Le Pecq, France) before use (to open their conformation for efficient binding). The surface morphology of TiO₂-NPs at different stages was characterized using scanning electron microscope (SEM XL 30 FEI/Philips, Philips Electronics Co., Netherlands).

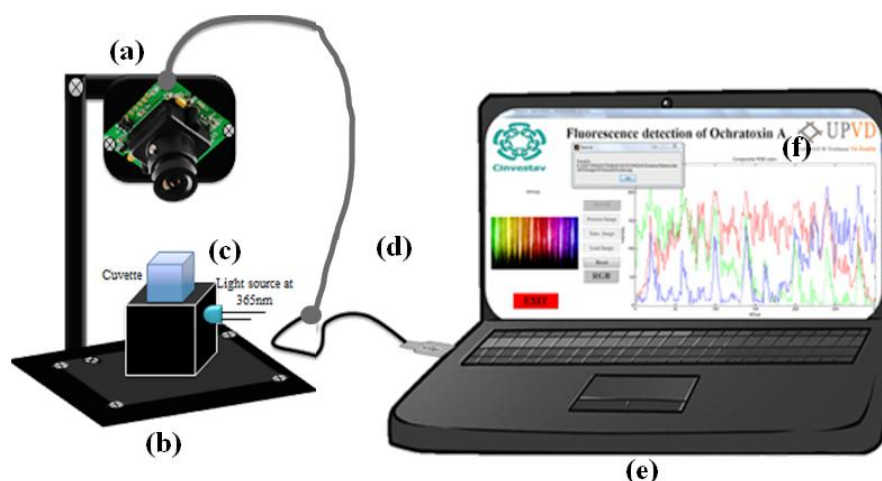


Figure 2.2: A portable and customized fluorescence imaging system (a) camera; (b) stage; (c) cuvette; (d) wire interface connection; (e) computer; (f) RGB component analysis.

For cross validation, the HPLC system Elite Lachrom L-2485 system consisted on a Merck (Merck GmbH, Germany), Hitachi pump L-7110 with a manual injector and a VWR Hitachi scanning fluorescence detector integrated with Borwin V 1.21 software version was used to

control the chromatograph and signal processing. The chromatographic separation was performed on a stainless steel Phenomenex 100, C₁₈ reversed-phase column (250 mm × 4.6 mm, 5 μm particle sizes) connected to a guard column, which protects all non-core shell and ≥ 3 μm particle size columns with 2-8 mm ID. The mixture of acetonitrile/water/acetic acid (48:51:1 v/v/v), at a flow-rate of 1.0 ml min⁻¹ was used as mobile phase and always degassed before use. The HPLC detector has λ_{ex} 330 nm and λ_{em} 460 nm. Sample injection was performed using 200 μL for standard/eluted samples. Each tested samples was measured in triplicate and peak deviation was calculated.

2.2.3 Solution preparation

2.2.3.1 Preparation of buffer

The binding buffers were prepared as follows: an appropriated amount of HEPES buffer containing 30 mM CaCl₂, 90 mM NaCl, 1.35 mM KCl and 5 mM MgCl₂ was dissolved in deionized Milli-Q water to prepare HEPES binding buffer (HBB) (25 mM, pH 7.4). The phosphate binding buffer (PBB) was prepared by dissolving an appropriate amount of Na₂HPO₄, KH₂PO₄, containing 5 mM MgCl₂, 1.35 mM KCl and 60 mM NaCl in deionized Milli-Q to prepare PBB (10 mM, pH 7.4). The pH of binding buffers was adjusted to 6.8-8.2 (until not optimized). All buffer solutions were stored at 4 °C when not in use.

2.2.3.2 Preparation of TiO₂-NPs and probe dilutions

To investigate the quenching efficiency of TiO₂-NPs, a known amount of TiO₂-NPs was dissolved in binding buffers (HBB and PBB) and further diluted in the range 2.5-1000 μg mL⁻¹. Similarly, the stock solution of FCM probe (0.2 mg mL⁻¹) was diluted in binding buffers to obtain the desired working range.

2.2.3.3 Preparation of OTA aptamer solutions

The stock solution of FAM-labelled anti-OTA aptamer (100 μM) and non-labelled anti-OTA (100 μM) aptamer were prepared in sterilized deionized Milli-Q water. The stock solution was further diluted in the range 5 nM to 5 μM (FAM-OTA aptamer) and 10 to 750 nM (non-labelled OTA-aptamer) in HBB. Before each experimentation, the aptamer sequences were pre-treated in thermocycler (Eppendorf, Le Pecq, France) with the following temperature

cycle: heated at 85 °C for 5 min to initial denaturation followed by a structure maintain step at 4 °C for 5 min.

2.2.3.4 Preparation of OTA and interferences standard solutions

For preparation of standards, OTA stock solution was prepared by dissolving 1 mg mL⁻¹ OTA powder in methanol and stored at -20 °C, when not in use. Subsequently, the stock solution was diluted in the range 17 nM to 20 µM in HBB (covering both strategies) before use. Similarly, for specificity studies of aptamer, OTB, warfarin and NAP standard solutions were prepared and diluted in binding buffer. All the working solutions were prepared freshly before use and stored at 4 °C when not in use.

2.2.3.5 Preparation of spiked sample for OTA analysis

To verify the performance of developed aptamer assays, the experiments were performed in spiked beer and wine samples. Matrix treatment was done because the presence of fluorescent compounds in beer and wine samples may lead to the false signal response.

2.2.3.5.1 OTA analysis using spiked beer samples

Beer samples were prepared as described elsewhere ([Visconti et al., 2000](#)) with our optimized protocol. In brief, the known concentration of OTA was spiked in the beer sample and mixture was degassed for 30 min and pH was adjusted to 7.4. The samples were cooled at 4 °C for 30 min to prevent frothing. The OTA spiked samples were filtered through 0.45 µm Minisart non-pyrogenic filters (Sartorius Stedim Biotech, USA). Subsequent dilutions were made with unspiked beer sample to obtain the different concentration of OTA i.e. 0.0031, 0.25 and 1.0 µM (Scheme-1) and 0.017, 0.125 and 1.0 µM (Scheme-2).

2.2.3.5.2 OTA analysis using spiked wine samples

For matrix matching, the wine sample was mixed with the binding buffer and methanol in 1:4:1 v/v ratio (wine:HBB:MeOH). The mixture was further degassed for 45 min, centrifuged at 10000 rpm (10 min) and filtered by using microfilters (0.45 µm). Then known quantities of 10 µM OTA was added to the prepared mixture (wine:HBB:MeOH) to prepare the different concentration of OTA in the range as described under beer samples preparation.

2.2.4 Quenching measurement using TiO₂-NPs

2.2.4.1 Quenching measurements against FAM-OTA aptamer

Prior to experiment, aptamer sequence was pre-treated as described under section (2.2.3.3). FAM-OTA aptamer and TiO₂-NPs were added in the binding buffer at a fixed concentration (total assay volume 150 μL , once optimized) and incubated at RT for 1 min. To study fluorescence quenching, the fluorescence measurements (λ_{ex} 485 nm; λ_{em} 538 nm) were performed continuously for 1 h at an interval of 5 min. Similarly, the control measurements were performed without addition of TiO₂-NPs keeping the assay volume constant (150 μL).

2.2.4.2 Quenching measurements against fluorescent probe (FCM)

The fluorescence quenching potential of TiO₂-NPs was evaluated before and after stabilization with target specific aptamer. TiO₂-NPs (2.5-1000 $\mu\text{g mL}^{-1}$) and FCM probe (10 μL of 100 $\mu\text{g mL}^{-1}$) were properly mixed with binding buffer (HBB) to make up volume 200 μL . The quenching measurements were performed at excitation (λ_{ex} 355 nm) and emission (λ_{em} 460 nm). Secondly, 10 μL of aptamer (250 nM) and 10 μL of TiO₂-NPs (at optimized conc. 300 $\mu\text{g mL}^{-1}$) were mixed with HBB and incubated for 1 h. Then, the FCM probe (10 μL of 100 $\mu\text{g mL}^{-1}$) was added to aptamer stabilized TiO₂-NPs and measurements were carried out immediately. For control, the measurements were performed with FCM keeping the concentration (100 $\mu\text{g mL}^{-1}$) other conditions same.

2.2.5 OTA detection based on fluorescence quenching

2.2.5.1 Labelled technique (OTA detection using fluorescently labelled aptamer)

For the quantification of OTA, FAM-OTA aptamer (optimized concentration i.e. 2.0 μM) was allowed to mix with the different concentrations of OTA (1.5 nM to 20 μM) and incubated. Then, 10 μL TiO₂-NPs (150 $\mu\text{g mL}^{-1}$) was added in microwell plate, mixed properly and incubated for 1 min at RT. The fluorescent measurements were carried out using Fluoroskan Ascent FL 2.6. Similarly, the control measurements were achieved without the addition of OTA in binding buffer under same experimental conditions.

2.2.5.2 Non-labelled technique (OTA detection using non-fluorescent labelled aptamer)

Different concentration of OTA (17 nM to 5.0 μM) were added and mixed with anti-OTA aptamer stabilized TiO_2 -NPs and incubated for 1 h. Finally, 10 μL of FCM (100 $\mu\text{g mL}^{-1}$) was added in each microwell and mixed properly. Measurements were carried out immediately after addition of FCM probe on Fluoroskan Ascent FL 2.6 plate reader at excitation (λ_{ex} 355 nm) and emission (λ_{em} 460 nm). Similarly, control measurements were performed without the addition of OTA and keeping other experimental conditions same.

2.3 Result and discussions

2.3.1 Labelled technique (OTA detection using fluorescently labelled aptamer)

2.3.1.1 UV-Vis spectroscopic analysis

The evidences of structure switching and interaction between aptamer and TiO_2 -NPs were characterized using UV-Vis measurements (Fig. 2.3). OTA showed the characteristics UV absorption at 355 nm (spectrum b). The characteristics absorption maximum (λ_{max}) of FAM-OTA aptamer was observed at 255 nm (spectrum c). The obtained results showed that the TiO_2 -NPs do not exhibit UV absorption at 255 nm (spectrum a). On addition of TiO_2 -NPs, the peak intensity of FAM-OTA aptamer UV absorption maxima significantly enhance without change in peak position (curve f) at 255 nm. These results emphasize the typical characteristic features of FAM-OTA aptamer- TiO_2 -NPs adsorption complex and electrostatic interaction (Kathiravan and Renganathan, 2009). On addition of OTA, hybridization of FAM-OTA aptamer-OTA complex formation results in the appearance of new absorption peak at 252 nm with decrease in peak intensity (spectrum e), indicating the target induced conformational changes in aptamer structure, which results in desorption of aptamer from TiO_2 -NPs surface. The UV spectrum of aptamer-OTA complex in the presence and absence of TiO_2 -NPs showed absorption maximum at 252 nm as shown in Fig. 2.3 (spectrum d and e). These results strongly suggested that the fluorescence recovery response in aptamer assay was due to the formation of target-aptamer quadruplex, resulting increase in distance between FAM group and TiO_2 -NPs. UV results have been summarized in Table 2.4.

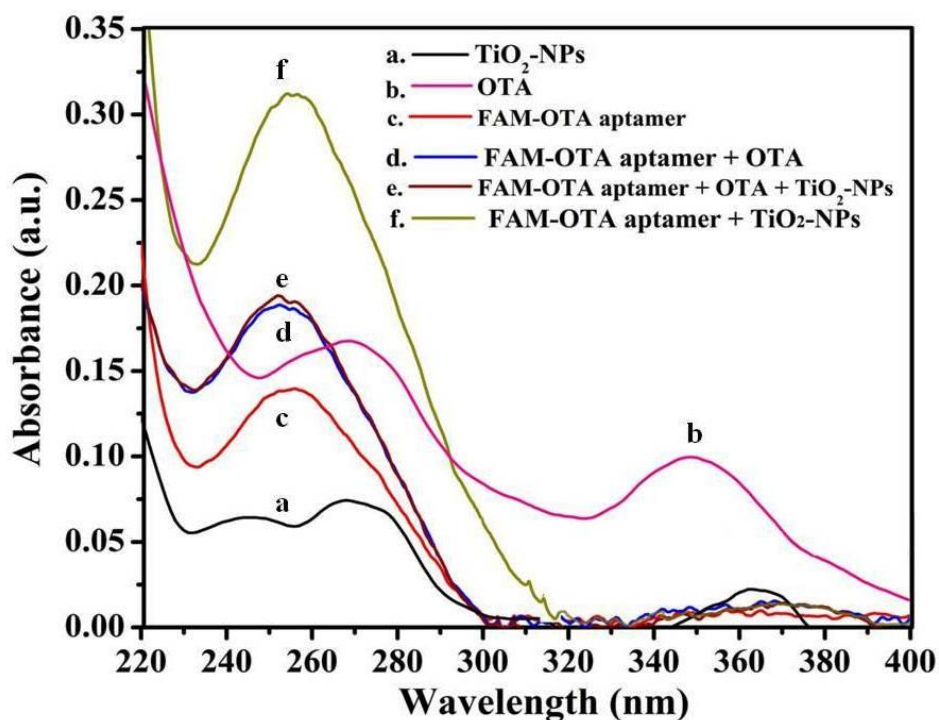


Figure 2.3: UV-Vis absorption analysis of aptamer-TiO₂-NPs complex for structure switching elucidation in HBB (pH 7.4).

Table 2.4: UV-Vis absorption results of structure switching aptamer assay in HBB (pH 7.4)

Spectrum	λ_{\max} (nm)	Description	Absorbance (a.u)
a.	255	TiO ₂ -NPs	-
b.	355	OTA	0.104
c.	255	FAM-OTA aptamer	0.139
d.	252	FAM-OTA aptamer + OTA (in absence of TiO ₂ -NPs)	0.186
e.	252	FAM-OTA aptamer + OTA+ (in presence of TiO ₂ -NPs)	0.193
f.	255	FAM-OTA aptamer + TiO ₂ -NPs	0.312

2.3.1.2 Fluorescence imaging study

The fluorescently labelled (FAM-OTA) aptamer exhibits strong fluorescence due to the presence of FAM molecules as depicted in Fig. 2.4a. Upon addition of TiO₂-NPs, the TiO₂-

NPs quenched the fluorescence of FAM-labelled OTA-aptamer, which was characterized by change in fluorescence intensity (green to blue) (Fig. 2.4b). On addition of OTA, the formation of FAM-OTA aptamer and OTA duplex results in the decrease in fluorescence intensity (blue intensity decrease), which is a strong evidence of target triggered formation of aptamer-target complex (Fig. 2.4c). The target induced conformational change resists the adsorption of aptamer on TiO₂-NPs surface and fluorescence recovered. The recorded fluorescence images were further decomposed into individual RGB components and analyzed using in house developed fluorescence imaging system integrated with MATLAB interface. The results have been summarized in Table 2.5.

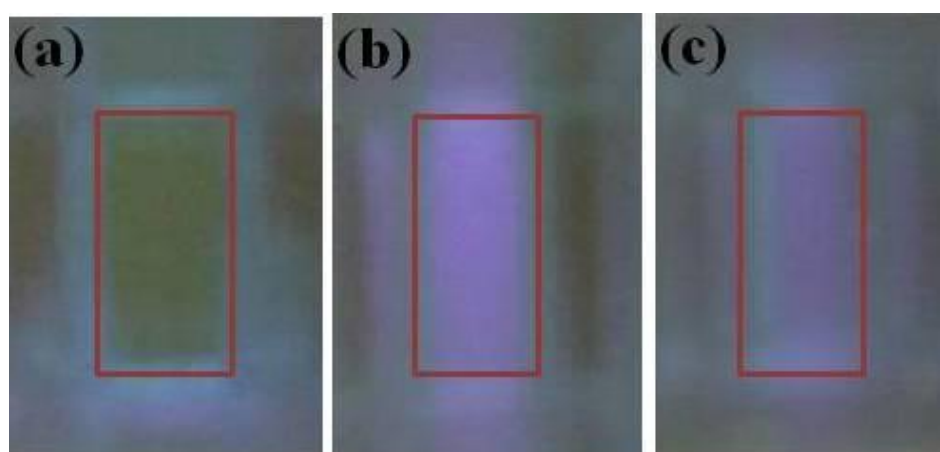


Figure 2.4: Fluorescence imaging of (a) FAM-OTA aptamer; (b) FAM-OTA aptamer+ TiO₂-NPs; (c) FAM-OTA+ OTA+ TiO₂-NPs in HBB (pH 7.4).

Table 2.5: Fluorescence magnitude value of blue components

Sample	Description	Blue component value
a.	FAM-OTA aptamer	22
b.	FAM-OTA aptamer + TiO ₂ -NPs	96
c.	FAM-OTA aptamer + OTA+ TiO ₂ -NPs	65

2.3.1.3 Optimization of experimental variables

Experimental variables such as aptamer concentration and TiO₂-NPs, buffer, pH, ionic strength, which could artifacts the performance of aptasensing platform were carefully investigated and optimized.

2.3.1.3.1 FAM-OTA aptamer concentration

It is important to identify the concentration of fluorophore labelled anti-OTA aptamer (FAM-OTA aptamer) for construction of quenching based aptasensing platform. The fluorescence intensity of FAM-OTA aptamer at various concentrations was studied (Fig. 2.5). It was found that the FAM-OTA aptamer at 2.0 μM exhibits enough fluorescence (λ_{ex} 485 nm; λ_{em} 538 nm) to further investigate the quenching potential of TiO₂-NPs.

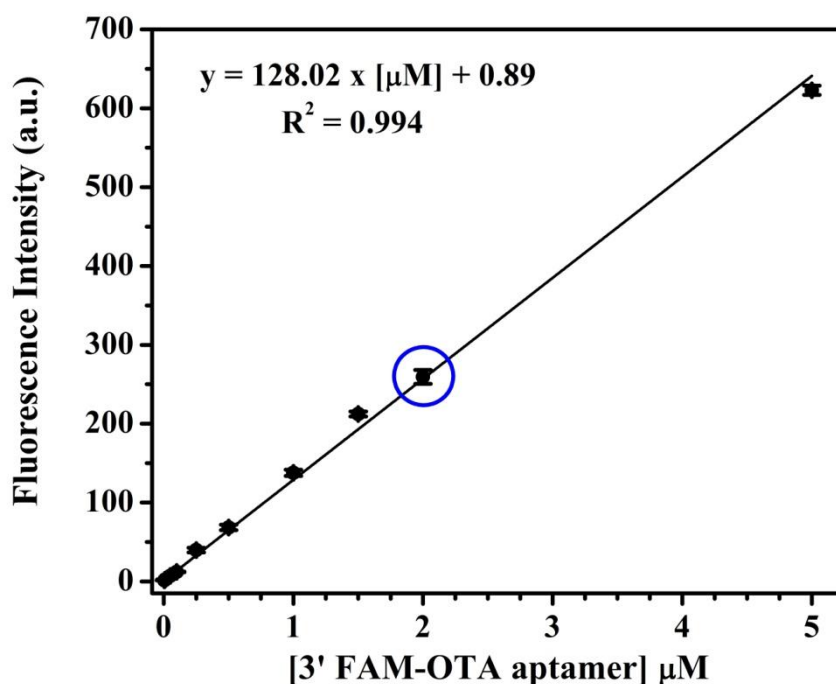


Figure 2.5: Fluorescence response of FAM-OTA aptamer with increasing concentration from 0.062-5.0 μM (optimized concentration for further experimentation encircled with blue).

2.3.1.3.2 TiO₂-NPs concentration

Different concentration of TiO₂-NPs (2.5-300 $\mu\text{g mL}^{-1}$) was evaluated against fixed concentration of FAM-OTA aptamer (2.0 μM). The fluorescence intensity of FAM-OTA aptamer gradually decreased with the increasing concentration of TiO₂-NPs ranging from 2.5-

150 $\mu\text{g mL}^{-1}$ in HBB (pH 7.4) (Fig. 2.6). No decrease in fluorescence intensity was observed with further increase in TiO_2 -NPs concentration, which confirms that the maximum quenching and 150 $\mu\text{g mL}^{-1}$ TiO_2 -NPs and used in further experimentations.

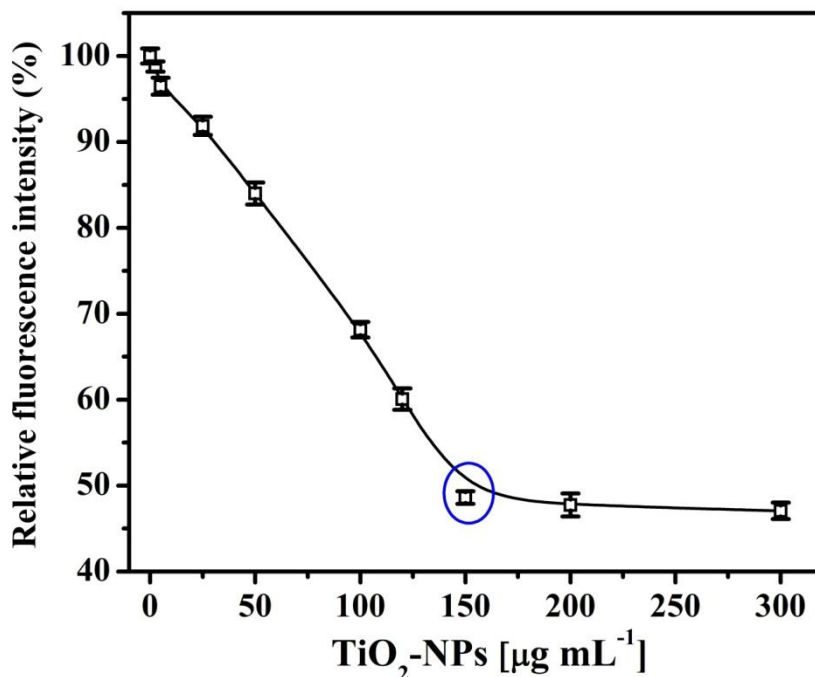


Figure 2.6: Quenching performance of TiO_2 -NPs (2.5-300 $\mu\text{g mL}^{-1}$) on fluorescence intensity of FAM-OTA aptamer (2.0 μM) in HBB (pH 7.4) (n=3).

2.3.1.3.3 Selection of buffer, pH and ionic strength

Non-specific adsorption of ionic species (buffer ions) on the surface of TiO_2 -NPs might hinder the adsorption of aptamer molecules, which could be responsible for decreasing quenching performance (Nelson et al., 2000; Zhang et al., 2014). Therefore, the quenching performance of TiO_2 -NPs was evaluated in two different buffers i.e. HBB and PBB. At optimized concentration of FAM-OTA aptamer (2.0 μM) and TiO_2 -NPs (150 $\mu\text{g mL}^{-1}$); maximum quenching by TiO_2 -NPs was obtained in the HBB (Fig. 2.7a). The pH of buffer has significant on generation of surface charge. The change in pH of buffer might leads to the variation in surface charge of TiO_2 -NPs, which could cause the aggregation or may render the electrostatic interaction of TiO_2 -NPs with FAM-OTA aptamer, resulting decrease in fluorescence quenching (Amano et al., 2010; Zhang et al., 2014). Maximum quenching was obtained in HBB at pH 7.4 (Fig. 2.7b).

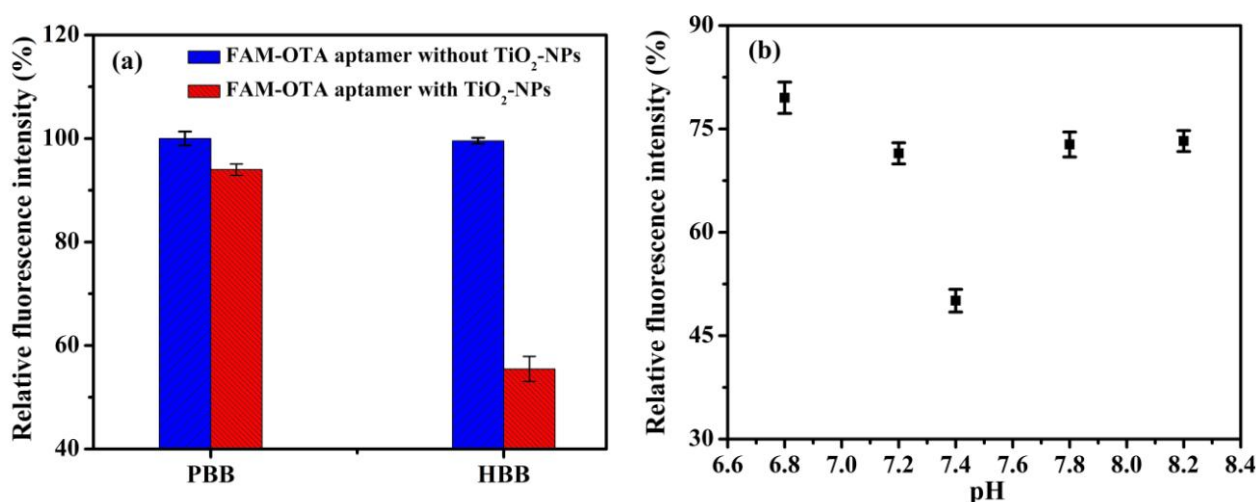


Figure 2.7: (a) Effect of HBB and PBB on quenching efficiency of TiO₂-NPs (150 $\mu\text{g mL}^{-1}$).

(b) Effect of pH (6.8-8.2) of HBB on quenching performance of TiO₂-NPs.

The optimal concentration of monovalent or divalent ions is highly important to obtain the maximum binding affinity of aptamer and quenching of TiO₂-NPs. The maximum binding efficacy of aptamer was evaluated against different salt concentrations present in the buffer. It is evident from the obtained (Fig. 2.8a) that the maximum response was obtained at 90 mM Na⁺ salt. The fluorescence intensity increased with further increase in Na⁺ concentration, which is a strong indication that the non-specific adsorption of Na⁺ on TiO₂-NPs surface decreasing the fluorescence quenching. The effect of divalent metal ions, which are important to maximize the binding affinity of aptamer and acted as ionic bridge enhances the electrostatic interaction in between aptamer and TiO₂-NPs were also evaluated (Sheng et al., 2011). The Mg²⁺ and Ca²⁺ salts showed the maximum response at 5 mM Mg²⁺ and 30 mM Ca²⁺ salt concentration (Fig. 2.8b and 2.8c). To avoid the involvement of excess salt concentration, the higher salt concentration has not been tested because these concentrations are optimal for binding interaction (Cruz-Aguado and Penner, 2008).

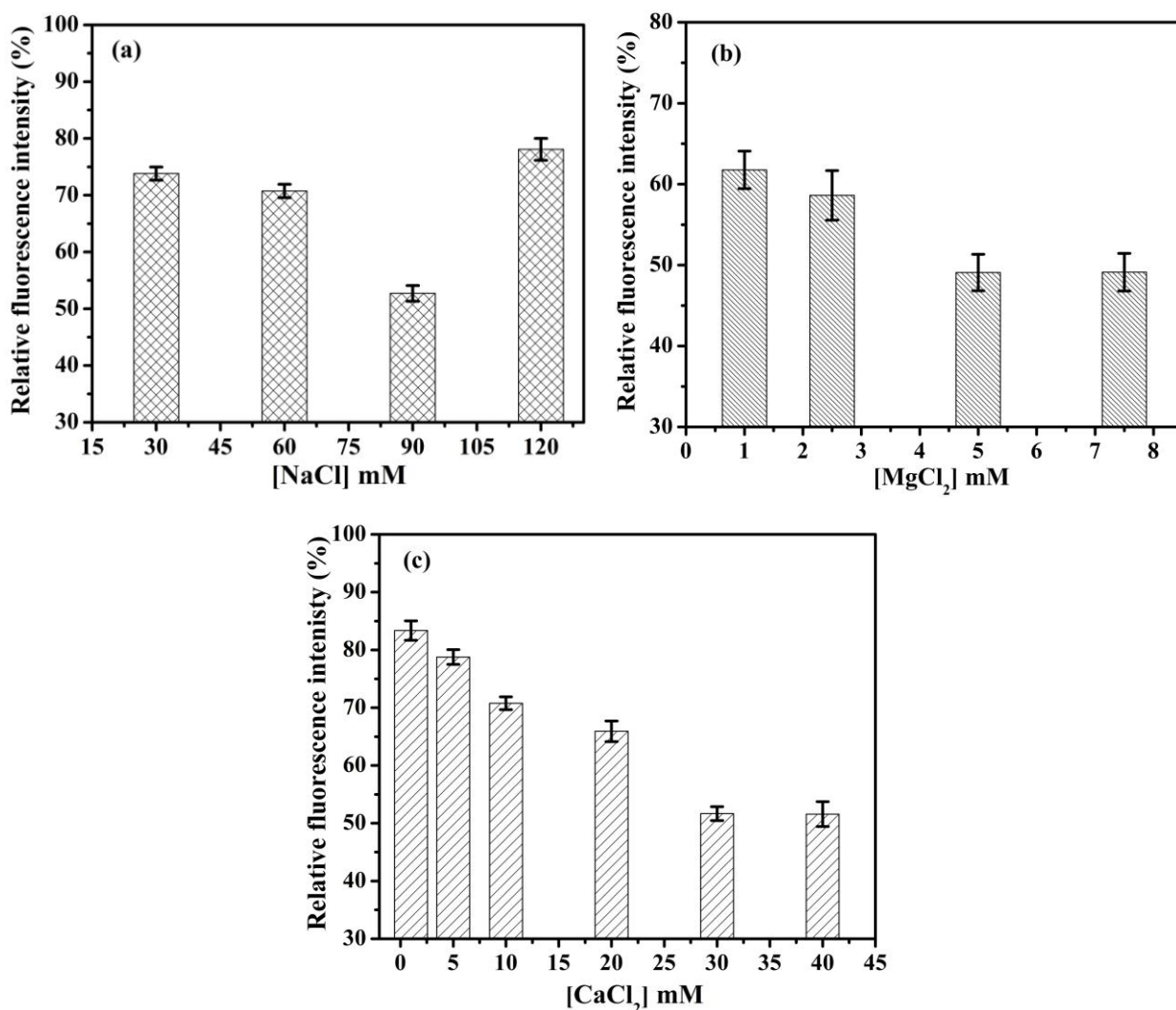


Figure 2.8: (a) Effect of various concentration of NaCl (30, 60, 90, 120 mM) on quenching efficiency of TiO₂-NPs in HBB (pH 7.4) (n=5); (b) Effect of various concentration of MgCl₂ (1, 2.5, 5 and 7.5 mM) on quenching efficiency of TiO₂-NPs in HBB (pH 7.4) (n=5); (c) Effect of various concentration of CaCl₂ (1, 5, 10, 20, 30 and 40 mM) on quenching efficiency of TiO₂-NPs in HBB (pH 7.4) (n=5).

2.3.1.4 Aptamer assay for OTA detection

Under optimized experimental conditions, the ability TiO₂-NPs to quench the fluorescence intensity of fluorescein labelled aptamer (FAM-OTA aptamer) was exploited for quantitative analysis of OTA. A calibration curve was performed against the different concentration of OTA ranging 1.5 nM to 20 μ M in HBB (pH 7.4) prior to real sample analysis. The recovered fluorescence intensity percentage response with an increasing OTA concentration from 1.5 nM to 20 μ M OTA has been plotted in Fig. 2.9. The obtained fluorescence recovery intensity

(%) response were in increase pattern corresponds to the concentration increased. This is due to the high binding affinity between FAM-OTA aptamer and OTA to form the stable anti-OTA aptamer-G-quadruplex complex, which resist the further quenching. The obtained linearity was from 1.5 nM to 1.0 μM with a line of equation $y = 17.01x [\mu\text{M}] + 49.83$ with $R^2 = 0.997$ and % R.S.D. = 3.65 ($n = 3$). A limit of detection (LOD) was calculated based on the standard deviation of baseline signal ($S/N = 3$) and found to be 1.5 nM. Similarly, the limit of quantification (LOQ) was calculated and found to be 3.1 nM. The obtained results that the presented assay could detect the OTA down to 1.5 nM compared to other fluorescence quenching based assay using nanoparticles (Table 2.2).

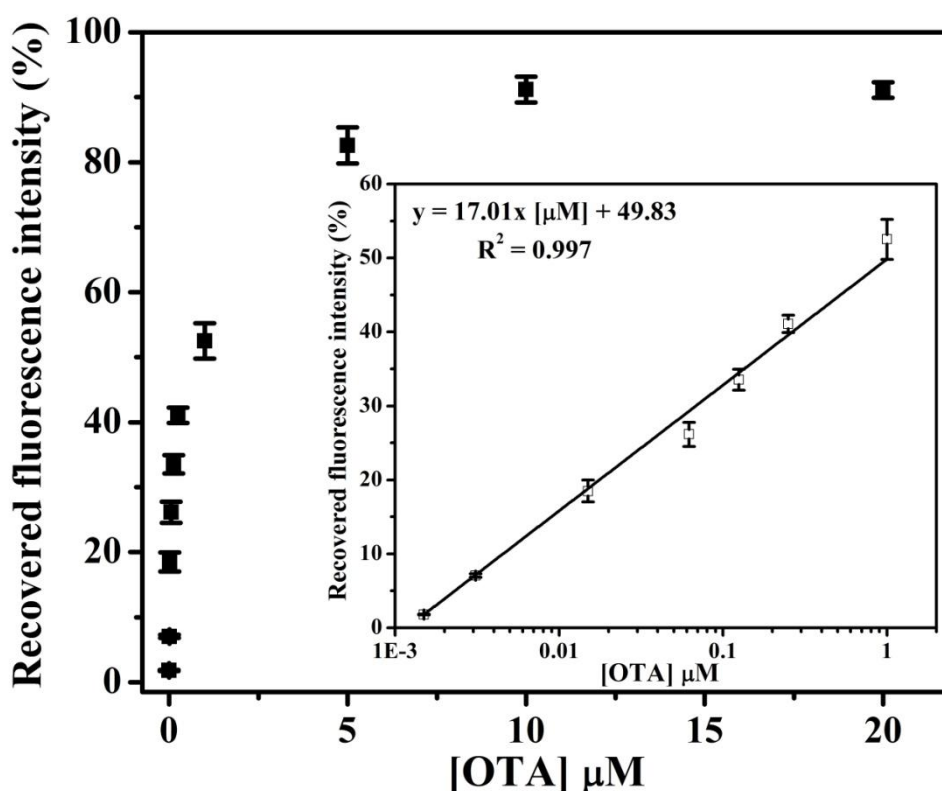


Figure 2.09: Calibration curve obtained for OTA (0.0015, 0.0031, 0.015, 0.062, 0.125, 0.25, 1.0, 5.0, 10.0, 20.0 μM) in HBB at pH 7.4 (Inset shows the logarithmic linear fit graph from 1.5 nM to 1.0 μM OTA).

2.3.1.5 Selectivity and specificity of aptamer assay

The selectivity and specificity of developed aptamer assay platform was investigated against the structural analogue of OTA for various concentrations of OTB (0.0031, 0.25 and 10.0

μM) spiked in the binding buffer. The obtained response of recovered fluorescence intensity percentage of OTB (red bar) was found to be more accurate with less than 10% ($n=3$) response of OTA (cyan bar) (Fig. 2.10). Results have been summarized in Table 2.6. These results confirmed that the recovered fluorescence response obtained with OTA was virtually due to high selectivity and specificity of FAM-OTA aptamer towards OTA.

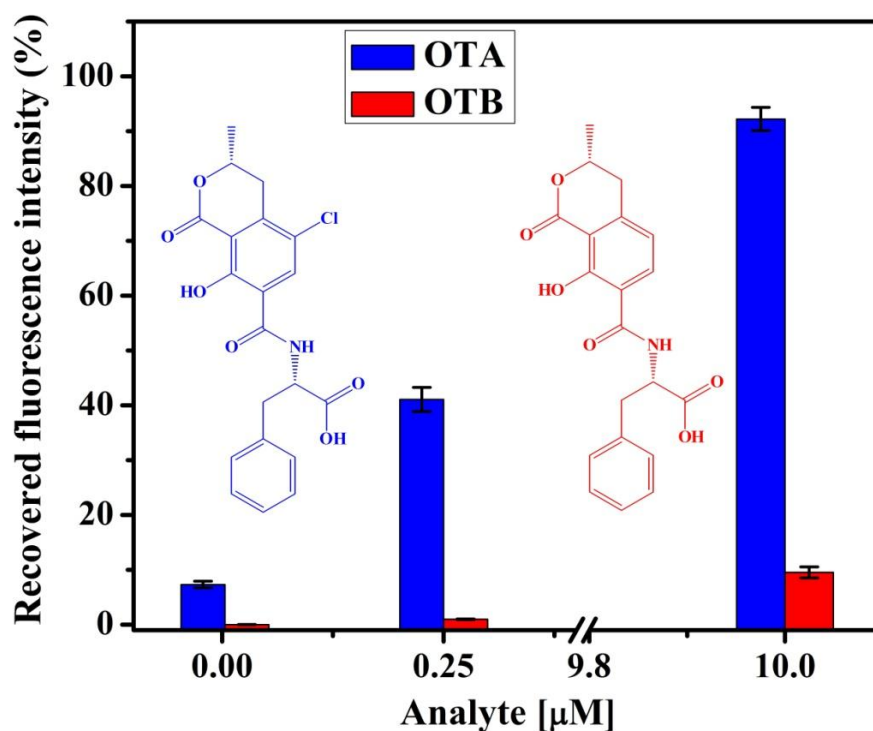


Figure 2.10: Bar graph representation of specificity studies of aptamer assay with structural (OTB) ($n=3$) at various concentrations (0.0031, 0.25 and 10.0 μM).

Table 2.6: Selectivity and specificity performance of assay platform for OTA detection

Conc ⁿ . [μM]	OTA		OTB		% response of OTB ($F_{\text{OTB}}/F_{\text{OTA}}$ $\times 100$)
	Recovered fluorescence intensity (%)		Recovered fluorescence intensity (%)		
	Mean \pm S.D. ($n=3$)	% R.S.D.	Mean \pm S.D. ($n=3$)	% R.S.D.	
0.0031	7.11 \pm 0.269	3.78	0.014 \pm 0.0005	3.57	0.197
0.25	41.07 \pm 2.199	5.35	0.961 \pm 0.0515	5.36	2.339
10.0	92.22 \pm 2.137	2.32	8.871 \pm 0.2055	2.32	9.619

2.3.1.6 Analytical performance of developed aptamer assay for OTA analysis

The analytical performance (repeatability and reproducibility) of aptamer assay was investigated by intra and inter day precision studies. The intra and inter day precision experiment was performed at 0.25 μM OTA under optimized experimental conditions. Similarly, control measurements were performed with each assay to calculate the recovered fluorescence intensity (%). Intraday precision with relative standard deviation of 2.89% (n=3) was calculated, indicating a very good reproducibility of aptamer assay. A % RSD from 1.74 to 6.50 (n=3) was calculated from interday analysis, which confirms that the results are reproducible. The results have been summarized in Table 2.7.

Table 2.7: Precision performance of developed assay for OTA analysis

Interday precision analysis					
Days	OTA [μM]	Recovered fluorescence intensity (%)		Mean \pm S.D.	% R.S.D.
Day-1	0.25	17.78		17.78 \pm 0.31	1.74
Day-2	0.25	16.76		16.76 \pm 1.09	6.50
Day-3	0.25	17.67		17.67 \pm 0.62	3.51
Intraday precision analysis					
OTA [μM]	Recovered FL Intensity (a.u.)			Mean \pm S.D.	% R.S.D.
	Response-1	Response-2	Response-3		
0.25	17.78	17.02	18.00	17.6 \pm 0.51	2.89

2.3.1.7 Feasibility of developed aptamer assay for OTA analysis in spiked beer and wine samples

The practical feasibility of developed aptamer assay platform was investigated in OTA spiked beer and wine sample. The recovery studies were performed at three different concentrations i.e. 0.0031, 0.25 and 1.0 μM OTA spiked in beer and wine samples. The OTA concentrations levels for real sample studies were selected from the calibration curve including lower and

higher values. Similarly, the controls were prepared by spiking the same amount of OTA in binding buffer. Obtained recoveries were found in good agreements, ranging from 94.30-102.68 % (n=3) with a maximum % R.S.D. 6.67 (n=3). The recoveries results have been summarized in Table 2.8, as percentage recovery (% recovery). These results prove the reliability and suitability of developed assay for OTA analysis in real matrices.

Table 2.8: Recovery performance of labelled assay platform for OTA determination in spiked beer and wine samples

Sample	OTA added [μM]	OTA found [μM]	Mean \pm S.D.	% RSD	% Recovery
Beer	0.0031	0.0029	0.0029 \pm 0.0001	3.44	94.30
	0.2500	0.2480	0.2480 \pm 0.0030	1.21	99.20
	1.0000	0.9910	0.9910 \pm 0.0100	1.00	99.10
Wine	0.0031	0.0032	0.0032 \pm 0.0002	6.67	103.22
	0.2500	0.2567	0.2567 \pm 0.0147	5.72	102.68
	1.0000	1.0169	1.0169 \pm 0.0321	3.16	101.69

2.3.2 Non-labelled technique (OTA detection using non-fluorescent labelled aptamer)

2.3.2.1 UV characterization of aptamer stabilized TiO₂-NPs

In UV-Vis analysis (methodology-2), the non-labelled anti-OTA aptamer showed a UV absorption maximum (λ_{max}) at 256 nm, whereas TiO₂-NPs do not absorb at the same wavelength (Fig. 2.12). The dispersion of anti-OTA aptamer stabilized TiO₂-NPs showed an increase in the absorption peak at 256 nm without change in the peak position (curve c and d). The reason was attributed to the electrostatic interaction between aptamer and TiO₂-NPs surface indicating presence of more anti-OTA aptamer molecule after stabilization of nanoparticles. The results have been tabulated in Table 2.9.

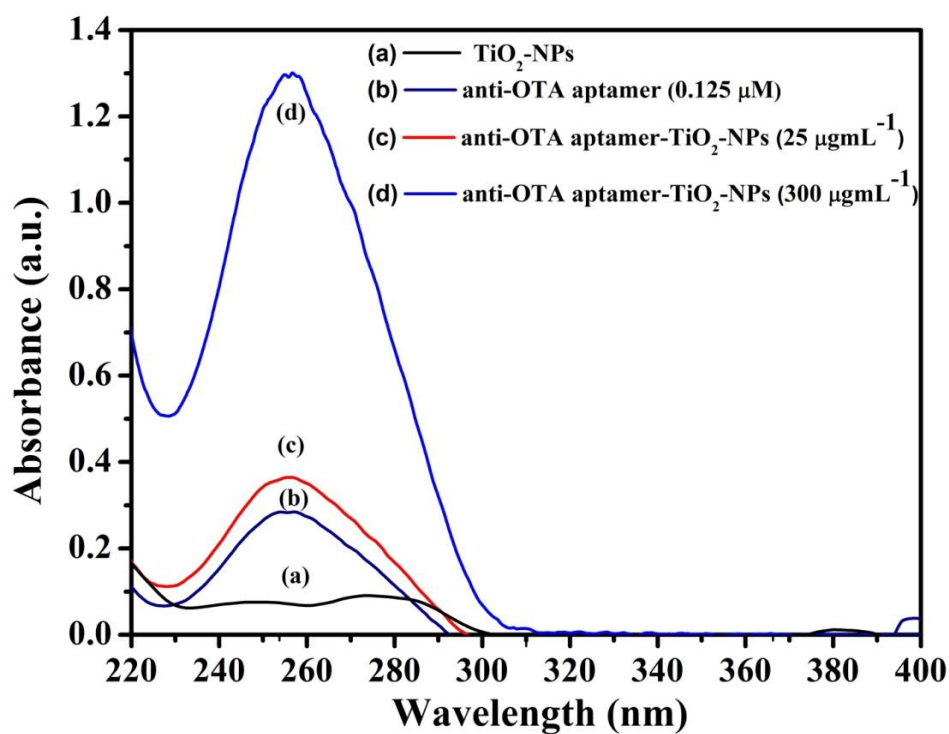


Figure 2.11: UV-Vis spectrum analysis of TiO_2 -NPs before and after stabilization with aptamer in HBB (pH 7.4)

Table 2.9: UV-Vis absorption characterization of aptamer assay in HBB (pH 7.4)

Spectrum	λ_{max} (nm)	Description	Absorbance (a.u.)
a.	256	TiO_2 -NPs	-
b.	256	anti-OTA aptamer	0.285
c.	256	anti-OTA aptamer + OTA (in absence of TiO_2 -NPs)	0.364
d.	256	anti-OTA aptamer+ OTA (in presence of TiO_2 -NPs)	1.299

2.3.2.2 Fluorescence imaging study

To establish the quenching assay mechanism, the fluorescence imaging studies were performed at each step. The high fluorescence of fluorescent probe (FCM) was quenched by TiO_2 -NPs and aptamer stabilized TiO_2 -NPs (Fig. 2.12). On addition of OTA, the OTA triggered conformational changes in reversible assembly of aptamer weakened the interaction between fluorescent probe and TiO_2 -NPs, results in the recovery of quenched fluorescence (Fig. 2.12e). The processed data from MATLAB interface based on RGB value is summarized in Table 2.10. On addition of OTA, the fluorescence magnitude of blue component of FCM increases in presence of TiO_2 -NPs, which is a strong indicative of target induced hybridization between anti-OTA aptamer and OTA molecule.

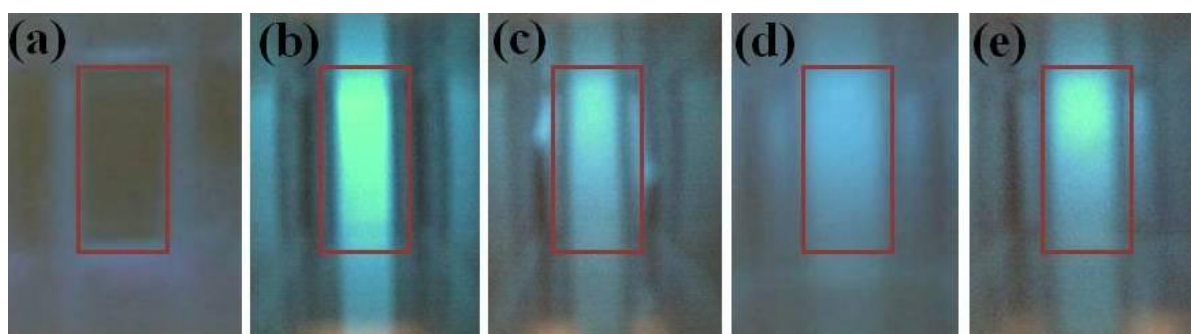


Figure 2.12: Fluorescence imaging of (a) OTA, (b) FCM, (c) FCM + TiO_2 -NPs, (d) FCM + anti-OTA aptamer- TiO_2 -NPs, (e) FCM + anti-OTA aptamer- TiO_2 -NPs + OTA in HBB (pH 7.4).

Table 2.10: Fluorescence magnitude value of blue components

Image	Description	Blue component value
a.	OTA	20
b.	FCM	160
c.	FCM + TiO_2 -NPs	115
d.	FCM + anti-OTA aptamer- TiO_2 -NPs	89
e.	FCM + anti-OTA aptamer- TiO_2 -NPs + OTA	120

2.3.2.3 SEM characterization of bare and aptamer stabilised TiO₂-NPs

The SEM micrographs of bare TiO₂-NPs (Fig. 2.14a) and anti-OTA aptamer stabilized TiO₂-NPs (Fig. 2.14b) were recorded on scanning electron microscope (SEM XL 30 FEI/Philips, Philips Electronics Co., Netherlands). The bare TiO₂-NPs showed the aggregation, whereas the morphology has been changes after stabilization and individual particle was visualized. It was observed that the TiO₂-NPs stabilized and started uniform distribution, which can be seen in Fig. 2.14b.

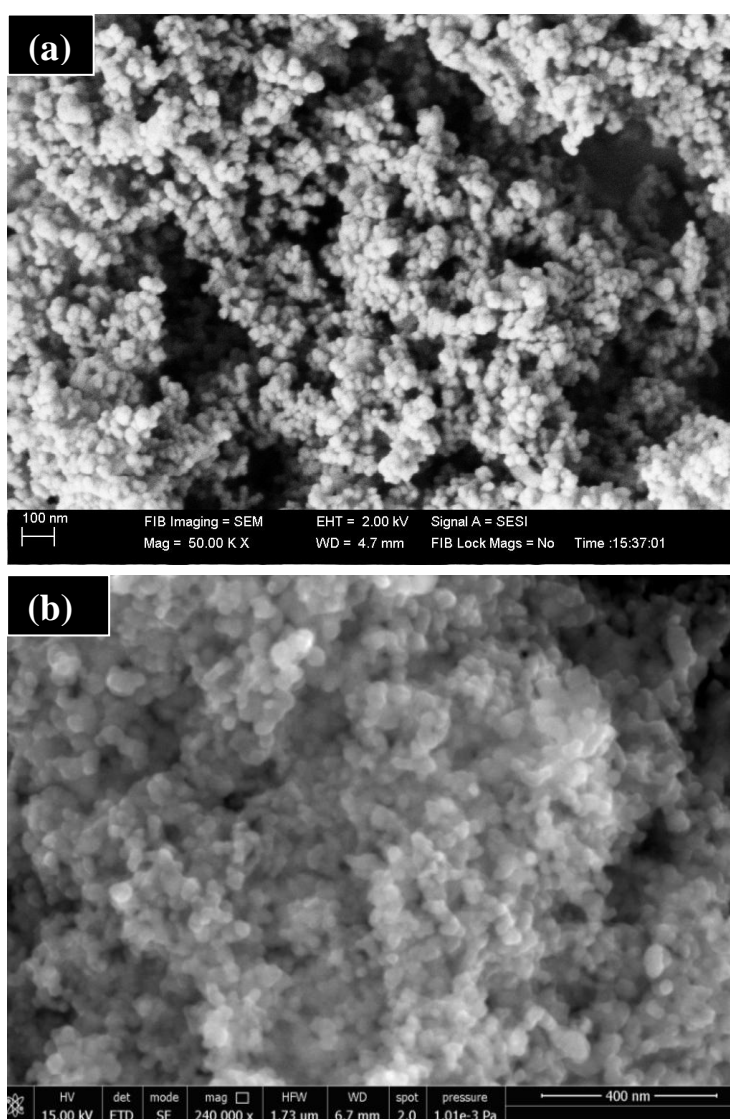


Figure 2.13: Scanning electron micrograph (a) bare TiO₂-NPs; (b) anti-OTA aptamer stabilized TiO₂-NPs.

2.3.2.4 Optimization of experimental parameters using non-labelled technique

2.3.2.4.1 TiO₂-NPs concentration

Quenching ability of TiO₂-NPs was evaluated against the fixed concentration of FCM probe (10 μ L of 100 μ g mL⁻¹ FCM in microwell). Various concentrations of TiO₂-NPs ranging from 2.5-1000 μ g mL⁻¹ were investigated. Fluorescence quenching increased with increasing TiO₂-NPs concentration from 2.5-300 μ g mL⁻¹ as shown in Fig. 2.15. Later, 300 μ g mL⁻¹ TiO₂-NPs was used as optimal concentration in further experimentation.

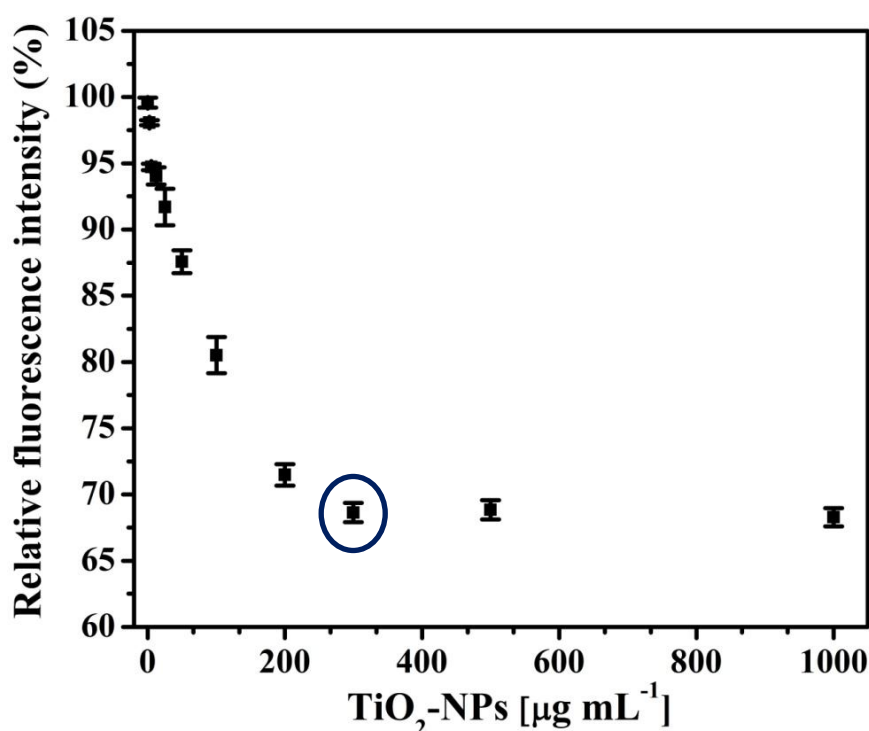


Figure 2.14: Optimization of TiO₂-NPs concentration (2.5-1000 μ g mL⁻¹) against FCM probe (10 μ L of 100 μ g mL⁻¹ FCM in microwell) for structure switching aptaswitch.

2.3.2.4.2 Aptamer concentration

In the present protocol, the optimization of aptamer concentration was the critical factor for the stabilization of TiO₂-NPs and OTA detection. Fluorescence intensity of FCM probe decreased with increased in anti-OTA aptamer concentration i.e. 10-750 nM (Fig. 2.15). The increased in quenching (decreased in fluorescence intensity) of FCM probe was attributed to the increased stability of TiO₂-NPs. This resulted in uniform dispersion of stabilized particle and quenching efficiency improved. Higher concentration of biomolecule might increases the

signal intensity meanwhile decreases the sensitivity due to increased background signal (Hayat et al., 2011), thus the 250 nM aptamer concentration was used as optimum.

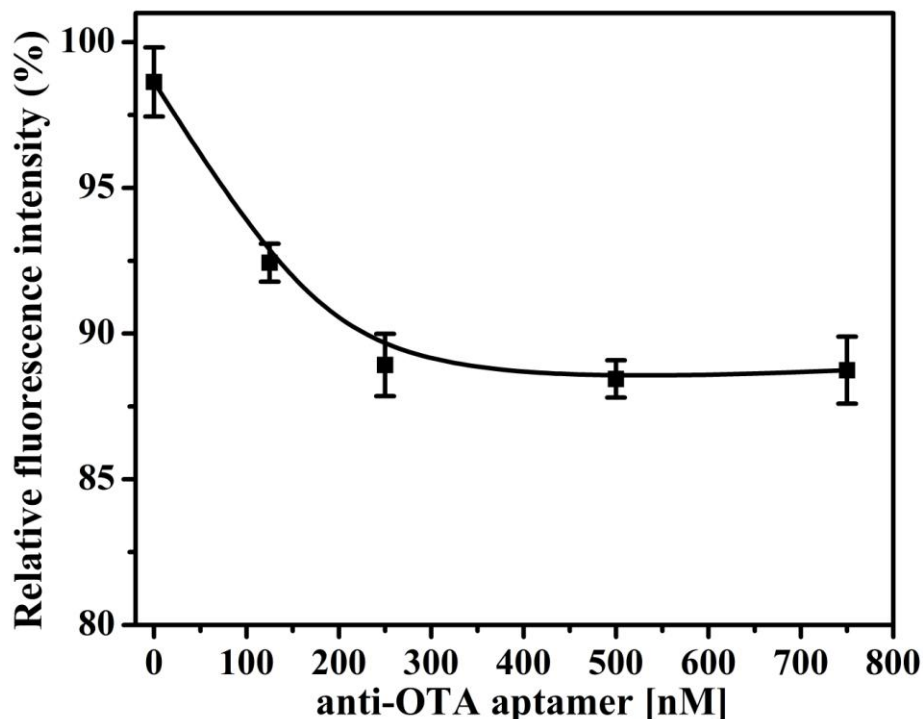


Figure 2.15: Effect of aptamer concentration on structure switching aptasensing platform.

2.3.2.4.3 Optimization of buffer, pH and salt concentrations

Undesirable adsorption of phosphate and other anionic buffer salt may cause the artifacts in the aptamer based stabilization or uniform dispersion TiO_2 -NPs surface, thus all the experiments were carried out in the HBB. The presence of surface charge at TiO_2 -NPs surface might be responsible for aggregation of NPs at high pH and alter the performance (Liao et al., 2009). TiO_2 -NPs showed a maximum quenching performance at pH 7.4 in HBB (Fig. 2.16a). The effect of pH was also investigated at aptamer stabilized TiO_2 -NPs. The maximum quenching efficiency was observed at pH 7.4 with 250 nM anti-OTA aptamer (Fig. 2.16b). Obtained results proves that the anti-OTA aptamer and TiO_2 -NPs complex is stable at pH 7.4 in HBB because binding buffer pH can significantly affect the adsorption kinetics and complex stability. On pH 7.4 condition the HBB activity was found to be maximum.

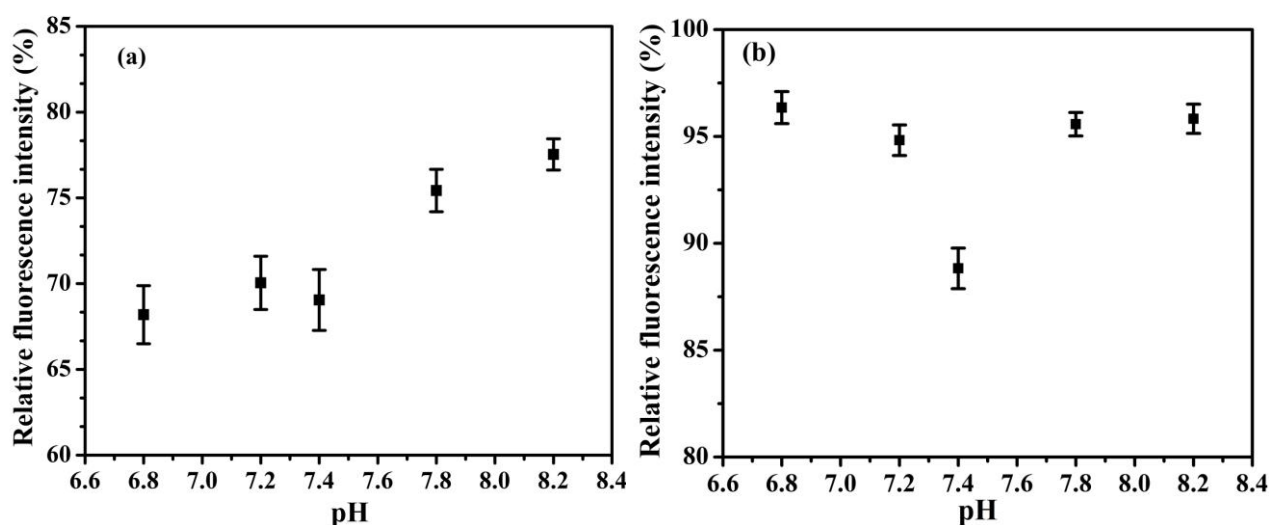


Figure 2.16: (a) Optimization of buffer pH (6.8-8.2) for development of structure signalling aptaswitch platform in HBB (n=3); (b) Effect of pH on quenching efficiency of anti-OTA aptamer stabilized TiO₂-NPs (aptamer- TiO₂-NPs complex) (n=3).

TiO₂-NPs carry a negative surface charge in HBB at pH 7.4. The variation in surface charge may cause the aggregation or render the electrostatic interaction resulting decreased fluorescence quenching efficiency (Amano et al., 2010). Owing to this, the effect of buffer salts was studied and optimized to overcome the electrostatic repulsion and obtained maximum response. The maximum response was obtained at 60 nM Na⁺ salt and 5 mM Mg²⁺ salt concentration (Fig. 2.17a and 2.17b). Similarly, the optimized time of incubation was 1 hr, because afterward the undesired agglomeration or multilayer adsorption of biomolecule might decrease the efficacy. Later on, the effect of dilution factor was shown to confirm the exponential decrease in the response and it was observed that the 200 μ L assay volume was optimum (Fig. 2.17c).

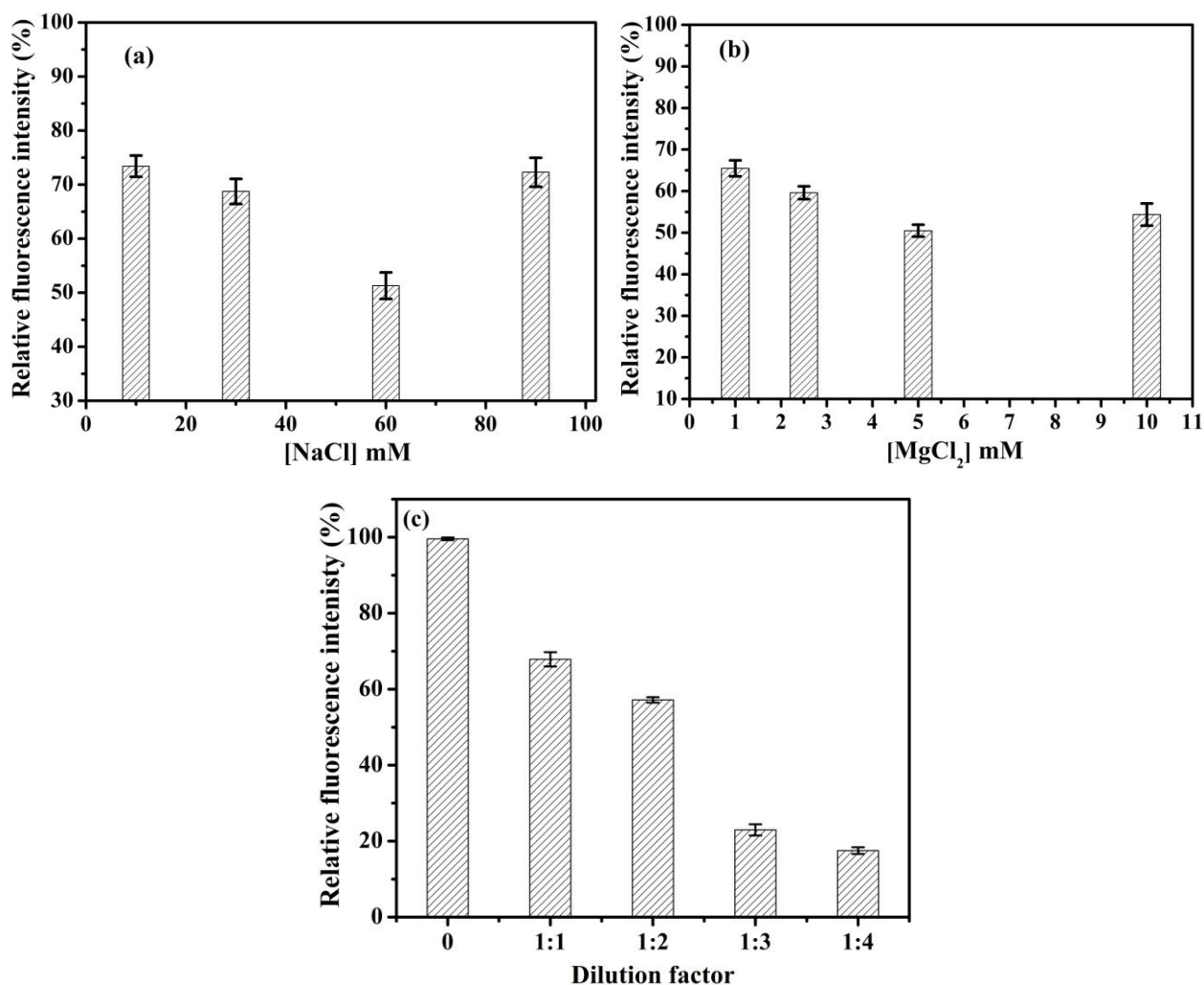


Figure 2.17: Effect of (a) NaCl concentration on quenching efficiency of anti-OTA aptamer stabilized TiO₂-NPs at optimized concentration; (b) MgCl₂ concentration on quenching efficiency of anti-OTA aptamer stabilized TiO₂-NPs at optimized concentration; (c) dilution factor (dilution with buffer) on assay performance. All measurements were performed in three replicate experiments (n=3).

2.3.2.5 OTA detection using label-free platform (FCM probe)

A calibration curve was performed for different concentrations of OTA spiked in the HBB. The recovered fluorescence intensity corresponds to the OTA was plotted as a function of increasing OTA concentrations i.e. 0.017-5.0 μ M in HBB, pH 7.4 (Fig. 2.18). The recovered fluorescence intensity was found to be increased with increasing OTA concentration, which is the result of high binding affinity of anti-OTA aptamer towards OTA to form the anti-OTA aptamer-G-quadruplex complex and resist further quenching. Calibration curve was fitted

using the linear equation and a line of equation as $y = 41.67 x (\mu\text{M}) + 6.604$ with $R^2 = 0.9913$ ($n=4$) and linearity from 0.017 to 5.0 μM OTA was calculated. The LOD was found to be 1.35 nM of OTA ($S/N = 3$). The developed aptaswitch platform showed the better LOD as compared to earlier reported methods based on fluorescence and colorimetric signal based aptaswitches for OTA detection as summarized in Table 2.3.

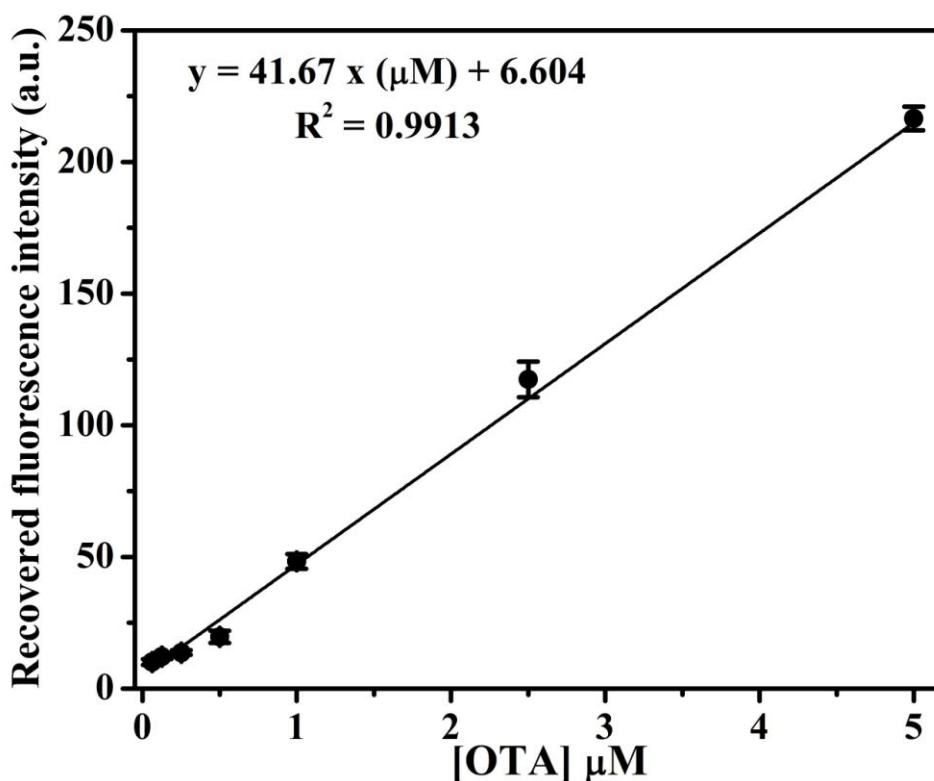


Figure 2.18: Calibration curve obtained for OTA (0.017-5.0 μM) in HBB (pH 7.0, $n=3$).

The present strategy exhibiting higher sensitivity than methodology -1, where the FAM-OTA aptamer (as recognition element and fluorophore) and TiO_2 -NPs (as quencher) were employed for OTA detection. The higher sensitivity of present aptaswitch was attributed to the stabilization of aptamer modulated nano surfaces, which offer an advantage of uniform dispersion and stability.

2.3.2.6 Selectivity and specificity of aptamer assay

The selectivity performance of developed assay platform was evaluated at varying concentration from 0.25, 1.0, 5.0 μM against structural (OTB) and non-structural analogues (*N*-acetyl-L-phenylalanine (NAP) and warfarin) spiked in the buffer. On addition of OTA the

recovered fluorescence intensity increased correspondingly (blue bar), whereas other analogues did not induced apparent fluorescence response at same concentrations (Fig. 2.19). It is evident from the results that recovered fluorescence response with OTA was due to the specific binding interaction of OTA and anti-OTA aptamer and negligible with other analogues. The selectivity response were found to be more accurate with less than 10 % (n=3) at three different concentrations as tabulated in Table 2.11.

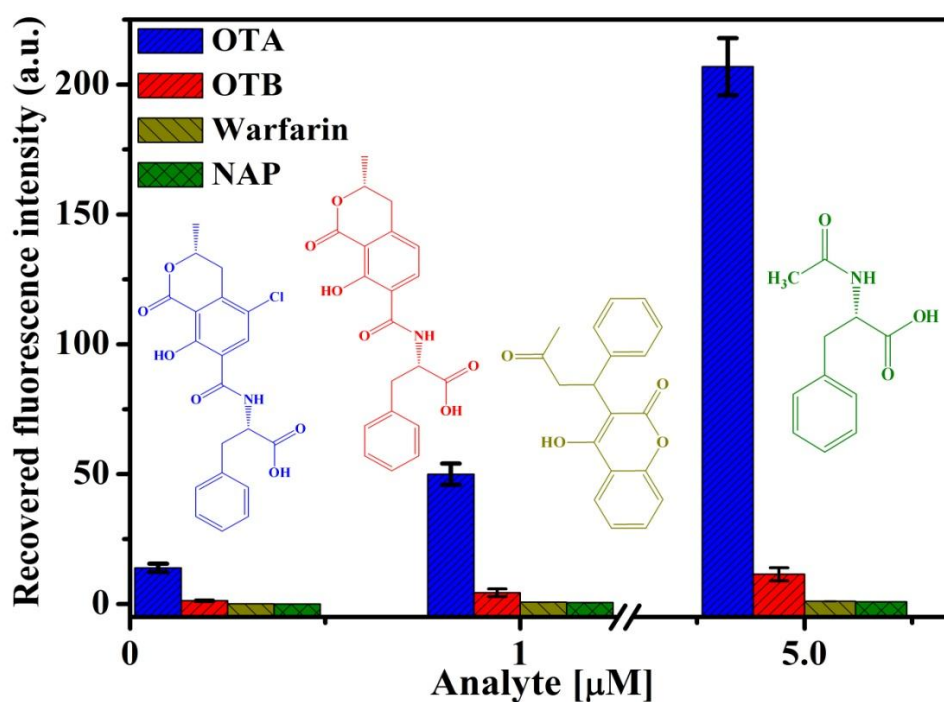


Figure 2.19: Bar graph representation of specificity studies of developed aptaswitch for OTA detection with structural and non-structural analogues (n=3) at various concentrations (0.25, 1.0 and 5.0 μM).

Table 2.11: Selectivity and specificity performance of assay platform for OTA detection

Specificity performance of fluorescence aptamer assay against other analogues											
Concⁿ. [μM]	OTA Recovered fluorescence intensity (a.u.)		OTB Recovered fluorescence intensity (a.u.)		% response of OTB (F_{OTB}/ F_{OTA} x 100)	Warfarin Recovered fluorescence intensity (a.u.)		% response of OTB (F_{warfarin} / F_{OTA} x 100)	NAP Recovered fluorescence intensity (a.u.)		% response of OTB (F_{NAP}/ F_{OTA} x 100)
	Mean ± S.D. (n=3)	% R.S.D	Mean ± S.D. (n=3)	% R.S.D.		Mean ± S.D. (n=3)	% R.S.D.		Mean ± S.D. (n=3)	% R.S.D.	
0.25	13.93 ± 1.19	8.54	1.27 ± 0.10	9.00	9.12	0.08 ± 0.01	12.5	0.57	0.06 ± 0.01	16.67	0.43
1.0	49.96 ± 1.94	5.88	4.36 ± 0.31	7.11	8.72	0.74 ± 0.06	8.11	1.48	0.53 ± 0.03	5.66	1.06
5.0	206.9 ± 9.60	4.64	11.44 ± 1.06	9.26	5.53	1.05 ± 0.09	8.57	0.51	0.89 ± 0.06	6.74	0.43

2.3.2.7 Analytical performance of developed platforms for OTA detection

The precision performance of developed aptaswitch was evaluated by intra and inters day precision studies. The precision studies were carried out at 0.25 μM OTA. Control measurements were performed for each assay without OTA. Intra assay precision with % R.S.D (n=3) of 5.04 was calculated for triplicate measurements of OTA. The inter assay precision with % R.S.D. (n=3) from 1.53 to 6.79 was calculated. The results from precision assay have been summarized in Table 2.12, which prove the applicability of sensing platform for real sample analysis.

Table 2.12: Analytical precision performance of developed aptaswitch

Interday precision performance of developed aptaswitch					
Days	OTA [μM]	Recovered fluorescence intensity (a.u.)	Mean \pm S.D.	% R.S.D.	
Day-1	0.25	13.73	13.73 \pm 0.87	6.33	
Day-2	0.25	14.13	14.13 \pm 0.96	6.79	
Day-3	0.25	13.65	13.65 \pm 0.21	1.53	
Intraday precision performance of developed aptaswitch					
OTA [μM]	Recovered fluorescence intensity (a.u.)			Mean \pm S.D.	% R.S.D.
	Response-1	Response-2	Response-3		
0.25	13.5	14.8	14.7	14.33 \pm 0.79	5.04

2.3.2.8 Analysis of OTA spiked beer and wine samples

The practical performance of present OTA aptaswitch was verified in the OTA spiked beer and wine samples. The recovery studies were performed at various concentrations spiked in the real samples i.e. 0.017, 0.125 and 1.0 μM OTA spiked in the buffer, beer and wine samples. Concentrations were selected from the calibration curve including lower and higher values. The recoveries were calculated based on the fluorescence response obtained in the buffer and OTA spiked samples. Obtained recoveries were in the range 96.79-101.5 % (n=3) with a maximum % R.S.D. 6.02. The results have been tabulated in Table 2.13 as % recovery

responses. The present results suggested that the present OTA aptaswitches could be further employed for detection of OTA in other matrices.

Table 2.13: Recovery performance of label-free platform for OTA spiked beer and wine samples

Sample	OTA added [μM]	OTA found [μM]	Mean ± S.D.	% RSD	% Recovery
Beer	0.0170	0.0166	0.0166 ± 0.0010	6.02	97.65
	0.1250	0.1210	0.1210 ± 0.0032	2.48	96.79
	1.0000	0.9940	0.9940 ± 0.0292	2.91	99.40
Wine	0.0170	0.0171	0.0171 ± 0.0010	5.85	100.50
	0.1250	0.1252	0.1252 ± 0.0052	5.72	100.16
	1.0000	1.0150	1.0150 ± 0.0321	3.16	101.50

2.3.3 Validation using HPLC method

The results obtained from the measurements on multiplate reader were cross validated against the standard chromatographic method HPLC. As a model the concentration of OTA at MRL and above were prepared spiked in beer and wine samples and tested using HPLC for cross validation. The HPLC was carried out using an extraction process to extract OTA from spiked beer and wine samples. The HPLC peak signal obtained for OTA spiked in wine samples have been shown (Fig. 2.20). The cross validation experiments against standard HPLC method confirmed the reliability of the developed platform. A good correlation and reliability was obtained for each concentration as each measured in triplicate. The co-relation observed in the data by both techniques is tabulated in Table 2.14. The recoveries were obtained by both the techniques were also in good agreements.

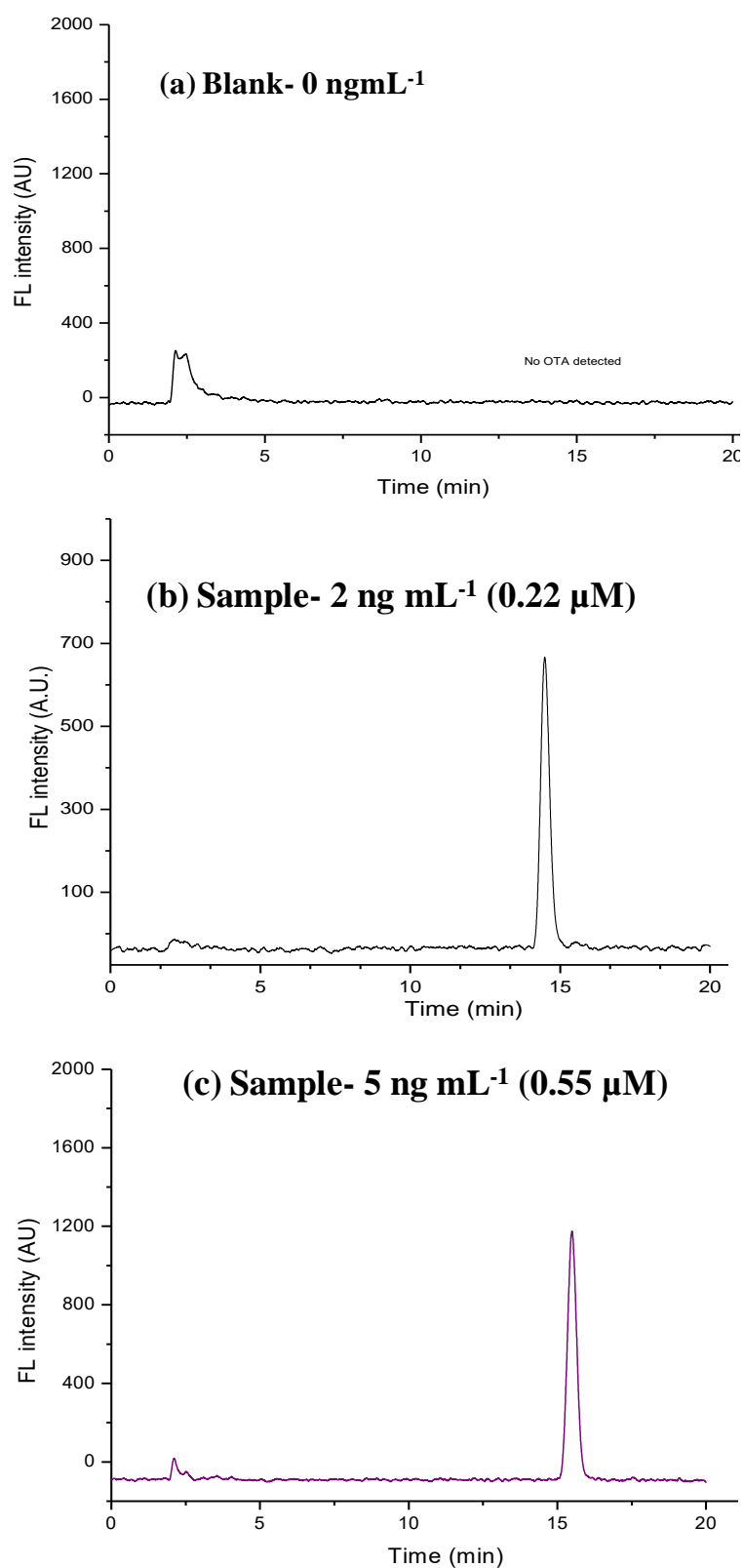


Figure 2.20: HPLC chromatograph for blank (a) 0 ng mL⁻¹ OTA; (b) OTA (2 ng mL⁻¹); (c) OTA (5 ng mL⁻¹) spiked in wine.

Table 2.14: Recovery performance of cross validation with HPLC method

Sample	OTA added [μM]	OTA added [μM]		Recovery (%)	
		Developed protocol	HPLC	Developed protocol	HPLC
Beer	0.22 (2.0 ng mL ⁻¹)	0.209 \pm 0.01	0.198 \pm 0.01	95.00	90.00
	0.55 (5.0 ng mL ⁻¹)	0.538 \pm 0.02	0.524 \pm 0.02	97.82	95.27
Wine	0.22 (2.0 ng mL ⁻¹)	0.212 \pm 0.01	0.202 \pm 0.01	96.36	91.82
	0.55 (5.0 ng mL ⁻¹)	0.544 \pm 0.02	0.528 \pm 0.02	98.90	96.00

2.3.4 Analytical performance comparison of developed assay protocols

The analytical performance of both the developed platforms were compared (Table 2.15). It is evident on the basis of the obtained results both the platform are enough sensitive for quantitative detection of the OTA in beer and wine samples meeting the requirements of regulatory standards. The methodology-1 was based on the conjugation of aptamer with fluorophore molecules, whereas, the methodology-2 capitalizes on the surface chemistry of nanoparticles to quench the response of fluorescence particles. The methodology-2 eliminates the need of bioconjugation with fluorophore and problems associated with nanomaterials based fluorescence quenching assays.

Table 2.15: Comparative analytical figures of merits of developed protocols

Parameter	Labelled technique	Label-free technique
Linear range	1.5 nM to 1.0 μM	17 nM to 5.0 μM
Limit of detection	1.5 nM	1.35 nM
Assay volume	150 μL	200 μL
Intraday precision	2.89 (% R.S.D.)	5.04 (% R.S.D.)
Analysis time	1 h	2 h
% Recovery	94.30-102.68 %	96.79-101.50 %

2.4 Conclusion

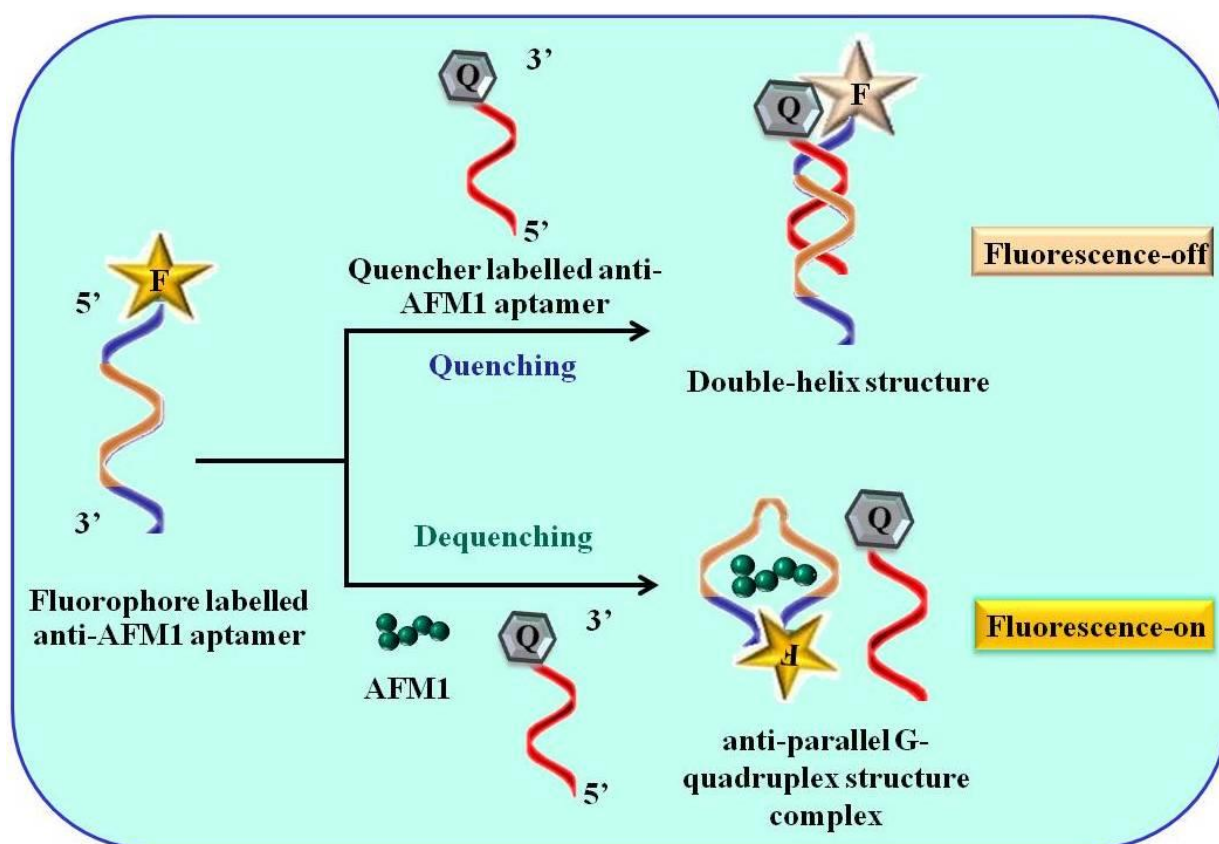
In conclusion, the present work demonstrates the development of structure signalling aptaswitches for OTA detection. In this work, the quenching ability of TiO₂-NPs (as nanoquencher) was employed against fluorophore labelled anti-OTA aptamer and aptamer stabilized TiO₂-NPs against fluorescent probe for quantitative determination of OTA. The work was divided in two parts; in first the assay development was based on the recovery of fluorescence quenched signal of fluorescently labelled anti-OTA aptamer by TiO₂-NPs. In second, the strategy capitalizes on the surface chemistry of nanoparticles to quench the fluorescence intensity of fluorophore particles, which eliminates the need of bioconjugation of aptamer molecule with fluorophore. The proposed assay platform exhibited the good linearity from 1.5 nM to 1.0 μM (methodology-1) and 17 nM to 5.0 μM (methodology-2), meeting the requirements of regulatory standards for OTA detection in alcoholic beverages (beer and wine i.e. 2.0 μg kg⁻¹ equal to 0.22 μM). Obtained recoveries were in the range of 94.30-102.68% (n=3) for OTA spiked in beer and wine samples. The precision performance proves the acceptability of developed aptaswitches platforms for OTA determination in comparison to existing method. However, we assumed that the present platform of fluorescence based aptamer assay will offer the new methodology for sensitive and specific detection of wide spectrum of analyte in food and environmental contamination.

CHAPTER 3

Structure switching aptamer assay for aflatoxin M1 (AFM1) analysis in milk sample

Novelty Statement:

- Structure switching aptamer assay employing the quenching-dequenching mechanism has been investigated for AFM1 detection in milk sample.
- Performance of anti-AFM1 aptamer sequences has been successfully evaluated against two complementary quencher sequences.
- No complex sample procedure required for detection of AFM1 in milk sample (AFM1 detection in the spiked raw milk).
- Developed strategies able to detect as low as 1 ng kg^{-1} AFM1 provided $15 \text{ }\mu\text{L}$ sample volume.



Graphical abstract of chapter content

3.1 Background

Mycotoxins are a large and varied group of fungal toxins or mold producing secondary metabolites, commonly encountered in variety of food and feed products. The presence of mycotoxins contamination in food and feed has initiated an alarming situation worldwide due to the increasing incidences and stubbornly high mortality of mycotoxin contamination (Nguyen et al., 2013; Guo et al., 2014). Among all, the aflatoxins (AFs) are the most relevant and usually found mycotoxins under a toxicological and legislative point of view. AFs (AFB1, AFB2) are naturally occurring secondary metabolites, produced by the molds i.e. *Aspergillus parasiticus*, *Aspergillus flavus* and *Aspergillus nomius* (Bakirci, I., 2001). When AFB1 contaminated feed is ingested by the lactating (or dairy) animals, it leads to the secretion of AFM1 in milk (Fig. 3.1). AFM1 is an enzymatic hydroxylated metabolite of the AFB1 metabolized by liver cytochrome P450 enzyme. It is secreted from the mammary glands of lactating cows in milk and known for its hepatotoxicity, carcinogenicity, DNA intercalation, gene mutation, base impairment and oxidative damage due to intracellular radical generation (Kanungo et al., 2011; Hamid et al., 2013). Based on episodes of AFM1 toxicity, severity of illness to human (especially in children and young infants) and environment, the regular monitoring and screening of AFM1 in milk and milk based products has been mandated (Shephard, G.S., 2008; Ashiq et al., 2014). International Agency for the Research on Cancer (IARC) has reclassified the AFM1 from Group 2B agents to Group 1 (IARC Monograph, 2002). To ensure the safety for food and providing quality to human health, several regulatory agencies have mandated the MRLs for AFM1 in milk and milk products, considering milk as the nutritional balanced food to young infants.

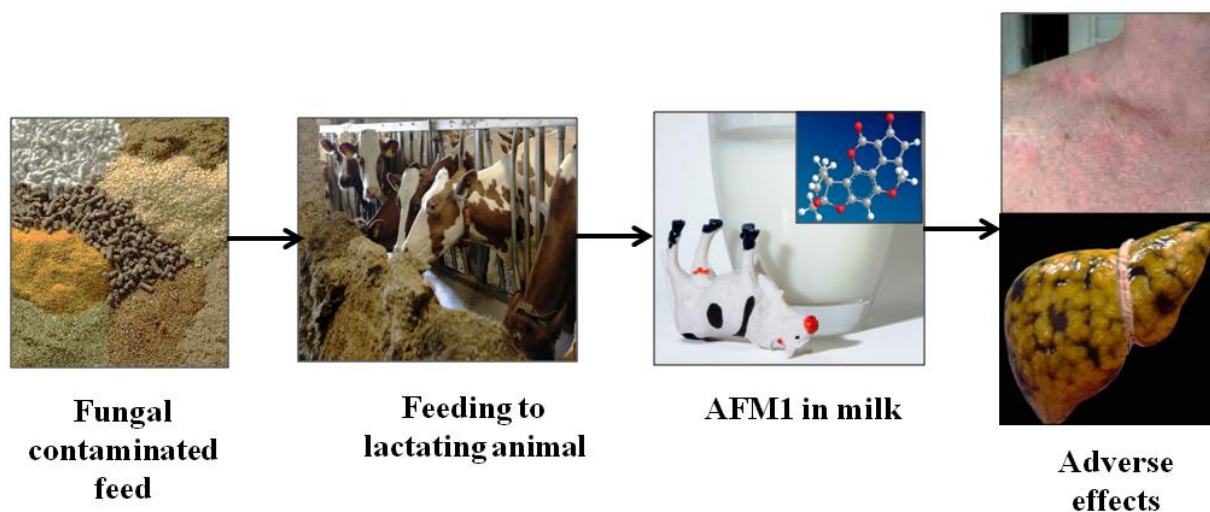


Figure 3.1: Source of AFM1 in milk and its toxic effect.

3.1.1 Regulatory legislation for AFM1 detection in milk samples

The MRLs for AFM1 in milk, regulated by the various regulatory agencies has been summarized in Table 3.1. The MRLs are even lower for the infants and baby formula because their vulnerability to toxins is higher (EU Commission Regulation, 2006). Hence, the demands of analytical methods with rapidity, high sensitivity, reproducibility and high throughput for AFM1 detection in raw milk sample are highly desired (US Food and Drug Administration (USFDA), 2000; Food Safety and Standard Authority of India (FSSAI), 2011; CODEX Alimentous Commission (CAC), 2000).

Table 3.1: Reported regulatory maximum residue limits for AFM1 in milk and infant formula (USFDA, FSSAI)

Analyte	MRLs (in milk and milk based products)			
	EU	USFDA	FSSAI	CODEX
Milk (Liquid)	50 ng kg ⁻¹	500 ng kg ⁻¹	500 ng kg ⁻¹	500 ng kg ⁻¹
Infant Milk formula	25 ng kg ⁻¹	Not specified	Not specified	Not specified

3.1.2 State of art for analysis of AFM1 in milk

Since the revolutionary outbreak of “turkey X disease” in England (in early 1960s), which was due to the consumption of AFM1 contaminated Brazilian peanut meal, the presence of AFs contamination in food has gathered significant attention (Kensler et al., 2011). Reports of AFs contamination in the European and Indian continent are rising concurrently with the change in environmental factors and feeding contaminated feed to milk producing animal (Hall and Wild, 1994; Medina et al., 2014). Milk is considered as healthy and nutritionally balanced food comprises essential nutrients for all age groups (Zhang et al., 2005). The presence of AFM1 contamination in milk causes an alarming situation to dairy and agriculture industry. The conventional techniques such as thin layer chromatography (TLC) (AOAC official method, 2000), high-performance liquid chromatography (HPLC) (Bognanno et al., 2006), liquid chromatography coupled with mass spectroscopy (LC-MS) (Cavaliere et al., 2006) and HPLC coupled fluorescence detector (HPLC-FD) (Iha et al., 2011) have been widely reported for AFM1 analysis in milk. Meanwhile, the enzyme-linked immunosorbent assays (ELISA) for AFM1 analysis have also gained significant attention with improved

sensitivity and high throughput (Rastogi et al., 2004; Kanungo et al., 2011; Vdovenko et al., 2014) (Fig. 3.2). The characteristics properties such as time consuming process, large sample volume, difficulty in automation, elevated cost of antibodies production, shorter shelf life and in-vivo production involving use of animals as immunization, involved in the chromatographic and immunological techniques limits their wider utility for on-site application (Istamboulié et al., 2016). There are reports on the sensitive detection of AFM1 in milk but their application to analysis of raw milk involving complex matrix treatment is always remained a challenge (Table 3.2). The high levels of AFM1 contamination in milk even at trace levels forced scientist to design and develop novel innovative analytical methods.

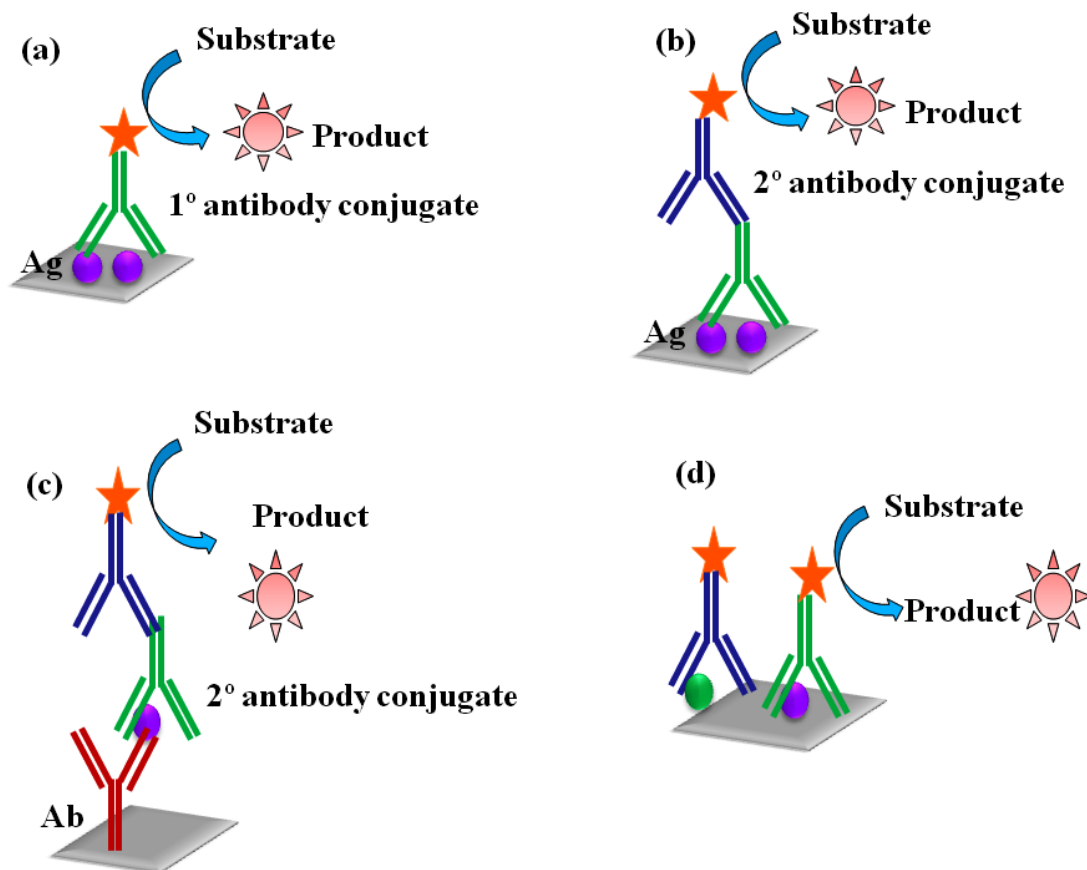


Figure 3.2: Schematic representation of (a) direct ELISA; (b) indirect ELISA; (c) sandwich ELISA; (d) competitive ELISA.

Table 3.2: Summary of reported immunosensor for analysis of AFM1

Methodology	Transduction principle	Linearity	LOD	Ref.
Flow-injection immunoassay (FI-IA)	Amperometric	20 and 500 ng kg ⁻¹	11.0 ng kg ⁻¹	(Badea et al., 2004)
Immunosensor	Chronoamperometry	30-160 ng kg ⁻¹	25.0 ng kg ⁻¹	(Micheli et al., 2005)
Immunoassay	Chemiluminescence	0.2-5000 ng kg ⁻¹	0.25 ng kg ⁻¹	(Mogliulo et al., 2005)
Enzyme immunoassay	Chemiluminescence	10-100 ng kg ⁻¹	5.0 ng kg ⁻¹	(Anfossi et al., 2008)
Immunosensor	Electrochemical	10-100 mg kg ⁻¹	10.0 mg kg ⁻¹	(Paniel et al., 2010)
Immunoassay	Chemiluminescence (based on gold magnetic nanoparticles)	6.25-250 ng kg ⁻¹	0.5 ng kg ⁻¹	(Kanungo et al., 2011)
Immunosensor	Electrochemical (impedimetric)	6.25-100 ng kg ⁻¹	1.0 ng kg ⁻¹	(Bacher et al., 2012)
Spore-inhibition-based enzymatic assay	Chemiluminescence	-	0.25 ng kg ⁻¹	(Singh et al., 2013)
Immuno chromatographic assay	Chemiluminescence (based on gold nanoparticles)	25-100 ng kg ⁻¹	50.0 ng kg ⁻¹	(Wu et al., 2016)
Immuno chromatographic assay	Fluorescence	10-320 ng kg ⁻¹	4.4 ng kg ⁻¹	(Zhang et al., 2016)

3.1.3 Aptasensing platforms for AFM1 analysis in milk

Recent trends in biosensor development report an extensive use of aptamer in combination with various transducing mechanism (optical and electrochemical). The high binding affinity, specificity and versatility of target along with the simplicity of in-vitro selection (SELEX)

process make aptamers as attractive molecular tools in bioanalytical applications (Malhotra et al., 2014). Various aptasensing strategies have been reported for detection AFM1 in milk (Table 3.3). Among them, the fluorescence signalling based aptaswitches or aptasensors are most desirable because of rapid response, simplicity, diverse measurement methods and availability of fluorophore-quencher pair for labelling (Lv et al., 2014). However, it is difficult to ensure the labelling of single aptamer molecule (monochromic approach). Therefore, researchers are focused to look for other alternatives for development of fluorescence based detection methods.

Table 3.3: Summary of reported aptasensors for analysis of AFM1 in milk samples

Methodology	Transduction principle	Linearity	LOD	Ref.
Electrochemical aptasensor (using DNA probe and gold nanoparticles)	CV and impedimetric	1-14 $\mu\text{g L}^{-1}$	-	(Dinckaya, et al., 2011)
Label free polyaniline based aptasensor	CV and SWV	6-60 ng L^{-1}	1.98 ng L^{-1}	(Nguyen et al., 2013)
SiON Ring Resonator-Based aptasensor	Ref. index	-	12.5 nM	(Guider et al., 2015)
Electrochemical aptasensor	Impedance	2 to 150 ng L^{-1}	1.15 ng L^{-1}	(Istamboulié et al., 2016)
qPCR-aptasensor	RT-qPCR amplification	1.0×10^{-4} to 1.0 $\mu\text{g L}^{-1}$	0.03 ng L^{-1}	(Guo et al., 2016)
Aptasensor	Resonator	-	1.64 $\mu\text{g L}^{-1}$	(Chalyan et al., 2017)

3.1.3.1 Structure switching signalling aptasensing platform

Due to the ease of conjugation between various fluorophore and quenchers labelled oligonucleotides/aptamers, it is easy to design fluorescence based aptaswitches. In principle, the structure switching aptaswitches recognition is based on the transduction of aptamer-

target interaction event into a measurable signal. Commonly two approaches are used in structure switching aptaswitches i.e. monochromophoric and bischromophoric approach. In monochromophoric approach, firstly, the aptamer molecule is labelled by one single fluorophore. Then, the binding of target molecule to aptamer triggers the structural conformational changes which alter the spectroscopic properties of attached fluorophore and generate signal (Fig. 3.3, (a) monochromophoric approach). In bischromophoric approach, the target induced conformational changes of the aptamer decreases the binding between fluorophore and quencher labelled complementary sequences, which alters the fluorescence properties of attached fluorophore resulting enhancement of fluorescence signal based on affinity of target analyte (Fig. 3.3, (b) bischromophoric approach) (Nutiu and Li, 2004). Herein, this effective signal generation/ enhancement come from effective fluorescence dequenching or FRET mechanism. The signal magnitude exhibited by the bischromophoric approach (aptamer beacons) is usually much higher than the single fluorophore labelled aptamer (Yamamoto et al., 2000). To date, such testimony using structure signalling platform that respond to their target analyte via conformational reformations resulting change in the fluorescence emission (FRET or fluorescence quenching) based optical detection have drawn the significant attention (Chen et al., 2012; Lv et al., 2014). To the best of our knowledge, there is no such report on structure switching aptamer assay for AFM1 detection in milk.

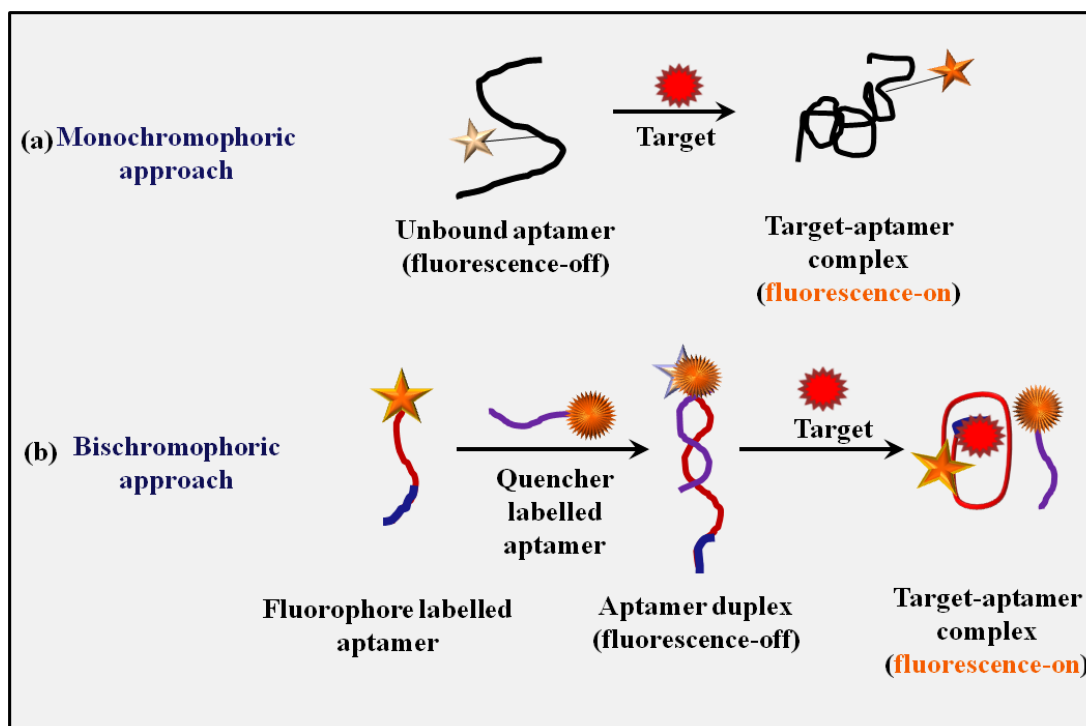


Figure 3.3: Schematic representation of structure signalling aptaswitches approaches (a) monochromatic approach, (b) bischromophoric approach.

3.1.3.2 Advantages of structure signalling aptasensing platforms

Based on tremendous advancement in aptamer technology, the aptasensing methods are best suited for analysis of mycotoxins. The bimolecular aptaswitches are aptamer/DNA/RNA molecules that reversibly changes between two or more conformations in response to the binding of specific ligand molecule. In fluorescence quenching based aptaswitches, a combination of fluorophore and quencher labelled complementary aptamer sequence based on universal phenomenon of adopting two different conformations have advantages of (Vallee-Belisle and Plaxco, 2010):

- (i) Specific-binding conformational changes transducing signal based on the hydrogen bonding and electrostatic interaction, not easily mimicked by non-specific analyte.
- (ii) Rapid, reversible and reagent-free signal transduction providing continuous and real-time monitoring.
- (iii) Versatility of approaches, allow changing the length of aptamer sequences as desired.

3.1.4 Objective

The proposed aim of this work was to develop structure switching signalling aptamer assay for quantitative detection of AFM1 and its exploration for AFM1 analysis in milk sample.

3.1.5 Methodology

For quantitative determination of AFM1, the structure switching signalling aptamer assay utilizing the rational concept of structure-switching/fluorescence-dequenching mechanism was designed to achieve the present objective (Fig. 3.4). The universal capability of aptamer to form two different conformational assemblies such as aptamer-aptamer duplex and antiparallel complex-G-quadruplex structure on target recognition was used. The fluorescein labelled anti-AFM1 aptamer sequences (F-aptamer, marked yellow) containing the AFM1 recognition site (marked blue) and its complementary sequences Q-aptamer (Quencher aptamer i.e. TAMRA-labelled aptamer sequence) were used. In the absence of AFM1, the aptamer duplex formation between fluorescence (F-aptamer) and quencher labelled aptamer (Q-aptamer) results in fluorescence-off. Because, in this arrangement the fluorophore and quencher comes in close proximity, thus resulting fluorescence quenching (Fig. 3.4a). When the AFM1 is added, due to the high affinity of F-aptamer toward AFM1, the aptamer duplex complex transformed into an AFM1-aptamer complex with a concomitant release of Q-

aptamer, which results in enhancement of fluorescence intensity corresponds to the AFM1 binding (Fig. 3.4b). This decreases the interaction between F-aptamer and Q-aptamer thus producing an increase in fluorescence intensity (dequenching). The quenching percentage (Q %) signal intensities were calculated as

$$Q (\%) = [1 - F_{-AFM1} / F_{+AFM1}] \quad (3.1)$$

where, F_{-AFM1} and F_{+AFM1} are the fluorescence intensity in the absence and presence of AFM1.

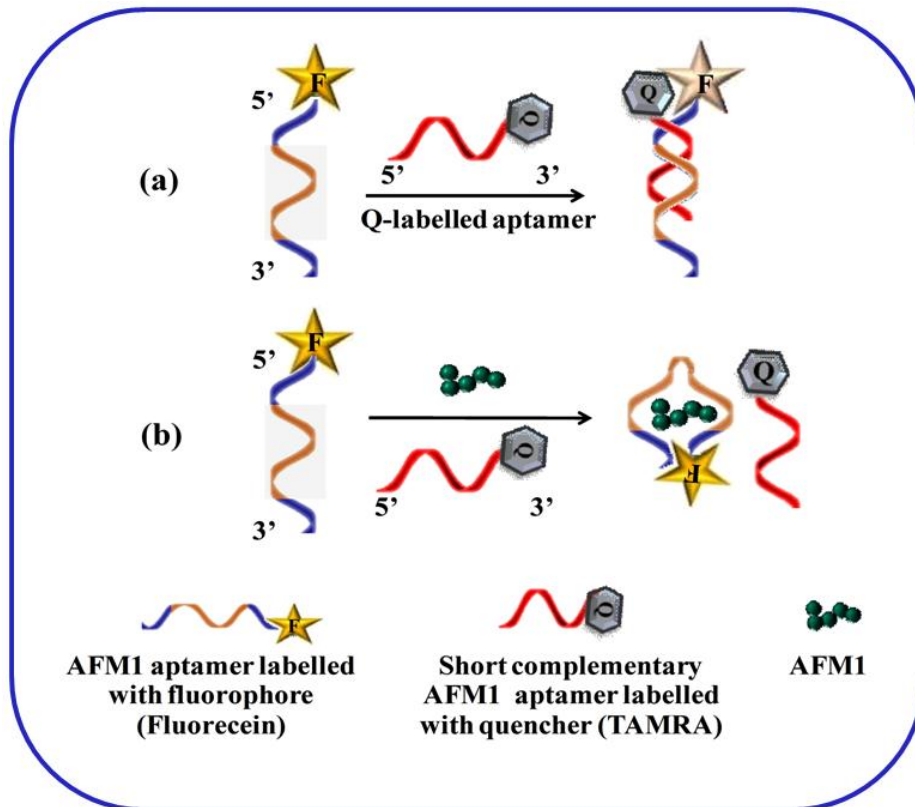


Figure 3.4: Principle of structure switching signalling aptamer assay for AFM1 detection.

3.2. Experimental section

3.2.1 Biochemicals and chemicals

HEPES sodium salt, potassium dihydrogen phosphate (KH_2PO_4), disodium hydrogen phosphate (Na_2HPO_4), magnesium chloride (MgCl_2), potassium chloride (KCl), calcium chloride (CaCl_2) and sodium chloride (NaCl) were procured from Sigma-Aldrich (France). AFM1 was purchased from Cluzeau Info Labo (France). Deionized Milli-Q water (Millipore,

Bedford, MA, USA) was used for reagent preparation. The AFM1 ELISA kit was procured from R-Biopharm AG (Darmstadt, Germany).

anti-AFM1 aptamers with 21 base sequences (7 base pairs) labelled with fluorescein (FAM) and its complementary sequences (TAMRA labelled, 7 and 9 base sequences) were prepared and purified by Microsynth (Switzerland). Different variants of FAM labelled (F-aptamer) and TAMRA labelled (Q-aptamer) complementary aptamer sequences were used. The details of aptamer sequences have been summarized in Table 3.4.

Table 3.4: Description of anti-AFM1 aptamer and complementary aptamer sequences used

S. No.	anti-AFM1 aptamer sequences (fluorescein labelled anti-AFM1 aptamer sequences)	anti-AFM1 complementary aptamer (TAMRA labelled anti-AFM1 aptamer sequences)
1.	F-aptamer (labelled at 5' end) 5'-FAM-ACT GCT AGA GAT TTT CCA CAT-3'	Q-aptamer (7 base sequences) 3'-TAMRA-TGA CGA T-5' Q-aptamer (9 base sequences) 3'-TAMRA-TGA CGA TCT-5'
2.	F-aptamer (labelled at 3' end) 5'-ACT GCT AGA GAT TTT CCA CAT-FAM-3'	Q-aptamer (7 base sequences) 3'-A GGTGTA-TAMRA-5' Q-aptamer (9 base sequences) 3'-AAA GGT GTA -TAMRA-5'

3.2.2 Instrumentation

All fluorescence measurements were carried out in standard 96 black microwell plate (Thermo Fisher Scientific, Denmark) format at excitation and emission wavelength of 485 nm and 538 nm respectively, using Fluoroskan Ascent FL 2.6 equipped with an Ascent software version 2.6 (Thermo Scientific-Finland). UV-visible spectrophotometer (UV-1800, Shimadzu, Japan) equipped with the TCC controller (TCC 240A) was used to measure the UV absorption characteristics of F-aptamer, aptamer duplex and aptamer-AFM1 complex.

3.2.3 Solution preparation

3.2.3.1 Preparation of binding buffer

The binding buffer was prepared by the following method: an appropriate amount of HEPES sodium salt containing 5 mM KCl, 5 mM MgCl₂ and 120 mM NaCl was dissolved in deionized Milli-Q water for preparation of HBB (50 mM, pH 7.0). All buffer solutions were stored at 4 °C when not in use.

3.2.3.2 Preparation of AFM1 standard solutions

AFM1 stock solution was prepared by dissolving AFM1 powder in 5 % ACN (v/v) in HBB at a concentration of 1 mg mL⁻¹ and stored at -20 °C, when not in use. Subsequently, the stock solution were diluted in HBB (containing 2 % ACN v/v) in the range 1-2000 ng kg⁻¹ to meet the regulatory requirements of European Commission i.e. 50 ng kg⁻¹ (milk) and 25 ng kg⁻¹ (infant milk formula).

3.2.3.3 Preparation of AFM1 aptamer solutions

Initially, the stock solution of anti-AFM1 F-aptamers and Q-aptamers were prepared in the sterilized deionized Milli-Q water. Subsequently, the stock solution of 100 μM anti-AFM1 F-aptamer and complementary Q-aptamer were diluted in the range of 0.062-2 μM in HBB. A PCR thermocycler (Mastercycler personal Eppendorf VWR, Leuven, Belgium) was used for aptamer pre-treatment. Before, each experimentation the aptamer solution was placed in a thermocycler with the following temperature profile: heating at 85 °C for 5 min to initial denaturation step, followed by a structure maintain step at 4 °C for 5 min.

3.2.3.4 Preparation of milk sample for AFM1 analysis

Performance of developed aptamer assay platform was verified in the AFM1 spiked milk samples. The raw milk sample (3% fat content) was purchased from the local market of Perpignan, France. The matrix treatment such as dissolving of fat by acid (trichloroacetic acid, TCA) decreases the real matrix composition. To avoid such problem, milk sample was first centrifuge at 5000 rpm for 10 min (at 27 °C). The supernatant was taken out and spiked with known concentration of AFM1. The pH and ionic strength of milk samples were checked and adjusted before analysis. Further, milk samples were diluted with non-contaminated centrifuged milk sample to obtain the desired concentration of AFM1 spiked milk samples i.e. 25, 50 and 500 ng kg⁻¹. A similar sample preparation procedure was adopted for the analysis of AFM1 using commercial ELISA Kit. For recovery studies, dilution factor was taken into consideration.

3.2.4 UV characterization

The structure switching confirmation of antiparallel G-quadruplex aptamer-AFM1 complex and aptamer-aptamer duplex were characterized by performing UV measurements in the range of 220-400 nm. The UV absorption measurement of F-aptamer (0.5 μM) was measured in the absence and presence of complementary sequence (Q-aptamers) and AFM1. The concentration of complementary sequence (0.5 μM) and AFM1 (50 ng kg^{-1}) were added individually and in mixture and incubated with F-aptamer before further measurements. Finally, the F-aptamer, AFM1 and Q-aptamers were mixed together to study the absorption characteristics of assay solution.

3.2.5 Fluorescence measurements

The optimized concentration of F-aptamer 0.5 μM (75 pmol) was incubated with variants concentration of Q-aptamer at different ratios 1:1, 1:2, 1:3 and 1:4. Optimized ratio with low background signal was selected for further experimentation. The evidence of structure switching or quenching studies was confirmed by temperature profiles studies as follows: the solution containing both F-aptamer and Q-aptamer was incubated for a total incubation time of 100 min at different temperature, first at 15 $^{\circ}\text{C}$ for 20 min, next at 30/ 37.5/ 45 $^{\circ}\text{C}$ for 60 min and finally at 22 $^{\circ}\text{C}$ for 20 min. Fluorescence intensities were recorded initially at every 5 min followed by 10 min at different increased temperatures. For quantitative determination of AFM1, F-aptamer was allowed to incubate with different concentration of AFM1 (1-2000 ng kg^{-1}) for 1 h followed by addition of equimolar concentration of Q-aptamer and incubated for 1 min at RT. The fluorescence responses were measured using Fluoroskan Ascent FL 2.6 and calculated for further analysis.

3.3 Results and Discussion

3.3.1 Optimization of experimental parameters

The analytical performance of structure switching signalling aptamer assay depends upon several parameters such as optimal concentration of fluorescent aptamer, ratio of fluorescent and quencher labelled aptamer sequences, pH, ionic strength and incubation time were optimized in 96 microplate platform.

3.3.1.1 Optimization of F-aptamer (fluorescein labelled anti-AFM1 aptamer)

For designing the structure switching signaling aptamer assay to detect AFM1 utilizing the fluorescence quenching-dequenching mechanism, selection of an optimal concentration of F-aptamer exhibiting the enough fluorescence intensity was highly important. Therefore, the fluorescence intensity of various F-aptamer (anti-AFM1 aptamer) concentrations ranging 0.062-2.0 μ M was studied. The F-aptamer (0.5 μ M) with fluorescence response of 105 ± 2.8 a.u (n=3, at λ_{ex} 485 nm; λ_{em} 538 nm) was selected as optimal for further experimentation (Fig. 3.5). Higher aptamer concentrations may increase the output signal but ultimately results in low sensitivity of the assay.

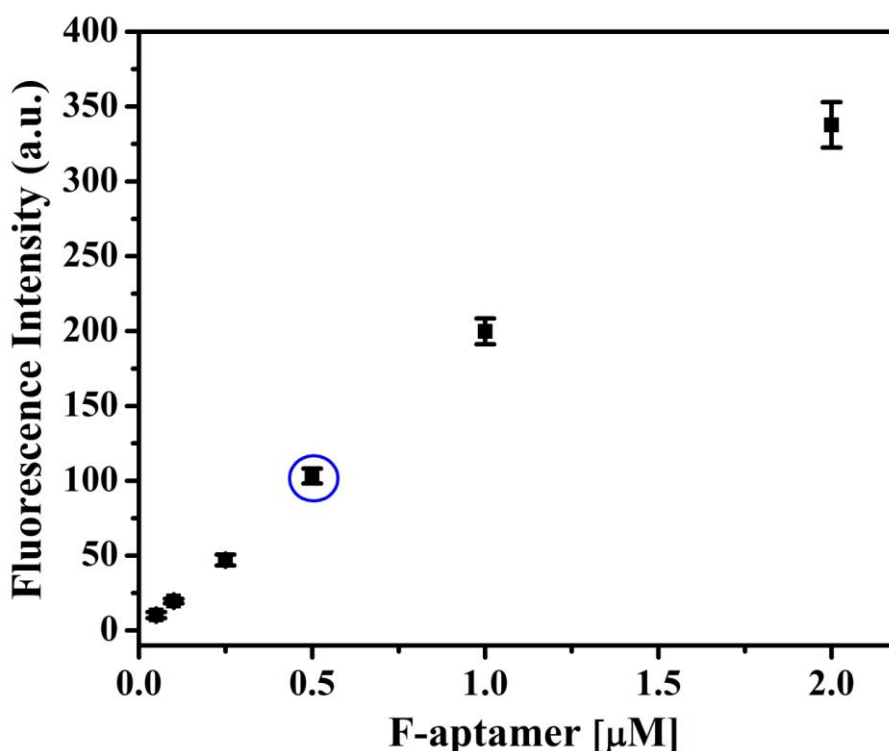


Figure 3.5: Fluorescence intensity response of different aptamer concentration in HBB (50 mM, pH 7.0).

3.3.1.2 Optimization of aptamer-quencher ratio

The quenching abilities of two complementary sequences of anti-AFM1 aptamer (Q-aptamers) were evaluated against the two specific anti-AFM1 aptamers (F-aptamers) labelled at different ends (as discussed under section 3.2.1). On hybridization, the formation of aptamer-aptamer duplex (F-aptamer : Q-aptamer duplex) resulted in fluorescence quenching against both the Q-aptamer sequences (7 and 9 bases). Different ratios F-aptamer : Q-aptamer

(1:1 to 1:4) was used to quantify the quenching magnitudes (Fig. 3.6). It is evident that the quenching percentage (Q %) was increased from 1:1 to 1:3 ratios with no further change in quenching efficiency was recorded with increase in quencher ratio. The maximum quenching of $\sim 70.83 \pm 1.04$ % (7 bases) and 91.23 ± 0.86 % (9 bases) was obtained at the optimal ratio. The quenching efficiency of Q-aptamers was also investigated against 3' labelled F-aptamer of AFM1. Maximum fluorescence recovery response was obtained with 5' labelled anti-AFM1 aptamer sequence. The reason was attributed to the presence of AFM1 binding domain, which is present near the 3' end, however, the fluorophore labelling at 3' end results in steric hindrance in AFM1 recognition and decrease responses.

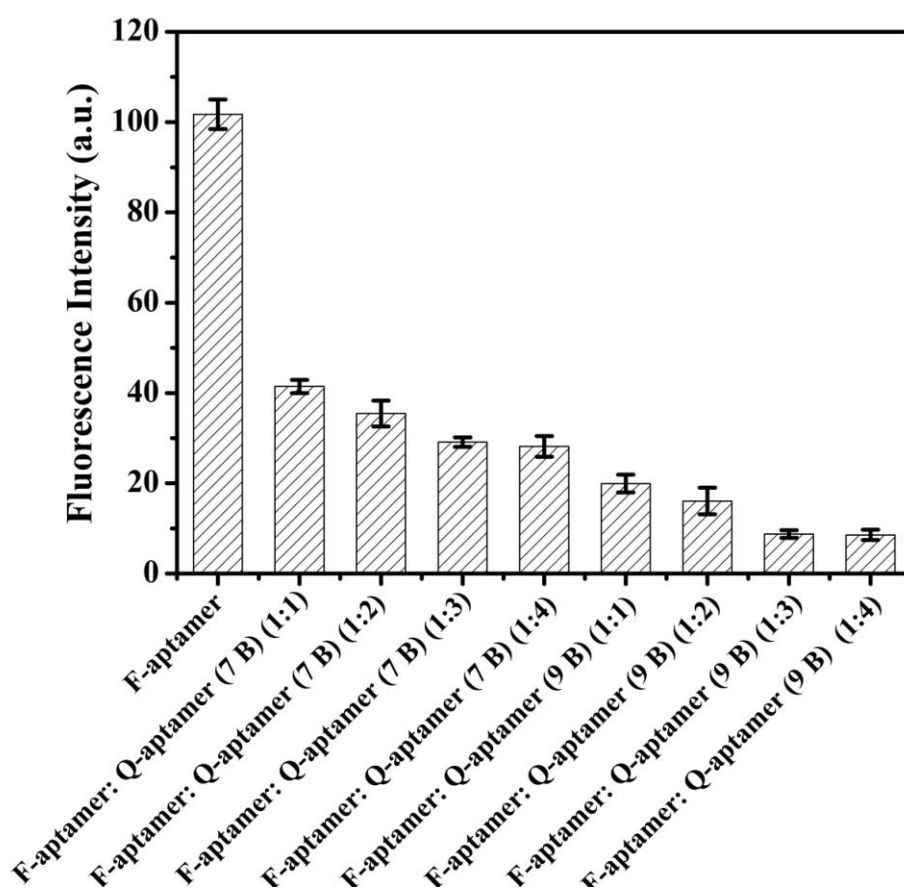


Figure 3.6: Optimization of F-aptamer: Q-aptamer ratio with two different quencher base complementary sequences (7 and 9 Bases).

3.3.1.3 Effect of buffer, ionic strength and pH

The effect of buffer, ionic strength and medium pH, which could significantly affects the binding interaction were investigated. The effects of two different buffer systems were studied to quantify the fluorescence and quenching phenomenon. Maximum quenching efficiency was observed in the HBB as shown in Fig. 3.7a. This was due to the non-specific

artifact effects of sodium ions (in PBB), which renders the hybridization (aptamer duplex formation) mechanism and quenching efficiency due to unfavorable effects on melting temperature and aptamer stability (Ponikova et al., 2008). The optimal ionic strength of binding buffer plays a significant role in aptamer recognition activity. Ionic strength of HBB was studied from 10 to 100 mM and maximum quenching was observed at 50 mM HBB (Fig. 3.7b). The activity of an aptamer (ssDNA) is based on pH-dependent conformational changes by folding/ unfolding of the 3D complex (triplex stem structure) at various pH (Porchetta et al., 2015). Therefore, the effect of pH was studied over a range of 6.8-7.6 in HBB. The maximum quenching performance due to the formation of aptamer duplex (F-aptamer and Q-aptamer duplex) was obtained at pH 7.0 HBB (Fig. 3.7c). This was a strong indication that

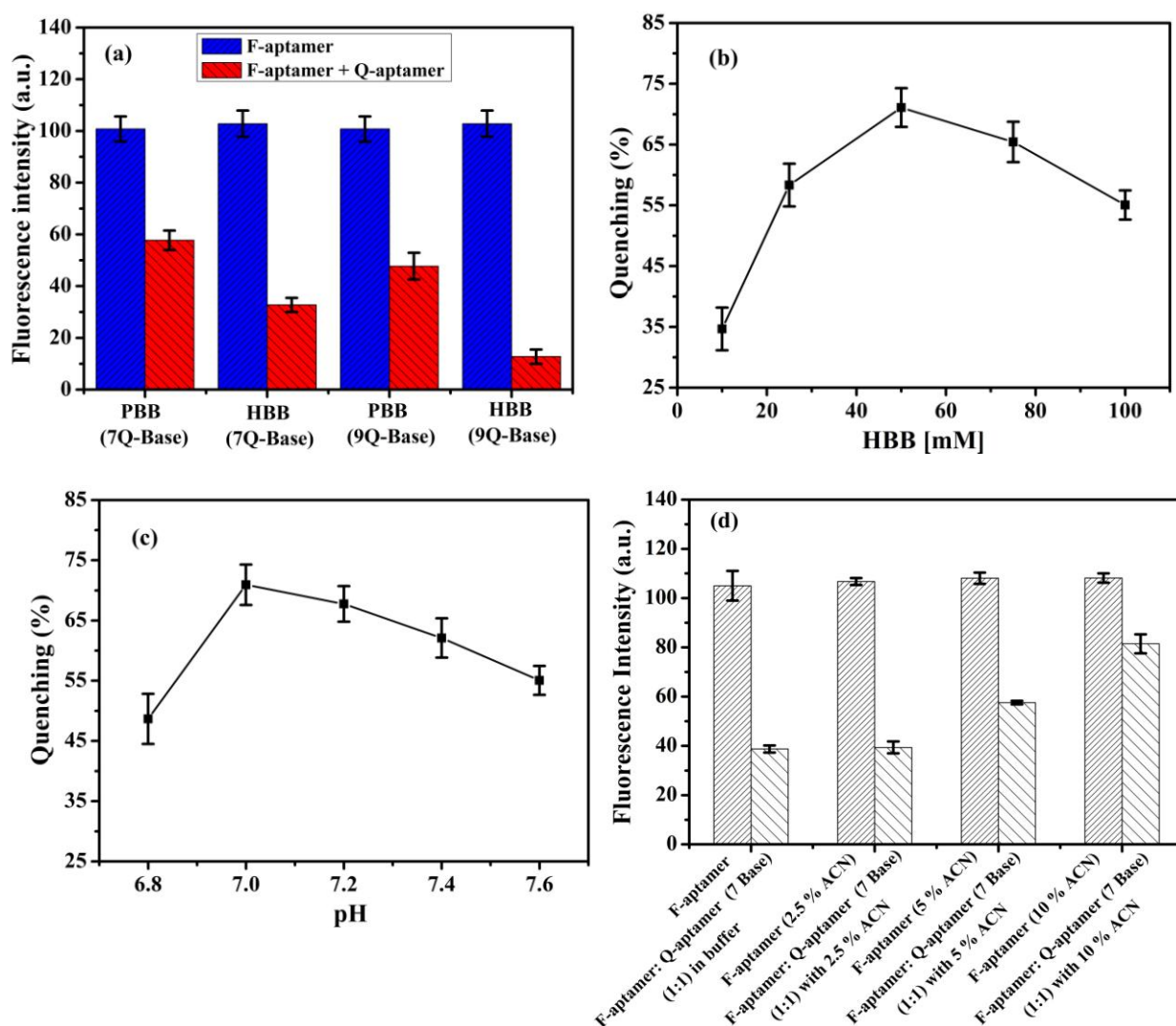


Figure 3.7: Effect of (a) Buffers (PBB and HBB); (b) ionic strength of HBB; (c) Effect of pH; (d) solvent (%) on quenching efficiency.

with increase in pH of binding buffer, the aptamer conformational structure is not stable. As discussed in experimental section, the AFM1 stock was initially prepared in the ACN solvent; therefore the effect of ACN on method performance was optimized. From Fig. 3.7d, with increase in ACN concentration the fluorescence quenching is decreasing, this might be due to interruption in the bonding interaction of aptamer sequences, which ultimately alters the aptamer stability. Experimentally, it was concluded that the ACN percentage below 2.5 % of total assay volume was optimal, which did not affect the quenching and fluorescence recovery performance (Fig. 3.7d).

3.3.1.4 Temperature-changing profile studies

To investigate the effect of temperature on structure switching of aptamer, a series of temperature mismatch fluorescence assays were performed (Fig. 3.8). In each studies, the F-aptamer/Q-aptamer duplex was incubated for a total incubation time of 100 min with varying temperature conditions as follow: first at 15 °C for 20 min, next at designated temperature (30, 37.5, 45 °C) for 60 min followed by an increase in temperature (1 °/min) and finally at 22 °C for 20 min. The low fluorescence response of aptamer duplex was observed with immediate formation of F-aptamer/ Q-aptamer duplex and it sustained at low temperature (15 °C), due to the aptamer duplex stability. With increase in the temperature, the transition of F-aptamer/Q-aptamer duplex occurred due to the unwinding of duplex, which is an indicative of denaturation of duplex assembly over heating (Nutiu and Li, 2003). The achievement of stable fluorescence intensity response with each rising temperature confirmed that equilibrium was occurred between free and bound Q-aptamer to duplex assembly. When the temperature was again lowered to 22 °C, the fluorescence intensity starts dropping owing to the reassociation of free Q-aptamer to aptamer duplex structure (Fig. 3.8a and 3.8b).

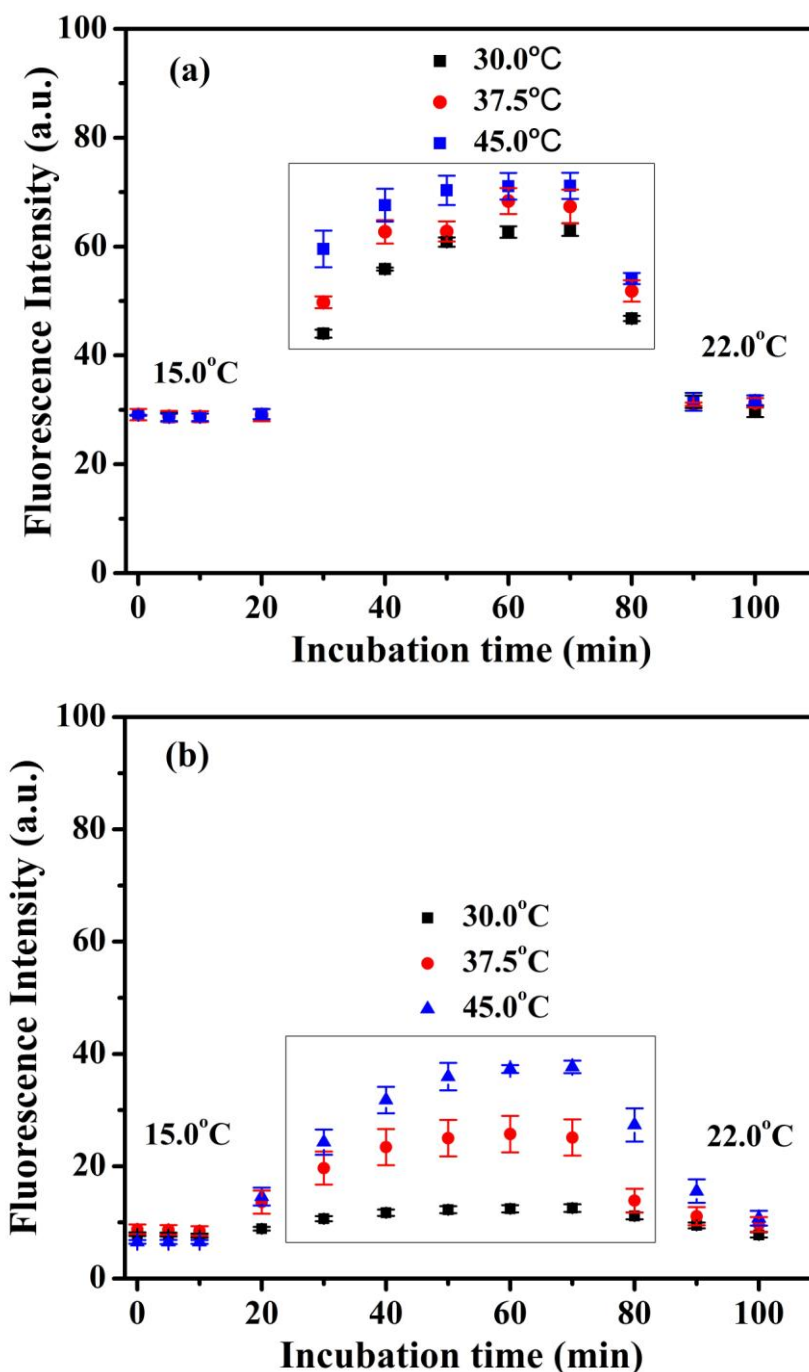


Figure 3.8: Temperature mismatch profile studies of structure switching of aptamer duplex against quencher (a) 7 bases and (b) 9 bases.

3.3.2 Evidences of structure switching mechanism

3.3.2.1 UV characterization

The evidence of structure switching mechanism was verified by UV spectral measurements (Fig. 3.9). The characteristics UV absorption maxima (λ_{\max}) of Q-aptamer and F-aptamer were obtained at 254 nm (Q-aptamer, spectrum a) and 259 nm (F-aptamer, spectrum b),

respectively. Upon hybridization of F and Q aptamer specific to AFM1, the aptamer duplex showed the appearance of new absorption peak at 257 nm with a change in peak intensity, which strongly emphasizes the formation of aptamer-aptamer duplex formation (spectrum e) (Islam et al., 2015). Due to the two different aptamer conformations, the UV absorption properties of aptamer complexes might also varied. The formation of antiparallel G-quadruplex AFM1-aptamer complex showed UV absorption at 259 nm (spectrum c) with increase in absorption intensity compared to F-aptamer (spectrum b), indicating the AFM1-aptamer interaction. On addition of AFM1 (50 ng kg⁻¹), the UV absorption of aptamer duplex is decreased with a change in peak position from 257 nm to 259 nm (spectrum d). The decrease in UV absorption peak intensity of aptamer duplex strongly indicates the target induced antiparallel G-quadruplex tertiary complex formation. These results strongly suggest that the obtained fluorescence recovery response were due to the AFM1 induced interaction between AFM1 and F-aptamer (Katilius et al., 2006). The comparative results have been tabulated in Table 3.5.

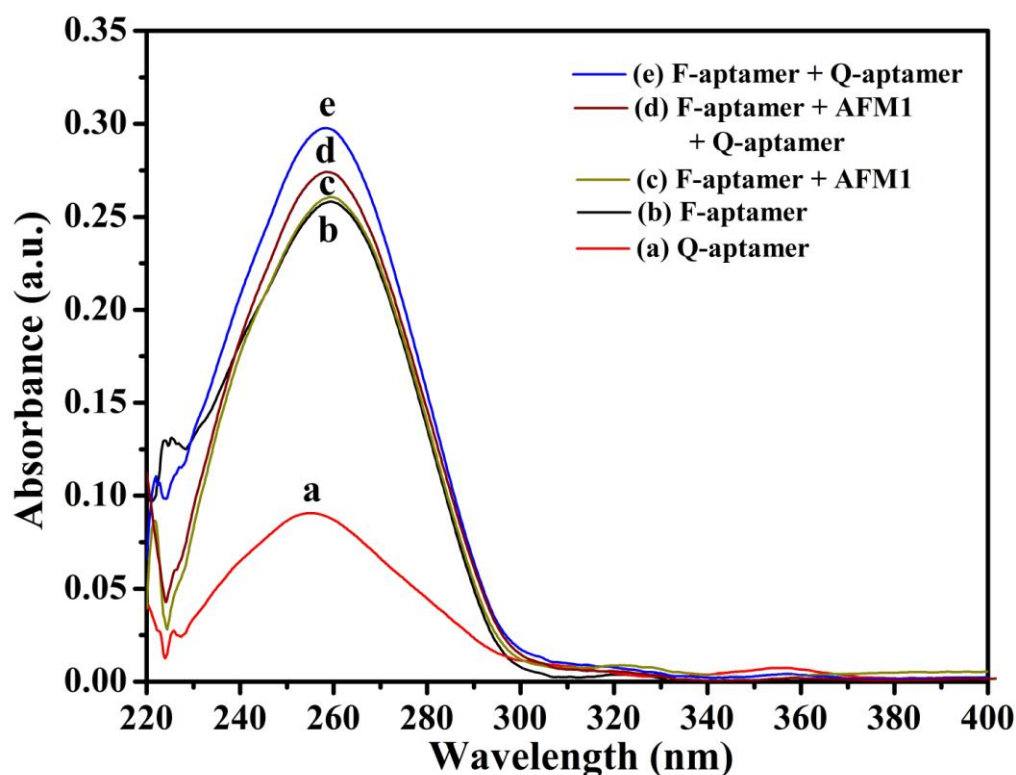


Figure 3.9: UV absorption characterizations for evidence of structure switching mechanism.

Table 3.5: UV absorption results for structure switching mechanism

Spectrum	Description	Wavelength (λ_{\max}) (nm)	Absorbance (a.u.)
a.	Q-aptamer	254	0.0909
b.	F-aptamer	259	0.2589
c.	F-aptamer + AFM1	259	0.2630
d.	F-aptamer + AFM1 + Q-aptamer	259	0.2706
e.	F-aptamer + Q-aptamer	257	0.2985

3.3.2.2 Response optimization

Under the optimized experimental conditions, the fluorescence measurements were recorded for AFM1 detection (50 ng kg^{-1}). The fluorescence recovery response was higher with Q-aptamer (7 bases) over the Q-aptamer (9 bases) (Fig. 3.10). No fluorescence recovery response was observed with 3'FAM labelled AFM1 aptamer. Thus, based on these observations and results, the structure switching signalling aptamer assay was performed for detection of AFM1.

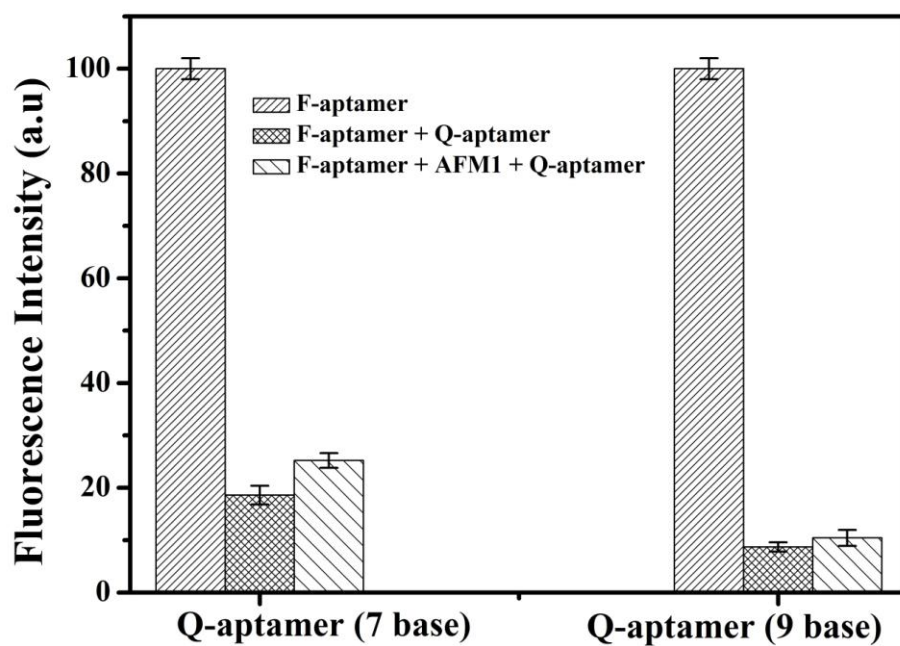


Figure 3.10: Fluorescence response studies of aptasensing platform with 7 and 9 based on Q-aptamer.

3.3.2.3 Fluorimetric measurements

Post optimization of response parameters, the fluorimetric spectral measurements were carried out against different AFM1 concentrations using Fluorimeter (Jasco, Japan). It is evident from the result that the fluorescence peak intensity of F-aptamer (spectrum e) quenched in presence of Q-aptamer (spectrum a) (Fig. 3.11) with slight change in peak position. Further, with increase in AFM1 concentration from 50, 500, 1000 ng kg⁻¹ (spectrum b-d), fluorescence signal intensity start increasing i.e. the quenched fluorescence recovered. This shows that the AFM1 molecule has highly specific binding interaction with F-aptamer (anti-AFM1 aptamer), which resulted in generation of AFM1 induced G-quadruplex AFM1-aptamer complex. The structural conformation increased the distance between F-aptamer and Q-aptamer, which is responsible for recovered fluorescence. These results were in strong agreement with the UV measurements (Fig. 3.9).

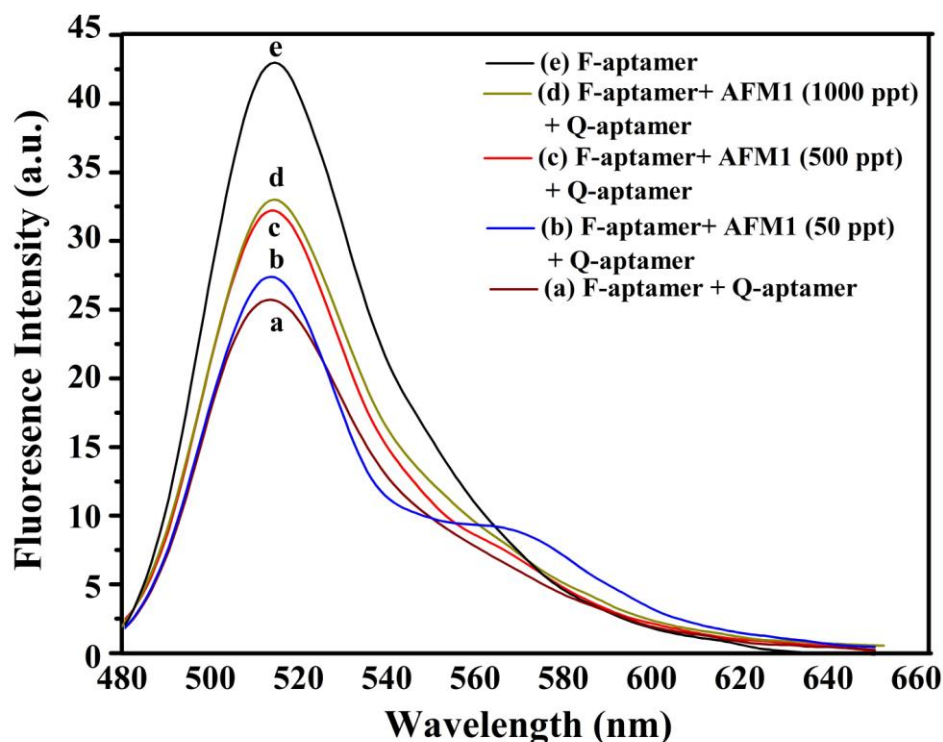


Figure 3.11: Fluorescence spectrum of structure switching aptaswitches for various concentration of AFM1 (50, 500, 1000 ng kg⁻¹).

3.3.3 Calibration curve for AFM1 detection

The ability of F-aptamer (anti-AFM1 aptamer) to selectively bind AFM1 was used for quantitative determination of AFM1. The efficiency of proposed structure switching aptamer assay was tested by exposing to different concentrations of AFM1. The calibration was

constructed in HBB (as the reference) prior to milk analysis. The recovered fluorescence intensity percentage corresponding to various AFM1 concentrations from 1.0-2000 ng kg⁻¹ has been plotted using the both combinations of F-aptamer and Q-aptamer (7 and 9 bases) (Fig. 3.12 and 3.13). Encouragingly, the recovered fluorescence intensity (%) was found to be increase corresponds to the increase in AFM1 concentrations. The increase in recovered fluorescence intensity (%) was due to the high binding affinity of AFM1 to form anti-AFM1 aptamer tertiary complex. Each experimental data is the mean of different individual aptamer assays measurements in triplicate.

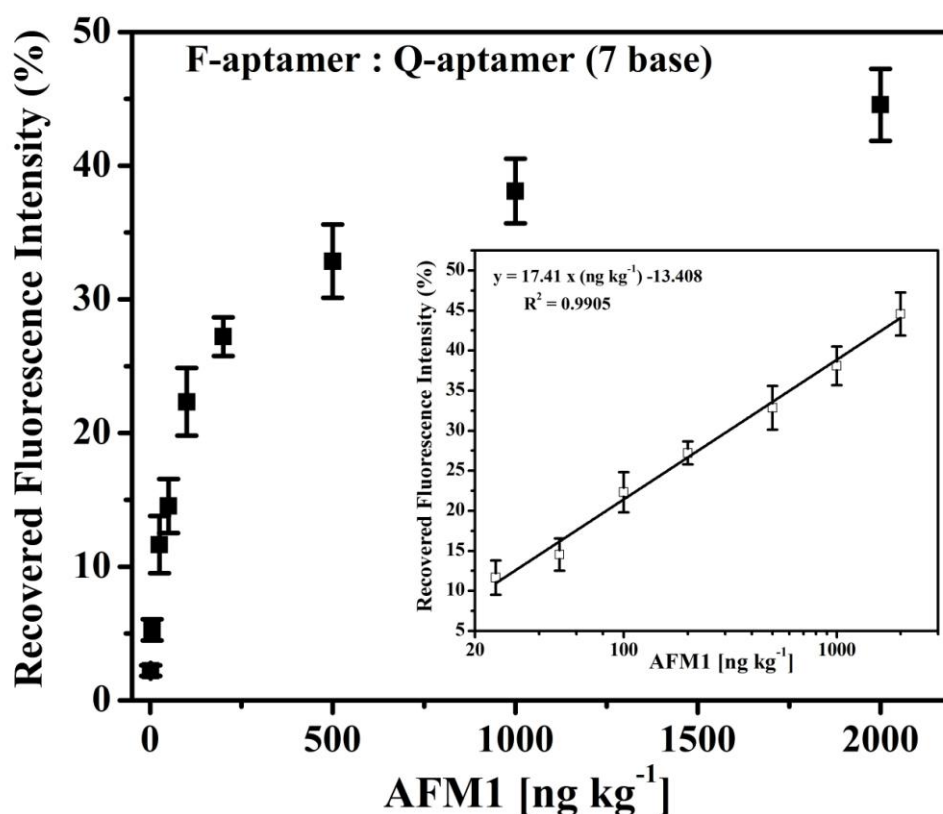


Figure 3.12: Calibration curve obtained for AFM1 in HBB at pH 7.4 with 7 Base quencher sequences (Inset show the linear fit graph).

A good linearity was obtained in the range 25-2000 ng kg⁻¹ with a line of equation $y = 17.41 x (\text{ng kg}^{-1}) - 13.408$ (7 bases), $R^2 = 0.9905$ (n=3) and $y = 14.70 x (\text{ng kg}^{-1}) - 12.354$ (9 bases), $R^2 = 0.9905$ (n=3). The sensitivity of 17.41 ng kg⁻¹ for 7 base quencher sequences and 14.70 ng kg⁻¹ for 9 base quencher sequences was calculated with a minimum detection limit (LOD) of 5.0 ng kg⁻¹ (S/N = 3) from both calibration curve. Similarly, the limit of quantification (LOQ) was calculated and found to be 25 ng kg⁻¹ (S/N = 10). These results strongly suggested

that the analytical figure of merits in presented structure switching assay are in good correlation with the reported literature as tabulated in Table 3.2 and 3.3.

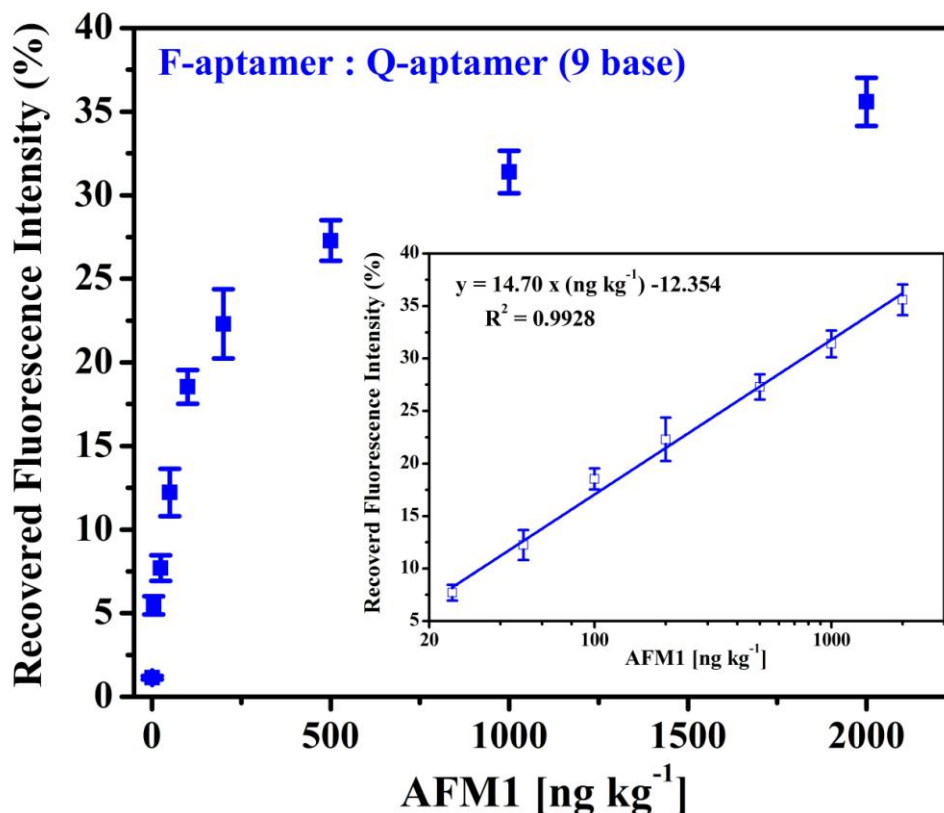


Figure 3.13: Calibration curve obtained for AFM1 in HBB at pH 7.4 with 9 base quencher sequences (Inset shows the linear fit graph).

3.3.4 Specificity and selectivity of aptamer assay

Before application to real sample analysis, the selectivity and specificity of developed platform were important parameters were investigated to evaluate the performance of method. The selectivity studies were performed against structural (AFB1) and non-structural analogue (OTA) at two different concentrations 50 and 500 ng kg^{-1} of each analyte spiked in HBB. The recovered fluorescence intensity (%) of AFB1 and OTA were found to be less than 10% ($n = 3$) compare to response of AFM1 (Fig. 3.14). The results have been tabulated in Table 3.6. This high specificity and selectivity of method were attributed to the aptamer sequence used, which has high selective binding to AFM1 in presence of other cross contaminants. Therefore, the obtained response was due to the formation of aptamer-AFM1 tertiary complex.

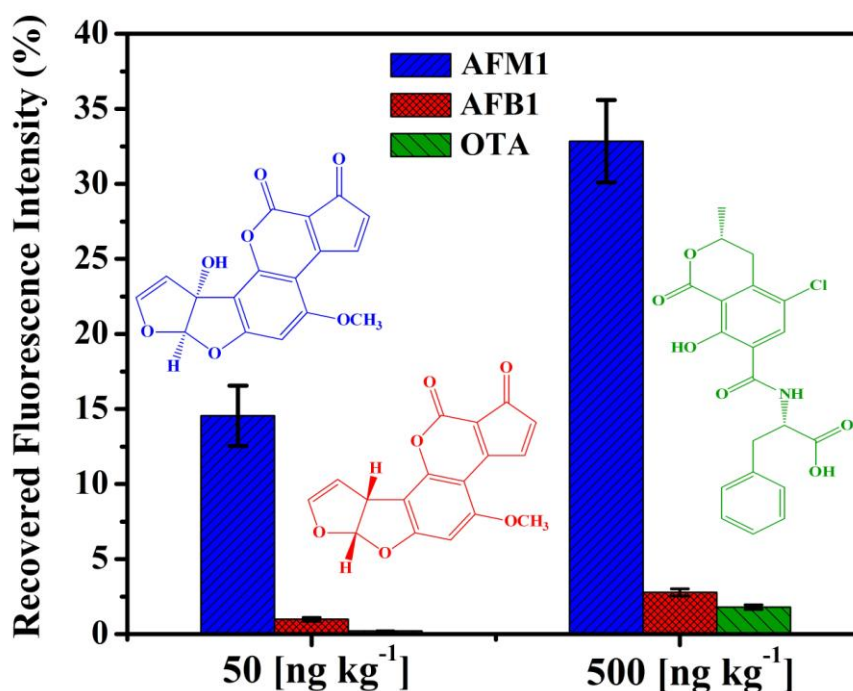


Figure 3.14: Specificity studies of aptamer assay with structural (AFB1) and non structural analogue (OTA) at 50 and 500 ng kg⁻¹.

Table 3.6: Selectivity performance of aptamer assay for AFM 1 detection

Analyte conc ⁿ . [ng kg ⁻¹]	AFM 1 recovered fluorescence intensity (%)		AFB 1 recovered fluorescence intensity (%)		OTA recovered fluorescence intensity (%)		% response of AFB1 (F _{AFB 1} /F _{AFM 1} X 100)	% response of OTA (F _{OTA} /F _{AFM 1} X 100)
	Mean ± S.D. (n=3)	% R.S.D.	Mean ± S.D. (n=3)	% R.S.D.	Mean ± S.D. (n=3)	% R.S.D.		
50	14.53 ± 2.01	13.84	0.98 ± 0.14	13.87	0.19 ± 0.03	14.11	6.75	1.31
500	32.84 ± 2.76	8.39	2.77 ± 0.23	8.36	1.79 ± 0.15	8.34	8.43	5.45

3.3.5 Milk analysis

The feasibility of developed structure switching aptamer assay was further investigated for analysis of AFM1 levels in spiked milk samples at varying concentration levels of 25, 50 and 500 ng kg⁻¹. The selection of spiked concentrations was from the dynamic range of calibration curve including regulatory levels. Similarly, the control milk samples were prepared by adding same amount of AFM1 (25, 50 and 500 ng kg⁻¹) in HBB (50 mM, pH 7).

Keeping the primary objective of work in mind, procedure was optimized in such a way that no requirement of complex matrix treatment required before milk sample analysis. The recoveries were calculated based on the response obtained from buffer and AFM1 spiked milk sample. Recoveries were found to be in good agreement i.e. 94.40-95.28% (n = 3) with the AFM1 spiked concentrations, ranging with a maximum % RSD of 4.34 for triplicate measurements. The results have been tabulated in the Table 3.7. It is evident that the developed assay platform paves the suitability of platform for detection of AFM1 in non-treated spiked milk samples.

Table 3.7: Recovery performance of structure switching aptamer assay for detection of AFM1 in spiked milk sample

Recovery calculation from AFM1 spiked milk sample					
Milk Sample	AFM 1 added [ng kg ⁻¹]	AFM 1 found [ng kg ⁻¹] Mean ± S.D. (n=3)	% R.S.D.	% R. E.	% Recovery
1.	25.00	23.60 ± 1.02	4.34	-95.66	94.40
2.	50.00	47.61 ± 1.82	3.83	-96.17	95.22
3.	500.00	476.40 ± 8.79	1.85	-98.15	95.28

3.3.6 Precision of developed assay

The reproducibility and repeatability (precision analytical parameters) of aptamer assay was investigated by intra and inter day precision studies. Precision studies were carried out at 50 ng kg⁻¹ AFM1 concentration under optimized experimental conditions. The control measurements were carried out to calculate the % recovery responses. All experiments were performed three times in triplicates. The intraday precision with % RSD of 3.47 (n=9) was calculated, which was an indicative of good reproducibility of structure switching fluorescence quenching based aptamer assay for AFM1 analysis. Similarly, for interday precision, the % RSD from 4.47 to 6.05 (n = 3) was calculated confirming the reliability and reproducibility of the method. The comparative and calculated results have been illustrated in Table 3.8.

Table 3.8: Precision performance of developed assay for detection of AFM1

Interday performance of fluorescence aptamer assay						
Days	AFM 1 added [ng kg⁻¹]	Recovered Fluorescence Intensity (%) Mean ± S.D. (n=3)			% R.S.D.	% R. E.
1.	50.00	14.54 ± 0.654			4.47	-95.53
2.	50.00	14.56 ± 0.772			5.27	-94.73
3.	50.00	14.40 ± 0.874			6.05	-93.95
Intraday performance of fluorescence aptamer assay						
AFM 1 added [ng kg⁻¹]	Recovered Fluorescence Intensity (%)			Mean ± S.D. (n=3)	% R.S.D.	
	Response-1	Response-2	Response-3			
50.00	14.44	15.42	14.64	14.83 ± 0.514	3.47	

3.3.7 Cross-validation of developed aptamer assay with AFM1 ELISA Kit

The applicability of developed aptamer assay was tested and cross validated against the commercially available AFM1 ELISA kit. To validate the precision, the milk samples were analyzed using the commercial colorimetric kit and developed platform at same time. The analytical merits of figures of quenching based structure switching AFM1 aptamer assay were compared with Ridascreen ELISA kit procured from R-Biopharm AG (Darmstadt, Germany). The ELISA kit detect AFM1 on basis of sandwich ELISA using two types of antibodies and a wider dynamic range of antigens (0-2000 ng L⁻¹) as per the instructions. In principle, the AFM1 concentrations were measured on basis of absorbance using a microwell plate reader at 450 nm. The intensity of absorbance was inversely proportional to the concentration of AFM1 present in milk samples. Measurements were carried out at three different levels of AFM1 (25, 50 and 500 ng kg⁻¹) and % recovery was calculated.

The results obtained from the developed structure switching aptamer assay and ELISA kit were analysed and compared. The recoveries from the developed structure switching signalling AFM1 aptamer assay (94.40-95.28% with % R.S.D. (n=3) 1.85 - 4.34) was similar

to the recoveries obtained from the commercial AFM1 ELISA kit (94.20-96.04%, % R.S.D. (n=3) 0.91 – 4.62). Good correlation in terms of sensitivity and reproducibility was observed as summarized in Table 3.9.

Table 3.9: Recovery studies of AFM1 in milk sample from aptamer AFM1 assay and commercial ELISA kit

Comparison of structure switching aptamer assay with commercial kit for AFM1 detection							
Milk	AFM 1 added [ng kg ⁻¹]	AFM 1 found [ng kg ⁻¹] Mean ± S.D. (n=3)		% RSD		% Recovery	
		Aptamer Assay	ELISA kit	Aptamer Assay	ELISA kit	Aptamer Assay	ELISA kit
1.	25.00	23.60 ± 1.02	23.55 ± 1.09	4.34	4.62	94.40	94.20
2.	50.00	47.61 ± 1.82	47.95 ± 1.05	3.83	2.19	95.22	95.90
3.	500.0	476.4 ± 8.79	480.2 ± 4.38	1.85	0.91	95.28	96.04

The dynamic range and the upper limit of detection for the AFM1 in milk sample using the developed assay and kit were found in the confidence level of more than 98 %. Analysis time for aptamer assay is 1 h for AFM1 analysis with high throughput of 32 samples/h in triplicate, whereas with commercial kit up to 48 samples could be analyzed (in duplicate) in 2 h. For, aptamer assay the response is faster due to high affinity between AFM1 and aptamer sequences and principle employed for determination of AFM1, whereas the sandwich ELISA involved in the ELISA kit involving incubation and multi reaction step increased with reaction time. Present studies suggested that the developed structure switching signalling aptamer assay for AFM1 shows good precision and accuracy in comparison to the commercially available ELISA kits for AFM1 detection as compared in Table 3.9.

Table 3.10: Comparison of analytical figures of merits of aptamer assay and ELISA kit

Parameters	Techniques		
	Structure switching aptamer assay	Ridascreen 30/15 kit	Ridascreen Fast kit
Dynamic range	5-2000 ng kg ⁻¹	0-80 ng kg ⁻¹	0-2000 ng kg ⁻¹
Limit of detection	1.0 ng kg ⁻¹	5 and 50 ng kg ⁻¹	<367 ng kg ⁻¹
Limit of quantification	5.0 ng kg ⁻¹	25 ng kg ⁻¹	500 ng kg ⁻¹
Recovery percentage with relative standard deviation	94.40-95.28% (%RSD= 1.85-4.34)	90.20-93.50% (% R.S.D= 3.50-8.62)	94.20-96.04% (% R.S.D= 0.91-4.62)
Time requirement	1.0 h/32 samples	1.5 h/48 samples	0.5 h/24 samples
Sample volume	15 µL	100 µL	50 µL
High throughput	96	96	48

3.4 Conclusions

In conclusion, the significance of the present work demonstrates the design of structure switching signalling fluorescence quenching based aptamer assay for the detection of AFM1. A novel structure switching signalling aptamer assay with the implementation of fluorescence quenching principle has been developed for quantification of AFM1 in milk samples (with no complex matrix matching procedure). The developed aptamer assay offers the advantage of simplicity of structure switching aptamer for AFM1 analysis. A linearity of 25-2000 ng kg⁻¹ with LOD -5 ng kg⁻¹ and LOQ- 25 ng kg⁻¹, meeting the requirements of regulatory standards in milk (50 ng kg⁻¹ for adults and 25 ng kg⁻¹ for infants) were obtained. Recoveries were in good agreement in the range of 94.40-95.28% (n = 3) for the AFM1 spiked milk samples. The precision studies prove the acceptability of assay platform for AFM1 analysis in comparison to existing commercial ELISA kit. Based on the successful demonstration with

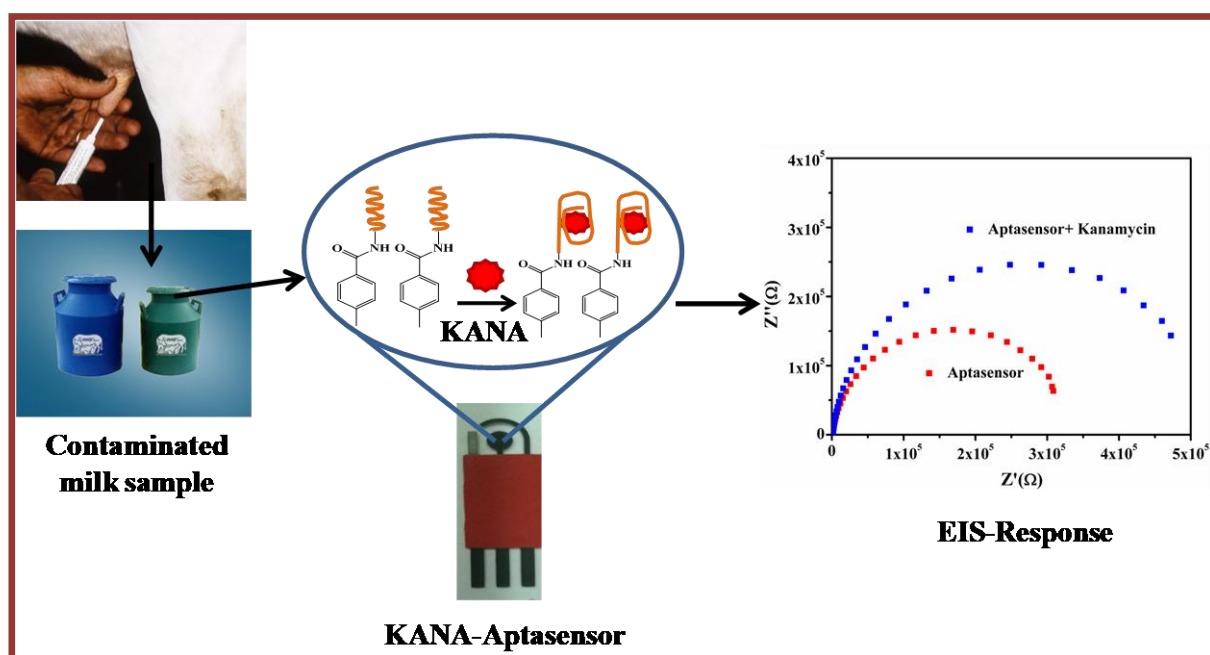
milk samples, it can be envisioned that this structure switching signalling fluorescence quenching based aptamer based can be extended to monitor AFM1 contamination in other matrices.

CHAPTER 4

Development of label-free and disposable impedimetric aptasensor for detection of kanamycin in milk sample

Novelty Statement:

- Label free and disposable SPCE integrated EIS based KANA-aptasensor has been developed.
- Developed aptasensor has been successfully employed for detection of kanamycin in spiked milk sample (untreated milk sample).
- Developed aptasensor exhibited the sensitivity limit i.e. $0.0080 \text{ ng mL}^{-1}$ KANA in milk.



Graphical abstract of chapter content

4.1 Background

In the modern era, the effect of revolutionary medicines (antibiotics) has been critical to enhance the productivity and improving the quality of food products and human health. Antibiotics are mainly used in the clinical therapy, prevention of infectious diseases and as growth promoters (in agriculture and dairy industries). Whereas, the emergence of increasing irrational use of antibiotics and microbial resistance against majority of antibiotics has resulted in sustainable side effects on human health and high mortality rates (Cabello, 2006; Daprà et al., 2013). Owing to the increasing incidences and prevalence for “suprainfection or secondary residual effect” of antibiotics, the early detection of residual antibiotic contamination has become a paramount interest (Sarmah et al., 2006; Leung et al., 2013). Food producing animals and foodstuffs are worldwide traded. Therefore, the use of antibiotics in prophylaxis and treatment of food producing animals with assurance to their complete dosage regimen is highly important (Pinacho et al., 2014). The commonly encountered side effects due to the antibiotic residual (aminoglycosides, tetracyclines etc.) contamination in food and foodstuffs are nephrotoxicity, hepatotoxicity, teratogenicity, gastritis etc. (Thi Hanh et al., 2016) (Fig. 4.1). Presently, up to 10% of global population have been diagnosed; those are hypersensitive/ allergic to antibiotics overdosing and contamination (Kivirand et al. 2015). Kanamycin (KANA) is an important chemotherapeutic agent of aminoglycoside derivatives produced by *Streptomyces kanamyceticus*. In principle, KANA inhibits the protein synthesis by binding to the 30S subunit of ribosomal RNA causes the misreading of genetic codes and interrupting the translation process that kills the microbes. KANA is widely used in therapeutic and prophylaxis of animal diseases, mastitis, modern agriculture and domestic animal stockbreeding (Hurd and Malladi, 2008). In recent years, the extensive use of KANA in food and dairy industries has increased its consumption and residual presence in foodstuffs.

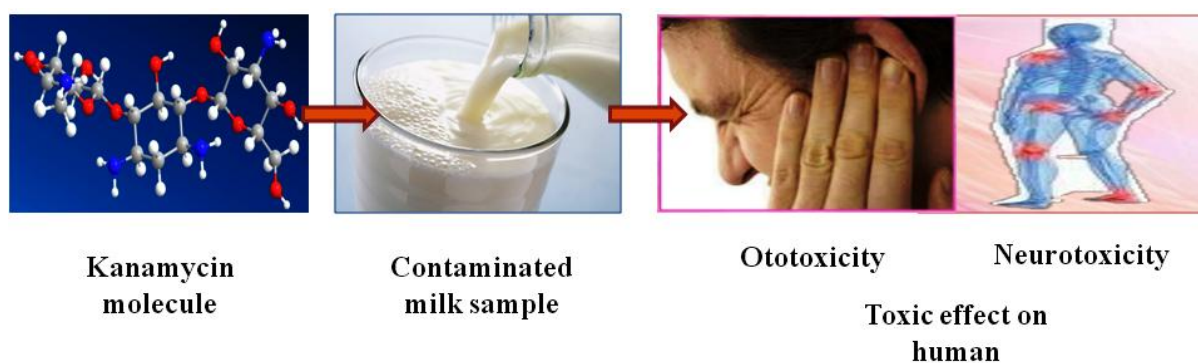


Figure 4.1: Structure (3D) and toxic effect of kanamycin in human.

4.1.1 Regulation for kanamycin contamination in milk samples

Among the various food matrices, milk has been considered as a complete balance diet due to its nutritional value and extensive usage in daily life. Milk is an excellent source of energy, proteins, minerals and vitamins for all age group and for young infants as main nutrient (Noyhouzer et al., 2009). To ensure the quality, safety of food (milk and milk products), and monitoring the human health, the maximum residual limits for KANA has been mandated in the milk samples (Table 4.1) (EU Regulation, 2003; Wang et al., 2013).

Table 4.1: Maximum residue limits of KANA residue in milk and milk products

Analyte	MRLs				
	EU	USFDA	FSSAI	CODEX	Korean Food and Drug Administration (KFDA)
Milk and milk products	150 $\mu\text{g kg}^{-1}$	125 $\mu\text{g kg}^{-1}$	200 $\mu\text{g kg}^{-1}$	200 $\mu\text{g kg}^{-1}$	0.1 mg kg^{-1}

4.1.2 State of art of KANA detection

KANA has a narrow therapeutic index and its overwhelming use in animal-derived foods cause particular side effects of aminoglycoside therapeutics (nephrotoxicity and ototoxicity), which can endanger the consumer (Oertel et al., 2004). In order to eliminate these adverse effects, a simple, sensitive and selective detection technique for monitoring of KANA in food samples is highly in demand. Until now, the identification and quantification of KANA are generally based on the conventional chromatographic methods (Yu et al., 2009; Lu et al., 2006; Blanchaert et al., 2013), enzyme-linked immunosorbent assay (ELISA) (Jin et al., 2006; Chen et al., 2008) and immunosensors (Yu et al., 2013). The earlier reported chromatographic method are sensitive and reliable, nevertheless the involvement of tedious process control and requirement of reagent limits their practical utility. Recently, the ELISA and immunosensing methods have also been widely explored for antibiotics determination in food samples because of their high sensitivity and selectivity. However, these methods also lack with shelf life, stability and involvement of *in-vivo* antibody production. The increase incidences of KANA contamination in milk sample forced scientist to design and develop

some novel innovative analytical methods. Therefore, a simple, rapid, specific, selective and robust analytical method for KANA residue detection is of immense need.

4.1.3 Electrochemical aptasensor for KANA detection

Since the discovery of aptamer the development of electrochemical biosensors containing aptamer as a bio-recognition element is growing field. In comparison to optical biosensors (as discussed in earlier chapters), electrochemical biosensors offer the advantages of portability, disposability, simplicity, rapidity, low-cost detection and low sample requirement (Robati et al., 2016). Moreover, the most electrochemical aptasensors are label-free that reduces both the cost and sensitivity of detection method (Mokhtarzadeh et al., 2015). Currently, the researchers have focused towards development of novel aptasensing platform with improved specificity and sensitivity of detection method providing on-line monitoring. In the year 2010, a RNA-based aptasensor was reported for detection of KANA (Rowe et al., 2010). The RNAs (as biorecognition element) are unstable and easily degraded during real sample analysis; whereas the single-stranded DNA (ssDNA) aptamers show the long-term stability at room temperature (Swensen et al., 2009). The above-mentioned properties of ssDNA aptamer make them an ideal candidate for development of new aptasensing platforms. Based on above facts, some optical based aptasensing platforms benefitting from a binding sequence of ssDNA aptamer have already been reported (Song et al., 2011; Leung et al., 2013; Sharma et al., 2014). The above reported optical aptasensor are impractical due to the difficulties in analyzing real samples, which has an inverse effect on method performance (Iliuk et al., 2011). Therefore, in the present thesis, aptamer-based electrochemical biosensors based on ssDNA anti-KANA aptamer have been developed for KANA residual detection. The electrochemical sensor platform plays an important role on immobilization of molecular probe, where the signal transduction generates from the electrochemical reaction occurred. The reported aptasensing platforms for KANA detection based one electrochemical transduction have been summarized in Table 4.2. Among all, the label-free electrochemical aptasensor has gained tremendous attention due to their simple preparation, cost effectiveness and conservation of structural integrity of biomolecule (Marchesini et al., 2008).

Table 4.2: Reported electrochemical based aptasensor for detection of KANA in milk samples

S. No.	Transduction principle	Dynamic range	Limit of detection (LOD)	Ref.
1.	LSV	25-4500 ng mL ⁻¹	4.7 ± 0.2 ng mL ⁻¹	Zhu et al., 2012
2.	EIS	5.0- 1.0x 10 ⁶ ng mL ⁻¹	-N.A.-	Dapra et al., 2013
3.	DPV	10×10 ³ -150×10 ³ ng mL ⁻¹	2.9 ng mL ⁻¹	Sun et al., 2014
4.	DPV	5×10 ⁻³ to 40 ng mL ⁻¹	4.6×10 ⁻³ ng mL ⁻¹	Xu et al., 2014
5.	DPV	5- 100 ng mL ⁻¹	4.3 ng mL ⁻¹	Li et al., 2014
6.	DPV	0.5-50×10 ³ ng mL ⁻¹	0.44 ng mL ⁻¹	Qin et al., 2015
7.	SWV	1-50 ng mL ⁻¹	0.92 ng mL ⁻¹	Liu et al., 2015
8.	Photochemical aptasensor	0.55-122.0 ng mL ⁻¹	0.20 ng mL ⁻¹	Li et al., 2014
9.	Label free impedimetric aptasensor	1.20-600 ng mL⁻¹	0.11 ng mL⁻¹ (0.206 nM)	Present work

4.1.3.1 Screen printed technology

Recently, the advancements and integration of SPCEs methodology have emerged out with the promising potential in the development of highly sensitive biosensors for clinical and environmental interest. The biosensors based on SPCEs are miniaturized systems, which enable the *in-vitro* and *in-vivo* analysis. SPCEs based sensors have enabled the production of disposable biosensors with the advantages of low cost, portability, disposability, miniaturization, versatility and feasibility for on-site analysis (Tudorache and Bala, 2007). However, it is cumbersome to use the conventional (rod type) and pattern integrated

electrodes due to the difficulties of many point calibration and design optimization (Lee et al., 2017). The SPCEs based electrochemical aptasensors have been explored for detection of various food and environmental contaminants (Kim et al., 2009; Bonel et al., 2011). In the present thesis, the SPCEs based technology has been used for development of a label-free electrochemical impedimetric aptasensor for KANA analysis.

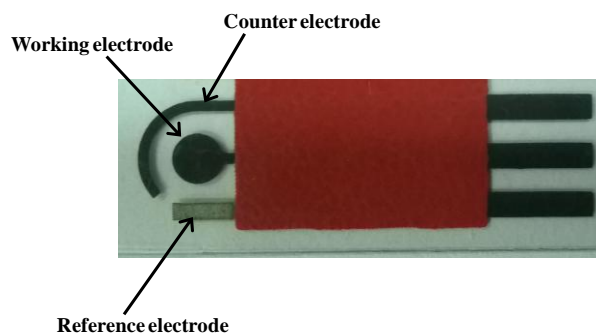


Figure 4.2: Customized screen printed carbon electrode (used in the present work).

4.1.3.2 Self assembled monolayer

Immobilization of bio-recognition element is an important step in construction of a biosensor based on SPCEs. The bio-analytical chemistry aims to improve the molecular detection sensitivity, selectivity and speed of detection method in complex real sample environment. The key factor for construction of a sensor device is to design the transducer surface, which is capable of selectively recognizing and binding a specific biological/ chemical analyte of interest. Integration of recognition molecule on the transducer surface is usually achieved by decorating the transducer surface either by covalent coupling using a coupling agent that enables the immobilization of the recognition species or physical adsorption process (Turner, 2013). Therefore, the intellectual fabrication of the recognition unit on transducer surface is essential to improve the analytical precision and accuracy of sensor. To modify the transducer surface, several surface modification techniques have been employed such as thiolation, click chemistry, diazotization and silanization to form the self assembled monolayer for better immobilization of biomolecule (Love et al., 2005; Wang et al., 2015). Of these alternative monolayer formation methods, the aryldiazonium coupling chemistry was reported by Pinson and co-workers in 1992 (Delamar et al., 1992). In electrochemical reduction, an aryldiazonium salts generates a reactive aryl radical, which bind to the carbon surface. Among all reported coupling mechanism, the diazonium salt chemistry is significantly important in SPCEs based electrochemical biosensing application. The diazotization coupling offers the advantages of better immobilization, rapid reaction time, lack of leakage of

biomolecule, uniform surface modification, compatibility with wide range of materials, stability, long shelf life and as well as lower limit of detection (Pchelintsev and Millner, 2007; Cao et al., 2017).

4.1.4 Research gap identified

Existing literature revealed that there is an immense need for sensitive and selective detection method for regular monitoring and quantification of antibiotic contamination. Therefore, a SPCEs integrated biosensing platform was employed for the construction of a label-free aptasensor. Investigation of developed aptasensor performance in the untreated milk samples.

4.1.5 Objective

The aim of present work was to develop a label-free and disposable impedimetric aptasensor for detection of kanamycin in raw milk sample.

4.2. Experimental Section

4.2.1 Biochemicals and reagents

Analytical grade reagents potassium dihydrogen phosphate, disodium hydrogen phosphate, sodium chloride, potassium chloride, magnesium chloride, 2-(*N*-morpholino) ethanesulfonic acid (MES) buffer, sodium nitrite (NaNO_2), 4-aminobenzoic acid (4-ABA), *N*-(3-dimethylaminopropyl)-*N*-ethyl-carbodiimide hydrochloride (EDC), *N*-hydroxysuccinimide (NHS), ethanolamine, sulphuric acid (98% v/v), hydrochloric acid (37.5 % v/v), potassium ferrocyanide ($\text{K}_4[\text{Fe}(\text{CN})_6]$) and potassium ferricyanide ($\text{K}_3[\text{Fe}(\text{CN})_6]$) were procured from Sigma-Aldrich (St. Quentin Fallavier Cedex, France). Kanamycin sulphate (derived from *Streptomyces kanamyceticus*) as reference standard was purchased from Sigma Aldrich (USA). For selectivity studies, the streptomycin and gentamicin were purchased from Sigma Aldrich (USA). The deionized Milli-Q water obtained from (Millipore, Bedford, MA, USA) was used for reagent preparation. For real sample analysis, the milk samples were procured from the local market. The amine modified ssDNA-KANA-aptamer was synthesized and purified by Microsynth (Schutzenstrasse, Balgach, Switzerland). The modified nucleotide sequence (7 base pairs) of ssDNA KANA-aptamer is shown below:

ssDNA anti-KANA aptamer (21 base sequences): amine modified anti-KANA aptamer

5'-TGG GGG TTG AGG CTA AGC CGA-NH₂-3'.

4.2.2 Instrumentation

The SPCEs consists of a conventional three electrode configuration with carbon electrode using carbon-based ink (as a working), an auxiliary electrode from carbon ink (as a counter) integrated with a pseudo reference electrode from a silver-based (Ag/AgCl) ink were fabricated using a DEK 248 screen-printing system (BAE Laboratory, Perpignan, France) (Fig. 4.2). For electrochemical measurements, an Autolab PGSTAT100 potentiostat/galvanostat station equipped with a frequency response analyzer system (Eco Chimie, Netherlands) and computerized controlled by two softwares, GPES 4.9 for voltammetric and FRA 4.9 for impedimetric measurements was used. Impedimetric measurements were recorded using a sinusoidal ac potential perturbation of 5 mV (rms) in the frequency range 10^3 - 0.1 Hz, superimposed on a dc potential of 0.1 V and readings were taken at 20 discrete frequencies per decade. All the measurements were carried out in a solution of 1.0 mM $[\text{Fe}(\text{CN})_6]^{4-/3-}$ in PBB (pH 7.0) as a background electrolyte. Fourier Transform Infrared (FT-IR) spectroscopy was used to characterize the surface modification of SPCEs at various step of aptasensor fabrication. The vibrational spectra were recorded using IR Affinity-1 attached with attenuated total reflectance (ATR) at Specac Diamond ATR AQUA (SHIMADZU, Japan). The spectra were recorded with 128 scans at 64 cm^{-1} resolution collected under vacuum conditions. Similarly, the scanning electron micrograph of modified SPCEs was recorded on scanning electron microscope (SEM XL 30 FEI/Philips, Philips Electronics Co., Netherlands). AFM topography studies were carried out using a multimode scanning probe microscope system operated in tapping (semicontact) mode using NTEGRA Prima (NT-MDT, Zelenograd, Moscow, Russia).

4.2.3 Solution preparation

4.2.3.1 Preparation of binding buffer solution

The phosphate binding buffer (10 mM) containing 30 mM KCl, 5 mM MgCl_2 and 90 mM NaCl was prepared in the deionized Milli-Q water. The pH of buffer was adjusted to 7.0. The binding buffer solution was freshly prepared and stored at 4 °C when not in use.

4.2.3.2 Preparation of aptamer solutions

For stock solution, the ssDNA anti-KANA aptamer was dissolved in the sterilized deionized Mili-Q water. Further, the stock was diluted in the range 0.125-4.0 μM ssDNA anti-KANA aptamer in PBB. The aptamer solution was placed in a thermocycler (Mastercycler personal

Eppendorf VWR, Leuven, Belgium) with the following temperature profile: heating at 90 °C for 5 min to initial denaturation step, followed by a structure maintain step at 4 °C for 5 min and room temperature for 10 min.

4.2.3.3 Preparation of kanamycin stock and working dilutions

Kanamycin stock solution was prepared by dissolving 1 mg mL⁻¹ KANA in sterilized deionized Milli-Q water. Subsequently, the stock was diluted in PBB (10 mM, pH 7.0) to obtain various working dilutions in the range of 1.20-600 ng mL⁻¹ KANA meeting regulatory standards (Table 4.1).

4.2.3.4 Matrix matching (milk sample preparation)

The raw milk sample (3% fat content) was purchased from the local market. The standard spiking method was used for milk sample analysis. The complex matrix treatment such as dissolving of fat by acid (trichloroacetic acid, TCA) could decrease the matrix composition. Thus, to avoid such problem, a simple strategy was worked out for analysis of milk sample. In brief, firstly, the milk sample was centrifuged at 10000 rpm for 10 min at room temperature. The supernatant was separated and milk spiked with a known concentration of KANA. Subsequently, the dilutions were made with non-contaminated centrifuged milk sample to obtain the different concentration of KANA (4.75, 9.5, 37.5 and 150 ng mL⁻¹).

4.2.4 Fabrication of KANA-aptasensor on diazotized SPCEs

4.2.4.1 SPCE surface cleaning

Prior to use, each SPCE surface was electrochemically pre-treated by applying cyclic voltammetry (CV) cycles (5 to 6 cycles) between 1.0 to -1.5 V vs. pseudo Ag/AgCl reference electrode in 0.5 M H₂SO₄ containing 0.1 M KCl. The SPCE pre-treatment was continuing until the CV characteristic of clean SPCE surface was obtained (Fig. 4.3).

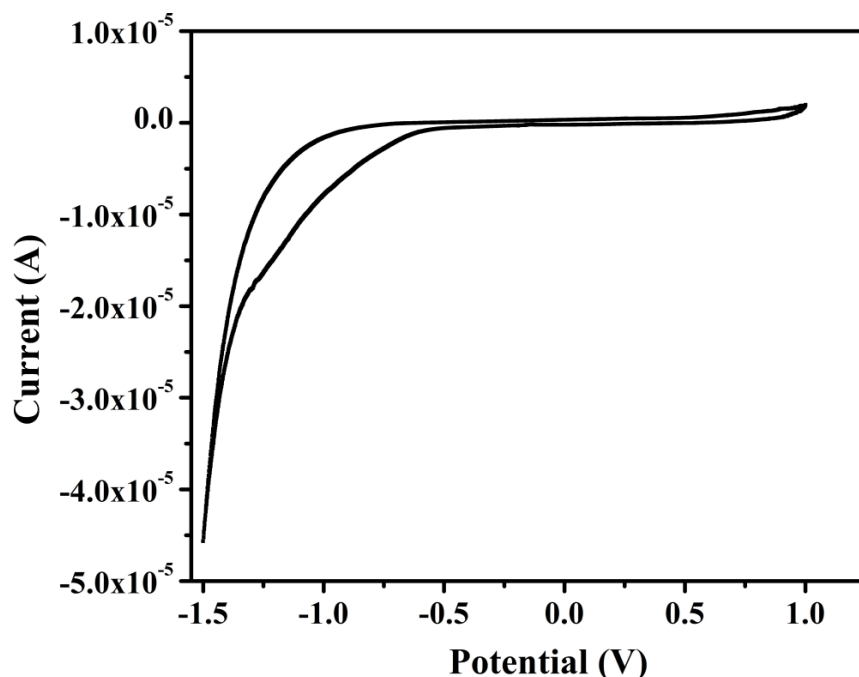


Figure 4.3: Cyclic voltammogram of bare SPCE during cleaning from 1.0 to -1.5 V vs. pseudo Ag/AgCl reference electrode in 0.5 M H₂SO₄ containing 0.1 M KCl.

4.2.4.2 Surface modification and end group activation

The pre-treated SPCEs surfaces were functionally modified by diazotization coupling mechanism (1:1 equivalents of NaNO₂ and 4-ABA) using electrografting method with modification (Baranton and Belanger, 2005). In brief, 20 μL of 0.1 NaNO₂ solution (final concentration 2 mM) was added to electrolytic solution (1.98 mL) containing 2 mM of 4-ABA in 0.5 M HCl. The mixture was stirred and allows keeping for 5 min under working condition (RT). The electrochemical reductive modification of SPCE with an *in-situ* generated 4-carboxyphenyl diazonium salt (4-COOH-Ar-N₂⁺) was carried out by a reductive linear sweep voltammetry (LSV) from 0.6 to 0.8 V vs. Ag/AgCl at a scan rate of 0.05 Vs⁻¹ (Fig. 4.4). Electrochemical reduction of diazonium species (4-COOH-Ar-N₂⁺) results in the generation of an aryl centered radical via one electron transfer with elimination of dinitrogen (-N₂) and covalently attached to the electrode surface. The potential applied in electrografting of aryl diazonium is an important parameter. The diazotization of SPCE surface has been incurred in first cycle at -0.3 V (Fig 4.5). Further no sign of diazotization signal was observed on SPCE surface after second cycle (inset Fig. 4.5), which signify the demonstration of uniform diazotized surface modification. In the present thesis, the diazotization coupling mechanism was explored due to advantages of high stability, ease of preparation and uniform modified surface formation, which provides the better immobilization of receptor element (Pchelintsev and Millner, 2007; Ocana and Del Valle, 2014). After modification, the 4-

CP/SPCEs were obtained and rinsed with copious amounts of distilled water for further use. The end terminal carboxylic groups on 4-CP/SPCEs modified electrodes were activated by immersing the modified electrodes into a solution of 100 mM EDC and 25 mM NHS in MES buffer (pH 5.5) for 60 min.

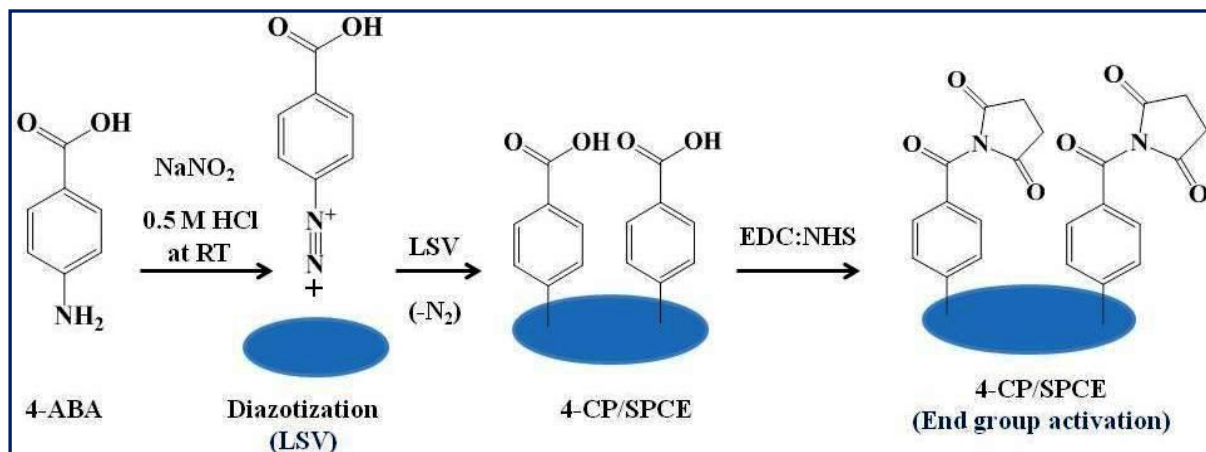


Figure 4.4: Electrografting of in-situ generated diazonium salt on SPCEs surface using linear sweep voltammogram (LSV).

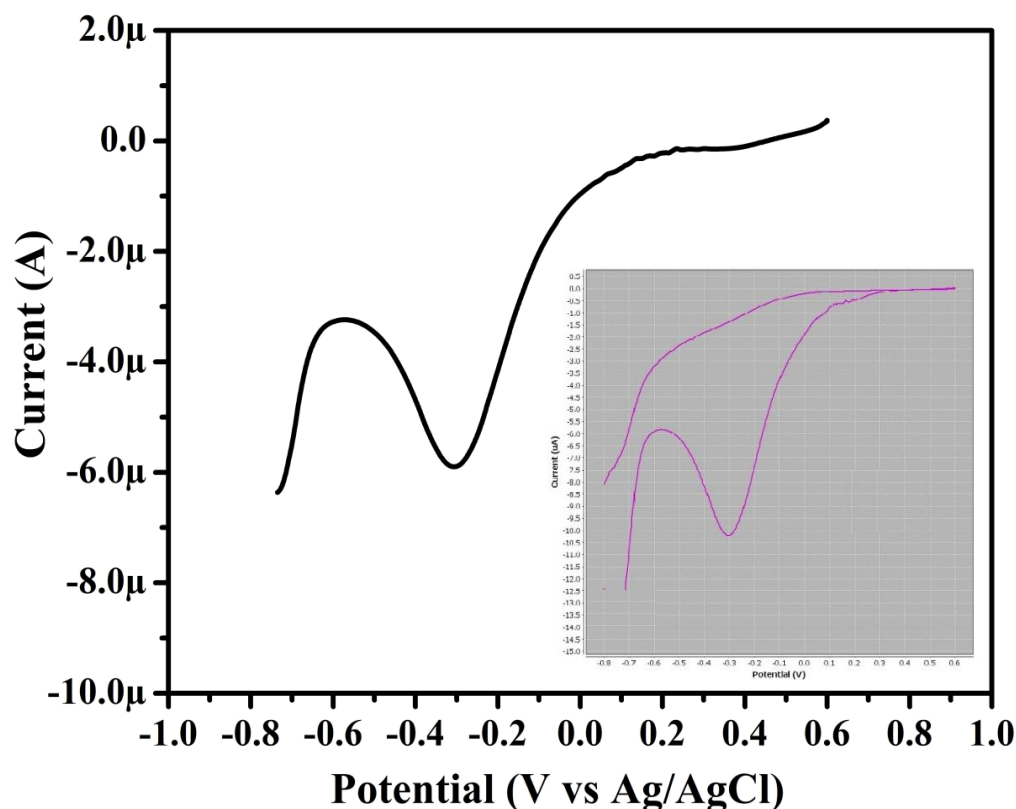


Figure 4.5: Linear sweep voltammogram (LSV) of bare SPCE electrode in the aqueous diazonium salt solution (NaNO_2 and 4-aminobenzoic acid 2 mM in 0.5 M HCl) in the potential range 0.6 to -0.8 V vs. Ag/AgCl. Inset showing the two consecutive cycles on same electrode.

4.2.4.3 Aptamer immobilization and blocking

The end group activated 4-CP/SPCEs were incubated with 20 μL of various concentrations of ssDNA anti-KANA aptamer in PBB (pH 7.0) for 4 h under humid environment. Aptamer immobilized 4-CP/SPCEs were again washed with PBB (Fig. 4.6). Further, to deactivate the remaining succinimide group and block reacted sites on the electrode surface, the aptamer immobilized electrodes were incubated with 20 μL of 1 M ethanolamine for 1 h and subsequently washed with distilled water. For milk analysis, the blocking was done using 20 μL of casein solution (1% casein) for 30 min to completely block the unbound sites of the SPCEs surface. The fabricated KANA-aptasensor integrated on modified SPCEs was used directly or stored at 4 $^{\circ}\text{C}$ for several days without any decrease in the sensitivity.

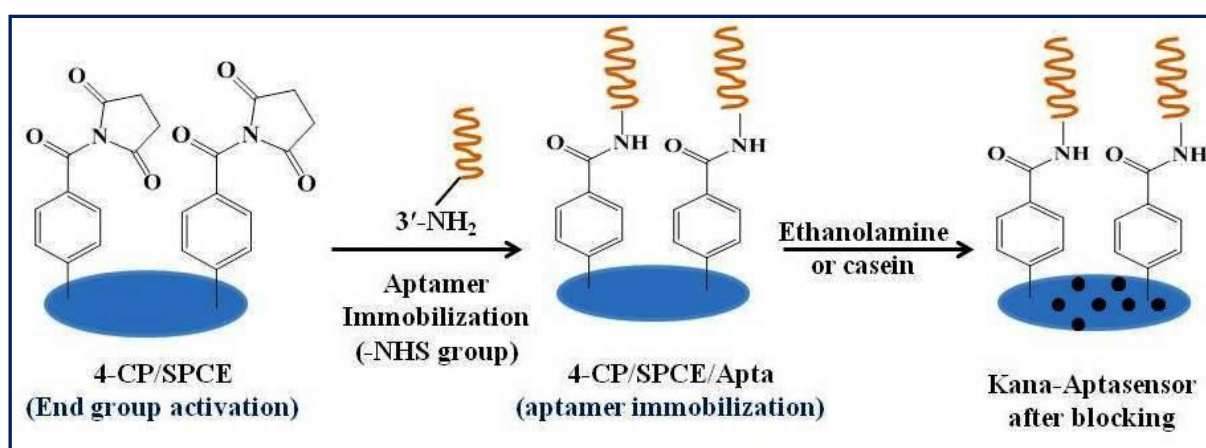


Figure 4.6: Immobilization of aptamer on diazotized SPCEs surface followed by blocking.

4.2.5 Impedimetric measurements

In the present work, the EIS (impedimetric) measurements were carried out at an applied potential of 0.1 V (vs. Ag/AgCl reference electrode) obtained from the redox potential of 1 mM $[\text{Fe}(\text{CN})_6]^{4-/3-}$ with a frequency range of 1 KHz to 0.1 Hz at an AC amplitude of 5 mV and a sampling rate of 100 points. The EIS data were recorded in the following order after each successive modification step: (1) bare electrode; (2) 4-CP/SPCE, (3) 4-CP/SPCE/activated, (4) 4-CP/SPCE/Apta and (5) 4-CP/SPCE/Apta/KANA incubated. The designed equivalent circuit diagram of an electrode-electrolyte interface known as Randles Circuit is showed in Fig. 4.7 and the parameters used were as follow:

R_{sol} = Solution resistance; R_{ct} = Charge transfer resistance between solution and the electrode surface; C_{dl} = Double layer capacitance; W = Warburg impedance corresponds to the diffusion of the redox probe

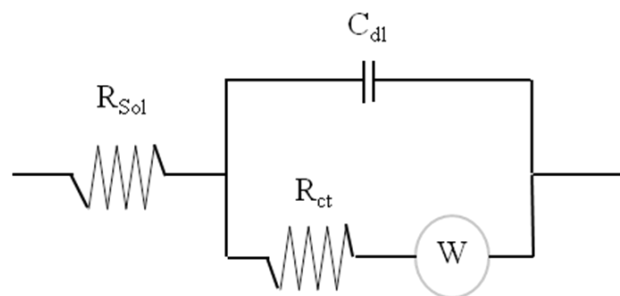


Figure 4.7: Design of a simple Randles Equivalent Circuit.

The obtained impedance spectrum (EIS spectrum) was plotted in the form of complex plane diagrams (known as Nyquist plots, $-Z_i$ vs. Z_r). The plotted spectra were fitted to a theoretical curve corresponding to an equivalent circuit obtained from FRA software. Further, to compare the results obtained from different aptasensor and to obtain independent, reliable and reproducible results, the relative and normalized signals were required. Accordingly, an analytical parameter, Δ_{ratio} , was defined using the R_{ct} values in the following equations:

$$\Delta_{\text{ratio}} = \Delta_s / \Delta_p$$

where, $\Delta_s = R_{\text{ct (KANA-aptamer)}} - R_{\text{ct (bare electrode)}}$

$$\Delta_p = R_{\text{ct (aptamer)}} - R_{\text{ct (bare electrode)}}$$

Where, $R_{\text{ct (KANA-aptamer)}}$ is the electron-transfer resistance of aptasensors measured after incubation with the KANA, $R_{\text{ct (aptamer)}}$ is the electron-transfer resistance of KANA-aptasensor and $R_{\text{ct (bare electrode)}}$ is the electron-transfer resistance of the bare electrode.

4.3 Results and discussion

Before sensitivity measurements, the fabricated KANA-aptasensor was characterized for each modification step. Various characterization techniques were employed to study the surface morphology and electrochemical behavior.

4.3.1 Surface characterization of KANA-aptasensor

4.3.1.1 Infrared spectroscopy (FT-IR)

Vibrational spectrum (FT-IR) recorded for diazotized SPCE, aptasensor and aptasensor incubated with KANA has been shown in Fig. 4.8. The diazotized SPCE showed the presence of broad absorption band at $3431\text{-}2921\text{ cm}^{-1}$ (ν_s) and two additional bands at 1633 cm^{-1} (ν_s , C=O of carboxyl) and out-of-plane bending (ν_d , -OH of acid) at 905 cm^{-1} (Fig. 4.8a). This is a

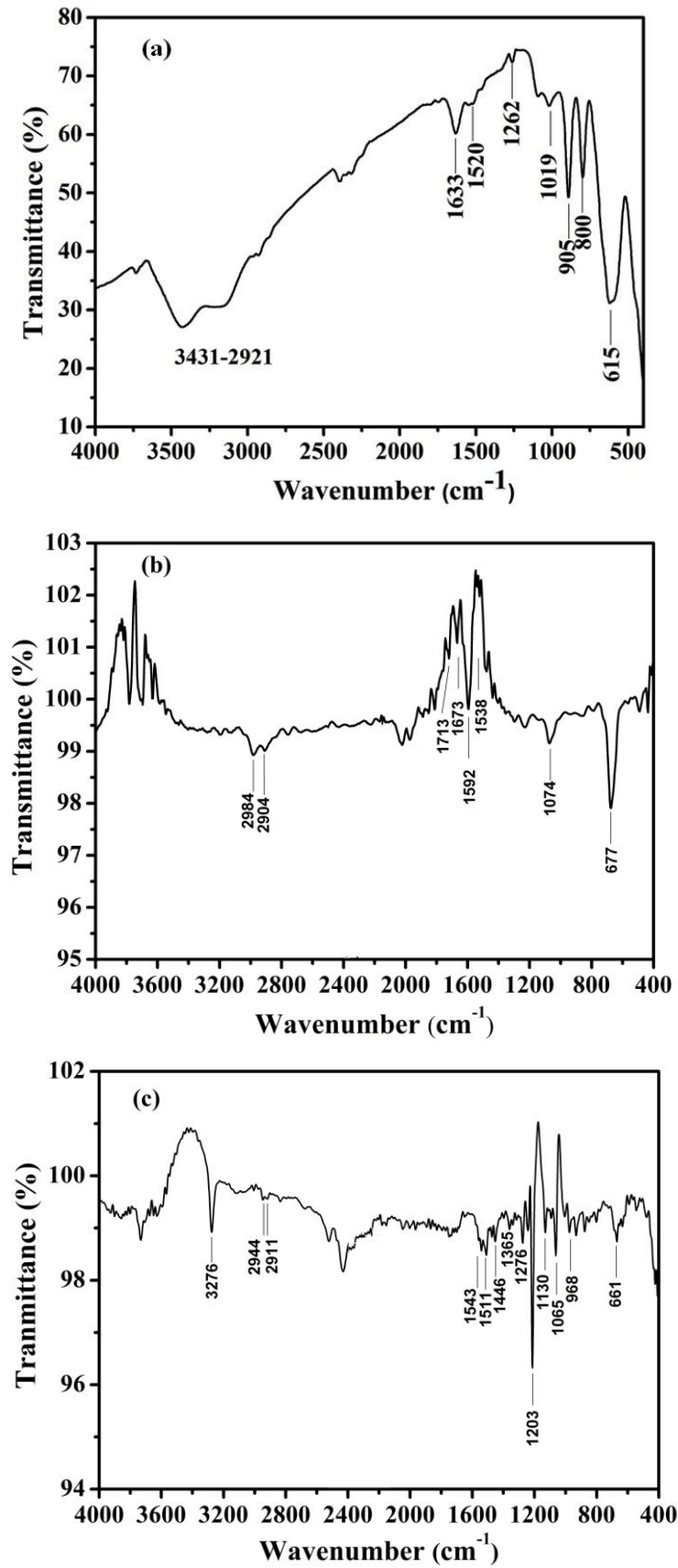


Figure 4.8: FT-IR spectrum of (a) 4-CP/SPCE modified; (b) 4-CP/SPCE/activated/Apta; (c) 4-CP/SPCE/activated/Apta/KANA electrodes recorded at 128 scans at 64 cm^{-1} resolution.

strong indication to the presence of free carboxylic groups on the surface of diazotized electrode (4-CP/SPCE) (Pavia et al., 2005). After immobilization of ssDNA anti-KANA aptamer, the appearance of two new vibrational bands at 1717 and 1673 cm^{-1} (ν_s , -C=O of carbonyl) corresponds to the guanine base and amide bond between diazotized surface and amine modified aptamer (Fig. 4.8b). Other vibrational bands at 1592, 1538 and 1074 cm^{-1} corresponds to the -C=C- and -C=N- bonds of ssDNA aptamer sequences (Andrushchenko et al., 2007) could also be seen. These vibrational spectra strongly suggested the presence of covalently immobilized aptamer on 4-CP/SPCE. Upon incubation with KANA, the appearance of new vibrational bands corresponds to the KANA at 3276 (ν_s , -NH₂ of KANA), 968 cm^{-1} (ν_d , -OH of KANA), 1103 cm^{-1} and 1230 cm^{-1} (ν_s , -C-O- of cyclic ring) were recorded (Fig. 4.8c). The appearance of new vibrational bands on KANA recognition confirmed the successful binding between KANA and with ssDNA anti-KANA aptamer.

4.3.1.2 Scanning electron microscopy (SEM)

The surface morphology of aptasensor at three different stages i.e. bare electrode (SPCE), KANA-aptasensor and aptasensor incubated with KANA has been illustrated in Fig. 4.9(a-c). The bare SPCEs showed a non-uniform surface with typical characteristics carbon based SPCEs (Fig. 4.9a). Upon diazotization, the 4-CP/SPCEs surface resulted in the formation of a uniform surface, which improves the immobilization process. After immobilization, a uniform surface cover with the immobilized ssDNA anti-KANA aptamer over diazotized electrode was observed (Fig. 4.9b). The universal mechanism of aptamer-target recognition is based on capability of aptamer to adopt an antiparallel complex-G-quadruplex structure formation upon target binding. Upon incubation with KANA (37.5 ng mL⁻¹), the binding interaction between ssDNA anti-KANA aptamer and KANA molecules led to KANA induced formation of G-quadruplex aptamer-KANA complex. It is evident that the recognition event caused the changes in structural form of aptamer, this could be concluded based on the presence non-uniformity in the surface morphology of aptamer immobilized SPCEs (Fig. 4.9c).

4.3.1.3 Atomic force microscopy (AFM)

Surface topography of fabricated aptasensor provided a clear indication about the surface modification and binding interaction between aptamer and KANA molecule on aptasensor surface. The typical AFM (3D micrographs) topographies of the fabricated aptasensor surface at different stages have been shown in Fig. 4.9(d-f). Average and root mean square roughness

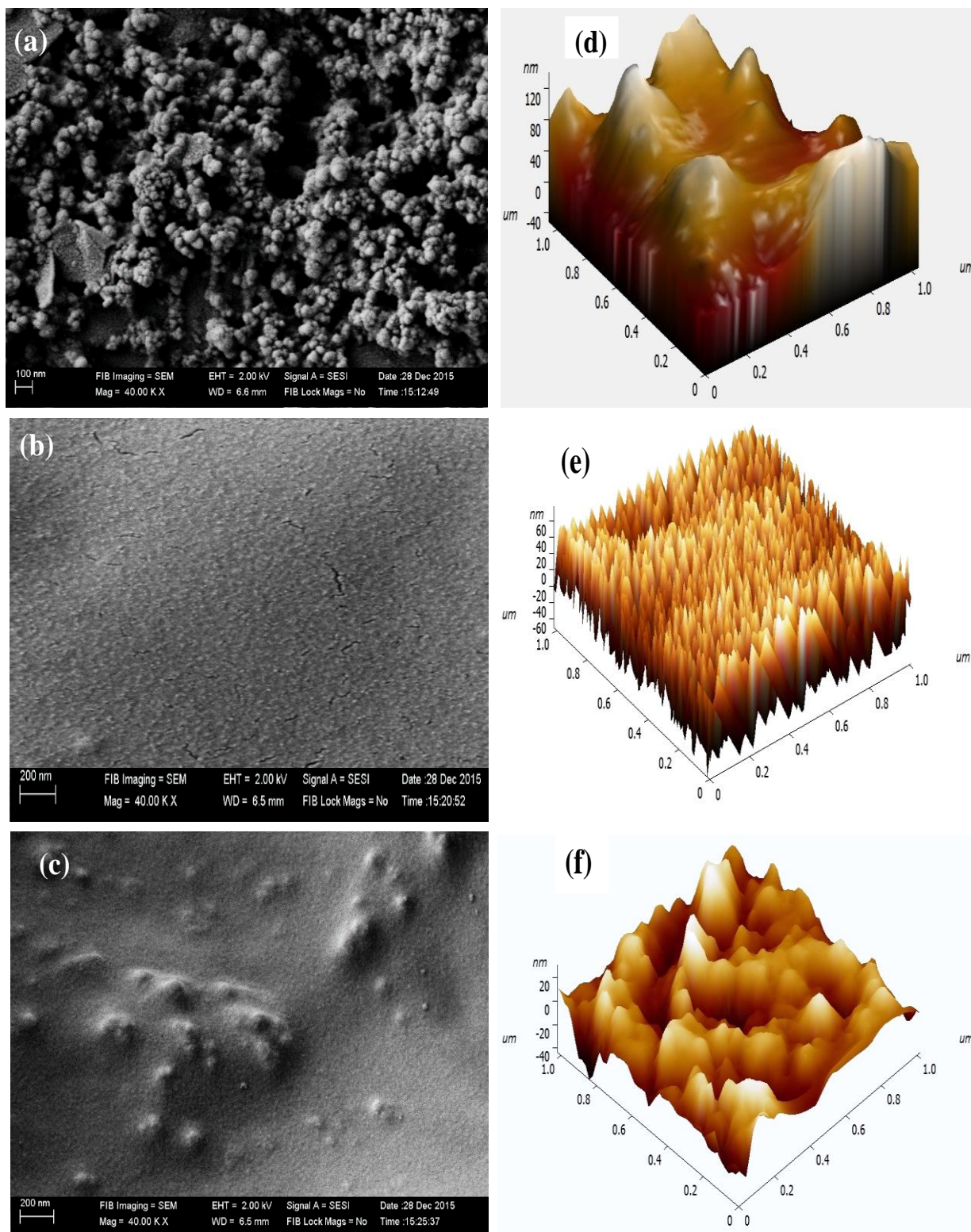


Figure 4.9: SEM images of (a) Bare SPCE; (b) 4-CP/SPCE/activated/ Apta immobilized; (c) 4-CP/SPCE/activated/Apta/KANA incubated electrode; AFM images (d) Bare SPCE; (e) 4-CP/SPCE/activated/Apta; (f) 4-CP/SPCE/activated/Apta/KANA incubated electrode in semicontact tapping mode.

value (RMS) of recorded AFM micrographs were calculated and analyzed for SPCE (bare electrode), KANA-aptasensor and KANA-aptasensor incubated with KANA. The results have been summarized in Table 4.3. The fabricated aptasensor showed a decrease in average roughness (Ra , 23.14 nm) and RMS (Rq , 27.55 nm) upon aptamer immobilization. Meanwhile, the height and spacing parameters also decreased to 1.5 times compare to the bare SPCE (Fig. 4.9e). Upon aptamer immobilization (4-CP/SPCE/activated/Apta), the decrease in roughness, lower peak spaces and spike planer surface covering the plane of electrode strongly indicated the successful immobilization of ssDNA anti-KANA aptamer on 4-CP/SPCE surface. Similarly, a uniform surface coverage observed during SEM analysis has been illustrated in the Fig. 4.9(b). On incubation with KANA (37.5 ng mL^{-1}), the surface topology was expected to be changed further due to formation of anti-KANA aptamer-KANA complex upon recognition of KANA. It was observed that upon KANA recognition by aptasensor, the surface roughness and average height have been decreased (Fig. 4.9f). The following results were approximately 2 fold smaller in roughness and height. However, the self similarity (fractal value, Rku) of aptasensor surface was increased from 1.945 to 3.044, which indicates the binding of KANA on aptasensor surface (Table 4.3).

Table 4.3: AFM topological parameters before and after modification for the screen printed carbon electrode, aptasensor and aptasensor incubated with analyte.

Parameter	Bare SPCE	ssDNA anti-KANA aptamer	Aptasensor incubated with KANA
Ra (nm)	25.19	23.14	10.37
Rq (nm)	31.46	27.55	13.11
Rpv (nm)	176.91	130.55	74.66
Rz (nm)	177.10	139.64	75.21
Rsk	-0.036	-0.055	-0.023
Rku	3.301	1.945	3.304

4.3.2 Electrochemical characterization of KANA-aptasensor

The surface interfacial properties of devised aptasensor after each modification were characterized using cyclic voltammetry and electrochemical impedance spectroscopy.

4.3.2.1 Cyclic voltammetry (CV)

The CV analysis was selected as a redox parameter to characterize the electrode surface at each modification step. The change in peak-to-peak separation and peak current in cyclic voltammograms are important characteristics, which relates the electron transfer-rate constant correspond to the electron transfer resistance. All electrochemical measurements were carried out in a relatively low concentration of the redox probe 1 mM $[\text{Fe}(\text{CN})_6]^{4-/3-}$ prepared in PBB (10 mM, pH 7.0) at scan rate of 100 mV s^{-1} . Because at higher concentration of electrolytic species might hinder the bioreceptor recognition (Wang et al., 2005). The presence of $[\text{Fe}(\text{CN})_6]^{4-/3-}$ redox probe allows the detection of a higher current response against the response obtained from an electrochemical inert solution.

Cyclic voltammograms after each assembly step of KANA aptasensor has been illustrated in Fig. 4.10. The sequential modification steps of fabricated KANA-aptasensor were confirmed by a decrease in the current response and an increase in the peak-to-peak separation. Bare SPCE showed a couple of well-defined redox peaks (quasi reversible) with the cathodic and anodic current peak ratio of approximately one and the peak-to-peak separation of 1.2 V (voltammogram a). After diazotization, the R_{et} (electron transfer resistance) between the probe and electrode surface has increased, which could attributed to formation of an organic layer at SPCEs surface due to the negatively charged carboxyl groups (COO^-). This layer acts as an electrostatic barrier and repelled redox probe $[\text{Fe}(\text{CN})_6]^{4-/3-}$ anions, indirectly retard the electron transfer between the redox probe and electrode. As a result, shape of redox couple for 4-CP/SPCEs was nearly disappeared indicating the successful coupling of 4-CP on electrode surface (voltammogram b). The activation of end-terminal group (EDC:NHS coupling) at 4-CP/SPCEs, introduced a succinimide moiety, which cause increase in current response due to devoid of negative charge groups (voltammogram c). When anti-KANA aptamer (ssDNA KANA-aptamer) was immobilized onto 4-CP/SPCE/activated, the peak current slightly decreased again due to the complex structure of aptamer and non-electrochemical activity (voltammogram d) (Guo et al., 2015). This partially blocks the electron transfer between $[\text{Fe}(\text{CN})_6]^{4-/3-}$ solution and the electrode surface. These obtained CV characteristic patterns showed that the ssDNA anti-KANA aptamer has been successfully immobilized onto the 4-CP/SPCEs surface. Upon recognition of KANA molecule a slight decrease in the current response was observed (voltammogram e) due to change in structural conformation of aptamer, which resist the charge further charge transfer.

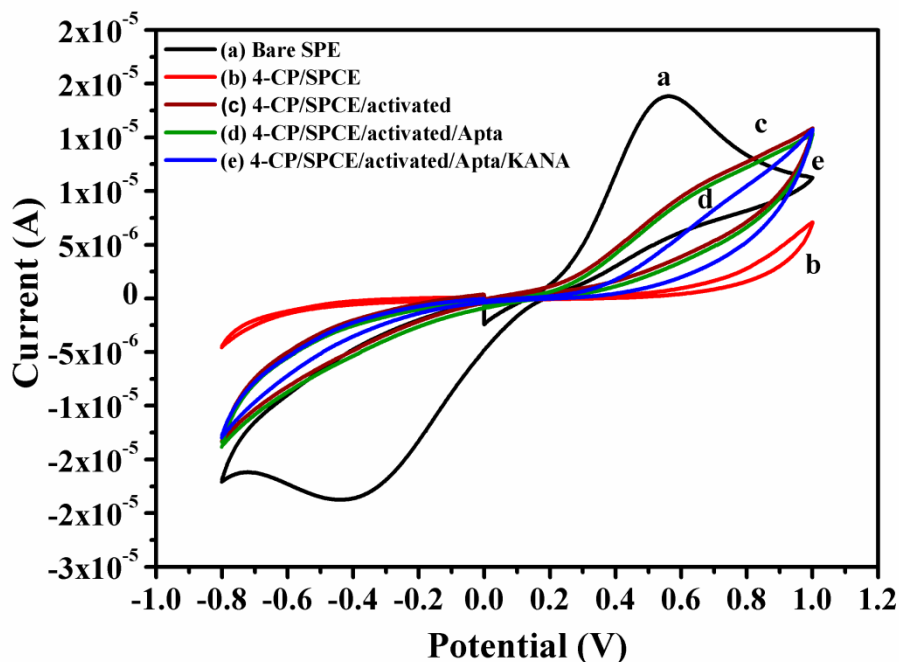


Figure 4.10: Cyclic voltammograms (a) bare SPCE; (b) 4-CP/SPCE; (c) 4-CP/SPCE/activated; (d) 4-CP/SPCE/activated/Apta; (e) 4-CP/SPCE/activated/Apta/KANA incubated electrodes in 1 mM $[\text{Fe}(\text{CN})_6]^{4-/3-}$ (prepared in PBB, pH 7.0) at scan rate of 100 mV s^{-1} .

4.3.2.2 Electrochemical impedance spectroscopy (EIS)

EIS characteristics were used as a power tool to study the change in surface properties after each modification step. The Nyquist diagram illustrating the EIS spectrum corresponds to the stepwise modification procedure using $[\text{Fe}(\text{CN})_6]^{4-/3-}$ as the redox probe has been plotted and shown in Fig. 4.11. The results obtained from EIS measurements were in the good agreement with the conclusions obtained from the CV studies (illustrated in Fig. 4.10). In the EIS spectrum (Nyquist plot) consists of a very small semicircle portion and a linear portion, the semicircle portion at higher frequencies relates to the electron-transfer resistance and the linear portion relates to the diffusion resistance (Reddi and Gobi, 2013). It can be seen that the bare SPCE exhibited a very small semicircle and showed a very low electron-transfer resistance (spectrum a). The R_{ct} value of the redox probe was calculated and found to be $44.4 \text{ k}\Omega \text{ cm}^2$. Compared to the bare SPCE, the diazotized electrodes (4-CP/SPCE) showed a spontaneously increased in the resistance up to $2650 \text{ k}\Omega \text{ cm}^2$ (spectrum b). This was because of the deposition of organic layer on electrode surface possessing negative terminal ($-\text{COO}^-$) and acts as an electrostatic barrier between electrode and the detection solution. A sharp fall in R_{ct} value ($320 \text{ k}\Omega \text{ cm}^2$, spectrum c) was noted after introducing succinimide moiety. The sharp fall in R_{ct} was correlated with the electrostatic interaction between positively charged

ester group (from succinimide moiety of -NHS) and negatively charged redox, which promote the electron transfer and decrease resistance (Yang et al., 2011). After anti-KANA aptamer immobilization on modified SPCEs surface, the R_{ct} value increased to $520 \text{ k}\Omega \text{ cm}^2$ (spectrum d). This was due to the presence of inert electron layers and electrostatic repulsion between phosphate groups of aptamer nucleotide sequences, which repel the negatively charged redox probe couple. The KANA recognized aptasensors showed the increase in R_{ct} value to $780 \text{ k}\Omega \text{ cm}^2$ (spectrum e). The reason for this increase in R_{ct} value was corresponds to the conformational changes in the aptamer structure and presence of various functional (phenolic or alcoholic) groups of KANA. The EIS spectrum results have been summarized in Table 4.4.

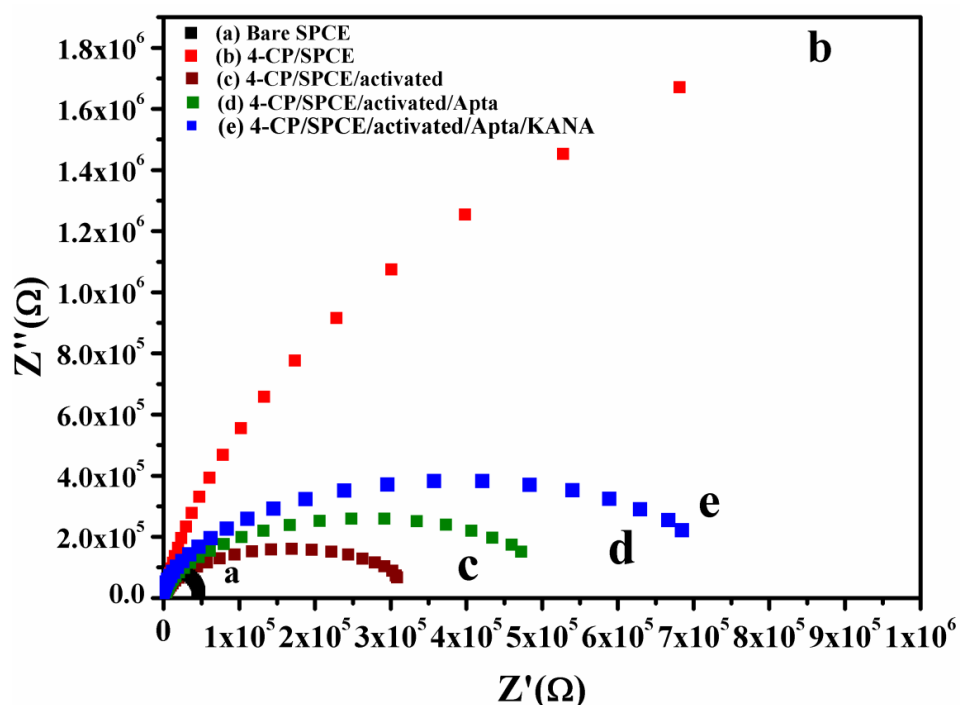


Figure 4.11: Nyquist plots (a) bare SPCE; (b) 4-CP/SPCE modified electrode; (c) 4-CP/SPCE/activated electrode; (d) 4-CP/SPCE/activated/Apta; (e) 4-CP/SPCE/activated/Apta/KANA incubated electrodes obtained in $1 \text{ mM } [\text{Fe}(\text{CN})_6]^{4-/3-}$ (prepared in PBB, pH 7.0) at an applied potential of 100 mV (vs. Ag/AgCl reference electrode) using a frequency range of 10 KHz to 0.5 Hz with an AC amplitude of 5 mV .

Table 4.4: Stimulated values of all elements in the equivalent electric circuit (Randles Circuit) for the various steps of the aptasensor fabrication

EIS spectrum	Electrode label	R_s (kΩ cm⁻²)	R_{ct} (kΩ cm⁻²)	C (μF)
a.	Bare SPCE	0.516	44.4	0.517
b.	4-CP/SPCE	0.522	2650	0.730
c.	4-CP/SPCE/activated	0.546	320	0.745
d.	4-CP/SPCE/activated/Apta	0.541	520	0.813
e.	4-CP/SPCE/activated/Apta/KANA	0.584	780	0.821

4.3.3 Equivalent circuit analysis and validation

Equivalent circuit is a key element to investigate the performance of an electrochemical cell, which has the same behaviour as the real cell under a given excitation conditions (Yang et al., 2003). The electrical parameters, which were used to design an equivalent circuit (Randles Circuit, Fig. 4.7) model for electrochemical curve fitting includes primarily, the ohmic/solution resistance (R_{sol}) of the electrolyte solution, the charge transfer resistance between solution and the electrode surface (R_{ct}), double layer capacitance element (Q_{dl} or C) and the Warburg impedance element (W) around each electrode. These factors contribute to the equivalent circuit model representing the experimental impedance data. The W and R_{sol} represented the bulk properties of the electrolyte solution and diffusion features of the redox probe in solution respectively. They are not much affected by modifications of the electrode surface. Q_{dl} magnitude also depends upon the dielectric constant of the layer separating the ionic charges and the electrode surface, electrode surface area and the thickness of the separation layer. During analysis, significant change in Q_{dl} was observed, when bare SPCE was modified with 4-CP layer. Moreover, relatively the small changes were quantified upon further modification. The R_{ct} value depends on the insulating feature at the electrode-electrolyte interface. In the present work, the changes in R_{ct} value were much larger than those in other impedance components (Table 4.4). Based on the observations, the R_{ct} was selected as a suitable signal for sensing the interfacial properties of the fabricated KANA-aptasensor. Fig. 4.12 shows the circuit fitting plot for experimental and fitted data for KANA

binding. The experimental data was fitted using Autolab FRA 4.9 software used for impedimetric measurements and optimized with phase, Z' and Z'' . The presented results suggested that the fitting parameters were in good agreement with experimental data, thus validating the equivalent circuit.

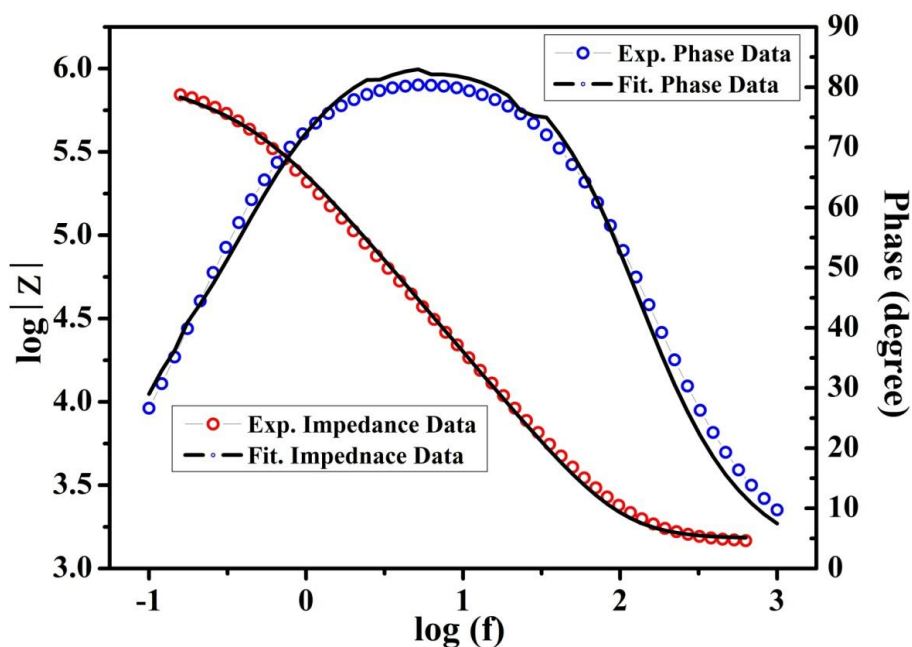


Figure 4.12: Fitting curve of impedance spectrum and phase at ac applied potential: 0.1 V; frequency range: 0.1 Hz to 1 KHz.

4.3.4 Optimization parameters for experimental conditions

Experimental variables, which could significantly affect the performance of an electrochemical aptasensor such as aptamer concentration, pH, incubation time and working temperature were studied and optimized. To establish the stability and sustainability of aptasensor, all the measurements were carried out at ambient temperature (working temperature i.e. 25 °C).

4.3.4.1 Influence of anti-KANA aptamer concentration

Sensitivity of an aptasensor is dependent of the aptamer concentration and plays an important role in the establishment of aptasensor performance. In order to study the effect of ssDNA anti-KANA aptamer concentration on sensor performance, the aptamer concentrations from 0.125 - 4 μM were investigated. Impedimetric response were calculated against KANA (37.5 ng mL^{-1}) and represented as Δ ratio with respect to aptamer concentration. It is evident from Fig. 4.13(a), that Δ ratio increased with increase in the concentration of ssDNA anti-KANA

aptamer. The Δ ratio reached to maximum level and attained equilibrium at 1 μM anti-KANA aptamer concentration and no further change in Δ ratio was recorded with increase in aptamer concentration. This was due to the fact that the signal of KANA-aptasensor at 1 μM was near to the saturation level for KANA (37.5 ng mL^{-1}). Based on the obtained results and to decrease the cost of aptamer used a compromise between aptasensor response (at high concentration) and cost led to the selection of 1 μM anti-KANA aptamer for further experiment.

4.3.4.2 Influence of incubation time

Incubation time is another important parameter that could influence the aptasensor efficiency. A short incubation time might lead to the incompleteness of reaction, whereas a long incubation time may cause the dissociation of complex (Guo et al., 2015). Under above optimized condition (1 μM anti-KANA aptamer and 37.5 ng mL^{-1} KANA), experiments were continued at varying incubation time from 10 to 120 min. It is illustrating from the results that the impedimetric response (Δ ratio) of KANA-aptasensor reached to the plateau stage at 60 min (Fig. 4.13b). After several experiment the 60 min was selected as optimal incubation time for impedimetric measurements.

4.3.4.3 Influence of pH

The pH of working buffer solution has a significant effect on structural integrity of ssDNA anti-KANA aptamer and aptamer-KANA complex, which could influence the recognition mechanism and aptasensor performance (Hainik et al., 2007). The KANA aptasensor response was studied in PBB containing 1 mM $[\text{Fe}(\text{CN})_6]^{4-/3-}$ with different pH of 6.6, 6.8, 7.0, 7.2, 7.4 and 7.6 and the relative changes in the Δ ratio were measured. The obtained results showed that the Δ ratio response increased from 6.6-7.0 pH (Fig. 4.13c) and decreased further. This confirms that the maximum response was observed at pH 7.0 PBB. The reason could be attributed to the activity and structural integrity of biomolecule, which can decline in acidic and alkaline conditions. The unfavourable working conditions may also lead to the dissociation of aptamer-target complex. Thus, pH 7.0 PBB was used in further experimentation.

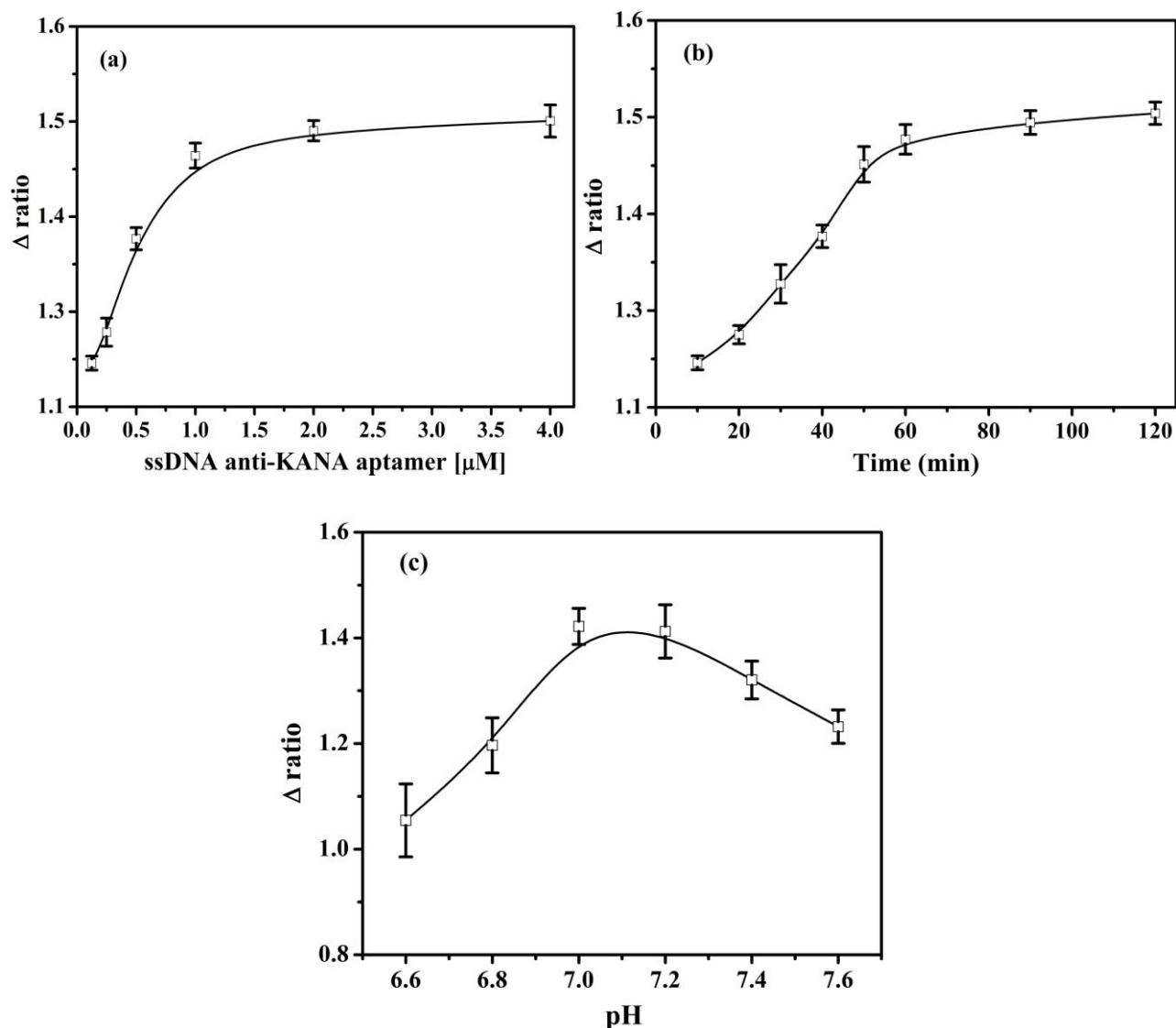


Figure 4.13: Influence of experimental variables (a) aptamer concentrations (0.125–4 μM); (b) incubation time; (c) pH on aptasensor performance at 37.5 ng mL^{-1} KANA in 1 mM $[\text{Fe}(\text{CN})_6]^{4-/3-}$ (prepared in PBB).

4.3.5 Sensitivity measurements for KANA detection (calibration curve)

Under optimized experimental conditions, the calibration curve was performed for quantification of KANA. The binding between KANA and anti-KANA aptamer was followed by an inhibition in the Faradaic response and resulted in an increase in the R_{ct} value (Fig. 4.14). This inhibition could be due to the formation of anti-KANA aptamer-G-quadruplex complex offers an additional negative charge on surface, which causes the decrease in the electron-transfer on SPCE surface.

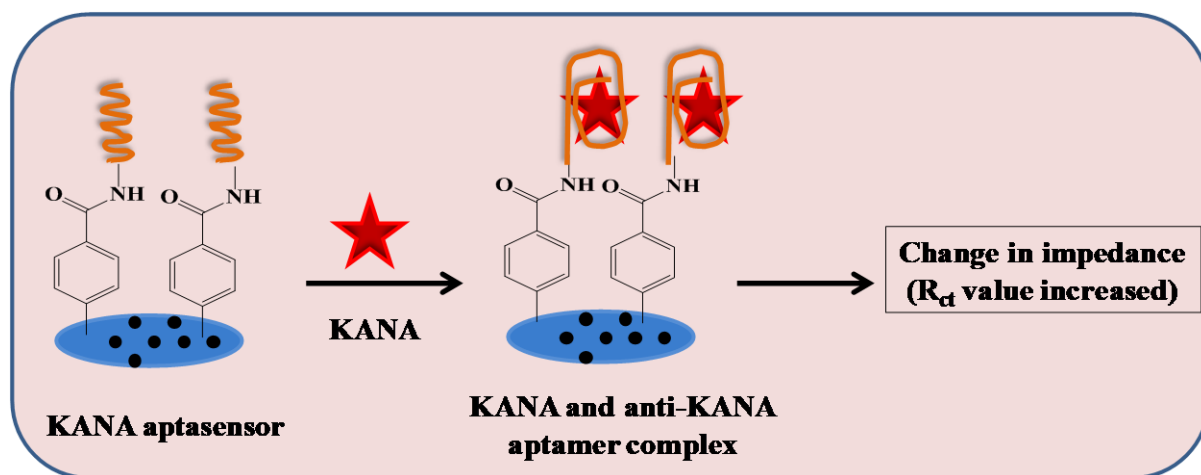


Figure 4.14: Binding and recognition of KANA molecule by ssDNA anti-KANA aptamer on aptasensor surface in PBB (10 mM, pH 7.0).

The obtained experimental points were fitted with the theoretical data points based on the Randles circuit diagram (Fig. 4.7). Binding of KANA with anti-KANA aptamer on aptasensor surface resulted in an increase of the R_{ct} values corresponds to the increase in KANA concentrations from 1.2-600 ng mL⁻¹. The Nyquist plots correspond to the KANA concentrations from 1.2-600 ng mL⁻¹ as larger semi-circular diameter has been shown in Fig. 4.15. The R_{ct} values were calculated from fitted experimental data with theoretical and plotted as Δ ratio corresponds to the various KANA concentrations in PBB (10 mM, pH 7.0) (Fig. 4.16). This label free EIS based aptasensor showed a broad detection range from 1.2-600 ng mL⁻¹ for KANA. The calibration curve was fitted using linear equation. A line of equation $y = 0.0079 x (\text{ng mL}^{-1}) + 1.0842$ with a coefficient of correlation, $R^2 = 0.9925$ ($n=4$) was calculated. A good linear relationship between the relative impedance change (Δ ratio) and KANA concentration in the range from 1.2-7.5 ng mL⁻¹ KANA was obtained. Similarly, the calibration curve was prepared for milk. A broad detection range from 1.2-600 ng mL⁻¹ KANA with linearity 1.2-75 ng mL⁻¹ KANA was calculated (Fig. 4.17). A line of equation obtained was $y = 0.0080 x (\text{ng mL}^{-1}) + 1.0810$ with a coefficient of correlation, $R^2 = 0.9935$ ($n=3$). Good linearity between relative impedance change (Δ ratio) and increasing KANA concentration from 1.2-7.5 ng mL⁻¹ KANA was observed. The LOD was calculated and found to be 0.11 ng mL⁻¹ KANA ($n=4$) ($S/N = 3$) in buffer and milk. The present method showed the lowest LOD among reported methods (Table 4.2). In the calibration curve, equilibrium was attained at concentration higher than 600 ng mL⁻¹, which might due to the binding of all the available active sites of the anti-KANA aptamer on the electrode surface.

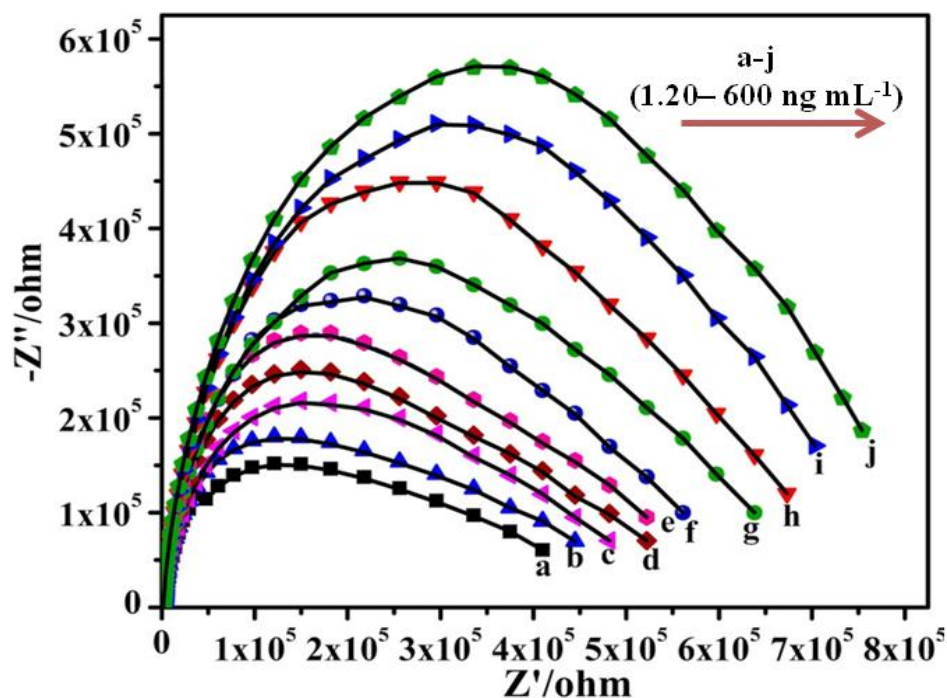


Figure 4.15: Nyquist plots of KANA aptasensor against different concentrations of KANA (a) 1.20, (b) 2.40, (c) 4.75, (d) 9.50, (e) 19.0, (f) 37.5, (g) 75.0, (h) 150, (i) 300 and (j) 600 ng mL^{-1} (vs. Ag/AgCl reference electrode) spiked in buffer with the fitted theoretical data obtained 1 mM $[\text{Fe}(\text{CN})_6]^{4-/3-}$ (prepared in PBB, pH 7.0).

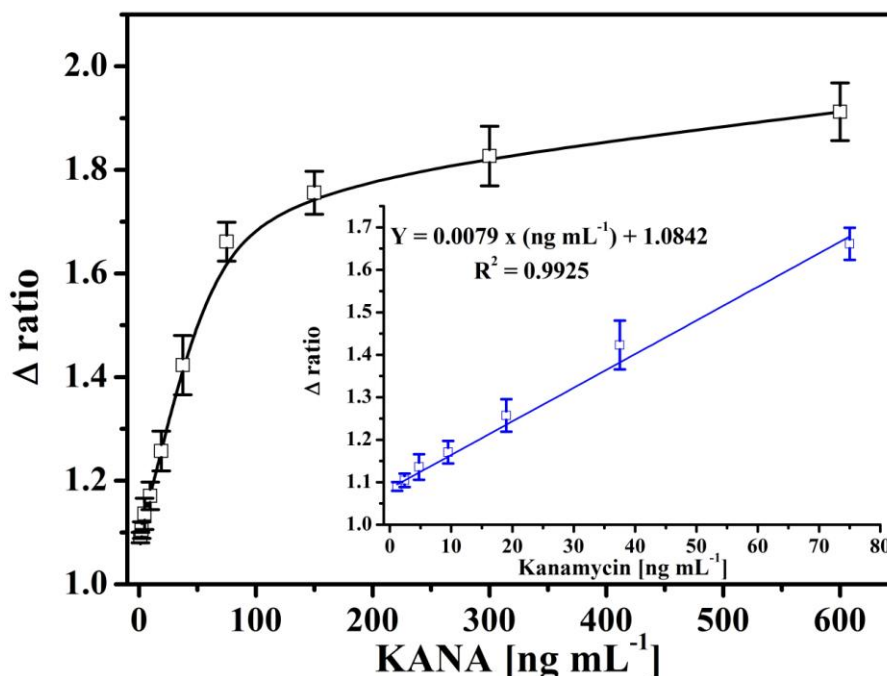


Figure 4.16: Calibration curve showing change in the Δ ratio vs KANA concentration (1.2–600 ng mL^{-1}) in PBB (10 mM, pH 7.0). Inset represents the linear curve from 1.2–7.5 ng mL^{-1} ($n=4$).

The higher sensitivity and low detection of presented KANA aptasensor was attributed to the following reasons (i) integration of SPCE technology employed in the fabrication of KANA aptasensor; (ii) the diazonium coupling mechanism provided better immobilization of anti-KANA aptamer; (iii) the aptamer sequences used was highly specific and selective to the KANA molecules.

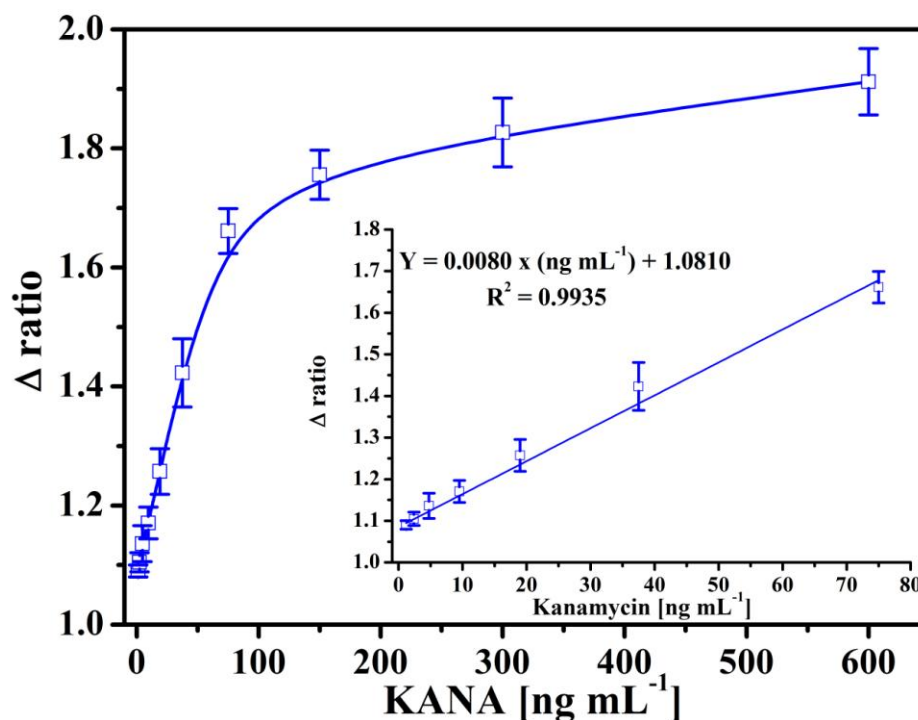


Figure 4.17: Calibration curve in milk showing the change in the Δ ratio vs various concentrations of KANA ($1.2\text{-}600 \text{ ng mL}^{-1}$). Inset represents the linear curve from $1.2\text{-}7.5 \text{ ng mL}^{-1}$ ($n=3$).

4.3.6 Selectivity performance of KANA-aptasensor

The specificity of developed detection method is always of paramount interest to evaluate the method performance. The devised KANA-aptasensor performance was verified in the presence of possible structural analogues streptomycin (SRT) and gentamicin (GENTA). All measurements were carried out at two different concentration levels of 9.5 and 37.5 ng mL^{-1} KANA, SRT, GENTA and binding buffer. It is evident from Fig. 4.18, the structural analogues (SRT and GENTA) showed negligible response compared to the KANA. The obtained Δ ratio histogram response of other analogues were found to be less than 10 % ($n=3$) response of KANA. The small response signal obtained with SRT and GENTA might be due to their high molecular weights, which impart a negative charge or retard the electron transfer, thus increased the impedance. Moreover, these results strongly suggested that the

responses obtained with KANA were due to the interaction between KANA with ssDNA anti-KANA aptamer. All the results were quantified and tabulated in Table 4.5.

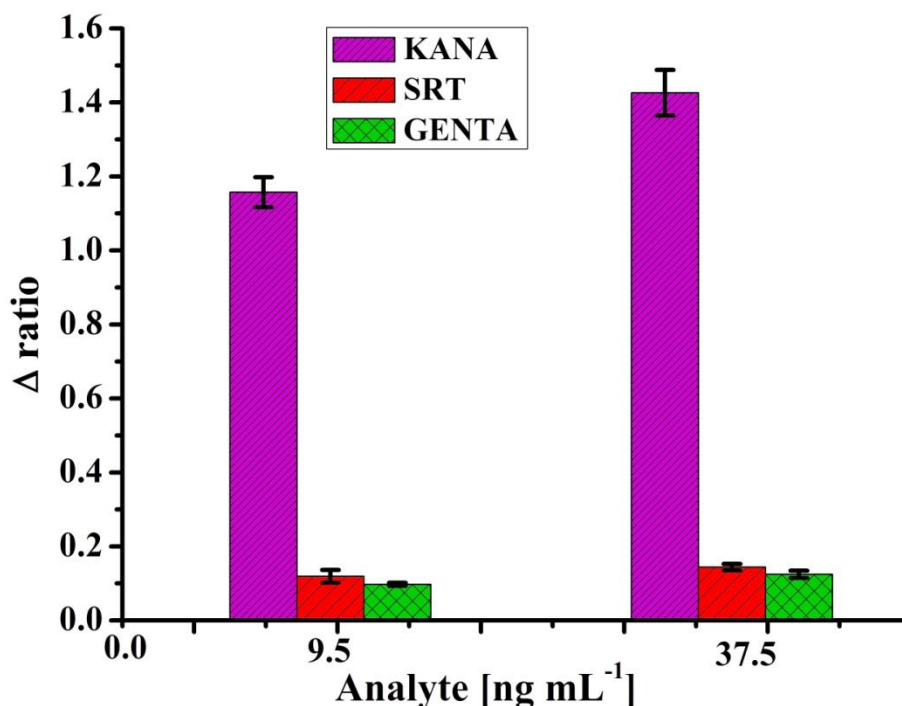


Figure 4.18: Impedimetric responses (Δ ratio) of fabricated aptamer for KANA, SRT and GENTA at concentration level 9.5 and 37.5 ng mL⁻¹ (n=3).

Table 4.5: Specificity and selectivity performance of KANA-aptasensor

Conc ⁿ . [ng mL ⁻¹]	KANA response (Δ ratio)		SRT response (Δ ratio)		SRT response (%)	GENTA response (Δ ratio)		GENTA response (%)
	Mean \pm S.D. (n=3)	R.S.D. %	Mean \pm S.D. (n=3)	R.S.D. %		Mean \pm S.D. (n=3)	R.S.D. %	
9.5	1.157 \pm 0.045	3.88	0.119 \pm 0.011	9.24	10.28	0.097 \pm 0.004	4.12	8.38
37.5	1.426 \pm 0.062	4.35	0.144 \pm 0.009	6.25	10.09	0.124 \pm 0.009	7.26	8.70

4.3.7 Application in milk sample

For practical application, the feasibility of developed KANA-aptasensor was further evaluated in milk samples using standard spiking method. The milk sample was treated as discussed under experimental section for matrix matching. For milk sample analysis, different concentrations of KANA were selected based on the calibration curve performed in the milk (Fig. 4.17). Three concentrations of KANA from the linear range (4.75, 9.5 and 37.5 ng mL⁻¹) and one corresponds to MRL (150 ng mL⁻¹) were studied for parallel measurements. Similarly, the controls were prepared by adding same concentration of KANA in the binding buffer. The obtained experimental data was fitted with theoretical points and plotted as Δ ratio against the spiked KANA concentrations (Fig. 4.19). The recoveries obtained were in the range of 96.88 to 100.5 % to the spiked concentrations with a maximum % RSD of 4.56 for parallel triplicate measurements (Table 4.6). The obtained recoveries were in good agreement indicating the analytical reliability and potential of KANA-aptasensor for KANA detection in non-treated milk samples.

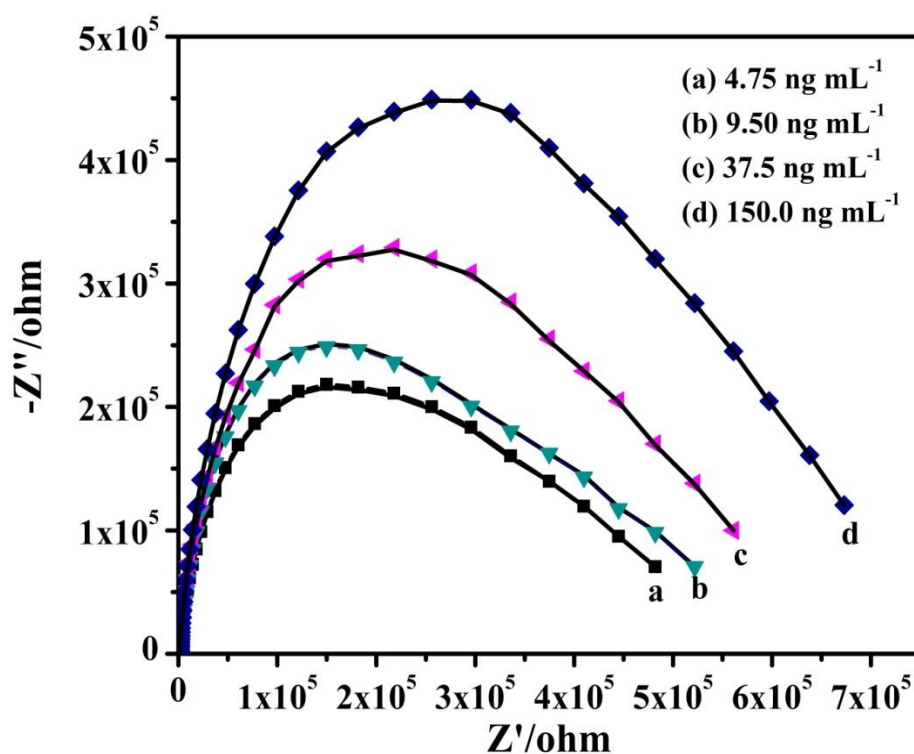


Figure 4.19: Nyquist plots of anti-KANA-aptamer modified SPCEs with different concentrations of KANA spiked in the milk sample (ng mL⁻¹); (a) 4.75, (b) 9.50, (c) 37.50 and (d) 150 obtained 1 mM [Fe(CN)₆]^{4-/3-} (prepared in PBB, pH 7.0) fitted theoretical data.

Table 4.6: Recovery calculation of KANA-aptasensor for KANA spiked milk samples

Recovery performance of aptasensor in spiked milk sample					
Milk sample	KANA added [ng mL ⁻¹]	KANA found [ng mL ⁻¹]	R.S.D. %	Recovery %	R.E. %
1.	4.75	4.65 ± 0.21	4.56	97.89	-2.11
2.	9.50	9.55 ± 0.19	2.01	100.5	0.50
3.	37.5	36.33 ± 1.04	2.86	96.88	-3.12
4.	150.0	148.95 ± 2.06	1.38	99.30	-0.70

4.3.8 Analytical performance of KANA-aptasensor

To evaluate the precision performance of devised KANA aptasensor, the reproducibility and repeatability of sensor are essential parameters. Under optimized experimental conditions, the inter-assay precision performance was evaluated for three different aptasensors prepared independently under similar experimental conditions for KANA detection (9.5 and 37.5 ng mL⁻¹). The percent relative standard deviations of three parallel measurements were found to be 3.44 % and 4.28 % for 9.5 and 37.5 ng mL⁻¹, respectively (Table 4.7). The results suggested that the devised KANA-aptasensor exhibited good precision and reproducibility.

Table 4.7: Precision performance of aptasensor for detection of KANA in milk sample

Inter-assay precision analysis					
KANA concentration [ng mL ⁻¹]	Δ ratio response			Mean ± S.D. (n=3)	R.S.D. %
	Exp-1	Exp-2	Exp-3		
9.5	8.95	9.40	9.70	9.31 ± 0.32	3.44
37.5	35.34	37.64	38.40	37.12 ± 1.59	4.28

The storage stability of KANA-aptasensor was further studied by comparing the Δ ratio over a period of two weeks after storage at 4 °C. The developed aptasensor showed the similar EIS and CV responses after a storage period of 2 weeks at 4 °C with a negligible drop in the

activity. This was due to the covalent immobilization of aptamer over diazonium modified electrodes (4-CP/SPCE), which prolonged the shelf-life and also prevented the leaking out of aptamer under optimized set of conditions. The merit of figures for the developed aptasensor has been tabulated in Table 4.8.

Table 4.8: Analytical figures of merits for devised KANA-aptasensor

Parameter	Findings
Linear range	1.20-75 ng mL ⁻¹
Dynamic range	1.20-600 ng mL ⁻¹
Limit of detection	0.11 ng mL ⁻¹
Sample volume	20 µL
Inter assay precision	3.44 and 4.28 %
Analysis time (response time)	Less than 3 min

4.4 Conclusion

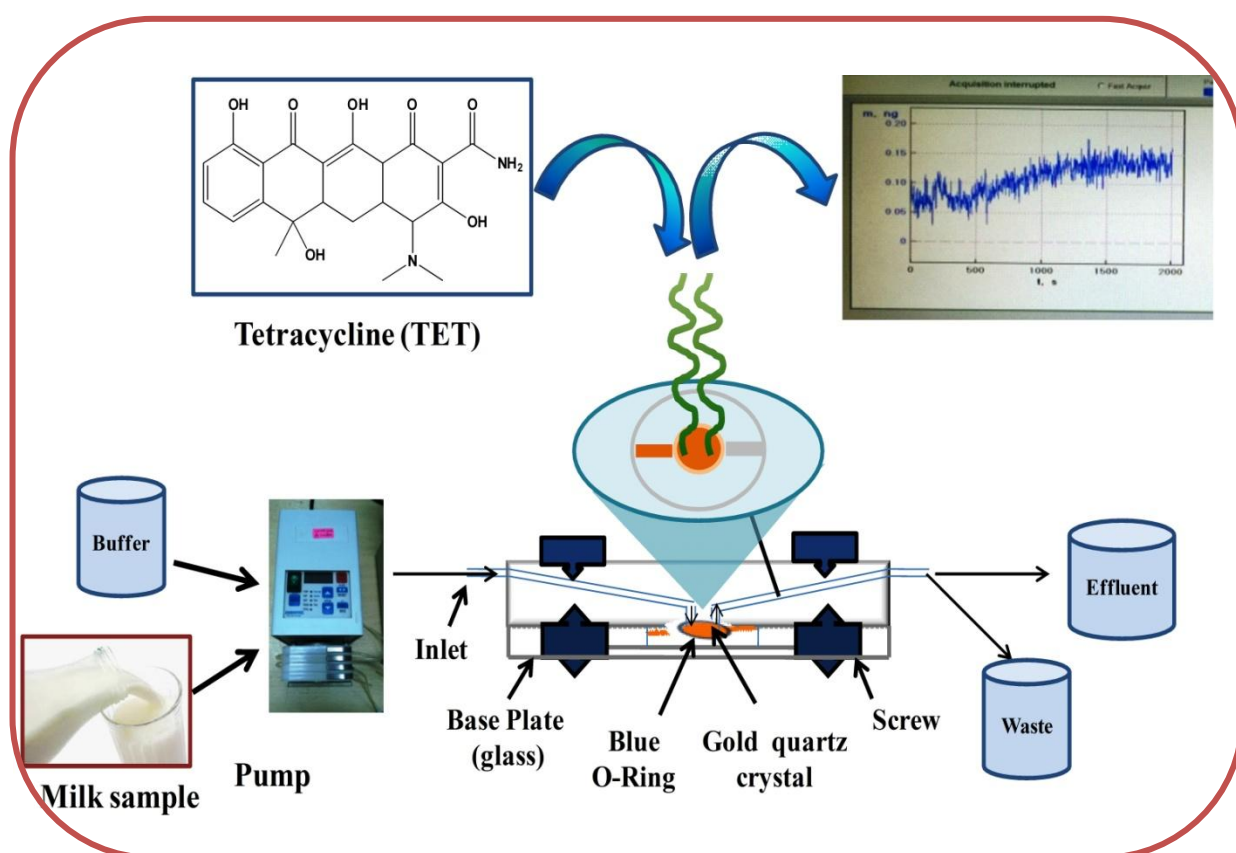
In the present work, a disposable and label-free SPCEs integrated impedimetric aptasensor for analysis of residual KANA analysis in buffer and milk sample has been demonstrated. The presented aptasensor meets the requirement of various regulatory authorities (Table 4.1). Implication of diazonium coupling mechanism and SPCEs technology offer the advantages of disposability, improved sensibility and stability. The aptasensor could detect the KANA down to the 0.11 ng mL⁻¹. The EIS based developed KANA-aptasensor could determine the presence of KANA in less than 3 min response times. The proposed aptasensor showed the recovery percentage between 96.88-100.5% in milk samples. The precision and accuracy studies prove that the presented aptasensor has the good selectivity, reproducibility and stability. The present results envisaged that the SPCEs based KANA aptasensor could be further extended to detect the KANA in other food matrices.

CHAPTER 5

Development of μ FIA-EQCN aptasensor for analysis of Tetracycline residue in milk sample

Novelty Statement:

- A μ FIA integrated EQCN aptasensor has been developed for detection of target analyte.
- Aptasensor performance was evaluated for on-line and real time analysis of tetracycline in milk sample.
- Developed aptasensor exhibited the sensitivity i.e. 0.531 ng mL^{-1} TET with no significant cross reactivity.



Graphical abstract for chapter content

5.1 Background

In view of successful development of disposable and label-free electrochemical aptasensor (Chapter 4), in this chapter, the focus was to develop a label free and real time aptasensor for on-line monitoring of antibiotic residual presence. Based on the availability of numerous ligand molecule and their well defined specificity towards cognate molecules to form the ligand-target complex, makes it possible to develop piezoelectric/mass sensitive biosensor for detection of wide range of analyte of interest. For development of real time aptasensor, a microfluidic flow injection analysis (μ FIA) platform integrated with piezoelectric transducer was developed for detection of tetracycline (TET).

5.1.1 Occurrence of antibiotic contamination in milk

Antibiotics are the one of the most important class of antimicrobial drugs, developed to stimulate a physiological response in humans, animals and other microorganisms. Unlike in human medicine, antibiotics are heavily used for the treatment and management of food producing animals mainly for two different purposes: (a) prevention and control of bacterial infections and (b) as growth promoters (Schwarz et al., 2001). In veterinary medicine and dairy industries, antibiotics are routinely used to treat mastitis in dairy cows. Antibiotics potential as growth enhancers also has led to their use in animal feed as feed supplements. In the last decades, with the increasing prudence of antimicrobial resistance, the antibiotic resistance and resistance to other anti-infective agents constitutes a major threat to the public health and ought to be recognized as such more widely than it is at present (Kümmerer, 2003). Tetracyclines (TCs) are commonly used broad-spectrum antibiotics containing four condensed rings. TCs are further divided into two sub-classes of natural TCs (tetracycline, oxytetracycline, aureomycin etc) and semi-synthetic TCs (doxycycline, minocycline etc.) (Chen et al., 2014). Among all, the tetracycline (TET) is widely used for the treatment of infectious diseases in fodder animals. The extensive use of TET in dairy and animal industries has led to the accumulation of TET in milk and other food products (Zhou et al., 2012). Meanwhile, the continuous occurrence and exposure of TET residues in food has also become a potential threat to the human health and environment. Indiscriminate use of TET may produce the TET contaminated milk and subsequently causes the liver damage, yellow coloration of teeth, allergic reaction and cross-contamination with ions (such as Ca^{2+}) present in milk (Gan et al., 2014). Therefore, the TET contamination has become one of the most

noticeable contaminations in milk and milk based products, since the presence of minute amount of TET can trigger the potential hazards (Conzuelo et al., 2013) (Fig. 5.1).



Figure 5.1: Toxicity effect of TET contamination on human health.

It is evident from the literature that TET has not been used as growth promoters in dairy industries in EU since 1980's but used in USA (Schwarz et al., 2001). It has now become important to develop a rapid, sensitive and specific method for TET analysis in milk and other food products. To safeguard and ensuring the food safety and human health, various regulations for TET have been mandated by the regulatory authorities (Table 5.1) (CAC joint FAO/WHO report 2003; FSSAI 2012; EU Regulation 2003).

Table 5.1: Recommended MRLs for TET in milk and milk based products

TET	MRLs			
	EU	USFDA	FSSAI	CODEX
Milk and milk products	100 $\mu\text{g kg}^{-1}$	100-300 $\mu\text{g kg}^{-1}$	100 $\mu\text{g kg}^{-1}$	200 $\mu\text{g kg}^{-1}$

5.1.2 State of art for TET analysis in milk

Since the identification of TET residue presence in milk samples, there has been lots of efforts to develop an analytical tool for detection of TET in milk/ milk based products. The commonly employed techniques reported for the detection of TET are HPLC (Ng and Linder, 2003), HPLC coupled with fluorescence detector (HPLC-FD) (Mesgari Abbasi et al., 2011),

capillary electrophoresis (Ibarra et al., 2011), liquid chromatography coupled with mass spectroscopy (LC-MS) (De Ruyck and De Ridder, 2007; Berendsen et al., 2013) and high-performance thin-layer chromatography–fluorescence detection and electrospray ionization mass spectrometry (HPTLC-FLD-ESI/MS) (Chen and Schwack, 2013) and polymer based fluorescent methods using transition metals (Tan et al., 2013). These reported methods suffer with the drawbacks of time-consuming process, large and expensive bench-top because they are often performed in conjunction with separating techniques, that lacks the specificity and always need a certified reference standards. Recently, the ELISA techniques and immunological methods due to the high sensitivity of antibody against their targets have been reported for TET detection (Conzuelo et al., 2013; Chen et al., 2016). The immunological methods are sensitive but their specificity is limited due to the potential cross-reactivity of interferents with structural similarities, which lead to the false positive results (Aga et al., 2005). These methods are commonly employed as screening tests. Moreover, the preparation processes of monoclonal antibody are rather complicated and nonspecific conjugation of antibody with appropriate labels often results in a low productivity of labelled-antibody. Currently, the looking for alternatives methods for label free and real time monitoring of TET residual presence in milk sample is on high demand.

5.1.3 Aptasensors for TET determination

Comparing to traditional immunological and chemical recognition molecules, aptamers provides high affinity, specificity and versatility in detection methods. Numerous aptasensors have been recently reported for the determination of TET in milk samples as summarized in Table 5.2. The mass based or gravimetric sensors (quartz crystal microbalance i.e. QCM) allow the detection of target molecule in complex matrix at quite a low level, which makes them suitable for various applications and industries. Owing to its simplicity, real time binding response and convenience, QCM has been increasingly explored for detection of antibiotic residues and other food contaminants (Karaseva and Ermolaeva, 2012; Melikhova et al., 2006; Karaseva and Ermolaeva, 2014). QCM has the advantages of minimal electrical requirements, diversity for adaptability to microfluidic techniques, integrity with flow cell, and label-free detection. One of such testimony is electrochemical quartz crystal nanobalance (EQCN) employed for detection of streptomycin (SRT) in milk using flow injection analysis (Mishra et al., 2015). The QCM biosensor integrated with flow injection analysis (μ FIA-QCM) system has the advantages in terms of reproducibility, speed of analysis, control of

contact time, label-free measurements and concentration profiling in kinetic studies (Malitesta et al., 2012).

Table 5.2: Summary of reported aptasensors for detection of TET in the milk samples

S. No.	Method	Dynamic range	LOD	Ref.
1.	Electrochemical aptasensor (CV)	0.1-100 ng mL ⁻¹	1.0 ng mL ⁻¹	Zhang et al., 2010
2.	Label free aptasensor (DPV)	44.4 ng mL ⁻¹ -222.2 μ g mL ⁻¹	2.22 μ g mL ⁻¹	Zhou et al., 2012
3.	Optical (ELAA)	14.044 μ g mL ⁻¹ -140 mg mL ⁻¹	0.210 ng mL ⁻¹	Jeong and Paeng et al., 2012
4.	Label free aptasensor (EIS)	5.0-5000 ng mL ⁻¹	1.0 ng mL ⁻¹	Chen et al., 2014
5.	Electrochemical aptasensor (DPV)	44.4 ng mL ⁻¹ -0.44 mg mL ⁻¹	1.866 ng mL ⁻¹	Guo et al., 2015
6.	Electrochemical aptasensor (EIS)	10-3000 ng mL ⁻¹	10 ng mL ⁻¹	Thi Hanh et al., 2016
7.	Electrochemical (CV)	666.6 ng mL ⁻¹ -2.2 mg mL ⁻¹	325.86 ng mL ⁻¹	Taghdisi et al., 2016
8.	μFIA-EQCN (First report)	1.562-2000 ng mL⁻¹	0.531 ng mL⁻¹	This work

5.1.4 Flow injection analysis (μ FIA)

Since the development of μ FIA in mid-70s, the μ FIA mode has proven itself as a powerful analytical technique in development of biosensing platforms (Hansen, 1996). In μ FIA, an injection of liquid sample into a moving and non-segmented continuous carrier stream is

carried out. The injected sample forming a zone is transported toward detector that continuously measures the change in signal resulting from the interaction between analyte and ligand molecules (Fig. 5.2). In principle, the μ FIA working is based on three different processes: firstly, the injection of metered sample volume then the reproducible and precise timing of sample injection and last the measurement of continuous transit signal at detector (Hansen et al., 2009). Existing literature suggests that until now, there is no such literature reported for TET detection using μ FIA-EQCN. In the present work, we have designed an EQCN aptasensor integrated with customized designed of flow cell (μ FIA-EQCN) for TET detection. This integration allows the on-line and real time monitoring of the binding interaction corresponds to the various TET concentrations.

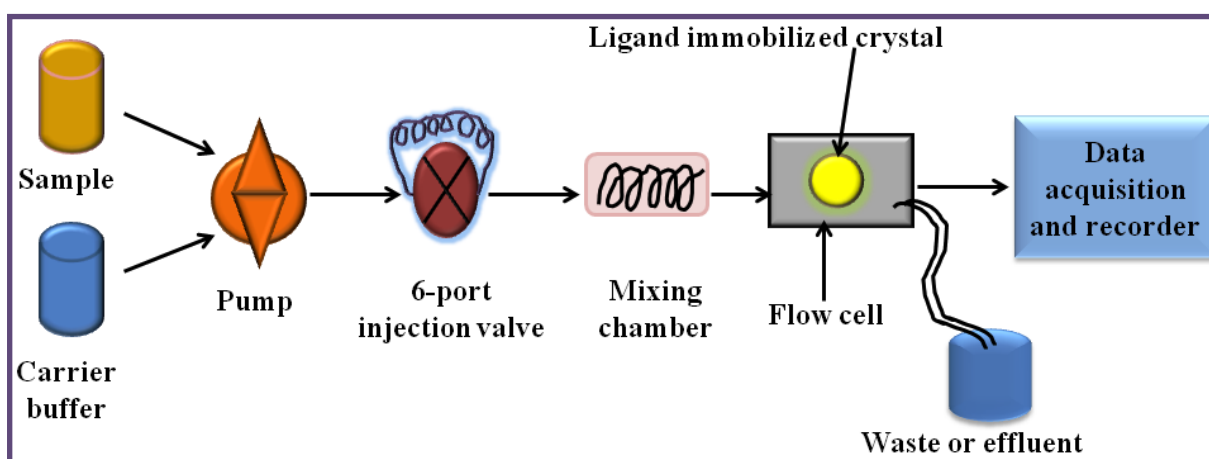


Figure 5.2: Flow diagram for the development of μ FIA-EQCN biosensor.

5.1.5 Working principle of EQCN

The working principle of QCM detection is based on the change in frequency of the AT-cut quartz crystal sandwiched between two metal electrodes. The quantitative relationship between the change in vibrational frequency of crystal and mass changes at the crystal surface can be quantified by well-known Sauerbrey equation (Sauerbrey, 1959).

$$\Delta f = \frac{-2\Delta m f_0^2}{A\sqrt{\rho_q \mu_q}} \quad (5.1)$$

Where, Δf is frequency change (Hz), Δm is the mass change (gm) on the sensor surface, f_0 is the fundamental frequency (Hz), A is the electrode surface area, and ρ_q and μ_q are the density (cm^3) and the shear modulus ($\text{gm cm}^{-1}\text{s}^{-2}$) of the QCM sensor, respectively.

The EQCN is a measurement system designed to monitor the extremely minute variation in the mass of a working electrode attached to a vibrating single gold coated quartz crystal. Thin wafers cut from a quartz crystal at a specific orientation ($35^{\circ}15'$ angle) with precise thickness (0.166 mm) oscillating at a characteristic fundamental frequency of 10 MHz were used. Here, the working electrode (gold electrode) was a thin metal film evaporated on one side of a quartz crystal wafer and sealed to the side opening in an electrochemical cell. A minute change in the mass attached to the working electrode results in the change of the vibrational frequency of quartz crystal. This change in frequency of the working quartz crystal is measured and compared with the vibrational frequency of the standard reference quartz crystal (with same fundamental frequency 10 MHz). Therefore, the frequency measurements are differential, i.e. the frequency of the reference quartz crystal is subtracted from the frequency of the working quartz crystal. Using a frequency-to-voltage converter, the obtained change in frequency is converted to an analog voltage and measured by a 16-bit analog-to-digital converter (ADC). The frequency shift corresponds to the mass change (Δm) of the working electrode. The EQCN experiments were completely computer controlled with the data logger DAQ-716 integrated with real-time VOLTSCAN data acquisition and control system (based on a 16-bit D/A converter and 16-bit A/D converters). In built Voltscan 5.0 software was used for all the data processing, graphing, and spreadsheet reporting. In the present EQCN 700 system, the resonant frequency of the gold crystal was 10MHz (10 x 10⁶ Hz) and calculated change of 1 Hz equals to 1.1040 ng of mass change. For results and analysis, the frequency change (Δf) was converted to the mass change (Δm) using following equation:

$$\Delta m = \frac{-\Delta f \times A \times \sqrt{\rho_q \mu_q}}{2f_0^2} \quad (5.2)$$

Where, Δm = mass Change (gm); Δf = resonant frequency change (Hz); A = piezoelectric active surface for reaction (0.25 cm²); μ_q = AT-cut quartz constant (2.947x10¹¹ gm cm⁻¹ s⁻²); ρ_q = quartz crystal density (2.65g cm³); f_0 = Reference or Resonant Frequency (Hz)

5.1.6 Research gap identified

The existing literature and prevalence of TET residual contamination revealed that there is an immense need to develop a sensitive and label-free method for on-line monitoring of TET contamination. To the best of our knowledge, there is no literature reported on μ FIA-EQCN system for detection of TET in milk sample.

5.1.7 Objective

The objective of present work was to develop a label-free and real time aptasensor for TET analysis in untreated raw milk sample using μ FIA integrated EQCN aptasensing platform.

5.2. Experimental section

5.2.1 Biochemicals and reagents

The tetracycline aptamer ATW0031 was purchased from Base Pair Biotechnologies (Pearland, Texas, USA). The functionally modified nucleotide sequence (40 bases) of ssDNA TET-aptamer attached with 10T linker was prepared and purified by Base Pair Biotechnologies and was used after pre-treatment. Tetracycline ELISA kit was procured from Bioscientific Austin, Texas, USA. All the analytical grade reagents Tris-HCl buffer, ethylenediaminetetraacetic acid, potassium dihydrogen phosphate, disodium hydrogen phosphate, sodium chloride, potassium chloride, magnesium chloride, *N*-hydroxysuccinimide (NHS), *N*-(3-dimethylaminopropyl)-*N*-ethyl-carbodiimide hydrochloride (EDC) and ethanolamine were procured from Merck kGaA (Darmstadt, Germany). Tetracycline hydrochloride as reference standard was purchased from Sigma Aldrich (USA). For specificity, the oxytetracycline, minocycline and doxycycline were also purchased from MP Biomedicals (Illkirch, France). The deionized Milli-Q water obtained from (Millipore, Bedford, MA, USA) was used for reagent preparation. For real sample analysis, the milk samples were procured from the local market of Goa, India.

5.2.2 Instrumentation

The EQCN-700 system integrated with microfluidic flow cell model FC-6 (Elchema, Potsdam, New York, USA) was used for the construction of μ FIA aptasensor for TET determination. A gold quartz crystal (10 MHz, AT cut) connected to the frequency-measuring unit, which contains a reference quartz crystal with the same frequency range as measuring crystal. An automated tubing pump (ISMATEC, Germany) was connected to a 6 port injection valve (Rheodyne, USA) to the flow-cell. The quartz crystal mounted flow cell was placed in a faraday cage to shield the crystal environment from the external electromagnetic sources. The output from the oscillator was measured by the frequency unit, which calculated the mass by using a conversion factor (1 Hz equivalent to 1.104 ng). A personal computer controlled the data acquisition. The sequential step of experimental setup used for the μ FIA aptasensor measurements has been shown in Fig. 5.2. Fourier Transform Infrared (FT-IR)

spectroscopy measurement was performed for surface characterization of aptasensor at various steps. The vibrational spectra were recorded using IR Affinity-1 attached with attenuated total reflectance (ATR) at Specac Diamond ATR AQUA (SHIMADZU, Japan). Spectrums were recorded with 128 scans at 64 cm^{-1} resolution collected under vacuum conditions. Surface topography was studied using AFM measurements at multimode scanning probe microscope system operated in tapping (semicontact) mode using NTEGRA Prima (NT-MDT, Zelenograd, Moscow, Russia). The scanning electron micrograph of fabricated aptasensor was recorded on scanning electron microscope (SEM XL 30 FEI/Philips, Philips Electronics Co., Netherlands) for various steps.

5.2.3 Solution preparation

5.2.3.1 Preparation of buffers

Tris-HCl EDTA buffer was prepared by dissolving an appropriate amount of Tris-HCl (315.2 mg, 10 mM) and EDTA (7.45 mg, 0.1 mM) in membrane filter (0.2 μM) deionized water (RO water). The pH of buffer was adjusted to pH 7.5 before use. The phosphate binding buffer (PBB, 10 mM) was prepared by dissolving appropriate amount of Na_2HPO_4 and KH_2PO_4 containing 137 mM NaCl, 2.7 mM KCl and 1.0 mM MgCl_2 in membrane filtered deionized water (RO water). HEPES binding buffer (HBB, 10 mM) containing 1.35 mM KCl, 5 mM MgCl_2 and 60 mM NaCl was prepared in the membrane filtered deionized water (RO water). The pH of the binding buffers was adjusted to 7.4 before use and stored at $4\text{ }^\circ\text{C}$ when not in use.

5.2.3.2 Preparation of TET standards

TET standards were prepared by dissolving a known amount of TET in HBB and subsequently diluted to meet the requirement of calibration curve ($1.56\text{-}2000\text{ ng mL}^{-1}$) and regulatory standards. All the solutions were freshly prepared before the experiment and stored at $4\text{ }^\circ\text{C}$ when not in use.

5.2.3.3 Aptamer preparation

For preparation of aptamer stock and working standard solutions, the protocol provided by Base Pair Technologies (Taxes, USA) was used. In brief, the ssDNA anti-TET aptamer stock solution was prepared by dissolving the lyophilized powder in Tris-EDTA buffer (10 mM). Then subsequent dilution was prepared in the binding buffer in the range $0.125\text{-}2.0\text{ }\mu\text{M}$ anti-

TET aptamer. Each aptamer concentration was treated on Light cycler 96 for unwinding of aptamer structure (RT-PCR, Roche Diagnostics, Mannheim, Germany). The following temperature profile was used for aptamer denaturation: heating at 90 °C for 5 min to initial denaturation step, followed by a structure maintain step at 4 °C for 5 min and room temperature for 15 min.

5.2.3.4 Matrix matching

The raw milk sample (1.5 % fat content) was purchased from the local market of Goa, India. The presence of fat content in milk may led to clogging of microfluidic channels and thus decrease the aptasensor performance. Whereas, the complex matrix treatment effect such as dissolving fat by acid treatment (trichloroacetic acid or ammonia solution) could disturb the matrix composition. Therefore, a simple method was optimized to address the matrix effect. In brief, the raw milk samples were centrifuged at 10000 rpm for 20 min at RT. Supernatant was filtered and spiked with known concentration of TET (600 ng mL⁻¹) and diluted further with unspiked milk samples and analyzed with the aptasensors.

5.2.4 Methodology for aptasensor construction

ssDNA anti-TET aptamer, which consists of a central region of 40 nucleotides flanked by 10-T linker and amine group at 3' end was used for designing the aptasensing platform. The ssDNA anti-TET aptamer was uniformly immobilized on gold coated quartz crystal surface that was used as transducer (Fig. 5.3). The surface of gold quartz crystal was prior cleaned with acid piranha (H₂O₂:H₂SO₄ in 1:3) solution. The gold quartz crystal surface was functionally modified using cross-coupling chemistry with 11-mercaptoundecanoic acid (11-MUA, 4 mM), cysteamenium (10 mM) and 4-aminothiophenol (4-ATP, 4 mM) until the cross-linker exhibiting maximum binding was achieved. After optimization, each gold coated quartz crystal was incubated with 100 μ L of 11-MUA as cross-linkers for 8 hr at RT under reduced pressure (Step-1). Afterward, crystal surface was washed with ethanol and copious amount of membrane filtered RO water to remove unbound fraction and dried under nitrogen environment. End-group activation of 11-MUA modified quartz gold surface was performed using EDC:NHS coupling chemistry by incubating SAMs modified crystal with EDC:NHS (3:1 ratio) for 1 h at RT under humid environment (Step-2). Activated crystal surface was washed with copious amount of membrane filtered water and binding buffer. Finally (Step-3), thiolated gold coated quartz crystal was incubated with 40 μ L of 1 μ M anti-TET aptamer solution in HBB (10 mM, pH 7.4) for 4 h under humid environment at RT (until the aptamer

concentration for maximum binding was optimized). The aptamer immobilized crystal was immersed in 0.01% v/v solution of tween 20 for 15 min and subsequently washed with the HBB and mounted on the flow cell to use in μ FIA mode.

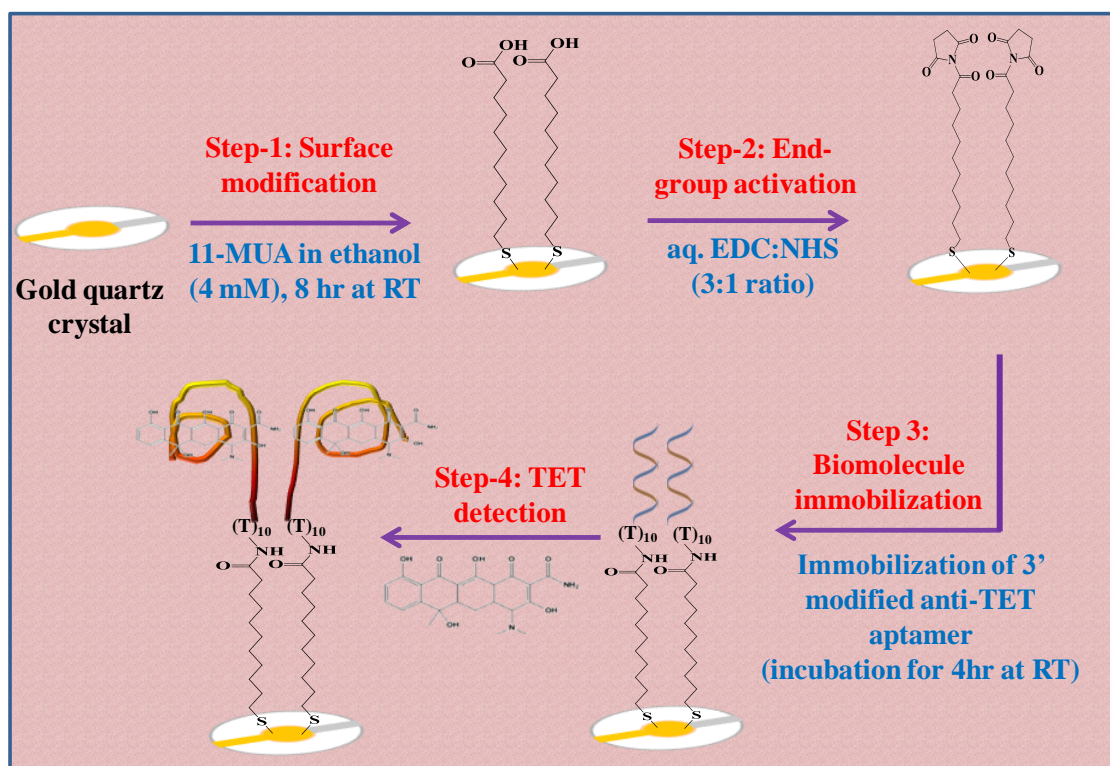


Figure 5.3: Schematic for fabrication of μ FIA-EQCN TET-aptasensor for TET analysis.

5.2.5 Design of flow cell (microfluidic system)

The ssDNA anti-TET aptamer immobilized on gold coated quartz crystal was placed in the plexiglass flow cell, which is sandwiched between flow cell and the blue O-ring (Fig. 5.4). Here, the upper electrode surface in contact with the liquid (flowing through the microfluidic cell) and the lower electrode in the air were connected through the microfluidic inlet and outlet channel and connected to electronic circuit via electrode. The diameter of quartz crystal was 14 mm, whereas the diameter of working electrode (gold surface) was 5 mm and a volume capacity of 50 μ L ($\varnothing = 8$ mm and height =1 mm). The automated pump was connected to the system providing the less pressure exerted on the crystal surface. Various samples were filled in the 6-port injection valve and injected to the flow cell through carrier buffer using a sample loop (100 μ L). Samples were passed through flow cell at a flow rate of 0.1 mL min^{-1} and real time binding response was recorded until the equilibrium attained.

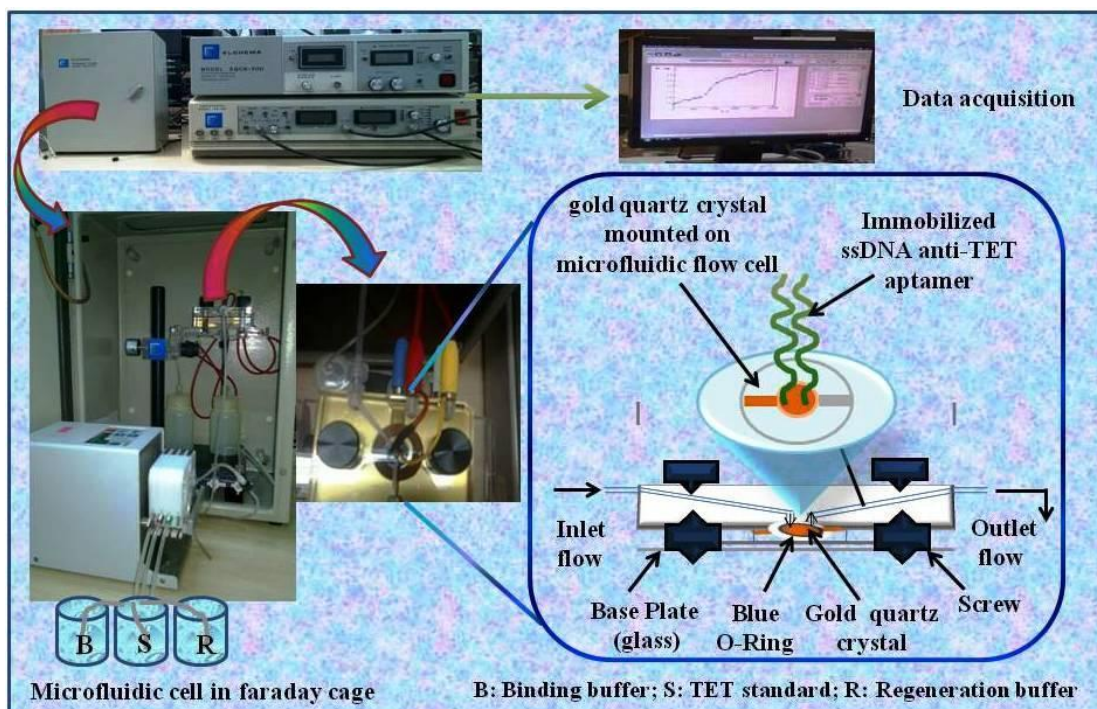


Figure 5.4: Design of microfluidic platform of μ FIA-EQCN aptasensor.

5.2.6 Binding assay of anti-TET aptamer

The mass binding kinetic studies were performed in flow mode (Fig 5.5). The ssDNA anti-TET aptamer pretreated in HBB (10 mM, pH 7.4 at 25 °C) as previously described (section 5.2.3.3). Then 50 μ L of aptamer solution was incubated on the SAMs modified gold quartz

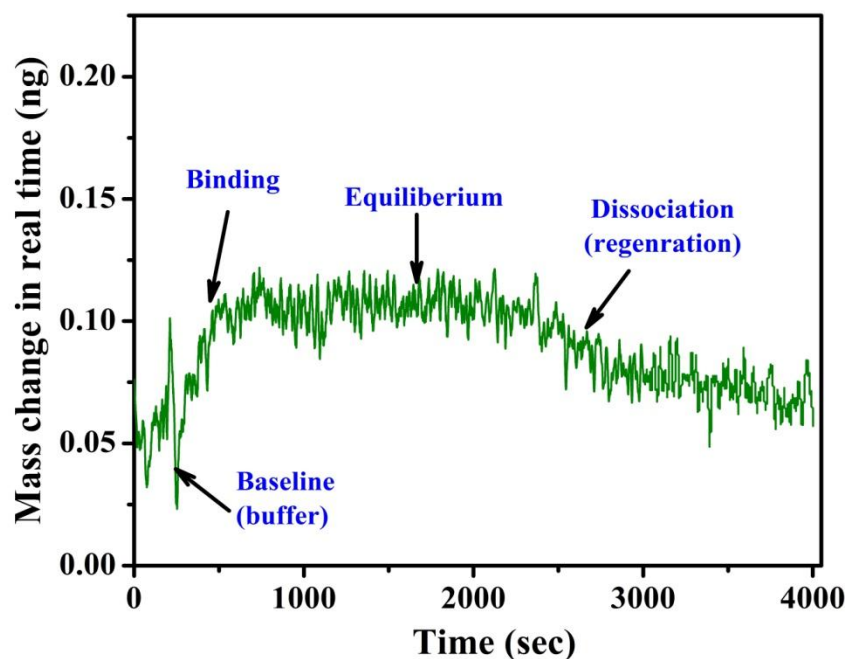


Figure 5.5: A real time sensogram of μ FIA-EQCN aptasensor for binding and regeneration of TET on aptasensor surface in binding buffer (10 mM, pH 7.0).

crystal for 4 h at RT under humid environment. The anti-TET aptamer concentrations from 1.56-200 μ M were immobilized on modified crystal surface. TET stock standard solution was dialyzed against HBB and injected passed over μ FIA-EQCN TET aptasensor. The change in mass (Δ ng) for each aptamer concentration was recorded and plotted. The reusability of TET-aptasensor was also determined by regenerating the surface with 4% w/v glycine buffer (regeneration buffer) in flow. Then the apparent equilibrium dissociation constant (K_d) value were calculated as the ratio of K_{diss}/K_{ass} using software Sigma Plot 13.0 (License version) and equilibrium mass binding signal at a function of analyte concentrations.

5.3 Result and discussions

5.3.1 Kinetics parameters for binding assay

It was evident from Fig. 5.5, that the binding of TET to the immobilized anti-TET aptamer was initially faster and then slowed down and attained equilibrium. Dissociation of bound TET was rapid in presence of regeneration buffer. The apparent K_d was calculated by applying the nonlinear fitting to the expression $y = V_{max} + x/(K_d + x)$, where V_{max} is the maximum binding capacity of the surface and x is the analyte concentration, using Sigma Plot 13.0 software. The calculated K_d value was found to be $3.030 \pm 0.5333 \mu\text{M}$ and V_{max} was 0.1496 ± 0.0048 mass change for the interaction of anti-TET aptamer and TET molecule.

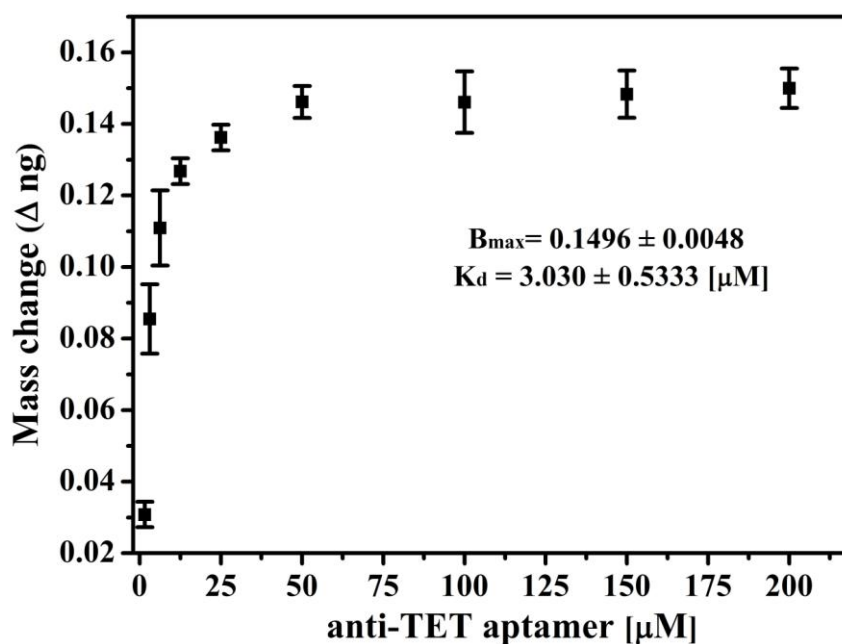


Figure 5.6: Binding affinity curves obtained using mass binding of TET (25 ng mL^{-1}) with various concentrations of ssDNA anti-TET aptamer.

5.3.2 Optimization of experimental parameters

5.3.2.1 Influence of self assembled monolayer's (SAMs)

To develop a protocol for producing a stable self assembled monolayer's (SAMs) on gold coated quartz crystal surface to immobilize ssDNA anti-TET aptamer was significantly important. The generation of thiol SAMs on metal surface provides a stable, robust and reproducible method, where the control over the orientation and distribution pattern is possible. For SAMs, various thiols with varying chain length (C3, C6 and C11) and structure (linear and aromatic) were employed for immobilization of ssDNA anti-TET aptamer. Different protocols were tested and optimized for SAMs formation of cysteamine (C-3), 11-MUA (C-11) and 4-ATP (aromatic, C-6) over gold crystal surface to impart an uniform surface coverage with minimum roughness and used further. From Fig. 5.7, ssDNA anti-TET aptamer immobilized over 11-MUA modified SAMs over gold quartz crystal showed the maximum mass change (Δm) of 91.9 ± 2.9 pg at 25 ng mL^{-1} TET against cysteamine (72.9 ± 2.3 pg) and 4-ATP (9.5 ± 1.0 pg). Inset (Fig. 5.7) showed the real time binding response of aptamer immobilized gold quartz crystal surface utilizing various thiols and the corresponding mass change responses in table, illustrating their chemical structure. Maximum binding response with 11-MUA could be attributed to the high affinity of terminal thiol towards gold surface, which improves the orientation of SAMs layer due to the presence of

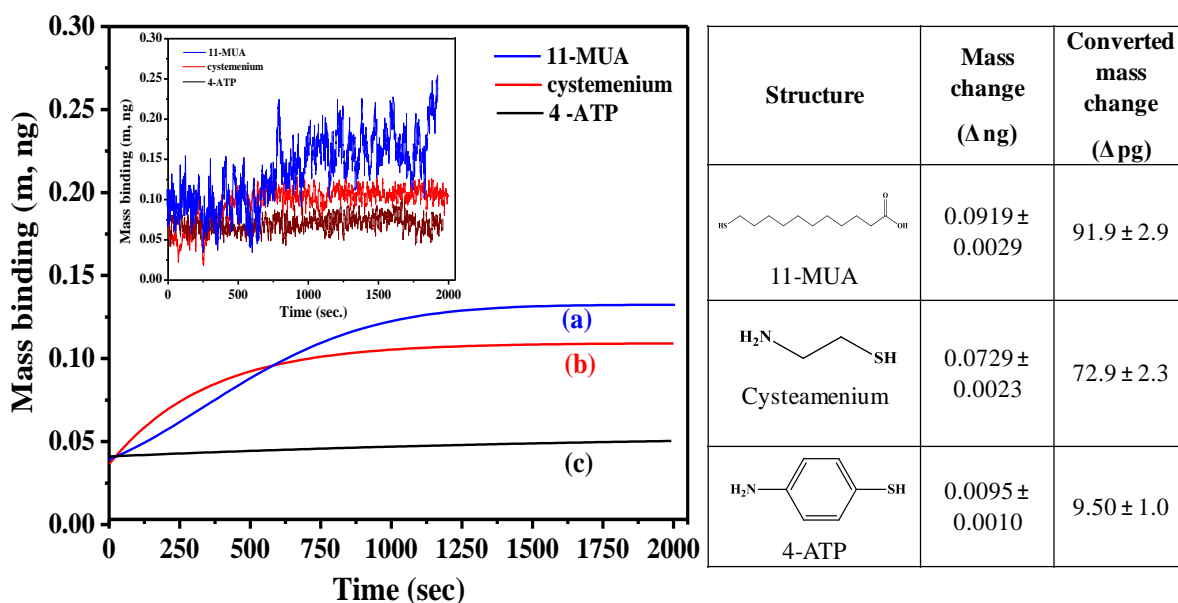


Figure 5.7: Optimization of binding response of aptasensor using different SAMs over gold surface curve at fixed concentration of TET (25 ng mL^{-1}) in binding buffer (10 mM, pH 7.0).

Inset showing the real time binding response for each SAMs.

long chain of alkane thiol (number of methylene groups > 10) (Porter et al., 1987). In addition to the tail functionality, the chain length is an important factor in determining the properties of the SAMs. Thiol with small functional group (such as amine, carboxyl) with longer alkyl chain consistently form more ordered and aligned SAMs than those formed from shorter chain length. 11-MUA SAMs response was found to be optimal over other thiol.

5.3.2.2 Influence of aptamer concentration

Sensitivity of an aptasensor platform is dependent of the aptamer density on sensing surface and plays a key role in establishment of aptasensor performance. To investigate the effect of aptamer concentration on sensor performance, various working dilutions of ssDNA anti-TET aptamer in the range 0.125-2.0 μ M was prepared and individually immobilized over 11-MUA modified gold quartz crystal surface and mounted in flow cell. With optimal control over the SAMs, the change in mass response was increased with increased concentration of aptamer immobilized from 0.125-1.0 μ M ssDNA anti-TET aptamer for fixed concentration of TET (Fig. 5.8). No further increased in mass change was observed with increased in aptamer concentration (Inset Fig. 5.8). Maximum mass change 92.3 ± 0.85 pg at 1.0 μ M ssDNA anti-TET aptamer was calculated and found to be maximum with optimal condition of SAMs. It is clear that concentration higher than 1.0 μ M aptamer reached equilibrium and showed decrease response. The lower binding against TET analyte at higher aptamer concentration

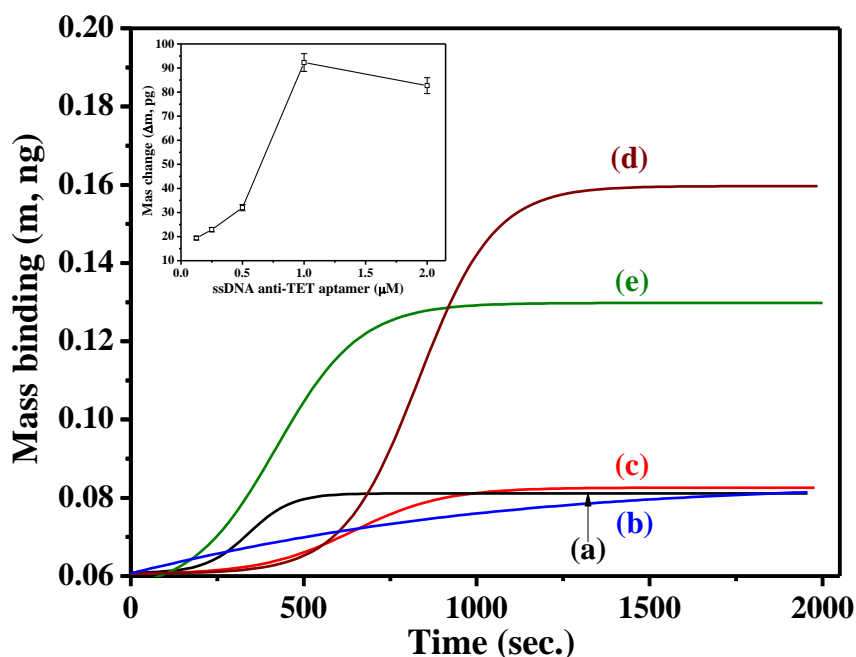


Figure 5.8: Binding response for ssDNA anti-TET aptamer (0.125-2.0 μ M) in HBB (10 mM, pH 7.4) at 25 ng mL^{-1} TET. Inset showing mass change for different aptamer concentration.

was attributed to the fact that too high concentration of aptamer on transducer surface (or density of probe) might alter the binding interaction due to the increased steric hindrance between immobilized aptamer molecules (White et al., 2008). This impedes the recognition mechanism and formation of G-quadruplex complex formation between ssDNA anti-TET aptamer and TET molecules. Moreover, the optimized concentration of ssDNA anti-TET aptamer (1.0 μ M) provided the flexibility to construct a calibration curve with broad dynamic range, whereas response calculated from lower aptamer concentrations (< 36 pg) were not enough due to the less change in mass for a fixed concentration of TET (25 ng mL⁻¹).

5.3.2.3 Influence of buffer, ionic strength, pH and flow rate

Influence of various experimental variables such as buffer, ionic strength, pH and flow rate, which could significantly affect the μ FIA-EQCN aptasensor were optimized. Measurements were carried out in different buffer (PBB and HBB), ionic strength (1, 5, 10, 25, 50 and 100 mM), pH (6.8, 7.2, 7.4, 7.8 and 8.2) and flow rate (0.01, 0.05, 0.1, 0.5 and 1.0 mL min⁻¹) (Fig. 5.9). It is evident from Fig. 5.9(a) that the maximum binding was obtained in HBB at

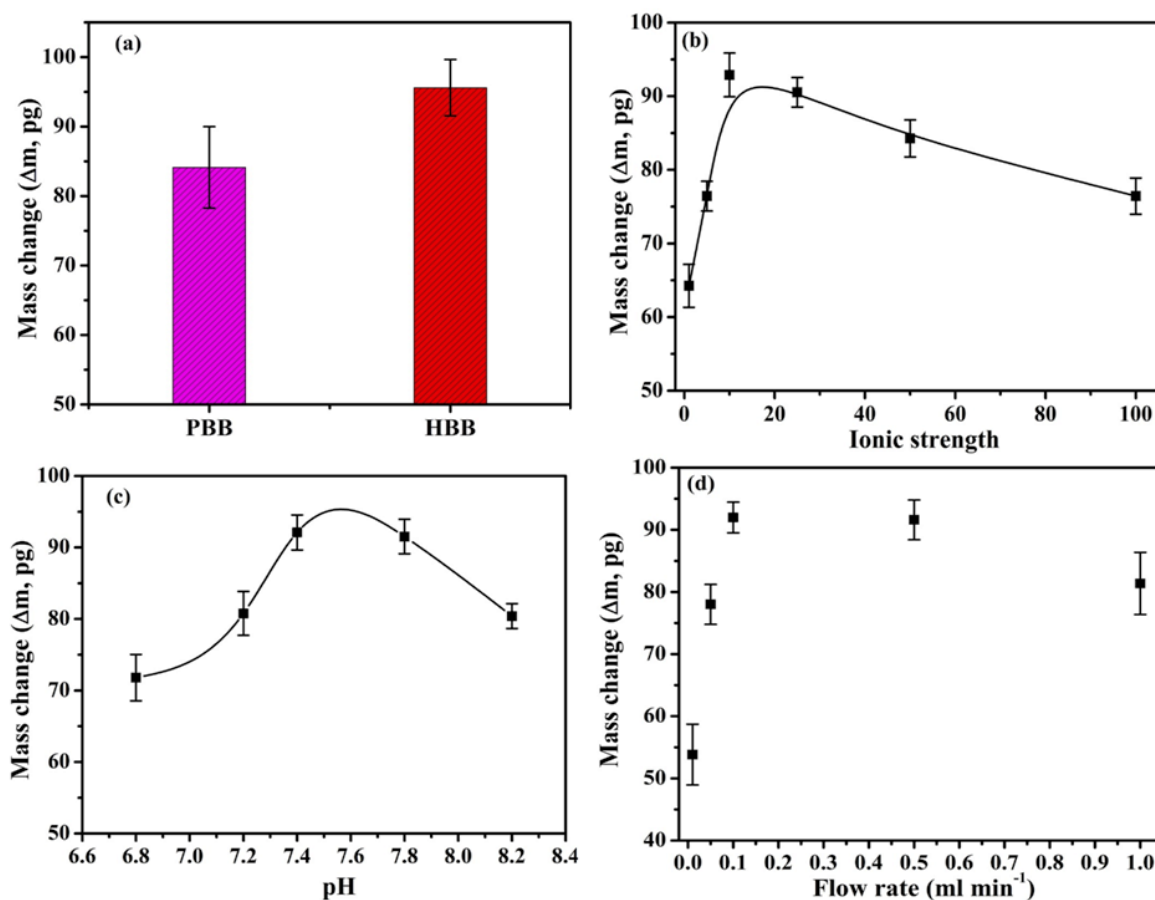


Figure 5.9: Optimization of various experimental variables (a) buffer; (b) ionic strength; (c) pH; (d) flow rate on binding performance of anti-TET aptamer to TET (25 ng mL⁻¹).

25 ng mL⁻¹ TET. Similarly, the ionic strength of binding buffer was also optimized. The presence of excess salt concentration hinders the interaction between anti-TET aptamer and TET molecules. This could be due to the presence of Na⁺ ion, which alters the binding mechanism of anti-TET aptamer (Hianik et al., 2007). Maximum mass change (Δm) was observed in 10 mM HBB for anti-TET aptamer and TET (Fig. 5.9b). The change in working pH has the significant effect on the structural integrity of aptamer and surface charge (Miodik et al., 2015). Therefore, the effect of HBB (10 mM) on binding of anti-TET aptamer binding with TET was studied with varying pH 6.8, 7.2, 7.4, 7.8 and 8.2 conditions. The TET induced specific binding interaction between anti-TET aptamer and TET (25 ng mL⁻¹) resulted in positive mass change at each pH, moreover the highest binding was obtained at pH 7.4 (Fig. 5.9c). In μ FIA mode, the optimization of flow rate of system is highly important because the little turbulence/ holding of fluid over the crystal surface for long time might cause the error in measurement. The μ FIA-EQCN TET aptasensor showed the maximum binding at flow rate of 0.1 mL min⁻¹ (Fig. 5.9d). The reason was attributed to the flow, that 0.1 mL min⁻¹ flow rate provided the sufficient contact time for binding of anti-TET aptamer and TET molecule. Thus, the further experimentation was performed on the optimized parameters.

5.3.3 Characterization of TET-aptasensor on transducer surface

5.3.3.1 Attenuated total reflection FT-IR (ATR-FTIR)

ATR-FTIR spectroscopy is a convenient non-destructive technique can be employed to characterize the immobilization of biomolecule on gold surface (Di Giambattista et al., 2011). Vibrational spectra of the bare, 11-MUA modified aptasensor and aptasensor incubated with TET have been shown in Figure (Fig. 5.10). It was observed that the bare gold crystal surface did not produce any significant features of vibration bands in the spectrum (Fig. 5.10a). The spectrum of 11-MUA treated gold crystal surface showed the presence of broad region from 3523-2700 cm⁻¹ (ν_s) with an out of plane (oop) bending at 936 cm⁻¹ confirms the presence of -COOH group of 11-MUA (Fig. 5.10a). The -C-H stretching vibrational band was observed at 2921 cm⁻¹. The appearance of two vibrational bands at 1698 and 1641 cm⁻¹ was associated to the carbonyl (-C=O) group of acid. Additionally, one -CH deformation (ν_d , scissoring) was found to be at 1446 cm⁻¹. Other characteristics vibrational bands of long chain methylene group were observed at 683, 625, 528 cm⁻¹ (Pavia et al., 2005). After immobilization of 3-amine modified anti-TET aptamer on 11-MUA modified crystal, the vibrational bands corresponding to the functional group of nucleic acid were observed as depicted in Fig. 5.10b

(Andrushchenko et al., 2007). The asymmetric (ν_a) and symmetric (ν_s) vibrational bands arising from $-\text{NH}_2$ group present in the 3-amine modified anti-TET aptamer and nitrogen base of aptamer sequence were buried in the broad band centered at $3488\text{--}3471\text{ cm}^{-1}$. The bands at 2928 and 2862 cm^{-1} were assigned to the asymmetric and symmetric vibrations of $-\text{CH}$ of $-\text{CH}_2$ groups present in the sugar phosphate backbone. The $-\text{NH}_2$ bending (ν_d) was observed at 1652 cm^{-1} with associated peak of $\text{C}=\text{C}$ at 1636 cm^{-1} . The band localized at 1296 cm^{-1} was due to base sugar moieties. The appearance of two additional bands at 1109 and 991 cm^{-1} was attributed P-O stretching (ν_s) vibration of phosphate backbone present (P-O-C groups). The presence of two additional bands at 683 and 644 cm^{-1} corresponds to the methylene long chain of 11-MUA confirms the successful immobilization of anti-TET aptamer over 11-MUA modified surface. On incubation with TET molecule (Fig. 5.10c), two new bands at 3443

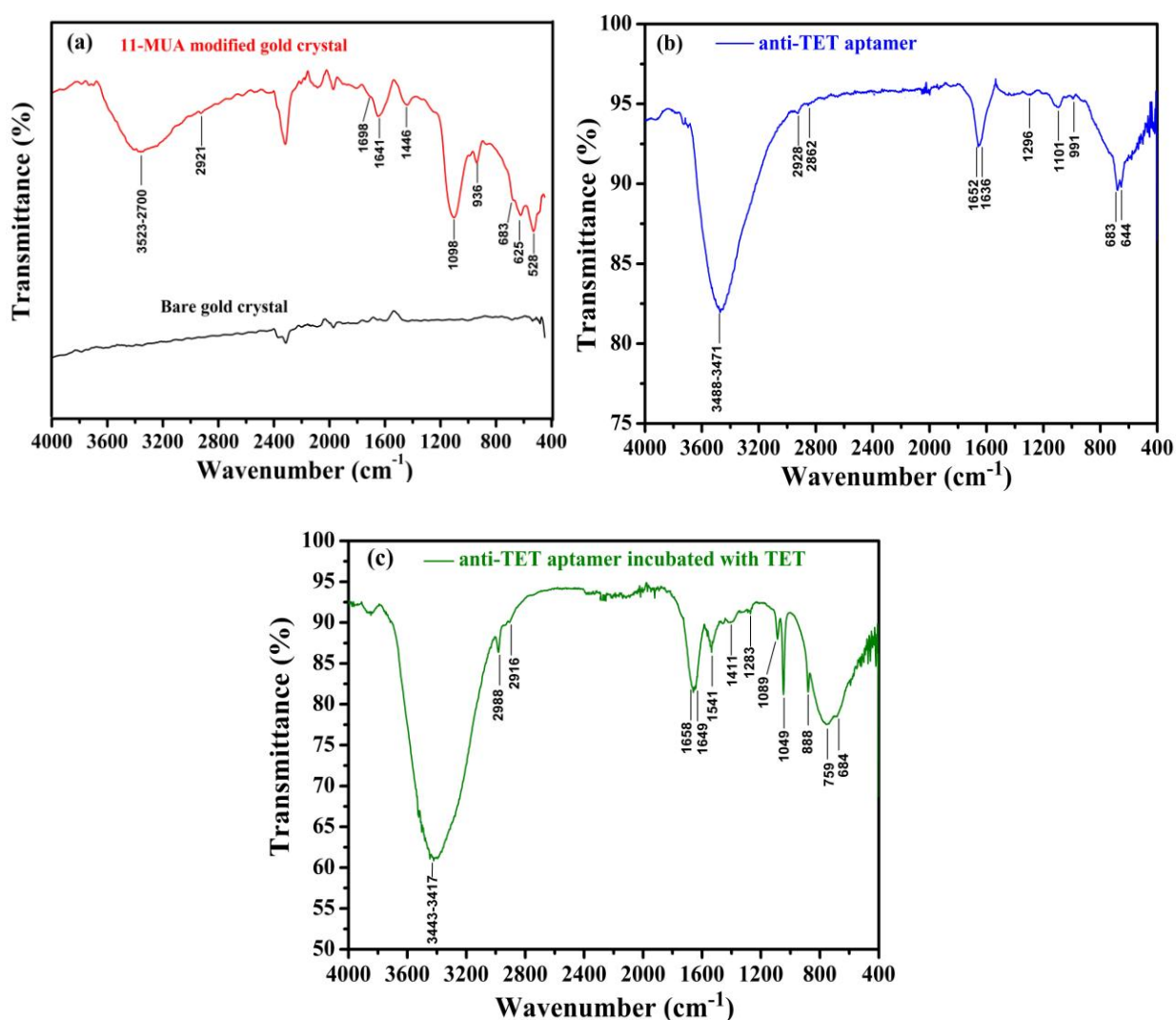


Figure 5.10: FT-IR spectra of (a) bare and 11-MUA modified gold surface; (b) ssDNA anti-TET aptamer immobilized over modified gold surface; (c) ssDNA anti-TET aptamer incubated with TET in ATR mode with 128 scans at 64 cm^{-1} resolution under vacuum.

and 3417 cm^{-1} corresponding to the binding of TET to anti-TET aptamer. The observed vibrational bands at 1658 and 1649 cm^{-1} were due to the amide of nucleic acid and amide present in tetracycline ring. The vibrational bands at 1541 cm^{-1} corresponds to C-H bending of ring $-\text{CH}_2$ group of TET and 1049 cm^{-1} corresponds to the C-O-C. These results strongly suggested and confirmed the binding of TET molecule to anti-TET aptamer.

5.3.3.2 Surface topography (using AFM analysis)

Upon surface modification, the fundamental frequency of crystal surface is not atomically same and changes with each modification step, which has direct correlation with the surface roughness (Kim and Jerkiewicz, 2017). Therefore, the surface roughness analysis was performed for each step of modification and analyzed. Herein, we considered the average roughness (R_a), root mean square roughness (R_q) and fractal surface (R_{ku}) parameters for comparative studies. The AFM monograph (Fig. 5.11a, 3D micrograph) showed the typical characteristic of bare gold surface with spherical particle in closely packed pattern (Rojas et al., 2008). The calculated value of parameters were found to be R_a (1.192 nm), R_q (1.532 nm) and R_{ku} (1.136 nm) (Fig. 5.11b). They are the characteristic of clean surface and reveal the usual features of smooth surface. Since, the 11-MUA (SAMs) possess a long chain of methylene group, which can provide the van der Waals attractive forces that results in uniform surface coverage with minimum roughness (Choi et al., 2001). Compare to the bare surface, 11-MUA coupled gold surface showed a well uniform surface coverage with an average height of R_a (2.228 nm) and R_q (2.394 nm) (Fig. 5.11) which is almost double the bare value. An increase in fractal value from 1.136 (bare surface) to 1.686 (11-MUA modified) suggests the successful SAMs formation on gold surface (Fig 5.11e). The histograms obtained for bare quartz crystal surface and 11-MUA modified surface have been depicted in Fig. 5.11 (c) and 5.11 (f). Upon immobilization of anti-TET aptamer, a fairly well organized array could be observed (Fig. 5.12a). The increased in R_a value from 2.228 nm to 22.66 nm and R_q value from 2.394 nm to 25.73 nm with decrease in fractal value can be seen upon aptamer immobilization (Fig. 5.12b). It could be clearly observed that the increase in peak height and spike planer surface covering the plane of 11-MUA coupled gold surface strongly suggested the covalent immobilization of anti-TET aptamer (amine modified with linker) immobilization (Fig. 5.12a and 5.12c). After incubation with TET (25 ng mL^{-1}), the surface topography was again expected to be changed that can be attributed to the formation of G-quadruplex anti-TET aptamer-TET complex, resulting in decrease in average height (Fig. 5.12d). The mean average height and root mean square roughness were further

decreased with an increase in fractal value of surface to 3.356 nm, this confirm the binding of TET on aptasensor surface (Fig. 5.12e).

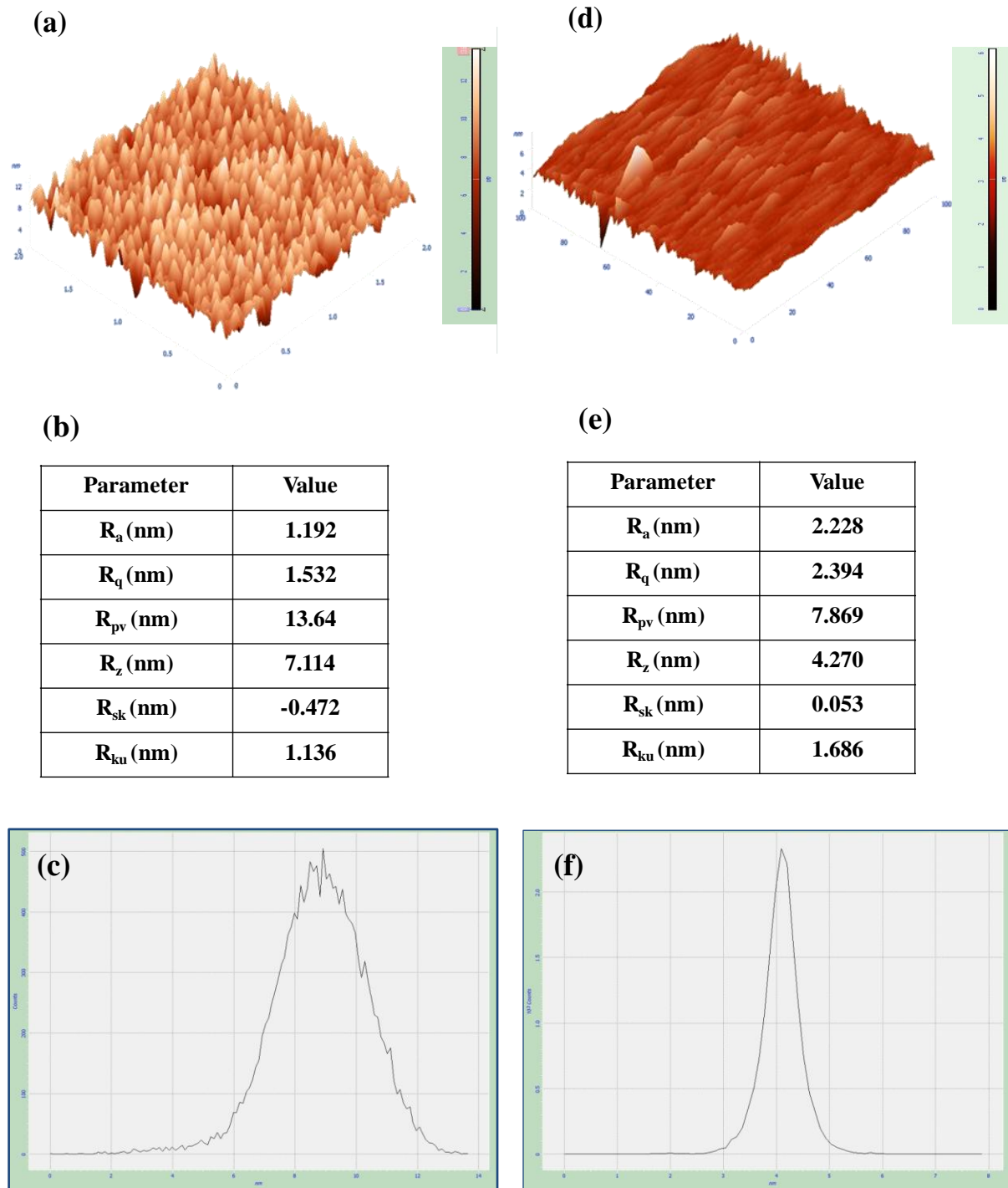


Figure 5.11: AFM micrographs of (a) bare gold quartz crystal surface (3D) micrograph; (b) different surface parameters calculated for bare quartz crystal; (c) histogram of bare gold quartz crystal surface; (d) 11-MUA modified gold quartz crystal surface (3D) micrograph; (e) different surface parameters calculated for 11-MUA modified gold quartz crystal surface (f) histogram of 11-MUA modified gold quartz crystal surface.

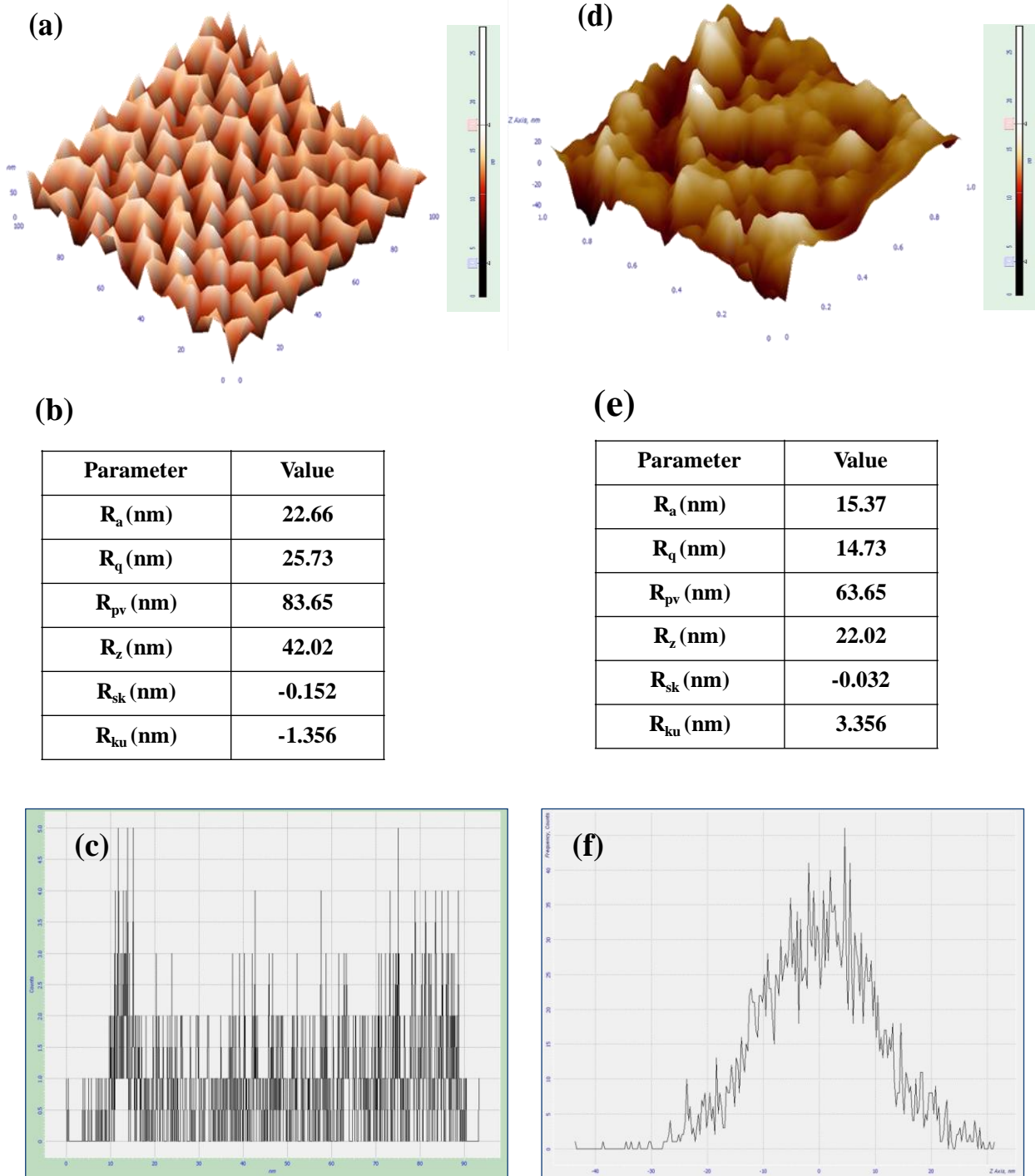


Figure 5.12: AFM micrographs of (a) anti-TET aptamer immobilized on 11-MUA modified gold quartz crystal surface (3D) micrograph; (b) different surface parameters calculated for 11-MUA coupled gold quartz crystal surface; (c) histogram of anti-TET aptamer immobilized on 11-MUA coupled gold quartz crystal surface; (d) anti-TET aptasensor incubated with TET (25 ng mL⁻¹) (3D) micrograph; (e) different surface parameters calculated for anti-TET aptasensor incubated with TET (25 ng mL⁻¹); (f) histogram of anti-TET aptasensor incubated with TET (25 ng mL⁻¹).

5.3.3.3 SEM analysis

The surface morphology of developed aptasensor for TET detection was also studied by SEM analysis at three different stages i.e. bare gold surface, 11-MUA modified gold surface and anti-TET aptamer immobilized on 11-MUA modified gold surface. The bare surface of gold quartz crystal showed a typical characteristic features of gold surface (Rojas et al., 2008) (Fig. 5.13a), which was in good agreement with the AFM monographs for bare gold surface (Fig. 5.11a). The surface modification using 11-MUA coupling mechanism resulted in the uniform pattern with the decrease in roughness over the bare surface (Fig. 5.13b). This improves the surface properties for bare surface and further immobilization of anti-TET aptamer over 11-MUA modified bare surface. After the immobilization of anti-TET aptamer on 11-MUA modified gold surface, a uniform surface coverage can be seen (Fig. 5.13c). The observed results strongly suggested the successful modification of bare gold surface and immobilization of anti-TET aptamer.

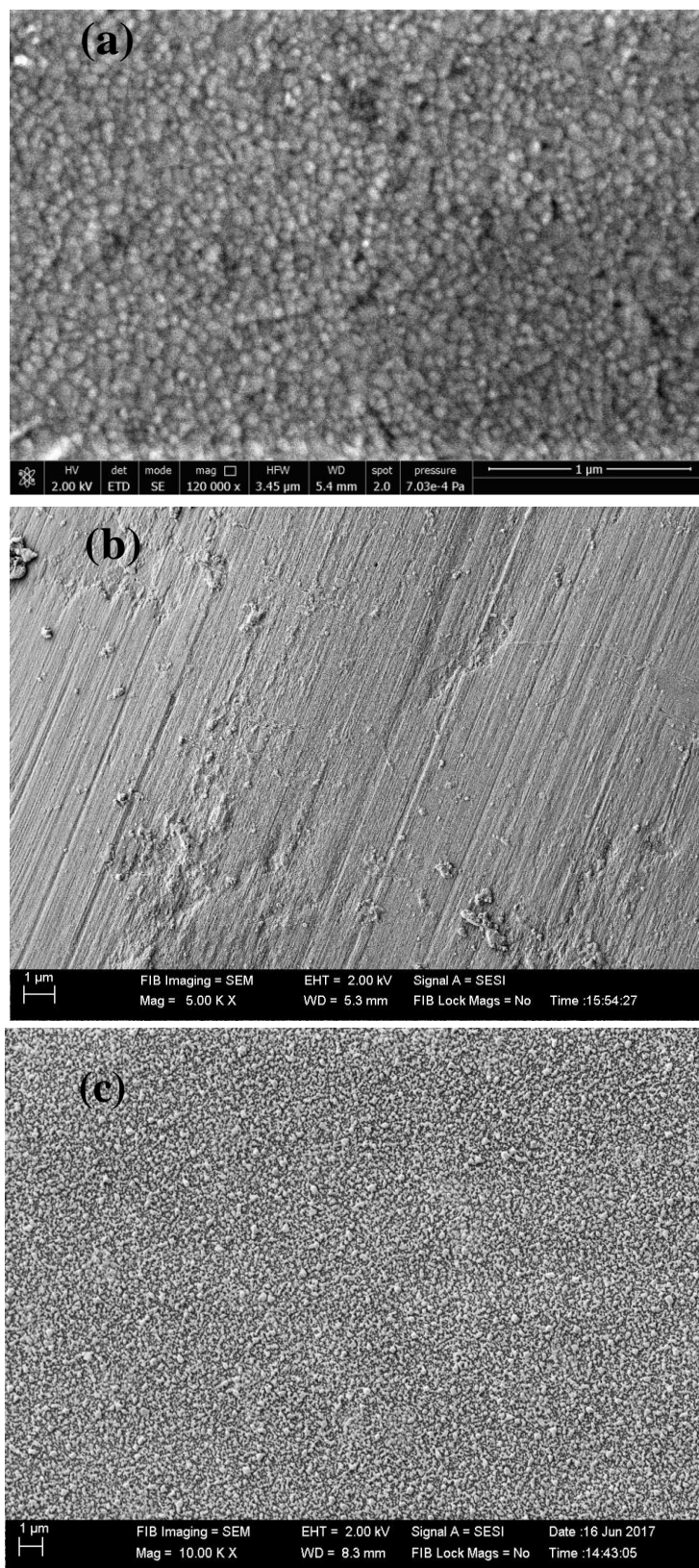


Figure 5.13: Scanning electron micrographs of (a) bare gold quartz crystal surface at scale of 1.0 μ m; (b) 11-MUA coupled (SAMs formation) on the surface of bare gold quartz crystal surface; (c) anti-TET aptamer immobilized on 11-MUA coupled gold surface.

5.3.4 Aptasensor performance for detection of TET (calibration curve)

Post optimization and characterization, aptasensor response to TET binding at various concentrations were recorded to construct the calibration curve. The devised TET-aptasensor was mounted on Plexiglas flow cell and degassed buffer (HBB, 10 mM, pH 7.4) was passed till the stable baseline achieved. Binding interactions between TET and TET-aptasensor on transducer surface were followed by a change in mass due to the formation of anti-TET aptamer-G-quadruplex complex between TET and ssDNA anti-TET aptamer. This change offers an additional mass over transducer surface resulting decrease in vibrational frequency of aptamer immobilized gold quartz crystal mounted in flow cell, which corresponds to the various TET concentrations. The freshly prepared TET standard (1.562-2000 ng mL⁻¹) in HBB (10 mM, pH 7.4) were injected into the μ FIA-EQCN system, starting from the lower to higher concentrations. Signal response respective to the TET concentrations were recorded using the data acquisition system (Voltascan 5 software) and further plotted as mass change (Δm) vs TET concentrations (Fig. 5.14). The data obtained from the Voltascan 5 software was further treated with OriginPro 8.1 software and best fit data was plotted. In μ FIA-EQCN TET-aptasensor, the obtained mass change (Δm) instead of change in frequency (Δf) was used for measurement due to the inbuilt conversion factor in the software of EQCN 700.

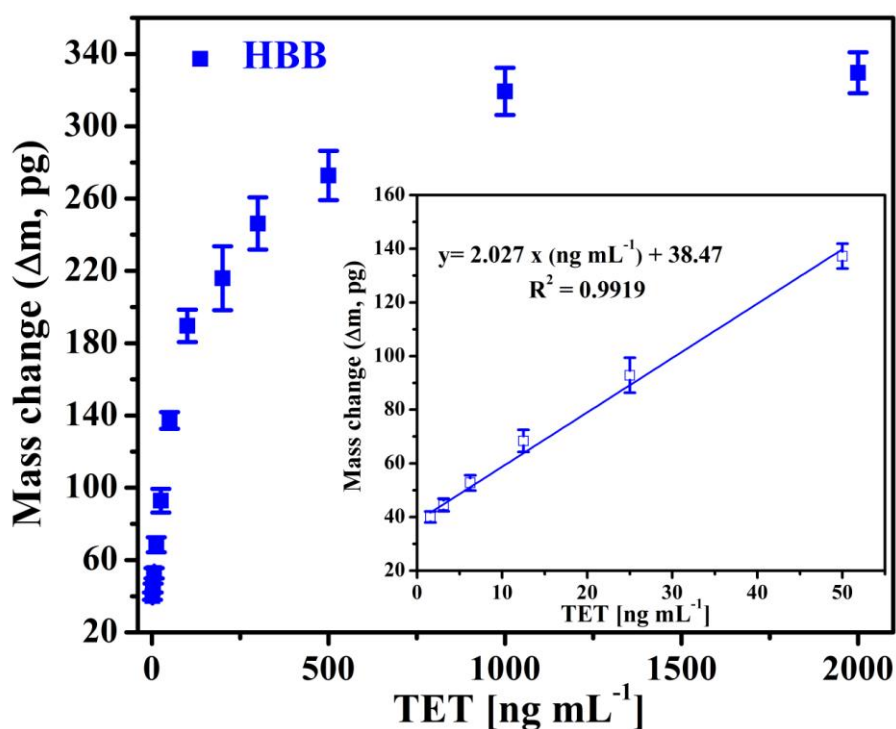


Figure 5.14: Calibration graph for analysis of TET (1.5-2000 ng mL⁻¹) in HBB (10 mM, pH 7.4) at 0.1 ml min⁻¹ flow rate. Inset showing the linear fit data for TET analysis in HBB.

In the presented μ FIA-EQCN TET-aptasensor, the obtained mass change (Δm) instead of change in frequency (Δf) was used for measurement due to the inbuilt conversion factor in the software of EQCN700 system. The recorded Δm values were converted from ng to pg scale to impart more clarity in the calibration graph plotted. A dynamic response range 1.562-2000 ng mL⁻¹ with a linearity 1.562-50 ng mL⁻¹ TET was obtained in HBB (Figure 6a). Calibration curve was fitted using the linear equation and the equation of line $y = 2.027 x$ (ng mL⁻¹) + 38.47 with, $R^2=0.9919$ (n=3) was calculated. All the measurements were performed in triplicate measurements and the error bars represent the standard deviation of the measurements with % RSD = 3.03-5.16 (n=3), demonstrating the high accuracy of the aptasensor. Furthermore, for practical utility, the performance of developed aptasensor was evaluated in milk sample. A good dynamic detection range was obtained in milk from 1.562-2000 ng mL⁻¹ TET. Obtained data was fitted using linear equation and a line of equation of $y = 2.094 x$ (ng mL⁻¹) + 35.86 with a linearity of 1.562-50 ng mL⁻¹ TET and $R^2 = 0.9889$ (n=3) in milk (Figure 6b). The sensitivity of method in calibration curve was 2.027 ng mL⁻¹ in HBB and 2.094 ng mL⁻¹ in milk with an excellent limit of detection (LOD) 0.531 ng mL⁻¹ (\approx 1.19 nM TET) in milk compared to the reported method (Table 5.2).

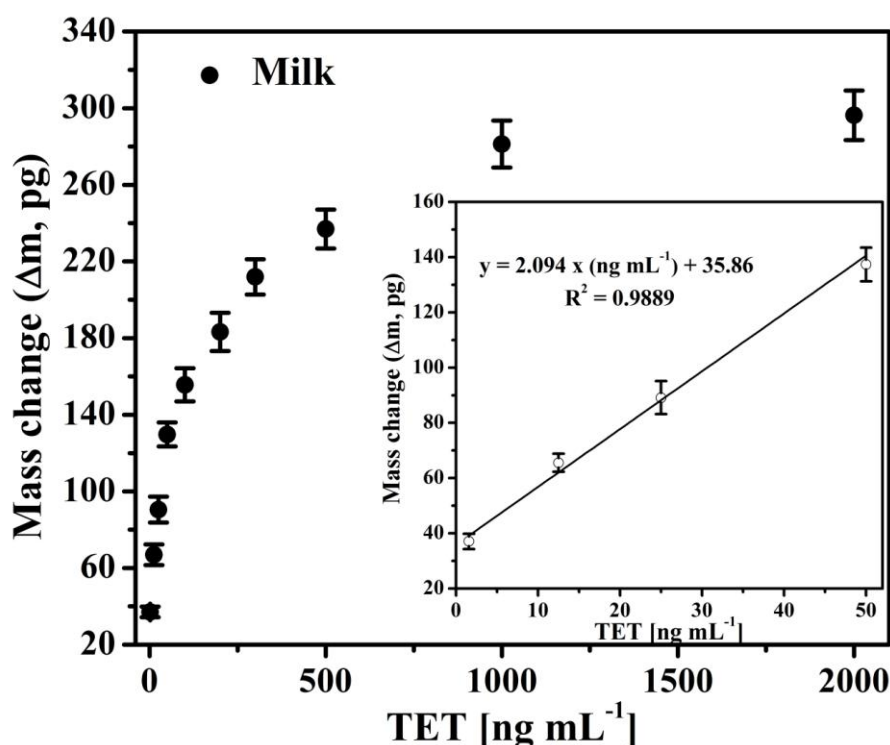


Figure 5.15: Calibration graph for analysis of TET in milk (spiked with 1.5-2000 ng ml⁻¹ TET) at 0.1 ml min⁻¹ flow arte. Inset showing the linear fit data for TET analysis in milk.

5.3.5 Specificity performance of μ FIA-EQCN aptasensor

Selectivity and specificity of the developed μ FIA integrated TET aptasensor was verified against structural analogues and non-structural analogues at 25 ng mL^{-1} . The cross reactants (OTC, DOXY, MINO and KANA) were selected based on the possibilities of their presence in milk sample, which might affect aptasensor performance. The specificity studies were carried in untreated milk sample (as discussed in section 5.2.3.4) against standard solution of each antibiotic as sample and unspiked milk sample as control. The anti-TET immobilized gold crystal surface was mounted in the flow cell and solution of each antibiotic was passed individually at a flow rate of 0.1 ml min^{-1} . The OTC, MINO and DOXY showed the negligible response compared to TET (Fig. 5.16). Whereas, the non-structural analogue (KANA) showed no response (data not shown since no response obtained). The obtained responses of Δm (pg) were plotted as histogram response and found to be less than 10 % (n=3) of TET response (Table 5.3). The results obtained with OTC and DOXY could be due to structural analogues, which impart a mass on transducer surface. Moreover, the results demonstrate that there was no significant interference produced by any other non-targeted antibiotics. Thus, obtained response was virtually due to the interaction of TET with anti-TET aptamer and confirms the remarkable specificity of aptamer sequence used for developing the μ FIA-EQCN aptasensor for TET analysis in milk samples.

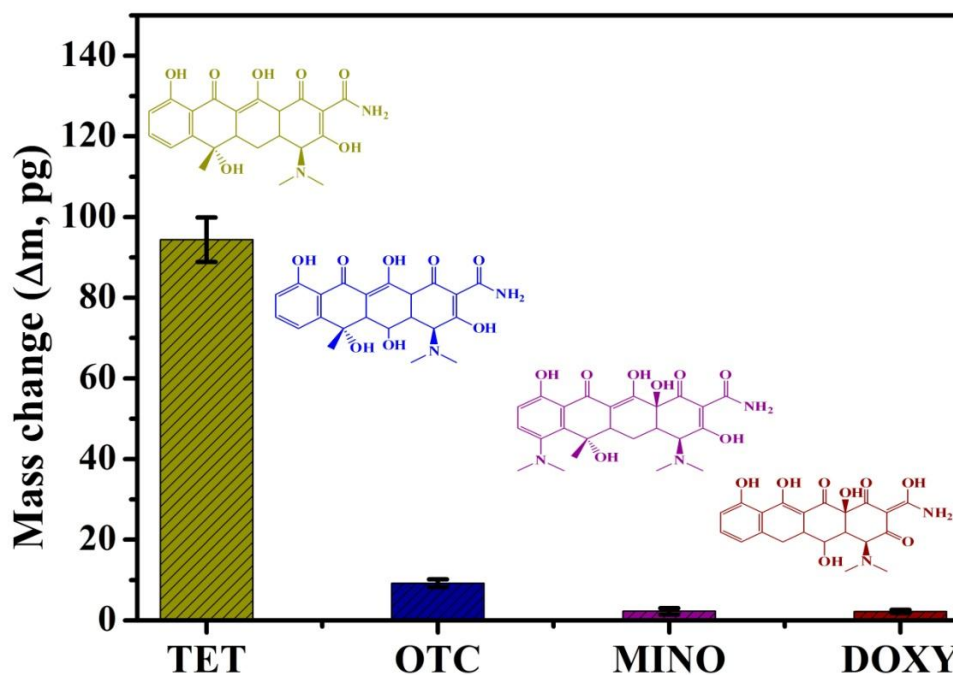


Figure 5.16: Cross-reactivity responses of developed μ FIA-EQCN TET-aptasensor for different analogues at 25 ng mL^{-1} (n=3) in spiked milk samples.

Table 5.3: Cross-reactivity studies of TET against structural and non-structural analogues in milk sample

Analyte	Conc ⁿ . added [ng mL ⁻¹]	Mass change (Δm , pg) Mean \pm S.D. (n= 3 x 2)	% R.S.D.	Response (%) (Analyte/ TET response x 100)
TET	25	94.39 \pm 5.527	5.856	100.0
OTC	25	9.198 \pm 0.961	9.855	9.745
MINO	25	2.243 \pm 0.204	9.103	2.376
DOXY	25	2.198 \pm 0.214	9.718	0.226
KANA	25	0.0 \pm 0.020	0.0	0.0

5.3.6 Recovery studies for TET spiked milk samples

The practical feasibility of developed μ FIA-EQCN TET-aptasensor was evaluated further in commercial milk samples using standard spiking method. Matrix matching was performed before analysis of each sample. Initially, the milk samples were assumed to be free of TET residual presence. For analysis, a known amount of TET (300 ng mL⁻¹) was added to the milk samples and further diluted with untreated milk samples in desired range, which were selected from linear range (1.562-50 ng mL⁻¹) and dynamic range (100-300 ng mL⁻¹) including MRLs i.e. 100-300 ng mL⁻¹. Thus, based on the response signal (Δm) recorded from μ FIA-EQCN aptasensor, recoveries were calculated and analyzed. The calculated recovery (%) obtained for TET spiked milk samples have been tabulated in Table 5.4. Recoveries were calculated 96.48-100.2 % from spiked TET milk samples with maximum % R.S.D. of 2.375 (n=6). The devised aptasensor showed a good % recovery, which indicated the potential application of the μ FIA-EQCN aptasensor for the detection of TET residual in milk samples.

Table 5.4: Recovery studies of TET spiked milk samples using μ FIA-EQCN aptasensor

Recovery performance of aptasensor in spiked milk samples					
Milk sample	TET added [ng mL ⁻¹]	TET found [ng mL ⁻¹] Mean \pm S.D. (n=3)	% R.S.D.	% Recovery	R.E. %
Milk-1	1.562	1.547 \pm 0.032	2.068	99.03	-0.970
Milk-2	12.50	12.06 \pm 0.285	2.375	96.48	-4.000
Milk-3	50.00	50.10 \pm 0.748	1.494	100.2	0.120
Milk-4	100.0	99.11 \pm 1.225	1.381	99.30	-0.700
Milk-5	200.0	195.8 \pm 3.540	1.809	97.90	-2.100
Milk-6	300.0	299.0 \pm 2.578	0.081	99.66	-0.034

5.3.7 Cross validation and comparison

The performance of developed μ FIA-EQCN aptasensor for TET analysis was cross validated with commercial TET-ELISA kit (Fig. 5.17a). The response signal (Δm) recorded from μ FIA-EQCN TET-aptasensor were compared with the signal obtained from TET-ELISA kit experiments for each TET concentrations. The % recovery was calculated from both experiments and compared. The recoveries obtained from the μ FIA-EQCN aptasensor ranging 97.43-102.6 % with % RSD 3.090-4.323 (n=6) was similar to the results obtained from the ELISA kit (96.90-102.5 %, % RSD 2.996-4.359, n=6). It is evident from Table 5.5 that the results from both the methods were in good agreement in terms of sensitivity and reproducibility. A good correlation was obtained between both the method with a value of $R^2 = 0.9962$ (n=3) (Fig. 5.17b). The developed μ FIA-EQCN TET-aptasensor was found to be reliable and precise as the commonly used ELISA kit and can be successfully employed for the detection of TET in milk samples for routine and continuous analysis in situations like milk processing plant. Thus, the developed μ FIA-EQCN aptasensor was found to be reliable and precise as the commonly used ELISA method for TET detection.

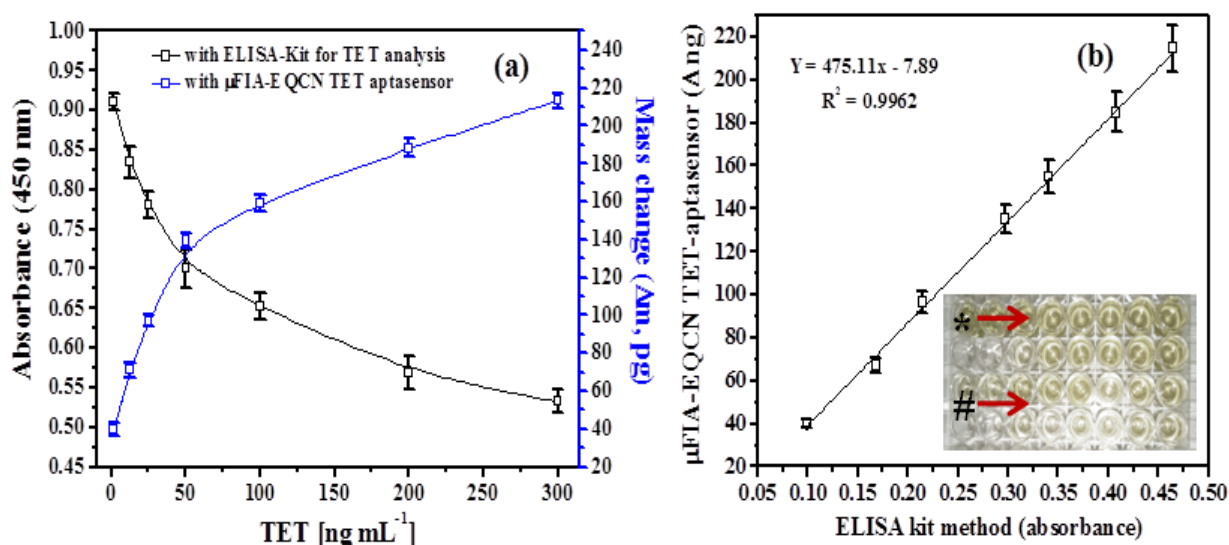


Figure 5.17: (a) Validation responses from μ FIA-EQCN TET-aptasensor and commercial ELISA Kit of TET analysis ($1.562\text{--}300\text{ ng mL}^{-1}$); (b) Correlation data between both techniques and inset showing the sample image in ELISA test (*ELISA TET standards $1.562\text{--}300\text{ ng mL}^{-1}$ and #Milk TET spiked sample $1.562\text{--}300\text{ ng mL}^{-1}$).

Table 5.5: Recovery performance of μ FIA-EQCN aptasensor and ELISA Kit for TET analysis

Milk sample spiked with TET [ng mL^{-1}]	TET found [ng mL^{-1}]		% R.S.D.		% Recovery	
	μ FIA-EQCN aptasensor (Mean \pm S.D.) (n=6)	ELISA Kit (Mean \pm S.D.) (n=6)	μ FIA-EQCN aptasensor	ELISA Kit	μ FIA-EQCN aptasensor	ELISA Kit
1.562	1.521 ± 0.06	1.531 ± 0.05	3.951	3.262	97.43	97.95
12.50	12.56 ± 0.50	12.60 ± 0.38	3.980	3.022	100.5	100.8
25.00	25.64 ± 1.03	25.63 ± 0.77	4.022	3.001	102.6	102.5
50.00	49.51 ± 2.14	49.34 ± 1.54	4.323	3.123	99.02	98.68
100.00	99.91 ± 3.09	96.90 ± 4.21	3.090	4.359	99.91	96.90
200.00	201.2 ± 6.95	200.4 ± 6.01	3.451	2.996	100.6	100.2
300.00	298.5 ± 12.61	298.9 ± 10.97	4.234	3.670	99.49	99.63

5.3.8 Precision and analytical performance of μ FIA-EQCN aptasensor

The precision of developed μ FIA-EQCN aptasensor was investigated by intra and inter run analysis on the same modified gold quartz crystal immobilized with anti-TET aptamer (after regeneration) and diverse set of crystals, respectively. A known amount of TET concentration (25 ng mL^{-1}) was spiked in untreated milk samples and successfully analyzed for aptasensor performance in four parallel experiments ($n=4$). Baseline signal was corrected before each analysis and Δm values were calculated based on the response obtained. The μ FIA-EQCN aptasensor showed a good reproducibility with standard deviation of 90.45 ± 3.80 and the calculated % R.S.D. ($n=4$) was 4.20 within the same crystal. Similarly, the inter-day precision performance was tested on diverse sets of immobilized crystals. For, interday precision, the % R.S.D. was calculated to be 1.60-3.69 ($n=4$). Precision analysis showed the good accuracy and reproducibility of aptasensor (Table 5.6). The storage stability of anti-TET aptamer immobilized crystals was also tested. The immobilized crystals were stored at 4°C for two weeks and used for measurements. The activity was retained until the two weeks for same concentration of TET providing no significant loss in mass binding response. The merit of figures for the developed μ FIA-EQCN TET-aptasensor has been tabulated in Table 5.7.

Table 5.6: Precision and reproducibility studies of μ FIA-EQCN aptasensor for TET

Intra-batch precision performance of μ FIA-EQCN aptasensor for TET							
TET [ng mL ⁻¹]	R1 (Δm , pg)	R2 (Δm , pg)	R3 (Δm , pg)	R4 (Δm , pg)	Mean \pm S.D. ($n=4$)	% RSD	
25	85.64	94.37	89.40	92.40	90.45 ± 3.80	4.20	
Inter-batch precision performance of μ FIA-EQCN aptasensor for TET							
Crystals	TET [ng mL ⁻¹]	R1 (Δm , pg)	R2 (Δm , pg)	R3 (Δm , pg)	R4 (Δm , pg)	Mean \pm S.D. ($n=4$)	% RSD
1.	25	84.64	92.37	90.40	89.60	89.25 ± 3.29	3.69
2.	25	84.46	86.40	90.20	91.40	88.12 ± 3.24	3.68
3.	25	92.00	93.00	88.60	90.00	90.90 ± 1.98	2.18
4.	25	92.30	88.80	90.80	91.00	90.73 ± 1.45	1.60

Table 5.7: Analytical figures of merit for devised μ FIA-EQCN TET-aptasensor

Parameter	Merits of figures
Linear range	1.562-50 ng mL ⁻¹
Dynamic range	1.562-2000 ng mL ⁻¹
Limit of detection	0.531 ng mL ⁻¹
Inter assay precision	% R.S.D. 0.35 (n=4)
Inter assay precision	% R.S.D. 1.60-3.69 (n=4)
Analysis time	Less than 17 min
Recovery	97.43-102.6 %
Sample treatment	No complex matrix treatment

5.4 Conclusion

In the present work, we first report the development of μ FIA integrated EQCN aptasensor for TET analysis. The ssDNA aptamer used exhibited the high affinity against TET with dissociation constant (K_d) value of 3.03 μ M. The detection method was based on the monitoring the change in mass on the aptasensor surface in FIA mode that is induced by the change in the aptamer configuration upon TET binding. The aptasensor showed fast response (17 min) and high sensitivity (0.531 ng mL⁻¹ TET) meeting the regulatory requirements (MRLs, 100-300 ng mL⁻¹). However, the developed TET aptasensor showed high affinity towards TET and did not show any significant cross reactivity with other structural and non-structural analogues. The μ FIA mode integrated with EQCN sensing platform provides improved sensitivity to the detection method. The aptasensor was also applied for detection of TET in milk sample showing high recovery percentages 97.43-102.6 % with % RSD 3.090-4.323 (n=6), that were in good agreement with the results obtained from the commercial ELISA kit method. The FIA mode provided the on-line and real time binding interaction. The precision and accuracy proves that the presented aptasensor has the good selectivity, reproducibility and stability. To the best of our knowledge, this is the first reported μ FIA-EQCN aptasensor based detection for TET residue in milk without much complex matrix treatment. The analysis can be performed directly in untreated milk samples.

This indicates that the present developed method showed great promising feature to be further employed as an alternatives to the traditional assays.

CHAPTER 6: CONCLUSION

The primary objectives of the work presented in the thesis were to develop novel biosensing platforms for determination of mycotoxin and antibiotics residual contaminants present in milk, beer and wine samples. Herein in the present work, the developed aptasensor technology uses the optical, EIS and piezoelectric transducers platforms for detection of mycotoxin and antibiotics in real samples. The significance of research lies in the development of high-throughput, sensitive, specific, stable and reproducible aptasensors for determination of OTA, AFM1, KANA and TET contamination. The lower detection limits at pg mL^{-1} were found without complex matrix treatments were the major outcomes of developed aptasensors.

Extensive experimental works were carried out for optimization of various experimental variables, characterization of biosensors, sensitivity measurements, stabilization of nanoparticles, optimization of fluorophore and quencher labelled aptamer sequences, immobilization of aptamer, selection of self assembled monolayer, cross-reactivity of biosensor with structural and non-structural analogues, real sample analysis and validation of developed biosensors. Various significantly important observations were notified. The overall conclusions of present thesis have been summarized chapter-wise as below:

1. Chapter 1: This chapter gave a detailed description about the background and motivation for present research, introduction to biosensors, types of bio(recognition) elements, various types of transducers, introduction to SELEX process, analytical aspects of biosensor performance, state of art for mycotoxin and antibiotics determination, introduction of nanomaterials in biosensors. This chapter also discussed about the gaps in the existing research and objective of proposed thesis work.

2. Chapter 2: This chapter gives detailed account for the development of fluorescence quenching based aptamer assay platform for OTA analysis in beer and wine samples. This chapter has two novel approaches, in first part a fluorescence quenching based aptasensing platform has been developed using fluorescently labelled aptamer (labelled technique) and TiO_2 -NPs as fluorescence quencher. In the second part, a non-labelled technique was developed using non-labelled ant-OTA aptamer, which capitalizes on the concept of aptamer assisted stability of TiO_2 -NPs and carboxylate modified microsphere nanoparticles as

fluorescent probe. The chapter include detailed account for characterization of aptamer and TiO₂-NPs interaction and optimization of experimental parameters. The OTA analysis is based on the fluorescence recovery response resulting from the binding interaction of the anti-OTA aptamer with OTA present in the sample. The analytical parameters of both aptasensing platforms compared. The developed platform can analysed OTA down to 1.5 nM with linearity of 1.5 nM- 1.0 μM (labelled techniques) and 1.35 nM with linearity of 17 nM- 5.0 μM (non-labelled technique) in beer and wine samples, which meets the regulatory standards (2.0 μg kg⁻¹ equal to 0.22 μM). The obtained recoveries were 94.30-102.68 % (methodology 1) and 96.79-101.50% (methodology 2) for triplicate measurements. The developed platforms showed very good precision with reproducibility of % R.S.D. 2.89 (n=3) and % R.S.D. 5.04 (n=3) for intraday analysis against methodology 1 and 2 respectively. Measurements of beer and wine samples and validation against HPLC method was carried out successfully. Based on successful demonstration of developed platforms, it proves their applicability in the beverages industries for OTA monitoring.

3. Chapter 3: This chapter gave the detailed account for the development of structure switching aptamer assay for the detection of aflatoxin M1 (AFM1) in milk. To avoid the complex matrix treatment process, the developed aptasensing platform was optimized in the untreated milk samples. The recommended MRLs of AFM1 in milk are 50 ng kg⁻¹ (for adults) and 25 ng kg⁻¹ (for infants). Various sequences of labelled aptamer specific to AFM1 and its complementary quencher sequences were studied to design the experiment. The developed platform demonstrates the dynamic range 1-2000 ng kg⁻¹ AFM1 with good linearity from 25-2000 ng kg⁻¹ with LOD of 1 ng kg⁻¹ AFM1 in milk including the requirements of AFM1 regulatory standards in milk (50 ng kg⁻¹ for adults and 25 ng kg⁻¹ for infants). Excellent recoveries were obtained in the range 94.40-95.28 % in the spiked milk samples comparative to the commercial ELISA kit. The assay showed the requirement of low sample volume (15 μL), fast response with high precision and accuracy representing intraday reproducibility % R.S.D. 3.47 (n=3).

4. Chapter 4: This chapter described the development of EIS based label-free and disposable impedimetric aptasensor for analysis of kanamycin in milk. The utilization of SPCEs technology and diazonium coupling mechanism for immobilization of aptamer provided the improved stability and sensitivity to aptasensor. The aptasensor was characterized using surface morphology and electrochemical techniques for each step of modification. Sensitivity and selectivity of developed aptasensor were evaluated by monitoring the change in

impedimetric response (R_{ct} value) on aptasensor surface after kanamycin was incubated on transducer surface. A linearity of 1.20-75 ng mL⁻¹ KANA was observed with increasing concentration of kanamycin and low sample requirement of 20 μ L. The LOD of KANA aptasensor was found to be 0.11 ng mL⁻¹ with an analysis time of less than 3 min. The devised aptasensor exhibited the recovery percentage 96.88-100.5% in KANA spiked milk samples. The high sensitivity of developed aptasensor was due to the enhanced stability and no leakage of aptamer molecule over diazotized surface. The developed aptasensor showed high selectivity to kanamycin providing a cost effective and disposable aptasensor with analysis time of less than 3 min.

5. Chapter 5: This chapter gave the detailed description about the development of μ FIA integrated EQCN aptasensor for TET analysis in raw milk samples. In this chapter, various parameters for μ FIA analysis were optimized including matrix matching for milk sample analysis and immobilization of the aptamer on the gold quartz crystal surface in a semi-automated mode. The ssDNA aptamer used exhibited the high affinity against TET with dissociation constant (K_d) value of 3.03 μ M. The successful characterization of devised μ FIA-EQCN TET-aptasensor proved aptasensor fabrication. The sensitivity of developed aptasensor was in the range of 1.562-600 ng mL⁻¹ with increase in the concentrations of TET in milk. The aptasensor poses the fast response (17 min) and high sensitivity (0.531 ng mL⁻¹ TET) meeting the regulatory standards (MRLs, 100-300 ng mL⁻¹). Observed recoveries for TET (97.43-100.60 %) over ELISA kit (97.95-100.18 %) suggested the applicability of μ FIA-EQCN-TET aptasensor for analysis of TET in milk sample. The developed TET aptasensor did not show any significant cross reactivity with other structural and non-structural analogues. Validation of presented aptasensor with commercial ELISA kit showed its potential to dairy industries involving no complex sample preparation involved.

Future scope of the work

- ❖ The developed fluorescence quenching based platform employed TiO₂-NPs can be further employed for OTA analysis in other matrices.
- ❖ The quenching potential of TiO₂-NPs could be further explored for other sensing protocols.
- ❖ The rational concept of fluorescence quenching-dequenching mechanism has enough potential to explore further.
- ❖ The novel coupling chemistry can be further investigated for immobilization of biomolecule on SPCEs and can be developed for commercial product.
- ❖ SPCEs integrated aptasensors could be further exaggerated for cost-effective and disposable aptasensor.
- ❖ μ FIA-EQCN technology can be successfully employed for antibiotic residue analysis in dairy industries for on-line monitoring.
- ❖ The μ FIA-EQCN platform can be explored for other analytes detection by employing the use of target specific aptamer sequences.

REFERENCES

1. Adrian, J., Pinacho, D.G., Granier, B., Diserens, J.M., Sanchez-Baeza, F., Marco, M.P., 2008. A multianalyte ELISA for immunochemical screening of sulfonamide, fluoroquinolone and ss-lactam antibiotics in milk samples using class-selective bioreceptors. *Analytical and Bioanalytical Chemistry* 391(5), 1703-1712.
2. Aga, D.S., O'Connor, S., Ensley, S., Payero, J.O., Snow, D., Tarkalson, D., 2005. Determination of the Persistence of Tetracycline Antibiotics and Their Degradates in Manure-Amended Soil Using Enzyme-Linked Immunosorbent Assay and Liquid Chromatography-Mass Spectrometry. *Journal of Agricultural and Food Chemistry* 53(18), 7165-7171.
3. Alivisatos, A.P., Johnsson, K.P., Peng, X., Wilson, T.E., Loweth, C.J., Bruchez, M.P., Schultz, P.G., 1996. Organization of 'nanocrystal molecules' using DNA. *Nature* 382(6592), 609-611.
4. Al-Taher, F., Banaszewski, K., Jackson, L., Zweigenbaum, J., Ryu, D., Cappozzo, J., 2013. Rapid method for the determination of multiple mycotoxins in wines and beers by LC-MS/MS using a stable isotope dilution assay. *Journal of Agricultural and Food Chemistry* 61(10), 2378-2384.
5. Amano, T., Toyooka, T., Ibuki, Y., 2010. Preparation of DNA-adsorbed TiO₂ particles-Augmentation of performance for environmental purification by increasing DNA adsorption by external pH regulation. *Science of The Total Environment* 408(3), 480-485.
6. Amaya-González, S., De-los-Santos-Álvarez, N., Miranda-Ordieres, A., Lobo-Castañón, M., 2013. Aptamer-Based Analysis: A Promising Alternative for Food Safety Control. *Sensors* 13(12), 16292.
7. Andrushchenko, V., Wieser, H., Bouř, P., 2007. DNA Oligonucleotide–cis-Platin Binding: Ab Initio Interpretation of the Vibrational Spectra. *The Journal of Physical Chemistry A* 111(39), 9714-9723.
8. Anfossi, L., Calderara, M., Baggiani, C., Giovannoli, C., Arletti, E., Giraudi, G., 2008. Development and application of solvent-free extraction for the detection of aflatoxin M1 in dairy products by enzyme immunoassay. *Journal of Agricultural and Food Chemistry* 56(6), 1852-1857.

9. Anli, E., Alkis, İ.M., 2010. Ochratoxin A and Brewing Technology: A Review. *Journal of the Institute of Brewing* 116(1), 23-32.
10. AOAC Official Method 986.16 Aflatoxins M1 and M2 in fluid milk, liquid chromatographic method. *Natural Toxins, Chapter-49, Official Methods of Analysis of AOAC International*, AOAC International, Gaithersburg, Maryland 20877–2417, USA, 2000, pp. 40–42.
11. Ashiq, S., Hussain, M., Ahmad, B., 2014. Natural occurrence of mycotoxins in medicinal plants: A review. *Fungal Genetics and Biology* 66, 1-10.
12. Aswani Kumar, Y.V.V., Renuka, R.M., Achuth, J., Venkataramana, M., Ushakiranmayi, M., Sudhakar, P., 2018. Development of Hybrid IgG-Aptamer Sandwich Immunoassay Platform for Aflatoxin B1 Detection and Its Evaluation Onto Various Field Samples. *Frontiers in Pharmacology* 9(271).
13. Bacher, G., Pal, S., Kanungo, L., Bhand, S., 2012. A label-free silver wire based impedimetric immunosensor for detection of aflatoxin M1 in milk. *Sensors and Actuators B: Chemical* 168, 223-230.
14. Badea, M., Micheli, L., Messia, M.C., Candigliota, T., Marconi, E., Mottram, T., Velasco-Garcia, M., Moscone, D., Palleschi, G., 2004. Aflatoxin M1 determination in raw milk using a flow-injection immunoassay system. *Analytica Chimica Acta* 520(1–2), 141-148.
15. Bakirci, I., 2001. A study on the occurrence of aflatoxin M1 in milk and milk products produced in Van province of Turkey. *Food Control* 12(1), 47-51.
16. Balcioglu, M., Rana, M., Robertson, N., Yigit, M.V., 2014. DNA-length-dependent quenching of fluorescently labeled iron oxide nanoparticles with gold, graphene oxide and MoS₂ nanostructures. *ACS Applied Materials & Interfaces* 6(15), 12100-12110.
17. Bamrungsap, S., Chen, T., Shukoor, M.I., Chen, Z., Sefah, K., Chen, Y., Tan, W., 2012. Pattern Recognition of Cancer Cells Using Aptamer-Conjugated Magnetic Nanoparticles. *ACS Nano* 6(5), 3974-3981.
18. Baranton, S., Bélanger, D., 2005. Electrochemical Derivatization of Carbon Surface by Reduction of in Situ Generated Diazonium Cations. *The Journal of Physical Chemistry B* 109(51), 24401-24410.
19. Barefoot, J.C., Grønbaek, M., Feaganes, J.R., McPherson, R.S., Williams, R.B., Siegler, I.C., 2002. Alcoholic beverage preference, diet, and health habits in the UNC Alumni Heart Study. *The American Journal of Clinical Nutrition* 76(2), 466-472.

20. (a) Barthelmebs, L., Jonca, J., Hayat, A., Prieto-Simon, B., Marty, J.-L., 2011. Enzyme-Linked Aptamer Assays (ELAAs), based on a competition format for a rapid and sensitive detection of Ochratoxin A in wine. *Food Control* 22(5), 737-743. (b) Barthelmebs, L., Hayat, A., Limiadi, A.W., Marty, J.-L., Noguera, T., 2011. Electrochemical DNA aptamer-based biosensor for OTA detection, using superparamagnetic nanoparticles. *Sensors and Actuators B: Chemical* 156(2), 932-937.
21. Bellver Soto, J., Fernández-Franzón, M., Ruiz, M.-J., Juan-García, A., 2014. Presence of Ochratoxin A (OTA) Mycotoxin in Alcoholic Drinks from Southern European Countries: Wine and Beer. *Journal of Agricultural and Food Chemistry* 62(31), 7643-7651.
22. Benito-Pena, E., Martins, S., Orellana, G., Moreno-Bondi, M.C., 2009. Water-compatible molecularly imprinted polymer for the selective recognition of fluoroquinolone antibiotics in biological samples. *Analytical and Bioanalytical Chemistry* 393(1), 235-245.
23. Berendsen, B.J.A., Stolker, L.A.M., Nielen, M.W.F., Nielen, M.W.F., 2013. Selectivity in the sample preparation for the analysis of drug residues in products of animal origin using LC-MS. *TrAC Trends in Analytical Chemistry* 43, 229-239.
24. Bhalla, N., Jolly, P., Formisano, N., Estrela, P., 2016. Introduction to biosensors. *Essays in Biochemistry* 60(1), 1-8.
25. Bhand, S.G., Soundararajan, S., Surugiu-Wärnmark, I., Milea, J.S., Dey, E.S., Yakovleva, M., Danielsson, B., 2010. Fructose-selective calorimetric biosensor in flow injection analysis. *Analytica Chimica Acta* 668(1), 13-18.
26. Blanchaert, B., Poderós Jorge, E., Jankovics, P., Adams, E., Van Schepdael, A., 2013. Assay of Kanamycin A by HPLC with Direct UV Detection. *Chromatographia* 76(21), 1505-1512.
27. Bognanno, M., La Fauci, L., Ritieni, A., Tafuri, A., De Lorenzo, A., Micari, P., Di Renzo, L., Ciappellano, S., Sarullo, V., Galvano, F., 2006. Survey of the occurrence of Aflatoxin M1 in ovine milk by HPLC and its confirmation by MS. *Molecular Nutrition & Food Research* 50(3), 300-305.
28. Bonel, L., Vidal, J.C., Duato, P., Castillo, J.R., 2011. An electrochemical competitive biosensor for ochratoxin A based on a DNA biotinylated aptamer. *Biosensors and Bioelectronics* 26(7), 3254-3259.
29. Boonen, J., Malysheva, S.V., Taevernier, L., Diana Di Mavungu, J., De Saeger, S., De Spiegeleer, B., 2012. Human skin penetration of selected model mycotoxins. *Toxicology* 301(1-3), 21-32.

30. Bueno, D., Valdez, L., Gutiérrez Salgado, J., Marty, J., Muñoz, R., 2016. Colorimetric Analysis of Ochratoxin A in Beverage Samples. *Sensors* 16(11), 1888.
31. Cabello, F.C., 2006. Heavy use of prophylactic antibiotics in aquaculture: a growing problem for human and animal health and for the environment. *Environmental Microbiology* 8(7), 1137-1144.
32. Cao, C., Zhang, Y., Jiang, C., Qi, M., Liu, G., 2017. Advances on Aryldiazonium Salt Chemistry Based Interfacial Fabrication for Sensing Applications. *ACS Applied Materials & Interfaces* 9(6), 5031-5049.
33. Castillo, G., Spinella, K., Poturnayová, A., Šnejdárková, M., Mosiello, L., Hianik, T., 2015. Detection of aflatoxin B1 by aptamer-based biosensor using PAMAM dendrimers as immobilization platform. *Food Control* 52, 9-18.
34. Cavaliere, C., Foglia, P., Pastorini, E., Samperi, R., Lagana, A., 2006. Liquid chromatography/tandem mass spectrometric confirmatory method for determining aflatoxin M1 in cow milk: comparison between electrospray and atmospheric pressure photoionization sources. *Journal of Chromatography. A* 1101(1-2), 69-78.
35. Chalyan, T., Pasquardini, L., Gandolfi, D., Guider, R., Samusenko, A., Zanetti, M., Pucker, G., Pederzoli, C., Pavesi, L., 2017. Aptamer- and Fab'- Functionalized Microring Resonators for Aflatoxin M1 Detection. *IEEE Journal of Selected Topics in Quantum Electronics* 23(2), 350-357.
36. Chen, D., Yao, D., Xie, C., Liu, D., 2014. Development of an aptasensor for electrochemical detection of tetracycline. *Food Control* 42, 109-115.
37. Chen, J., Fang, Z., Liu, J., Zeng, L., 2012. A simple and rapid biosensor for ochratoxin A based on a structure-switching signalling aptamer. *Food Control* 25(2), 555-560.
38. Chen, J., Zhang, X., Cai, S., Wu, D., Chen, M., Wang, S., Zhang, J., 2014. A fluorescent aptasensor based on DNA-scaffolded silver-nanocluster for ochratoxin A detection. *Biosensors and Bioelectronics* 57, 226-231.
39. Chen, Y., Kong, D., Liu, L., Song, S., Kuang, H., Xu, C., 2016. Development of an ELISA and Immunochromatographic Assay for Tetracycline, Oxytetracycline, and Chlortetracycline Residues in Milk and Honey Based on the Class-Specific Monoclonal Antibody. *Food Analytical Methods* 9(4), 905-914.
40. Chen, Y., Schwack, W., 2013. Planar chromatography mediated screening of tetracycline and fluoroquinolone antibiotics in milk by fluorescence and mass selective detection. *Journal of Chromatography A* 1312, 143-151.

41. Chen, Y., Wang, Z., Wang, Z., Tang, S., Zhu, Y., Xiao, X., 2008. Rapid Enzyme-Linked Immunosorbent Assay and Colloidal Gold Immunoassay for Kanamycin and Tobramycin in Swine Tissues. *Journal of Agricultural and Food Chemistry* 56(9), 2944-2952.
42. Choi, H.-G., Min, J., Han, K.-K., Choi, J.-W., Lee, W.H., 2001. Photoelectric conversion of bacteriorhodopsin films fabricated by self-assembly technique. *Synthetic Metals* 117(1-3), 141-143.
43. Codex Alimentarius Commission, Joint FAO/WHO Food Standards Programme (2003) Report of the fourteenth session of The Codex Committee on Residues of Veterinary Drugs in Foods, CI 2003/11-Rvdf.
44. Codex Alimentarius (2000) Codex Committee on Food Additives and Contaminants. CL 1999/13 GEN-CX 0016 FAC-Agenda item 16a. ALINORM 99/37, paras 103-105. Draft maximum level for aflatoxin M1 in milk, 20–24 March.
45. Conzuelo, F., Campuzano, S., Gamella, M., Pinacho, D.G., Reviejo, A.J., Marco, M.P., Pingarrón, J.M., 2013. Integrated disposable electrochemical immunosensors for the simultaneous determination of sulfonamide and tetracycline antibiotics residues in milk. *Biosensors and Bioelectronics* 50, 100-105.
46. Cordewener, J.H., Luykx, D.M., Frankhuizen, R., Bremer, M.G., Hooijerink, H., America, A.H., 2009. Untargeted LC-Q-TOF mass spectrometry method for the detection of adulterations in skimmed-milk powder. *Journal of Separation Science* 32(8), 1216-1223.
47. Cox, J.C., Ellington, A.D., 2001. Automated selection of anti-Protein aptamers. *Bioorganic & Medicinal Chemistry* 9(10), 2525-2531.
48. Craig, A.P., Franca, A.S., Irudayaraj, J., 2013. Surface-Enhanced Raman Spectroscopy Applied to Food Safety. *Annual Review of Food Science and Technology* 4(1), 369-380.
49. Cruz-Aguado, J.A., Penner, G., 2008. Determination of Ochratoxin A with a DNA Aptamer. *Journal of Agricultural and Food Chemistry* 56(22), 10456-10461.
50. Cui, Y., Wei, Q., Park, H., Lieber, C.M., 2001. Nanowire Nanosensors for Highly Sensitive and Selective Detection of Biological and Chemical Species. *Science* 293(5533), 1289.
51. Dai, S., Wu, S., Duan, N., Chen, J., Zheng, Z., Wang, Z., 2017. An ultrasensitive aptasensor for Ochratoxin A using hexagonal core/shell upconversion nanoparticles as luminophores. *Biosensors and Bioelectronics* 91, 538-544.

52. Dai, S., Wu, S., Duan, N., Wang, Z., 2016. A luminescence resonance energy transfer based aptasensor for the mycotoxin Ochratoxin A using upconversion nanoparticles and gold nanorods. *Microchimica Acta* 183(6), 1909-1916.
53. Damborsky, P., Svitel, J., Katrik, J., 2016. Optical biosensors. *Essays in Biochemistry* 60(1), 91-100.
54. Daprà, J., Lauridsen, L.H., Nielsen, A.T., Rozlosnik, N., 2013. Comparative study on aptamers as recognition elements for antibiotics in a label-free all-polymer biosensor. *Biosensors and Bioelectronics* 43, 315-320.
55. De Ruyck, H., De Ridder, H., 2007. Determination of tetracycline antibiotics in cow's milk by liquid chromatography/tandem mass spectrometry. *Rapid Communications in Mass Spectrometry* 21(9), 1511-1520.
56. Delamar, M., Hitmi, R., Pinson, J., Saveant, J.M., 1992. Covalent modification of carbon surfaces by grafting of functionalized aryl radicals produced from electrochemical reduction of diazonium salts. *Journal of the American Chemical Society* 114(14), 5883-5884.
57. Di Giambattista, L., Pozzi, D., Grimaldi, P., Gaudenzi, S., Morrone, S., Castellano, A.C., 2011. New marker of tumor cell death revealed by ATR-FTIR spectroscopy. *Analytical and Bioanalytical Chemistry* 399(8), 2771-2778.
58. Dinckaya, E., Kinik, O., Sezginturk, M.K., Altug, C., Akkoca, A., 2011. Development of an impedimetric aflatoxin M1 biosensor based on a DNA probe and gold nanoparticles. *Biosensors and Bioelectronics* 26(9), 3806-3811.
59. Duan, N., Wu, S., Ma, X., Chen, X., Huang, Y., Wang, Z., 2012. Gold Nanoparticle-Based Fluorescence Resonance Energy Transfer Aptasensor for Ochratoxin A Detection. *Analytical Letters* 45(7), 714-723.
60. Duarte, S.C., Lino, C.M., Pena, A., 2010. Mycotoxin food and feed regulation and the specific case of ochratoxin A: a review of the worldwide status. *Food Additives & Contaminants. Part A, Chemistry, Analysis, Control, Exposure & Risk Assessment* 27(10), 1440-1450.
61. Durán, N., Marcato, P.D., 2013. Nanobiotechnology perspectives. Role of nanotechnology in the food industry: a review. *International Journal of Food Science and Technology* 48(6), 1127-1134.
62. Emrani, A.S., Danesh, N.M., Lavaee, P., Ramezani, M., Abnous, K., Taghdisi, S.M., 2016. Colorimetric and fluorescence quenching aptasensors for detection of streptomycin

- in blood serum and milk based on double-stranded DNA and gold nanoparticles. *Food Chemistry* 190, 115-121.
63. European Agency for the Evaluation of Medical Products (EMA) London: 2003. Regulation No. EMA/MRL/886/03-FINAL.
 64. European Commission (2002). Commission Regulation EC 472/2002 of the 12 March 2002 amending regulation (EC) No. 466/2001 setting maximum levels for certain contaminants in foodstuffs, *Off. J. Eur. Union*, 2002.
 65. European Commission (2005). Commission Regulation (EC) No 123/2005 of 26 January 2005. Amending Regulation (CE) No 466/2001 as regards ochratoxin A. *Journal of the European Union*, L25/3-25/5.
 66. European Commission, Commission Regulation (EC) (No. 1881/2006) maximum levels for certain contaminant in foodstuffs, 2006, 5-24.
 67. Food Safety and Standard Authority of India (FSSAI) “Manual of Methods for analysis of Foods – Antibiotics and Hormone Residue” *Lab Manual* 2012, 15: 1-57.
 68. Food Safety and Standards (CONTAMINANTS, TOXINS AND RESIDUES) REGULATIONS (F.No. 2-15015/30/2010), Chapter 1, 2011.
 69. Gan, T., Shi, Z., Sun, J., Liu, Y., 2014. Simple and novel electrochemical sensor for the determination of tetracycline based on iron/zinc cations-exchanged montmorillonite catalyst. *Talanta* 121, 187-193.
 70. Gautschi, G., 2002. Piezoelectric Sensors. *Piezoelectric Sensorics: Force Strain Pressure Acceleration and Acoustic Emission Sensors Materials and Amplifiers*, pp. 73-91. Springer Berlin Heidelberg, Berlin, Heidelberg.
 71. Giesen, C., Jakubowski, N., Panne, U., Weller, M.G., 2010. Comparison of ICP-MS and photometric detection of an immunoassay for the determination of ochratoxin A in wine. *Journal of Analytical Atomic Spectrometry* 25(10), 1567-1572.
 72. Gold, L., Janjic, N., Jarvis, T., Schneider, D., Walker, J.J., Wilcox, S.K., Zichi, D., 2012. Aptamers and the RNA world, past and present. *Cold Spring Harbor Perspectives in Biology* 4(3).
 73. González-Fernández, E., de-los-Santos-Álvarez, N., Lobo-Castañón, M.J., Miranda-Ordieres, A.J., Tuñón-Blanco, P., 2011. Impedimetric aptasensor for tobramycin detection in human serum. *Biosensors and Bioelectronics* 26(5), 2354-2360.
 74. Goud, K.Y., Sharma, A., Hayat, A., Catanante, G., Gobi, K.V., Gurban, A.M., Marty, J.L., 2016. Tetramethyl-6-carboxyrhodamine quenching-based aptasensing platform for

- aflatoxin B1: Analytical performance comparison of two aptamers. *Analytical Biochemistry* 508, 19-24.
75. Grieshaber, D., MacKenzie, R., Vörös, J., Reimhult, E., 2008. Electrochemical Biosensors-Sensor Principles and Architectures. *Sensors (Basel, Switzerland)* 8(3), 1400-1458.
 76. Shruthi, G.S., Amitha, C.V., Blessy Baby Mathew, 2014. Biosensors: A Modern Day Achievement. *Journal of Instrumentation Technology* 2(1), 26-39.
 77. Guider, R., Gandolfi, D., Chalyan, T., Pasquardini, L., Samusenko, A., Pucker, G., Pederzoli, C., Pavesi, L., 2015. Design and Optimization of SiON Ring Resonator-Based Biosensors for Aflatoxin M1 Detection. *Sensors (Basel, Switzerland)* 15(7), 17300-17312.
 78. Guo, X., Wen, F., Zheng, N., Li, S., Fauconnier, M.L., Wang, J., 2016. A qPCR aptasensor for sensitive detection of aflatoxin M1. *Analytical and Bioanalytical Chemistry* 408(20), 5577-5584.
 79. Guo, X.; Wen, F.; Zheng, N.; Luo, Q.; Wang, H.; Wang, H.; Li, S.; Wang, J. 2014. Development of an ultrasensitive aptasensor for the detection of aflatoxin B1. *Biosensors and Bioelectronics* 56, 340-344.
 80. Guo, Y., Wang, X., Sun, X., 2015. A label-free Electrochemical Aptasensor Based on Electrodeposited Gold Nanoparticles and Methylene Blue for Tetracycline Detection. *International Journal of Electrochemical Science* 10, 3668 – 3679
 81. Guo, Z., Ren, J., Wang, J., Wang, E., 2011. Single-walled carbon nanotubes based quenching of free FAM-aptamer for selective determination of ochratoxin A. *Talanta* 85(5), 2517-2521.
 82. Hall, A.J.; Wild, C.P. Epidemiology of aflatoxin-related disease. In *The Toxicology of Aflatoxins: Human Health, Veterinary, and Agricultural Significance*; Eaton, D.L., Groopman, J.D., Eds.; Academic Press: San Diego, CA, USA, 1994; pp. 233–258
 83. Hamid, A.S., Tesfamariam, I.G., Zhang, Y., Zhang, Z.G., 2013. Aflatoxin B1-induced hepatocellular carcinoma in developing countries: Geographical distribution, mechanism of action and prevention. *Oncology Letters* 5(4), 1087-1092.
 84. Hansen, E.H., 1996. Principles and applications of flow injection analysis in biosensors. *Journal of Molecular Recognition* 9(5-6), 316-325.
 85. Hansen, E.H., Miró, M., Flickinger, M.C., 2009. Flow Injection Analysis in Industrial Biotechnology. *Encyclopedia of Industrial Biotechnology*. John Wiley & Sons, Inc.

86. Hayat, A., Barthelmebs, L., Marty, J.-L., 2011. Enzyme-linked immunosensor based on super paramagnetic nanobeads for easy and rapid detection of okadaic acid. *Analytica Chimica Acta* 690(2), 248-252.
87. Hayat, A., Marty, J., 2014. Disposable Screen Printed Electrochemical Sensors: Tools for Environmental Monitoring. *Sensors* 14(6), 10432.
88. Hayat, A., Sassolas, A., Marty, J.-L., Radi, A.-E., 2013. Highly sensitive ochratoxin A impedimetric aptasensor based on the immobilization of azido-aptamer onto electrografted binary film via click chemistry. *Talanta* 103, 14-19.
89. Hianik, T., Ostatna, V., Sonlajtnerova, M., Grman, I., 2007. Influence of ionic strength, pH and aptamer configuration for binding affinity to thrombin. *Bioelectrochemistry (Amsterdam, Netherlands)* 70(1), 127-133.
90. Hurd, H.S., Malladi, S., 2008. A stochastic assessment of the public health risks of the use of macrolide antibiotics in food animals. *Risk analysis : an official publication of the Society for Risk Analysis* 28(3), 695-710.
91. Hwang, J.-H., Lee, K.-G., 2006. Reduction of aflatoxin B1 contamination in wheat by various cooking treatments. *Food Chemistry* 98(1), 71-75.
92. IARC (1993). Some Naturally Occurring Substances: Food Items and Constituents, Heterocyclic Aromatic Amines, and Mycotoxins. IARC (International Agency for Research on Cancer) 56, 489.
93. Ibarra, I.S., Rodriguez, J.A., Miranda, J.M., Vega, M., Barrado, E., 2011. Magnetic solid phase extraction based on phenyl silica adsorbent for the determination of tetracyclines in milk samples by capillary electrophoresis. *Journal of Chromatography A* 1218(16), 2196-2202.
94. Iha, M.H., Barbosa, C.B., Favaro, R.M., Trucksess, M.W. 2011. Chromatographic method for the determination of aflatoxin M1 in cheese, yogurt, and dairy beverages. *Journal of AOAC International* 94, 1513-1518.
95. Iliuk, A.B., Hu, L., Tao, W.A., 2011. Aptamer in Bioanalytical Applications. *Analytical Chemistry* 83(12), 4440-4452.
96. International Agency for Research on Cancer, Monograph on the Evaluation of Carcinogenic Risk to Humans, World Health Organization, Lyon, France, 2002, 171.
97. Islam, M., Fujii, S., Sato, S., Okauchi, T., Takenaka, S., 2015. A Selective G-Quadruplex DNA-Stabilizing Ligand Based on a Cyclic Naphthalene Diimide Derivative. *Molecules* 20(6), 10963.

98. Istamboulié, G., Paniel, N., Zara, L., Granados, L.R., Barthelmebs, L., Noguera, T., 2016. Development of an impedimetric aptasensor for the determination of aflatoxin M1 in milk. *Talanta* 146, 464-469.
99. IUPAC. Compendium of Chemical Terminology, 2nd ed. (the "Gold Book"). Compiled by A. D. McNaught and A. Wilkinson. Blackwell Scientific Publications, Oxford (1997). XML on-line corrected version: <http://goldbook.iupac.org> (2006) created by M. Nic, J. Jirat, B. Kosata; updates compiled by A. Jenkins. ISBN 0-9678550-9-8. doi: 10.1351/goldbook.
100. James, W., 2006. Aptamers. *Encyclopedia of Analytical Chemistry*. John Wiley & Sons, Ltd.
101. Janshoff, A., Galla, H.J., Steinem, C., 2000. Piezoelectric Mass-Sensing Devices as Biosensors-An Alternative to Optical Biosensors? *Angewandte Chemie (International ed. in English)* 39(22), 4004-4032.
102. Jayasena, S.D., 1999. Aptamers: An Emerging Class of Molecules That Rival Antibodies in Diagnostics. *Clinical Chemistry* 45(9), 1628-1650.
103. Jeong, S., Rhee Paeng, I., 2012. Sensitivity and Selectivity on Aptamer-Based Assay: The Determination of Tetracycline Residue in Bovine Milk. *The Scientific World Journal*, 1-10.
104. Ji, J., Gu, W., Sun, C., Sun, J., Jiang, H., Zhang, Y., Sun, X., 2016. A novel recombinant cell fluorescence biosensor based on toxicity of pathway for rapid and simple evaluation of DON and ZEN. *Scientific Reports* 6, 31270.
105. Jin, Y., Jang, J.-W., Han, C.-H., Lee, M.-H., 2006. Development of immunoassays for the detection of kanamycin in veterinary fields. *Journal of Veterinary Science* 7(2), 111-117.
106. Joshi, K.A., Tang, J., Haddon, R., Wang, J., Chen, W., Mulchandani, A., 2005. A Disposable Biosensor for Organophosphorus Nerve Agents Based on Carbon Nanotubes Modified Thick Film Strip Electrode. *Electroanalysis* 17(1), 54-58.
107. Kantiani, L., Llorca, M., Sanchís, J., Farré, M., Barceló, D., 2010. Emerging food contaminants: a review. *Analytical and Bioanalytical Chemistry* 398(6), 2413-2427.
108. Kanungo, L., Pal, S., Bhand, S., 2011. Miniaturised hybrid immunoassay for high sensitivity analysis of aflatoxin M1 in milk. *Biosensors & bioelectronics* 26(5), 2601-2606.
109. Karaseva, N.A., Ermolaeva, T.N., 2012. A piezoelectric immunosensor for chloramphenicol detection in food. *Talanta* 93, 44-48.

110. Karaseva, N.A., Ermolaeva, T.N., 2014. Piezoelectric immunosensors for the detection of individual antibiotics and the total content of penicillin antibiotics in foodstuffs. *Talanta* 120, 312-317.
111. Kathiravan, A., Renganathan, R., 2009. Photoinduced interactions between colloidal TiO₂ nanoparticles and calf thymus-DNA. *Polyhedron* 28(7), 1374-1378.
112. Katilius, E., Katiliene, Z., Woodbury, N.W., 2006. Signaling Aptamers Created Using Fluorescent Nucleotide Analogues. *Analytical Chemistry* 78(18), 6484-6489.
113. Kensler, T.W., Roebuck, B.D., Wogan, G.N., Groopman, J.D., 2011. Aflatoxin: a 50-year odyssey of mechanistic and translational toxicology. *Toxicological sciences: an official journal of the Society of Toxicology* 120 Suppl 1, S28-48.
114. Kim, C.-H., Lee, L.-P., Min, J.-R., Lim, M.-W., Jeong, S.-H., 2014. An indirect competitive assay-based aptasensor for detection of oxytetracycline in milk. *Biosensors and Bioelectronics* 51, 426-430.
115. Kim, E., Baaske, M.D., Vollmer, F., 2017. Towards next-generation label-free biosensors: recent advances in whispering gallery mode sensors. *Lab on a chip* 17(7), 1190-1205.
116. Kim, J., Jerkiewicz, G., 2017. Influence of the Surface Roughness of Platinum Electrodes on the Calibration of the Electrochemical Quartz-Crystal Nanobalance. *Analytical chemistry*.
117. Kim, Y.-J., Kim, Y.S., Niazi, J.H., Gu, M.B., 2009. Electrochemical aptasensor for tetracycline detection. *Bioprocess and Biosystems Engineering* 33(1), 31.
118. Kivirand, K., Kagan, M., Rinken, T., 2015. Biosensors for the detection of antibiotic residues in milk *Nanotechnology and Nanomaterial "Biosensors - Micro and Nanoscale Applications"* (Book reference).
119. Kuang, H., Chen, W., Xu, D., Xu, L., Zhu, Y., Liu, L., Chu, H., Peng, C., Xu, C., Zhu, S., 2010. Fabricated aptamer-based electrochemical "signal-off" sensor of ochratoxin A. *Biosensors and Bioelectronics* 26(2), 710-716.
120. Kumar, V., Basu, M.S., Rajendran, T.P., 2008. Mycotoxin research and mycoflora in some commercially important agricultural commodities. *Crop Protection* 27(6), 891-905.
121. Kümmerer, K., 2003. Significance of antibiotics in the environment. *Journal of Antimicrobial Chemotherapy* 52(1), 5-7.
122. Lakowicz, J.R. *Principle of Fluorescence Spectroscopy*; Kluwar Academic/Plenum: New Work, NY, USA, 1999.

123. Lechuga, L.M., 2005. Chapter 5 Optical biosensors. *Comprehensive Analytical Chemistry*, pp. 209-250. Elsevier.
124. Lee, S.X., Lim, H.N., Ibrahim, I., Jamil, A., Pandikumar, A., Huang, N.M., 2017. Horseradish peroxidase-labeled silver/reduced graphene oxide thin film-modified screen-printed electrode for detection of carcinoembryonic antigen. *Biosensors and Bioelectronics* 89, Part 1, 673-680.
125. Leung, K.-H., He, H.-Z., Chan, D.S.-H., Fu, W.-C., Leung, C.-H., Ma, D.-L., 2013. An oligonucleotide-based switch-on luminescent probe for the detection of kanamycin in aqueous solution. *Sensors and Actuators B: Chemical* 177, 487-492.
126. Li, H., Sun, D.-e., Liu, Y., Liu, Z., 2014. An ultrasensitive homogeneous aptasensor for kanamycin based on upconversion fluorescence resonance energy transfer. *Biosensors and Bioelectronics* 55, 149-156.
127. Li, R., Liu, Y., Cheng, L., Yang, C., Zhang, J., 2014. Photoelectrochemical Aptasensing of Kanamycin Using Visible Light-Activated Carbon Nitride and Graphene Oxide Nanocomposites. *Analytical Chemistry* 86(19), 9372-9375.
128. Liao, D.L., Wu, G.S., Liao, B.Q., 2009. Zeta potential of shape-controlled TiO₂ nanoparticles with surfactants. *Colloids and Surfaces A: Physicochemical and Engineering Aspects* 348(1-3), 270-275.
129. Liu, C., Lu, C., Tang, Z., Chen, X., Wang, G., Sun, F., 2015. Aptamer-functionalized magnetic nanoparticles for simultaneous fluorometric determination of oxytetracycline and kanamycin. *Microchimica Acta* 182(15), 2567-2575.
130. Liu, J., 2012. Adsorption of DNA onto gold nanoparticles and graphene oxide: surface science and applications. *Physical Chemistry Chemical Physics* 14(30), 10485-10496.
131. Liu, J., Lu, Y., 2005. Fast colorimetric sensing of adenosine and cocaine based on a general sensor design involving aptamers and nanoparticles. *Angewandte Chemie (International ed. in English)* 45(1), 90-94.
132. Love, J.C., Estroff, L.A., Kriebel, J.K., Nuzzo, R.G., Whitesides, G.M., 2005. Self-assembled monolayers of thiolates on metals as a form of nanotechnology. *Chemical Reviews* 105(4), 1103-1169.
133. Lu, C.Y., Feng, C.H., 2006. On-line concentration of neomycin and screening aminoglycosides in milk by short capillary column and tandem mass spectrometry. *Journal of Separation Science* 29(14), 2143-2148.

134. Luan, Y., Chen, J., Li, C., Xie, G., Fu, H., Ma, Z., Lu, A., 2015. Highly Sensitive Colorimetric Detection of Ochratoxin A by a Label-Free Aptamer and Gold Nanoparticles. *Toxins* 7(12), 5377-5385.
135. Luo, Y., Xu, J., Li, Y., Gao, H., Guo, J., Shen, F., Sun, C., 2015. A novel colorimetric aptasensor using cysteamine-stabilized gold nanoparticles as probe for rapid and specific detection of tetracycline in raw milk. *Food Control* 54, 7-15.
136. Luong, J.H.T., Male, K.B., Glennon, J.D., 2008. Biosensor technology: Technology push versus market pull. *Biotechnology Advances* 26(5), 492-500.
137. Lv, L., Cui, C., Liang, C., Quan, W., Wang, S., Guo, Z., 2016. Aptamer-based single-walled carbon nanohorn sensors for ochratoxin A detection. *Food Control* 60, 296-301.
138. Lv, Z., Chen, A., Liu, J., Guan, Z., Zhou, Y., Xu, S., Yang, S., Li, C., 2014. A Simple and Sensitive Approach for Ochratoxin A Detection Using a Label-Free Fluorescent Aptasensor. *PLOS ONE* 9(1), e85968.
139. Ma, X., Wang, W., Chen, X., Xia, Y., Wu, S., Duan, N., Wang, Z., 2014. Selection, identification, and application of Aflatoxin B1 aptamer. *European Food Research and Technology* 238(6), 919-925.
140. Magliulo, M., Mirasoli, M., Simoni, P., Lelli, R., Portanti, O., Roda, A., 2005. Development and validation of an ultrasensitive chemiluminescent enzyme immunoassay for aflatoxin M1 in milk. *Journal of Agricultural and Food Chemistry* 53(9), 3300-3305.
141. Malitesta, C., Picca, R.A., Mazzotta, E., Guascito, M.R., 2012. Tools for the Development of Electrochemical Sensors: an EQCM Flow Cell with Flow Focusing. *Electroanalysis* 24(4), 790-797.
142. Malhotra, B.D., Srivastava, S., Ali, M.A., Singh, C., 2014. Nanomaterial-based biosensors for food toxin detection. *Applied biochemistry and biotechnology* 174(3), 880-896.
143. Malhotra, S., Pandey, A.K., Rajput, Y.S., Sharma, R., 2014. Selection of aptamers for aflatoxin M1 and their characterization. *Journal of molecular recognition : JMR* 27(8), 493-500.
144. Maragos, C., 2009. Biosensors for mycotoxin analysis: recent developments and future prospects. *World Mycotoxin Journal* 2(2), 221-238.
145. Marchesini, G.R., Buijs, J., Haasnoot, W., Hooijerink, D., Jansson, O., Nielen, M.W.F., 2008. Nanoscale Affinity Chip Interface for Coupling Inhibition SPR Immunosensor Screening with Nano-LC TOF MS. *Analytical Chemistry* 80(4), 1159-1168.

146. Marin, S., Ramos, A.J., Cano-Sancho, G., Sanchis, V., 2013. Mycotoxins: Occurrence, toxicology, and exposure assessment. *Food and Chemical Toxicology* 60, 218-237.
147. Mateo, R., Medina, Á., Mateo, E.M., Mateo, F., Jiménez, M., 2007. An overview of ochratoxin A in beer and wine. *International Journal of Food Microbiology* 119(1–2), 79-83.
148. Medina, A., Rodriguez, A., Magan, N., 2014. Effect of climate change on *Aspergillus flavus* and aflatoxin B(1) production. *Frontiers in Microbiology* 5, 348.
149. Megoulas, N.C., Koupparis, M.A., 2005. Direct determination of kanamycin in raw materials, veterinary formulation and culture media using a novel liquid chromatography–evaporative light scattering method. *Analytica Chimica Acta* 547(1), 64-72.
150. Mejri-Omrani, N., Miodek, A., Zribi, B., Marrakchi, M., Hamdi, M., Marty, J.-L., Korri-Youssoufi, H., 2016. Direct detection of OTA by impedimetric aptasensor based on modified polypyrrole-dendrimers. *Analytica Chimica Acta* 920, 37-46.
151. Melikhova, E.V., Kalmykova, E.N., Eremin, S.A., Ermolaeva, T.N., 2006. Using a piezoelectric flow immunosensor for determining sulfamethoxazole in environmental samples. *Journal of Analytical Chemistry* 61(7), 687-693.
152. Mesgari Abbasi, M., Babaei, H., Ansarin, M., Nourdadgar, A.-o.-s., Nemati, M., 2011. Simultaneous Determination of Tetracyclines Residues in Bovine Milk Samples by Solid Phase Extraction and HPLC-FL Method. *Advanced Pharmaceutical Bulletin* 1(1), 34-39.
153. Micheli, L., Grecco, R., Badea, M., Moscone, D., Palleschi, G., 2005. An electrochemical immunosensor for aflatoxin M1 determination in milk using screen-printed electrodes. *Biosensors and Bioelectronics* 21(4), 588-596.
154. Miodek, A., Regan, E.M., Bhalla, N., Hopkins, N.A.E., Goodchild, S.A., Estrela, P., 2015. Optimisation and Characterisation of Anti-Fouling Ternary SAM Layers for Impedance-Based Aptasensors. *Sensors (Basel, Switzerland)* 15(10), 25015-25032.
155. Mishra, G.K., Sharma, A., Bhand, S., 2015. Ultrasensitive detection of streptomycin using flow injection analysis-electrochemical quartz crystal nanobalance (FIA-EQCN) biosensor. *Biosensors and Bioelectronics* 67, 532-539.
156. Mishra, R.K., Hayat, A., Catanante, G., Istamboulie, G., Marty, J.-L., 2016. Sensitive quantitation of Ochratoxin A in cocoa beans using differential pulse voltammetry based aptasensor. *Food Chemistry* 192, 799-804.

157. Mokhtarzadeh, A., Ezzati Nazhad Dolatabadi, J., Abnous, K., de la Guardia, M., Ramezani, M., 2015. Nanomaterial-based cocaine aptasensors. *Biosensors and Bioelectronics* 68, 95-106.
158. Monaci, L., Palmisano, F., 2004. Determination of ochratoxin A in foods: state-of-the-art and analytical challenges. *Analytical and Bioanalytical Chemistry* 378(1), 96-103.
159. Mosbach, K., Ramstrom, O., 1996. The Emerging Technique of Molecular Imprinting and Its Future Impact on Biotechnology. *Nature Biotechnology* 14(2), 163-170.
160. Moser, J., Graetzel, M., 1984. Photosensitized electron injection in colloidal semiconductors. *Journal of the American Chemical Society* 106(22), 6557-6564
161. Murphy, P.A., Hendrich, S., Landgren, C., Bryant, C.M., 2006. Food Mycotoxins: An Update. *Journal of Food Science* 71(5), R51-R65.
162. Murugaiyan, S.B., Ramasamy, R., Gopal, N., Kuzhandaivelu, V., 2014. Biosensors in clinical chemistry: An overview. *Advanced Biomedical Research* 3, 67.
163. Musheev, M.U., Krylov, S.N., 2006. Selection of aptamers by systematic evolution of ligands by exponential enrichment: addressing the polymerase chain reaction issue. *Analytica Chimica Acta* 564(1), 91-96.
164. Naik, L., Sharma, R., Mann, B., Lata, K., Rajput, Y.S., Surendra Nath, B., 2017. Rapid screening test for detection of oxytetracycline residues in milk using lateral flow assay. *Food Chemistry* 219, 85-92.
165. Narsaiah, K., Jha, S.N., Bhardwaj, R., Sharma, R., Kumar, R., 2012. Optical biosensors for food quality and safety assurance-a review. *Journal of Food Science and Technology* 49(4), 383-406.
166. Nelson, B.P., Candal, R., Corn, R.M., Anderson, M.A., 2000. Control of Surface and ζ Potentials on Nanoporous TiO_2 Films by Potential-Determining and Specifically Adsorbed Ions. *Langmuir* 16(15), 6094-6101.
167. Ng, K., Linder, S.W., 2003. HPLC separation of tetracycline analogues: comparison study of laser-based polarimetric detection with UV detection. *Journal of Chromatographic Science* 41(9), 460-466.
168. Nguyen, B.H., Tran, L.D., Do, Q.P., Nguyen, H.L., Tran, N.H., Nguyen, P.X., 2013. Label-free detection of aflatoxin M1 with electrochemical Fe_3O_4 /polyaniline-based aptasensor. *Materials Science and Engineering: C* 33(4), 2229-2234.
169. Noyhouzer, T., Kohen, R., Mandler, D., 2009. A new approach for measuring the redox state and redox capacity in milk. *Analytical Methods* 1(2), 93-99.

170. Nutiu, R., Li, Y., 2003. Structure-switching signalling aptamers. *Journal of the American Chemical Society* 125(16), 4771-4778.
171. Nutiu, R., Li, Y., 2004. Structure-Switching Signalling Aptamers: Transducing Molecular Recognition into Fluorescence Signalling. *Chemistry-A European Journal* 10(8), 1868-1876.
172. O'Sullivan, C.K., Guilbault, G.G., 1999. Commercial quartz crystal microbalances – theory and applications. *Biosensors and Bioelectronics* 14(8–9), 663-670.
173. Ocaña, C., del Valle, M., 2014. A comparison of four protocols for the immobilization of an aptamer on graphite composite electrodes. *Microchimica Acta* 181(3), 355-363.
174. Paniel, N., Radoi, A., Marty, J.-L., 2010. Development of an Electrochemical Biosensor for the Detection of Aflatoxin M1 in Milk. *Sensors* 10(10), 9439-9448.
175. Park, J.-H., Byun, J.-Y., Mun, H., Shim, W.-B., Shin, Y.-B., Li, T., Kim, M.-G., 2014. A regeneratable, label-free, localized surface plasmon resonance (LSPR) aptasensor for the detection of ochratoxin A. *Biosensors and Bioelectronics* 59, 321-327.
176. Pavia, D.L., Lampman, G.M., Kriz, G.S. Introduction to spectroscopy, fifth ed., New York, 2005. *Infrared Spectroscopy* (Chapter 2).
177. Pchelintsev, N.A., Millner, P.A., 2007. Development of Surface Activated Screen-Printed Carbon Transducers for Biosensors Application. *Analytical Letters* 40(7), 1317-1332.
178. Pérez-López, B., Merkoçi, A., 2011. Nanomaterials based biosensors for food analysis applications. *Trends in Food Science & Technology* 22(11), 625-639.
179. Piacentini, K.C., Savi, G.D., Olivo, G., Scussel, V.M., 2015. Quality and occurrence of deoxynivalenol and fumonisins in craft beer. *Food Control* 50, 925-929.
180. Pinacho, D., Sánchez-Baeza, F., Pividori, M.-I., Marco, M.-P., 2014. Electrochemical Detection of Fluoroquinolone Antibiotics in Milk Using a Magneto Immunosensor. *Sensors* 14(9), 15965.
181. Ponikova, S., Antalík, M., Hianik, T., 2008. A circular dichroism study of the stability of guanine quadruplexes of thrombin DNA aptamers at presence of K^+ and Na^+ ions. *General Physiology and Biophysics* 27(4), 271-277.
182. Porchetta, A., Idili, A., Vallée-Bélisle, A., Ricci, F., 2015. General Strategy to introduce pH-Induced Allostery in DNA-Based Receptors to Achieve Controlled Release of Ligands. *Nano Letters* 15(7), 4467-4471.
183. Porter, M.D., Bright, T.B., Allara, D.L., Chidsey, C.E.D., 1987. Spontaneously organized molecular assemblies. 4. Structural characterization of n-alkyl thiol monolayers on gold

- by optical ellipsometry, infrared spectroscopy, and electrochemistry. *Journal of the American Chemical Society* 109(12), 3559-3568.
184. Prelle, A., Spadaro, D., Denca, A., Garibaldi, A., Gullino, M.L., 2013. Comparison of clean-up methods for ochratoxin A on wine, beer, roasted coffee and chili commercialized in Italy. *Toxins* 5(10), 1827-1844.
185. Qin, X., Guo, W., Yu, H., Zhao, J., Pei, M., 2015. A novel electrochemical aptasensor based on MWCNTs-BMIMPF₆ and amino functionalized graphene nanocomposite films for determination of kanamycin. *Analytical Methods* 7(13), 5419-5427.
186. Rasooly, A., Herold, K.E., 2006. Biosensors for the analysis of food- and waterborne pathogens and their toxins. *Journal of AOAC International* 89(3), 873-883.
187. Rastogi, S., Dwivedi, P.D., Khanna, S.K., Das, M., 2004. Detection of Aflatoxin M1 contamination in milk and infant milk products from Indian markets by ELISA. *Food Control* 15(4), 287-290.
188. Reddy, K.K., Gobi, K.V., 2013. Artificial molecular recognition material based biosensor for creatinine by electrochemical impedance analysis. *Sensors and Actuators B: Chemical* 183, 356-363.
189. (a) Rhouati, A., Hayat, A., Hernandez, D.B., Meraihi, Z., Munoz, R., Marty, J.-L., 2013. Development of an automated flow-based electrochemical aptasensor for on-line detection of Ochratoxin A. *Sensors and Actuators B: Chemical* 176, 1160-1166. (b) Rhouati, A., Yang, C., Hayat, A., Marty, J.-L., 2013. Aptamers: A Promising Tool for Ochratoxin A Detection in Food Analysis. *Toxins* 5(11), 1988-2008.
190. Ricci, F., Volpe, G., Micheli, L., Palleschi, G., 2007. A review on novel developments and applications of immunosensors in food analysis. *Analytica Chimica Acta* 605(2), 111-129.
191. Robati, R.Y., Arab, A., Ramezani, M., Langroodi, F.A., Abnous, K., Taghdisi, S.M., 2016. Aptasensors for quantitative detection of kanamycin. *Biosensors and Bioelectronics* 82, 162-172.
192. Rodriguez Velasco, M.L., Calonge Delso, M.M., Ordonez Escudero, D., 2003. ELISA and HPLC determination of the occurrence of aflatoxin M(1) in raw cow's milk. *Food Additives and Contaminants* 20(3), 276-280.
193. Rojas, E., Gallego, M., Reviakine, I., 2008. Effect of sample heterogeneity on the interpretation of quartz crystal microbalance data: impurity effects. *Analytical Chemistry* 80(23), 8982-8990.

194. Rowe, A.A., Miller, E.A., Plaxco, K.W., 2010. Reagentless Measurement of Aminoglycoside Antibiotics in Blood Serum via an Electrochemical, Ribonucleic Acid Aptamer-Based Biosensor. *Analytical Chemistry* 82(17), 7090-7095.
195. Sabet, F.S., Hosseini, M., Khabbaz, H., Dadmehr, M., Ganjali, M.R., 2017. FRET-based aptamer biosensor for selective and sensitive detection of aflatoxin B1 in peanut and rice. *Food Chemistry* 220, 527-532.
196. Sarmah, A.K., Meyer, M.T., Boxall, A.B., 2006. A global perspective on the use, sales, exposure pathways, occurrence, fate and effects of veterinary antibiotics (VAs) in the environment. *Chemosphere* 65(5), 725-759.
197. Sauerbrey, G. (1959) Verwendung von Schwingquarzen zur Wägung dünner Schichten und zur Mikrowägung, *Z. Physik* 155, 206-222.
198. Schwarz, S., Kehrenberg, C., Walsh, T.R., 2001. Use of antimicrobial agents in veterinary medicine and food animal production. *International Journal of Antimicrobial Agents* 17(6), 431-437.
199. Seok, Y., Byun, J.Y., Shim, W.B., Kim, M.G., 2015. A structure-switchable aptasensor for aflatoxin B1 detection based on assembly of an aptamer/split DNAzyme. *Analytica Chimica Acta* 886, 182-187.
200. Sharma, R., Ragavan, K.V., Thakur, M.S., Raghavarao, K.S.M.S., 2015. Recent advances in nanoparticle based aptasensors for food contaminants. *Biosensors and Bioelectronics* 74, 612-627.
201. Sharma, T.K., Ramanathan, R., Weerathunge, P., Mohammadtaheri, M., Daima, H.K., Shukla, R., Bansal, V., 2014. Aptamer-mediated 'turn-off/turn-on' nanozyme activity of gold nanoparticles for kanamycin detection. *Chemical Communications* 50(100), 15856-15859.
202. Sheng, L., Ren, J., Miao, Y., Wang, J., Wang, E., 2011. PVP-coated graphene oxide for selective determination of ochratoxin A via quenching fluorescence of free aptamer. *Biosensors and Bioelectronics* 26(8), 3494-3499.
203. Shephard, G.S., 2008. Determination of mycotoxins in human foods. *Chemical Society Reviews* 37(11), 2468-2477.
204. Shi, J., Tian, F., Lyu, J., Yang, M., 2015. Nanoparticle based fluorescence resonance energy transfer (FRET) for biosensing applications. *Journal of Materials Chemistry B* 3(35), 6989-7005.

205. Shim, W.-B., Mun, H., Joung, H.-A., Ofori, J.A., Chung, D.-H., Kim, M.-G., 2014. Chemiluminescence competitive aptamer assay for the detection of aflatoxin B1 in corn samples. *Food Control* 36(1), 30-35.
206. Sieber, M., Wagner, S., Rached, E., Amberg, A., Mally, A., Dekant, W., 2009. Metabonomic Study of Ochratoxin A Toxicity in Rats after Repeated Administration: Phenotypic Anchoring Enhances the Ability for Biomarker Discovery. *Chemical Research in Toxicology* 22(7), 1221-1231.
207. Singh, N.A., Kumar, N., Raghu, H.V., Sharma, P.K., Singh, V.K., Khan, A., Raghav, N., 2013. Spore inhibition-based enzyme substrate assay for monitoring of aflatoxin M1 in milk. *Toxicological & Environmental Chemistry* 95(5), 765-777.
208. Siontorou, C.G., Nikolelis, D.P., Miernik, A., Krull, U.J., 1998. Rapid methods for detection of Aflatoxin M1 based on electrochemical transduction by self-assembled metal-supported bilayer lipid membranes (s-BLMs) and on interferences with transduction of DNA hybridization. *Electrochimica Acta* 43(23), 3611-3617.
209. Skladal, P., dos Santos Riccardi, C., Yamanaka, H., da Costa, P.I., 2004. Piezoelectric biosensors for real-time monitoring of hybridization and detection of hepatitis C virus. *Journal of Virological Methods* 117(2), 145-151.
210. Song, K.M., Cho, M., Jo, H., Min, K., Jeon, S.H., Kim, T., Han, M.S., Ku, J.K., Ban, C., 2011. Gold nanoparticle-based colorimetric detection of kanamycin using a DNA aptamer. *Analytical Biochemistry* 415(2), 175-181.
211. Song, S., Wang, L., Li, J., Fan, C., Zhao, J., 2008. Aptamer-based biosensors. *TrAC Trends in Analytical Chemistry* 27(2), 108-117.
212. (a) Song, K.-M., Jeong, E., Jeon, W., Cho, M., Ban, C., 2012. Aptasensor for ampicillin using gold nanoparticle based dual fluorescence–colorimetric methods. *Analytical and Bioanalytical Chemistry* 402(6), 2153-2161. (b) Song, K.-M., Jeong, E., Jeon, W., Jo, H., Ban, C., 2012. A coordination polymer nanobelt (CPNB)-based aptasensor for sulfadimethoxine. *Biosensors and Bioelectronics* 33(1), 113-119.
213. Songsermsakul, P., Razzazi-Fazeli, E., 2008. A Review of Recent Trends in Applications of Liquid Chromatography-Mass Spectrometry for Determination of Mycotoxins. *Journal of Liquid Chromatography & Related Technologies* 31(11-12), 1641-1686.
214. Stoltenburg, R., Reinemann, C., Strehlitz, B., 2007. SELEX--a (r) evolutionary method to generate high-affinity nucleic acid ligands. *Biomolecular Engineering* 24(4), 381-403.

215. Su, S., Wu, W., Gao, J., Lu, J., Fan, C., 2012. Nanomaterials-based sensors for applications in environmental monitoring. *Journal of Materials Chemistry* 22(35), 18101-18110.
216. Suarez, G., Jin, Y.H., Auerswald, J., Berchtold, S., Knapp, H.F., Diserens, J.M., Leterrier, Y., Manson, J.A., Voirin, G., 2009. Lab-on-a-chip for multiplexed biosensing of residual antibiotics in milk. *Lab on a chip* 9(11), 1625-1630.
217. Sun, X., Li, F., Shen, G., Huang, J., Wang, X., 2014. Aptasensor based on the synergistic contributions of chitosan-gold nanoparticles, graphene-gold nanoparticles and multi-walled carbon nanotubes-cobalt phthalocyanine nanocomposites for kanamycin detection. *Analyst* 139(1), 299-308.
218. Swensen, J.S., Xiao, Y., Ferguson, B.S., Lubin, A.A., Lai, R.Y., Heeger, A.J., Plaxco, K.W., Soh, H.T., 2009. Continuous, Real-Time Monitoring of Cocaine in Undiluted Blood Serum via a Microfluidic, Electrochemical Aptamer-Based Sensor. *Journal of the American Chemical Society* 131(12), 4262-4266.
219. Taghdisi, S.M., Danesh, N.M., Ramezani, M., Abnous, K., 2016. A novel M-shape electrochemical aptasensor for ultrasensitive detection of tetracyclines. *Biosensors and Bioelectronics* 85, 509-514.
220. Tan, H., Ma, C., Song, Y., Xu, F., Chen, S., Wang, L., 2013. Determination of tetracycline in milk by using nucleotide/lanthanide coordination polymer-based ternary complex. *Biosensors and Bioelectronics* 50, 447-452.
221. Thakur, M.S., Ragavan, K.V., 2013. Biosensors in food processing. *Journal of Food Science and Technology* 50(4), 625-641.
222. Thevenot, D.R., Toth, K., Durst, R.A., Wilson, G.S., 2001. Electrochemical biosensors: recommended definitions and classification. *Biosensors and Bioelectronics* 16(1-2), 121-131.
223. Thi Hanh, L., Van Phuc, P., Thi Huyen, L., Thi Binh, P., Quang Huan, L., 2016. Electrochemical aptasensor for detecting tetracycline in milk. *Advances in Natural Sciences: Nanoscience and Nanotechnology* 7(1), 015008.
224. Thompson, V.S., Maragos, C.M., 1996. Fiber-Optic Immunosensor for the Detection of Fumonisin B1. *Journal of Agricultural and Food Chemistry* 44(4), 1041-1046.
225. Toh, S.Y., Citartan, M., Gopinath, S.C.B., Tang, T.-H., 2015. Aptamers as a replacement for antibodies in enzyme-linked immunosorbent assay. *Biosensors and Bioelectronics* 64, 392-403.

226. Tombelli, S., Minunni, M., Mascini, M., 2005. Piezoelectric biosensors: strategies for coupling nucleic acids to piezoelectric devices. *Methods* (San Diego, Calif.) 37(1), 48-56.
227. Tothill, I., 2011. Biosensors and nanomaterials and their application for mycotoxin determination. *World Mycotoxin Journal* 4(4), 361-374.
228. Tudorache, M., Bala, C., 2007. Biosensors based on screen-printing technology, and their applications in environmental and food analysis. *Analytical and Bioanalytical Chemistry* 388(3), 565-578.
229. Turner, A.P., 2013. Biosensors: sense and sensibility. *Chemical Society Reviews* 42(8), 3184-3196.
230. U.S. Food & Drug Administration (Guidance for Industry: Action Levels for Poisonous or Deleterious Substances in Human Food and Animal Feed), 2000.
231. Vallee-Belisle, A., Plaxco, K.W., 2010. Structure-switching biosensors: inspired by Nature. *Current Opinion in Structural Biology* 20(4), 518-526.
232. Van Dorst, B., Mehta, J., Bekaert, K., Rouah-Martin, E., De Coen, W., Dubruel, P., Blust, R., Robbens, J., 2010. Recent advances in recognition elements of food and environmental biosensors: A review. *Biosensors and Bioelectronics* 26(4), 1178-1194.
233. Vasapollo, G., Sole, R.D., Mergola, L., Lazzoi, M.R., Scardino, A., Scorrano, S., Mele, G., 2011. Molecularly Imprinted Polymers: Present and Future Prospective. *International Journal of Molecular Sciences* 12(9), 5908-5945.
234. Vdovenko, M.M., Lu, C.C., Yu, F.Y., Sakharov, I.Y., 2014. Development of ultrasensitive direct chemiluminescent enzyme immunoassay for determination of aflatoxin M1 in milk. *Food Chemistry* 158, 310-314.
235. Vinayaka, A.C., Thakur, M.S., 2011. Photoabsorption and Resonance Energy Transfer Phenomenon in CdTe-Protein Bioconjugates: An Insight into QD-Biomolecular Interactions. *Bioconjugate Chemistry* 22(5), 968-975.
236. Virolainen, N., Karp, M., 2014. Biosensors, antibiotics and food. *Advances in biochemical engineering/biotechnology* 145, 153-185.
237. Visconti, A., Pascale, M., Centonze, G., 2000. Determination of ochratoxin A in domestic and imported beers in Italy by immunoaffinity clean-up and liquid chromatography. *Journal of Chromatography A* 888(1-2), 321-326.
238. Wackerlig, J., Schirhagl, R., 2016. Applications of Molecularly Imprinted Polymer Nanoparticles and Their Advances toward Industrial Use: A Review. *Analytical Chemistry* 88(1), 250-261.

239. Wang, C., Dong, X., Liu, Q., Wang, K., 2015. Label-free colorimetric aptasensor for sensitive detection of ochratoxin A utilizing hybridization chain reaction. *Analytica Chimica Acta* 860, 83-88.
240. Wang, C., Liu, C., Wang, Y., Shen, T., 1998. Spectral Characteristics and Photosensitization Effect on TiO₂ of Fluorescein in AOT Reversed Micelles. *Journal of Colloid and Interface Science* 197(1), 126-132.
241. Wang, J., Carmon, K.S., Luck, L.A., Suni, I.I., 2005. Electrochemical impedance biosensor for glucose detection utilizing a periplasmic E. coli receptor protein. *Electrochemical and Solid-State Letters* 8(8), H61-H64.
242. Wang, J., Wu, F., Watkinson, M., Zhu, J., Krause, S., 2015. "Click" Patterning of Self-Assembled Monolayers on Hydrogen-Terminated Silicon Surfaces and Their Characterization Using Light-Addressable Potentiometric Sensors. *Langmuir : the ACS journal of surfaces and colloids* 31(35), 9646-9654.
243. Wang, L., Chen, W., Ma, W., Liu, L., Ma, W., Zhao, Y., Zhu, Y., Xu, L., Kuang, H., Xu, C., 2011. Fluorescent strip sensor for rapid determination of toxins. *Chemical Communications (Cambridge, England)* 47(5), 1574-1576.
244. Wang, R., Xiang, Y., Zhou, X., Liu, L.-h., Shi, H., 2015. A reusable aptamer-based evanescent wave all-fiber biosensor for highly sensitive detection of Ochratoxin A. *Biosensors and Bioelectronics* 66, 11-18.
245. Wang, R.E., Zhang, Y., Cai, J., Cai, W., Gao, T., 2011. Aptamer-Based Fluorescent Biosensors. *Current Medicinal Chemistry* 18(27), 4175-41.
246. Wang, Y., Bao, L., Liu, Z., Pang, D.W., 2011. Aptamer biosensor based on fluorescence resonance energy transfer from upconverting phosphors to carbon nanoparticles for thrombin detection in human plasma. *Analytical Chemistry* 83(21), 8130-8137.
247. Wang, Y., Zou, M., Han, Y., Zhang, F., Li, J., Zhu, X., 2013. Analysis of the Kanamycin in Raw Milk Using the Suspension Array. *Journal of Chemistry* 2013, 4-7.
248. Wei, Y., Zhang, J., Wang, X., Duan, Y., 2015. Amplified fluorescent aptasensor through catalytic recycling for highly sensitive detection of ochratoxin A. *Biosensors and Bioelectronics* 65, 16-22.
249. White, R.J., Phares, N., Lubin, A.A., Xiao, Y., Plaxco, K.W., 2008. Optimization of Electrochemical Aptamer-Based Sensors via Optimization of Probe Packing Density and Surface Chemistry. *Langmuir : the ACS journal of surfaces and colloids* 24(18), 10513-10518.

250. Wu, C., Liu, D., Peng, T., Shan, S., Zhang, G., Xiong, Y., Lai, W., 2016. Development of a one-step immunochromatographic assay with two cutoff values of aflatoxin M1. *Food Control* 63, 11-14.
251. Wu, H.P., Cheng, T.L., Tseng, W.L., 2007. Phosphate-modified TiO₂ nanoparticles for selective detection of dopamine, levodopa, adrenaline, and catechol based on fluorescence quenching. *Langmuir : the ACS journal of surfaces and colloids* 23(14), 7880-7885.
252. Wu, J., Chu, H., Mei, Z., Deng, Y., Xue, F., Zheng, L., Chen, W., 2012. Ultrasensitive one-step rapid detection of ochratoxin A by the folding-based electrochemical aptasensor. *Analytica Chimica Acta* 753, 27-31.
253. Wu, S., Duan, N., Ma, X., Xia, Y., Wang, H., Wang, Z., Zhang, Q., 2012. Multiplexed Fluorescence Resonance Energy Transfer Aptasensor between Upconversion Nanoparticles and Graphene Oxide for the Simultaneous Determination of Mycotoxins. *Analytical Chemistry* 84(14), 6263-6270.
254. Wu, S., Duan, N., Wang, Z., Wang, H., 2011. Aptamer-functionalized magnetic nanoparticle-based bioassay for the detection of ochratoxin a using upconversion nanoparticles as labels. *Analyst* 136(11), 2306-2314.
255. Xu, W., Wang, Y., Liu, S., Yu, J., Wang, H., Huang, J., 2014. A novel sandwich-type electrochemical aptasensor for sensitive detection of kanamycin based on GR-PANI and PAMAM-Au nanocomposites. *New Journal of Chemistry* 38(10), 4931-4937.
256. Yamamoto, R., Baba, T., Kumar, P.K., 2000. Molecular beacon aptamer fluoresces in the presence of Tat protein of HIV-1. *Genes to cells: devoted to molecular & cellular mechanisms* 5(5), 389-396.
257. Yan, Z., Gan, N., Li, T., Cao, Y., Chen, Y., 2016. A sensitive electrochemical aptasensor for multiplex antibiotics detection based on high-capacity magnetic hollow porous nanotracers coupling exonuclease-assisted cascade target recycling. *Biosensors and Bioelectronics* 78, 51-57.
258. Yang, C., Wang, Y., Marty, J.-L., Yang, X., 2011. Aptamer-based colorimetric biosensing of Ochratoxin A using unmodified gold nanoparticles indicator. *Biosensors and Bioelectronics* 26(5), 2724-2727.
259. Yang, G., Jin, W., Wu, L., Wang, Q., Shao, H., Qin, A., Yu, B., Li, D., Cai, B., 2011. Development of an impedimetric immunosensor for the determination of 3-amino-2-oxazolidone residue in food samples. *Analytical Chimica Acta* 706(1), 120-127.

260. Yang, L., Ruan, C., Li, Y., 2003. Detection of viable *Salmonella typhimurium* by impedance measurement of electrode capacitance and medium resistance. *Biosensors and Bioelectronics* 19(5), 495-502.
261. Yu, C.-Z., He, Y.-Z., Fu, G.-N., Xie, H.-Y., Gan, W.-E., 2009. Determination of kanamycin A, amikacin and tobramycin residues in milk by capillary zone electrophoresis with post-column derivatization and laser-induced fluorescence detection. *Journal of Chromatography B* 877(3), 333-338.
262. Yu, F.Y., Chi, T.F., Liu, B.H., Su, C.C., 2005. Development of a Sensitive Enzyme-Linked Immunosorbent Assay for the Determination of Ochratoxin A. *Journal of Agricultural and Food Chemistry* 53(17), 6947-6953.
263. Yu, S., Wei, Q., Du, B., Wu, D., Li, H., Yan, L., Ma, H., Zhang, Y., 2013. Label-free immunosensor for the detection of kanamycin using Ag@Fe₃O₄ nanoparticles and thionine mixed graphene sheet. *Biosensors and Bioelectronics* 48, 224-229.
264. Zhang, J., Zhang, B., Wu, Y., Jia, S., Fan, T., Zhang, Z., Zhang, C., 2010. Fast determination of the tetracyclines in milk samples by the aptamer biosensor. *Analyst* 135(10), 2706-2710.
265. Zhang, J., Zhang, X., Yang, G., Chen, J., Wang, S., 2013. A signal-on fluorescent aptasensor based on Tb³⁺ and structure-switching aptamer for label-free detection of Ochratoxin A in wheat. *Biosensors and Bioelectronics* 41, 704-709.
266. Zhang, X., Wang, F., Liu, B., Kelly, E.Y., Servos, M.R., Liu, J., 2014. Adsorption of DNA Oligonucleotides by Titanium Dioxide Nanoparticles. *Langmuir* 30(3), 839-845.
267. Zhang, X., Wen, K., Wang, Z., Jiang, H., Beier, R.C., Shen, J., 2016. An ultra-sensitive monoclonal antibody-based fluorescent microsphere immunochromatographic test strip assay for detecting aflatoxin M₁ in milk. *Food Control* 60, 588-595.
268. Zhang, Y., Muench, S.B., Schulze, H., Perz, R., Yang, B., Schmid, R.D., Bachmann, T.T., 2005. Disposable Biosensor Test for Organophosphate and Carbamate Insecticides in Milk. *Journal of Agricultural and Food Chemistry* 53(13), 5110-5115.
269. Zheng, M., Jagota, A., Semke, E.D., Diner, B.A., McLean, R.S., Lustig, S.R., Richardson, R.E., Tassi, N.G., 2003. DNA-assisted dispersion and separation of carbon nanotubes. *Nature Material* 2(5), 338-342.
270. Zheng, W., Teng, J., Cheng, L., Ye, Y., Pan, D., Wu, J., Xue, F., Liu, G., Chen, W., 2016. Hetero-enzyme-based two-round signal amplification strategy for trace detection of aflatoxin B₁ using an electrochemical aptasensor. *Biosensors and Bioelectronics* 80, 574-581.

271. Zhou, L., Li, D.-J., Gai, L., Wang, J.-P., Li, Y.-B., 2012. Electrochemical aptasensor for the detection of tetracycline with multi-walled carbon nanotubes amplification. *Sensors and Actuators B: Chemical* 162(1), 201-208.
272. Zhou, N., Zhang, J., Tian, Y., 2014. Aptamer-based spectrophotometric detection of kanamycin in milk. *Analytical Methods* 6(5), 1569-1574.
273. Zhu, Y., Chandra, P., Song, K.-M., Ban, C., Shim, Y.-B., 2012. Label-free detection of kanamycin based on the aptamer-functionalized conducting polymer/gold nanocomposite. *Biosensors and Bioelectronics* 36(1), 29-34.
274. Zimmerli, B., Dick, R., 1995. Determination of ochratoxin A at the ppt level in human blood, serum, milk and some foodstuffs by high-performance liquid chromatography with enhanced fluorescence detection and immunoaffinity column cleanup: methodology and Swiss data. *Journal of Chromatography B: Biomedical Sciences and Applications* 666(1), 85-99.

List of Publications

List of publication counted in the thesis

1. **Atul Sharma** and Sunil Bhand, “Aptamer Integrated Microfluidic Quartz Crystal Biosensing Platform: Application to on-line Determination of Tetracycline in Milk”. Submitted to Analytical Chemistry: Manuscript ID: ac-2017-02618p (Output from chapter 5) (Scopus listed).
2. **Atul Sharma**, Reem Khan, Gaelle Catanante, Tauqir A. Sherazi, Sunil Bhand, Akhtar Hayat, Jean Louis Marty, “Designed strategies for fluorescence based biosensors for the detection of mycotoxins”, *Toxins (Special Issue- Advances sensors for Toxins)*, 2018, 10(4), 197 (Output from chapter 1) (Scopus listed, IF-3.03)
3. **Atul Sharma**, Georges Istamboulie, Akhtar Hayat, Gaëlle Catanante, Sunil Bhand*, Jean Louis Marty, “Disposable and portable aptamer functionalized impedimetric sensor for detection of kanamycin in milk sample”, *Sensors and Actuators B: Chemical*, 2017, 245, 507-515 (Citation-13) (Output from chapter 4) (Scopus listed, IF- 5.401).
4. **Atul Sharma**, Gaëlle Catanante, Akhtar Hayat, Georges Istamboulie, Ben Rejeb Ines, Sunil Bhand, Jean Louis Marty, “Development of structure signalling aptamer assay for detection of aflatoxin M1 in milk sample”, *Talanta*, 2016, 158, 35-41 (Citation-20) (Output from chapter 3) (Scopus listed, IF- 4.162).
5. **Atul Sharma**, Akhtar Hayat, Rupesh K. Mishra, Gaëlle Catanante, Sunil Bhand and Jean Louis Marty, “Design of fluorescence aptaswitch based on the aptamer modulated nano-surface impact on the fluorescence particles”, *RSC Advances*, 2016, 6, 65579-65587. (Citation-4) (Output from chapter 2) (Scopus listed, IF- 3.108).
6. **Atul Sharma**, Akhtar Hayat, Rupesh K. Mishra, Gaëlle Catanante, Sunil Bhand and Jean Louis Marty, “Titanium Dioxide Nanoparticles (TiO₂) Quenching Based Aptasensing Platform: Application to Ochratoxin A Detection”, *Toxins* 2015, 7, 3771- 3784. (Citation-10) (Output from chapter 2) (Scopus listed, IF- 3.03).

7. **Atul Sharma**, Kotagiri Yugender Goud, Akhtar Hayat, Sunil Bhand, Jean Louis Marty, “Recent Advances in Electrochemical Based Sensing Platforms for Aflatoxins Detection”, *Chemosensors*, 2017, 7, 1-14. (Citation-6) (Output from chapter 1) (Scopus listed).
8. **Atul Sharma**, Aruna Chandra Singh, Gautam Bacher, Sunil Bhand, “Recent Advances in Aptamer - Based Biosensors for Detection of Antibiotic Residues”, *Aptamers and Synthetic Antibodies*, 2016, 2(2), 43-54. (Citation-1) (Output from chapter 1).

Other publications not counted in the thesis

9. Diana Bueno, **Atul Sharma**, Sunil Bhand, Jean Louis Marty, Roberto Muñoz, “Effect of pH, solvent and salt composition on the fluorescence emission behaviour of Ochratoxin A”, *Food Analytical Methods* (Manuscript Submitted, 2018) (Scopus listed, IF-2.04).
10. K. Yugender Goud, **Atul Sharma**, Akhtar Hayat, Gaëlle Catanante, K. Vengatajalabathy Gobi, Ana Maria Gurban and Jean Louis Marty, “TAMRA Quenching Based Aptasensing Platform for Aflatoxin B1: Analytical performance comparison of two aptamers”, *Analytical Biochemistry*, 2016, 508, 19-24 (Citation-10) (Scopus listed, IF- 2.334).
11. Geetesh K. Mishra*, **Atul Sharma***, Sunil Bhand “Ultrasensitive detection of Streptomycin using Flow Injection Analysis Electrochemical quartz crystal Nanobalance (FIA-EQCN) biosensor”, *Biosensors and Bioelectronics*, 2015, 67, 532-539 (*Author with Equal Contribution) (Citation-20) (Scopus listed, IF- 7.78).
12. Geetesh K. Mishra, **Atul Sharma**, Kanchanmala Deshpande, Sunil Bhand* “Flow Injection Analysis biosensor for urea analysis in urine using Enzyme Thermistor”, *Applied Biochemistry and Biotechnology*, 2014, 174 (3), 998-1009 (Citation-9) (Scopus listed, IF- 1.751).

Conference and workshop attended

1. Aptamer integrated microfluidic quartz crystal biosensing platform: Application for determination of tetracycline in milk”, **Atul Sharma** and Sunil Bhand (**Poster No., P3.016**). Abstract accepted for Poster Presentation in World Biosensor Congress 2018, 12-15 June, 2018.
2. **Atul Sharma** and Sunil Bhand, “Molecularly Imprinted Polymeric Nanoparticles for Selective Determination of Antibiotic Residue in Milk Sample”, Poster presentation in ICONN 2017 (4th INTERNATIONAL CONFERENCE ON NANOSCIENCE AND NANOTECHNOLOGY, 9-11th August, 2017, SRM University, Chennai, INDIA) (**Poster**

No. 749)

3. **Oral presentation** at 2nd National Conference on NEW FRONTIERS IN CHEMISTRY – FROM FUNDAMENTALS TO APPLICATIONS-II, 28-29 January, 2017 at Department of Chemistry, BITS Pilani, K K Birla Goa Campus entitled “Novel biosensing platform for detection of antibiotics in food sample”, Sunil Bhand, **Atul Sharma**, Geetesh K. Mishra.
4. **Oral presentation and presented a poster** at Symposium on Recent Advancements in Chemical Sciences and RSC Research Scholar Meet 2016, Goa, India organized by BITS Pilani- K K Birla Goa Campus, INDIA, 13th November, 2016 entitled “Design of a nanomaterial based fluorescence aptaswitch using aptamer modulated nano-surface impact on the fluorescence particles”, Atul Sharma, Akhtar Hayat, Rupesh K. Mishra, Gaëlle Catanante, Sunil Bhand and Jean Louis Marty. (Oral presentation 2 and Poster No. 08).
5. **Presented poster** at AMAN-2016 organized by BITS- Pilani K. K. Birla Goa Campus jointly with University of Leeds, UK from 11-12th January 2016 entitled “Structure signaling aptasensing platform for detection of aflatoxin M1 in milk”, Atul Sharma, Gaëlle Catanante, Akhtar Hayat, George Istamboulie, Sunil Bhand and Jean Louis Marty (Poster No. 14).
6. **Presented poster** at TMSB 2015 organized by UPVD Perpignan, France from 1-2 October, 2015 entitled “Quenching based aptamer assay: A sensing platform for detection of target analyte”, Atul Sharma, Akhtar Hayat, Rupesh K. Mishra, Gaëlle Catanante, Sunil Bhand and Jean Louis Marty (Poster no 4).
7. **Oral presentation and presented a poster** at 11th Workshop on Biosensors and Bioanalytical Microtechniques in Environmental, Food and Clinical Analysis (BBMEC-11th) organized by University of Regensburg, Germany from 26-30 September, 2015 entitled “Aptamer assay: A nanomaterial based sensing platform for detection of target molecule”, Atul Sharma, Akhtar Hayat, Rupesh K. Mishra, Gaëlle Catanante, Sunil Bhand and Jean Louis Marty presented in (Oral presentation no. 9 and Poster no P 53).
8. Attended and participated in the Fourth International Conference on Advanced Oxidation Processes (AOP-2016) organized by BITS, Pilani- K.K. Birla Goa Camps in association with Society of Environmental Chemistry and Allied Sciences (SECAS), INDIA, from 17-20th December, 2016.
9. Attended as co-instructor in BRNS-AEACI Twelfth School on Analytical Chemistry-2016 (SAC-12) organized by BRNS and BITS Pilani-K K Birla Goa Campus, 15-22 November, 2016.
10. Attended 1st National Conference on NEW FRONTIERS IN CHEMISTRY – FROM

FUNDAMENTALS TO APPLICATIONS-II, 28-29 January, 2015 at Department of Chemistry, BITS Pilani, K K Birla Goa Campus entitled.

11. Actively Participated in International Conference on Emerging Technologies: Micro to Nano 2013 (ETMN 2013), organized by BITS Pilani- K K Birla Goa Campus, INDIA, 23-24th February, 2013.
12. Actively Participated in workshop on Intellectual Property and Innovation Management in Knowledge Economy, organized by national Research Development Corporation, New Delhi and Goa University, December, 2013 INDIA.

Abstract accepted in the conferences

1. **Oral presentation** at International Conference on Electrochemical Sensors (Matrafured 2017) 11-16 June, 2017, Visegrád, Budapest entitled “Disposable and portable aptamer functionalized impedimetric sensor for detection of kanamycin residue in milk sample”, Atul Sharma, Sunil Bhand, Jean Louis Marty.
2. Abstract accepted for poster presentation at International Symposium in Electroanalytical Chemistry (ISEAC), Changchun, China, 13-16 August, 2015 entitled “OTA bio-sensing in real matrix using folding based electrochemical aptasensor”, Rupesh K. Mishra, Atul Sharma, Akhtar Hayat, Sunil Bhand, Jean-Louis Marty (Poster no-106).
3. Abstract accepted for poster presentation at 24th Anniversary World Congress on Biosensors, 27-30 May, 2014, Australia entitled “Ultrasensitive detection of streptomycin using Flow injection analysis-Electrochemical quartz crystal nanobalance (FIA-EQCN), Geetesh K. Mishra, Atul Sharma, Sunil Bhand (BIOS2014_0153).
4. Poster presentation at India-Japan Workshop on “Biomolecular Electronics and Organic Nanotechnology for Environment Preservation” IJWBME 2013, 13-15 December 2013, DTU, Delhi, India entitled “Flow Injection Analysis biosensor for urea analysis in urine using Enzyme Thermistor”, Geetesh K. Mishra, Atul Sharma, Sunil Bhand, (Poster No. PP. 70).

Brief Biography of the candidate

Name: Atul Sharma
Date of Birth: 27th April, 1987
Education: M. Pharmacy (Pharmaceutical Chemistry), 2011 from U.P. Technical University, Lucknow (U.P.), India
B. Pharmacy (Pharmacy), 2009 from U.P. Technical University, Lucknow (U.P.), India
D. Pharmacy (Pharmacy), 2006 from Delhi Institute of Pharmaceutical Sciences and Research (DIPSAR), Delhi, India
Email: a2Lpharm@gmail.com; p20120407@goa.bits-pilani.ac.in

Research Experience (4 years 6 Month)

1. Presently working as Institute Research Scholar in the Department of Chemistry, BITS, Pilani-K.K. Birla Goa Campus, Goa. Supervisor: Prof. Sunil Bhand (November 2015 onwards).
2. Worked as Erasmus Mundus Fellow (Doctoral Research Fellowship awarded by EUPHRATES Program, 2014-15) at University of Perpignan Via Domitia (UPVD), Perpignan, CEDEX, France, Thesis Co-Supervisor: Prof. Jean Louis MARTY.
3. Worked as Senior Research Fellow (NFBSFARA Project, a consortium based project sponsored by ICAR, Delhi) at BITS Pilani-K. K. Birla Goa Campus, Goa. CPI: Prof. Sunil Bhand (Jan 2014 to 6th November, 2014).
4. Worked as Senior Research Fellow (National Agricultural Innovation Project, a consortium based project sponsored by ICAR, India and the World Bank at BITS, Pilani-K. K. Birla Goa Campus, Goa. CPI: Prof. Sunil Bhand (June 2013 to December 2013).
5. Worked as Institute Research Scholar in the Department of Chemistry, BITS, Pilani-K.K. Birla Goa Campus, Goa. Notional Supervisor: Prof. Sunil Bhand (Jan 2013 to May 2013).

Research publications

09 (research and review) publications in international journals

Work Experience

1. Worked as Assistant Professor in Department of Pharmaceutical Chemistry, Siddhartha Institute of Pharmacy, Dehradun (Uttarakhand), India (September 2012- January 2013).
2. Worked as Assistant Professor in Department of Pharmaceutical Chemistry, Shree Ram College of Pharmacy, Rambha, Karnal (Haryana), India (January 2012- August 2012).

Award and Honours

1. **First Prize** in Poster Competition in INDO-UK International Workshop on Advanced Materials and Their Applications in Nanotechnology (AMAN 2016).
2. **Meritorious position (4th Rank)** in the poster presentation in Symposium on Recent Advancements in Chemical Sciences and RSC Research Scholar Meet 2016 organized on 13th November at BITS, Pilani-KK Birla Goa Campus, INDIA
3. **Travel award** to present Oral and poster in 11th Workshop on Biosensors and Bioanalytical Microtechniques in Environmental, Food and Clinical Analysis (BBMEC-11th) at Regensburg, Germany, 2015.
4. Awarded Erasmus Mundus Doctoral Fellowship for One year research work (2014-15).
5. Awarded among top 20 best posters at International Symposium in Electroanalytical Chemistry (ISEAC), Changchun, China, 13-16 August, 2015 (P-106).

Brief Biography of the Supervisor

Name: Prof. Sunil Bhand

Date of Birth: 17.03.1969

Academic Position: Professor, Department of Chemistry, BITS, Pilani-KK Birla
Goa Campus

Administrative Position: Dean (University Wide),
Sponsored Research and Consulting Division (SRCDD)

Address: C-211 BITS, Pilani-KK Birla Goa Campus, NH17B Bypass,
Zuari Nagar Goa 403726 India

Email: sunilbhand@goa.bits-pilani.ac.in; sgbhand@gmail.com

Education: Ph.D., 1996, M.Sc., 1990 (First in University Merit)

Post-Doctoral Experience

1. Department of Pure and Applied Biochemistry, Lund University Sweden 2001-2002,
2. Short term visits 2003, 2004, 2005, 2007, 2008
3. Visiting Scientist Jul-August, 2011 at Acromed Invest AB, Lund, Sweden.
4. Visiting Scientist June 2013 at FBS University of Leeds, UK.
5. Visiting Scientist June 2016 at Acromed Invest AB, Lund, Sweden.

No. of Sponsored Research Projects

(a) Completed projects

1. Joint Indo-Swedish Project on Biosensors for Environmental analysis 2003-2007 funded by Swedish Research Council (Prof. B. Danielsson and Prof. Sunil Bhand as joint PIs), Rs. 27 lakhs.
2. CSIR Project 2006-2010 (3 years) on biosensors for analysis of pesticides in sea water, Rs. 16.5 lakhs.
3. Consortium PI for NAIP, ICAR New Delhi funded project on “Development of biosensors and micro techniques for analysis of pesticide residues, aflatoxin, heavy metals and bacterial contamination in milk, Rs. 450.5 lakhs, in collaboration with IITD, NDRI and PU Patiala.

4. Consortium Co-PI, NAIP project on “Detection and mitigation of dairy pathogens and detection of adulterants using chemical biology”, Rs. 92 lakhs.

5. Multi-institute Consortium Project entitled “Imprinted polymer for sensing and removal of selected antibiotic and pesticide residue” Funding Agency: National Funds for Basic and Strategic Research in Frontier Areas of Agricultural Science, ICAR, New Delhi, Rs. 54 lakhs.

(b) Ongoing Projects:

1. Multi-institute Consortium Project entitled “Development of sensing system for residual pesticide and harmful chemical detection in fruits and vegetables” funded by R.D Tata Trust, Aug. 2016-Jul 2018. Total amount Rs. 212 lakh in collaboration with CDAC Kolkata and Jadavpur University Kolkata for a period of two years.

2. Multi-institute Consortium Project entitled “Nano-based detection of organophosphate pesticides using metal-organic framework conjugates” funded by National Agricultural Science Fund, ICAR Govt. of India. (Jan. 2017-Dec 2019), Total amount Rs. 212 lakh (BITS Goa share Rs. 43.20 lakh) in collaboration with Amity Institute of Nanotechnology and Indian Agricultural Research Institute IARI, New Delhi.

3. Development of field portable device for the analysis of contaminant in water” funded by BRNS, DAE Govt of India. Total amount Rs. 24.138 lakhs for 3 years in collaboration with Dr R. Balasubramaniam, Ashwin Rathod (PED, BARC) and Dr VK Suri (MGM,Mumbai).

4. Centre of Research Excellence in Water, Waste water and Energy Management (CORE WWEM) funded by BITS, Pilani. Subproject title: Development of Field Deployable biosensor for analysis of bacterial contaminant in potable water. Rs. 41 lakh.

5. International: Swedish Research Council project entitled “Functional composite materials and their application in smart sensors” for 3 years. Invited PI: Prof. Sunil Bhand (funding for Exchange visit of PI and researcher), BITS Goa in collaboration with PI: Dr. Cedric Dicko, Pure and Applied Biochemistry, Lund University Sweden.

Honours and awards

- Prof. Sunil Bhand has been presented “Joseph Wang Award 2015”, by Cognizure publishing in recognition of his research excellence in the area of Analytical Chemistry.
- Member, expert committee (international program) Department of Biotechnology N. Delhi India (2014-16).

- Received certificate of appreciation from American Chemical Society ACS USA as a reviewer for ACS Journals 2012.
- Faculty opponent at the Department of Science and Technology, Linköping University Sweden, Dissertation No. 1376 Sept 02, 2011.
- Best Poster award “Biosensors for arsenic analysis” 7th Intl Conference on Biogeochemistry of trace elements 2003 Uppsala Sweden.
- UV Rao memorial awards for young scientists by Indian Chemical Society 1998.

Publications

1. 09 Patents (04 International including 02 PCT and 01 Australian & 1 US Patent and 06 Indian) and more than 60 publications in international journals, 2 Book chapters (RSC and Springer).
2. Membership of societies: Affiliate member IUPAC since 2000 IAEAC Switzerland, AAAS, USA, 2012.

Reviewer for international journals

Biosensors and Bioelectronics, Analytical Letters, International Journal of Environmental and Analytical Chemistry, Applied Biochemistry and Biotechnology, Journal of Agriculture and Food Chemistry, IEEE Sensors.

No of Ph.D. Students

1. Awarded as Supervisor: 06
2. Ongoing as Supervisor: 04
3. Ongoing as Co-supervisor: 02

No of Conferences and workshops organized: 05

Brief Biography of the Co-supervisor

Name: Prof. Jean Louis MARTY

Date of Birth: 30.04.1950

Academic Position: Professor “Classe exceptionnelle” in Biotechnology,
Université de Perpignan Via Domitia, Perpignan, France

Administrative Position: Vice President for International Relations 2012-2016
Responsible ERASMUS Exchanges 2008-2012
Director of IMAGES Laboratory 2003-2008

Address: BAE-LBBM, Université de Perpignan, 52 avenue Paul
Alduy, 66860 Perpignan Cedex France

Email: jlmarty@univ-perp.fr

Education: Doctorat d’Etat, Université de Perpignan Via Domitia, 1987
PhD in Biochemistry, Université de Montpellier, 1980
Engineer in Biochemistry, INSA Lyon 1973

Post-Doctoral Experience

1. R.C.A.S.T., Research Center for Advanced Science and Technology (Pr. Isao Karube), University of Tokyo 1988 (April to December).
2. R.C.A.S.T., Research Center for Advanced Science and Technology (Pr. Isao Karube), University of Tokyo, 1989 (November to December).

No. of Sponsored Research Projects

Ongoing Projects:

1. 2016-2019: INTERREG POCTEFA

Title: Eco-friendly and healthy Food plastic packaging (Foodyplast), Participants: 6 (3 Spanish, 3 Spanish)

2. 2016-2019: INTERREG SUDOE

Title: Alianza tecnológica para completar el ciclo de producción agroindustrial y forestal (Redvalue), Participants: 8 (4 Spanish, 2 Spanish, 3 Portuguese)

3. 2016-2019: PHC Peridot (project France-Pakistan)

Title: Cooperative partnership to design early warning, site portable bioassays for biomedical applications, Participants: 2 (Pakistani, French)

4. 2016-2018: FAPEMA (Brazil)

Title: biossensores para determinação de antioxidantes em frutos da amazônia e pré-amazônia maranhense, Participants: 3 (Brazilian, French, Romanian)

5. 2016-2018: PHC BALATON (France-Hungary)

Title: Innovating biosensors for the detection of zearalenone and other mycotoxines, Participants: 2 (Hungarian, French)

6. 2014-2017: Région Languedoc-Roussillon: Aide à La Recherche en partenariat avec les entreprises (ARPE)

Title: Mise au point d'un capteur pour la détection de l'OTA, Participants: 1

2015-2018: Call NATO

Title: Development of optical biosensors for detection of bio toxins (BIOTOX)

Participants: 5 (English, French, Hungarian, Ukrainian, Israeli)

Honours and awards

1. Doctor Honoris Causa of University of Bucharest, 2000.
2. Honorary Professor of Transylvania University of Brasov, 2005.
3. Invited Professor by JST (Japan Science Technology), 2007.
4. Invited Professor by JST (Japan Science Technology), 2010.

Publications

More than 180 publications including international journals and book chapter.

Reviewer for international journals

Talanta, Chemosensors, Frontiers in Analytical Chemistry, The Open Current Process Chemistry Journal (Bentham Science), The Open Analytical Chemistry Journal (Bentham Science), Romanian Biotechnological Letters (Bulletin of Transylvania University of Brasov, Chemical sensor , Journal of Analytical Methods in Chemistry.

No of Ph.D. Students

Completed 28, Registered 04 (Co-supervisor),

No of Conferences organized: More than 32

Appendix v

Reprint of publications

Review

Recent Advances in Electrochemical-Based Sensing Platforms for Aflatoxins Detection

Atul Sharma ^{1,2}, Kotagiri Yugender Goud ^{2,3}, Akhtar Hayat ^{2,4}, Sunil Bhand ¹ and Jean Louis Marty ^{2,*}

¹ Biosensor Lab, Department of Chemistry, BITS, Pilani K. K. Birla Goa Campus, Zuarinagar, 403726 Goa, India; p2012407@goa.bits-pilani.ac.in (A.S.); sgbhand@gmail.com (S.B.)

² BAE Laboratoire, Université de Perpignan Via Domitia, 52 Avenue Paul Alduy, 66860 Perpignan, France; yugenderkotagiri@gmail.com (K.Y.G.); akhtarloona@gmail.com (A.H.)

³ Department of Chemistry, National Institute of Technology, Warangal, 506004 Telangana, India

⁴ Interdisciplinary Research Centre in Biomedical Materials (IRCBM), COMSATS Institute of Information Technology (CIIT), Lahore 54000, Pakistan

* Correspondence: jlmarty@univ-perp.fr; Tel.: +33-04-6866-2254; Fax: +33-04-6866-2223

Academic Editors: Paolo Ugo and Ligia Moretto

Received: 25 August 2016; Accepted: 20 December 2016; Published: 26 December 2016

Abstract: Mycotoxin are small (MW ~700 Da), toxic secondary metabolites produced by fungal species that readily colonize crops and contaminate them at both pre- and post-harvesting. Among all, aflatoxins (AFs) are mycotoxins of major significance due to their presence in common food commodities and the potential threat to human health worldwide. Based on the severity of illness and increased incidences of AFs poisoning, a broad range of conventional and analytical detection techniques that could be useful and practical have already been reported. However, due to the variety of structural analogous of these toxins, it is impossible to use one common technique for their analysis. Numerous recent research efforts have been directed to explore alternative detection technologies. Recently, immunosensors and aptasensors have gained promising potential in the area of sample preparation and detection systems. These sensors offer the advantages of disposability, portability, miniaturization, and on-site analysis. In a typical design of an aptasensor, an aptamer (ssDNA or RNA) is used as a bio-recognition element either integrated within or in intimate association with the transducer surface. This review paper is focused on the recent advances in electrochemical immuno- and aptasensing platforms for detection of AFs in real samples.

Keywords: aflatoxins; electrochemical techniques; aptasensor; biosensor; food

1. Introduction

With the increasing incidence and stubbornly high mycotoxin mortality around the world, the earlier diagnosis of mycotoxin contamination has drawn significant attention. The presence of mycotoxin in food and feed due to their associated toxic effects on human health and the environment has now become a primary concern [1]. Mycotoxins are the toxic fungal metabolites produced by fungi (micromycetes and macromycetes) under specific conditions of temperature and moisture [2]. The optimal condition of temperature for mycotoxin-producing molds ranging between 24 °C and 35 °C and a relative humidity of $\geq 70\%$. Toxicity of these metabolites in human and warm-blooded animals is commonly known as mycotoxicosis. More than 300 mycotoxins (aflatoxins, ochratoxins, trichothecane) commonly exist, but only some of them are practically important. Among all, the most commonly studied groups of mycotoxins are aflatoxins (AFs). Initially, AFs were isolated and identified after the death of young turkeys on poultry farms in England, which were found to be related due to the consumption of a Brazilian peanut meal. AFs are the difuranocoumarin derivatives mainly produced by *Aspergillus parasiticus*, *Aspergillus flavus*, and rarely by *Aspergillus nomius* [3].

Review Article

Recent Advances in Aptamer- Based Biosensors for Detection of Antibiotic Residues

Atul Sharma¹, Aruna Chandra Singh¹, Gautam Bacher^{1,2}, Sunil Bhand^{1*}

¹Biosensor Lab, Department of Chemistry; ²Department of Electrical and Electronics Engineering, BITS, Pilani-K.K. Birla Goa Campus, Goa 403726, India.

Abstract | Antibiotics are widely used as bacteriostatic or bactericidal agents either to kill or inhibit the growth of microorganisms. Their abuse results in various side effects on the human health, environment and agriculture. The occurrence of bacterial “suprainfection” with tolerance to antibiotics has attracted the significant attention, mainly due to the consequences of multi drug resistance and potential threat to human health and the environment. With the increasing incidences of antimicrobial contamination, especially in food, dairy products, agriculture and environment, their regular monitoring is on prime interest. Aptamers are synthetic short sequences of single stranded (ss) oligonucleotides (ss-RNA or DNA), which are developed by an *in-vitro* selection process known as “Systematic Evolution of Ligands by Exponential Enrichment (SELEX)” technique. Among the receptors available for biosensing, aptamer exhibit the advantages of high specificity, selectivity, stability, facile labelling and modification, which makes them ideal candidates for development of new biosensing applications for detection of specific target molecules. In the present review, we concentrate on the recent advances in the development of aptasensors for antibiotics residue analysis based on electrochemical signal generation. Aptamers possesses the strong potential as receptors for the development of biosensors for antibiotics detection; therefore, a specially designed aptamer specific to an antibiotic may be suitable for this purpose. In this review, the importance of detection of antibiotic residue contamination, reported analytical methods, advancement in biosensing platform especially regarding electrochemical transduction are discussed in detail. Finally, future prospects toward the development of selective and sensitive aptasensors for antibiotic detection are presented.

Editor | Dr. Tarun Kumar Sharma, Centre for Biodesign and Diagnostics, NCR Biotech Science Cluster, 3rd Milestone, Faridabad-Gurgaon Expressway, Faridabad, India.

Received | August 29, 2016; **Accepted** | October 14, 2016; **Published** | November 23, 2016

***Correspondence** | Sunil Bhand, Biosensor Lab, Department of Chemistry, BITS, Pilani- K.K. Birla Goa Campus, Goa 403726, India; **Email:** sunilbhand@goa.bits-pilani.ac.in

Citation | Sharma A, Singh AC, Bacher G, Bhand S. 2016. Recent advances in aptamer- based biosensors for detection of antibiotic residues. *Aptamers and Synthetic Antibodies*, 2(2): 43-54.

Keywords | Antibiotics, Aptamer, SELEX, Electrochemical detection, Biosensor, Milk

Due to the increasing prevalence and incidence of antibiotic residue contamination and drug resistance around the world, early and specific detection of antibiotic residues has garnered significant attention. The emergence of microorganisms resistant towards important antibiotics results in consistently high mortality rates (White et al., 2011; CDC, 2006). However, indiscriminate antibiotic use or abuse re-

sults in serious clinical infections, requiring aggressive therapy and as growth promoters in aquaculture and agriculture, antibiotics have become a global concern, due to the serious side effects and multidrug resistance affecting the human health and the environment (Rogatsky and Stein, 2005; Cabello, 2006; Dapra et al., 2013; Leung et al., 2013). Despite these problems, the increased incidences of “suprainfection” caused by

Review

Designed Strategies for Fluorescence-Based Biosensors for the Detection of Mycotoxins

Atul Sharma ^{1,2,5}, Reem Khan ^{1,3,4}, Gaelle Catanante ¹, Tauqir A. Sherazi ³, Sunil Bhand ², Akhtar Hayat ^{4,*} and Jean Louis Marty ^{1,*}

¹ BAE: Biocapteurs-Analyses-Environnement, Université de Perpignan Via Domitia, 52 Avenue Paul Alduy, 66860 Perpignan CEDEX, France; p20120407@goa.bits-pilani.ac.in (A.S.); kreemjadoon@gmail.com (R.K.); gaelle.catanante@univ-perp.fr (G.C.)

² Biosensor Lab, Department of Chemistry, Birla Institute of Technology and Science, Pilani K. K. Birla Goa Campus, Zuarinagar, Goa 403726, India; sgbhand@gmail.com

³ Department of Chemistry, COMSATS Institute of Information Technology, Abbottabad 22060, Pakistan; sherazi@ciit.net.pk

⁴ Interdisciplinary Research Centre in Biomedical Materials (IRCBM), COMSATS Institute of Information Technology, Lahore 54000, Pakistan

⁵ School of Pharmaceutical Sciences, MVN University-Palwal, Haryana-121105, India

* Correspondence: akhtarhayat@ciitlahore.edu.pk (A.H.); jlmarty@univ-perp.fr (J.L.M.); Tel.: +33-468-662-254 (J.L.M.); Fax: +33-468-662-223 (J.L.M.)

Received: 23 April 2018; Accepted: 8 May 2018; Published: 11 May 2018



Abstract: Small molecule toxins such as mycotoxins with low molecular weight are the most widely studied biological toxins. These biological toxins are responsible for food poisoning and have the potential to be used as biological warfare agents at the toxic dose. Due to the poisonous nature of mycotoxins, effective analysis techniques for quantifying their toxicity are indispensable. In this context, biosensors have been emerged as a powerful tool to monitor toxins at extremely low level. Recently, biosensors based on fluorescence detection have attained special interest with the incorporation of nanomaterials. This review paper will focus on the development of fluorescence-based biosensors for mycotoxin detection, with particular emphasis on their design as well as properties such as sensitivity and specificity. A number of these fluorescent biosensors have shown promising results in food samples for the detection of mycotoxins, suggesting their future potential for food applications.

Keywords: mycotoxins; fluorescence assay; biosensors; nanomaterials; fluorescence quenching; food samples

Key Contribution: This review paper provides an insight on the development of fluorescence-based biosensors with a particular focus on the selection and properties of fluorescence probes. Impact of nanomaterial in mycotoxins detection and various fluorescent aptasensing platforms were concluded.

1. Introduction

Mycotoxins are low molecular weight and thermally stable secondary metabolites of toxigenic molds that mainly belong to the genera: *Aspergillus*, *Penicillium*, *Alternaria*, and *Fusarium* [1,2]. Mycotoxins readily colonize crops and contaminate them at both pre and post harvesting level. For example, *Fusarium* and *Alternaria* produce toxic metabolites in the field while *Penicillium* and *Aspergillus* contaminate the food stuff during drying and storage processes. These toxins are present in the mycelium and spores of the toxic molds [3]. In the literature, approximately 100 different species of mycotoxins producing fungi have been reported, which can produce more than 400 toxigenic metabolites. The food regulatory authority

Article

Titanium Dioxide Nanoparticles (TiO₂) Quenching Based Aptasensing Platform: Application to Ochratoxin A Detection

Atul Sharma ^{1,2}, Akhtar Hayat ^{1,3}, Rupesh K. Mishra ^{1,4}, Gaëlle Catanante ¹, Sunil Bhand ² and Jean Louis Marty ^{1,*}

¹ BAE Laboratory, Université de Perpignan Via Domitia, 52 Avenue Paul Alduy, Perpignan 66860, France; E-Mails: p2012407@goa.bits-pilani.ac.in (A.S.); akhtarloona@gmail.com (A.H.); rupeshmishra02@gmail.com (R.K.M.); gaelle.catanante@univ-perp.fr (G.C.)

² Biosensor Lab, Department of Chemistry, BITS, Pilani- K. K. Birla Goa Campus, Zuarinagar, Goa 403726, India; E-Mail: sgbhand@gmail.com

³ Interdisciplinary Research Centre in Biomedical Materials (IRCBM), COMSATS Institute of Information Technology (CIIT), Lahore 54000, Pakistan

⁴ Department of Biosciences and Biotechnology, Banasthali University, Rajasthan 304022, India

* Author to whom correspondence should be addressed; E-Mail: jlmarty@univ-perp.fr; Tel.: +33-4-68-66-2254; Fax: +33-4-68-66-2223.

Academic Editor: Michelangelo Pascale

Received: 30 August 2015 / Accepted: 16 September 2015 / Published: 22 September 2015

Abstract: We demonstrate for the first time, the development of titanium dioxide nanoparticles (TiO₂) quenching based aptasensing platform for detection of target molecules. TiO₂ quench the fluorescence of FAM-labeled aptamer (fluorescein labeled aptamer) upon the non-covalent adsorption of fluorescent labeled aptamer on TiO₂ surface. When OTA interacts with the aptamer, it induced aptamer G-quadruplex complex formation, weakens the interaction between FAM-labeled aptamer and TiO₂, resulting in fluorescence recovery. As a proof of concept, an assay was employed for detection of Ochratoxin A (OTA). At optimized experimental condition, the obtained limit of detection (LOD) was 1.5 nM with a good linearity in the range 1.5 nM to 1.0 μM for OTA. The obtained results showed the high selectivity of assay towards OTA without interference to structurally similar analogue Ochratoxin B (OTB). The developed aptamer assay was evaluated for detection of OTA in beer sample and recoveries were recorded in the range from 94.30%–99.20%. Analytical figures of the merits of the developed aptasensing platform confirmed its applicability to real


 CrossMark
 click for updates

 Cite this: *RSC Adv.*, 2016, 6, 65579

Design of a fluorescence aptaswitch based on the aptamer modulated nano-surface impact on the fluorescence particles†

 Atul Sharma,^{ab} Akhtar Hayat,^{ac} Rupesh Kumar Mishra,^{ad} Gaëlle Catanante,^a Shakir Ahmad Shahid,^e Sunil Bhand^b and Jean Louis Marty^{*a}

The concept of DNA based stabilization of nanostructures to enhance the surface reactivity has been the focus of great interest in the design of colorimetric aptaswitches. Whereas, colorimetric methodologies have limited sensitivity, this concept is rarely considered for other sensing approaches such as those based on fluorescence detection. In this paper, we have investigated the impact of reversible assembly of a single strand DNA aptamer on nanoparticle surface chemistry, involving target tuneable electrostatic and steric repulsion phenomena for fluorescence based detection of molecular interactions. In the same context, literature reported fluorescence based aptamer assays are prone to certain limitations such as complicated labelling chemistry, low conjugation yield, low binding affinity and elevated cost per assay. Alternatively, our designed aptaswitch capitalizes on the surface chemistry of nanoparticles to quench the response of fluorescence particles, eliminating the need of bioconjugation with a fluorophore. As a proof of concept, the proposed methodology was used for the detection of ochratoxin A with TiO₂ nanoparticles as a representative nanomaterial. We expect that this concept may pave a new way to probe aptamer-target binding events, since any nanomaterials with fluorescence quenching characteristics can be regulated in the same manner.

 Received 27th April 2016
 Accepted 30th June 2016

DOI: 10.1039/c6ra10942j

www.rsc.org/advances

1. Introduction

Since the discovery of DNA-functionalized gold nanoparticle conjugates in 1996,^{1,2} many nanomaterials have been utilized to design DNA structure switchable nanosensors based on their plasmon resonance properties.³ These DNA/aptamer based switches are mainly based on materials such as gold nanoparticles,⁴ silver nanoparticles,⁵ quantum dots,⁶ magnetic nanoparticles,⁷ and dye-doped silica nanoparticles.⁸ As bulk materials are devoid of a band gap, nanomaterials must be extremely small to exhibit their distinct and intrinsic properties. In general, a colloidal dispersion of nanoparticles exhibits well defined redox activity, while aggregated nanoparticles pose negligible surface activities.⁹ Based on this observation, the

concept of DNA based stabilization of nanostructures to enhance the surface reactivity has been focus of great interest in the design of colorimetric aptaswitches.¹⁰ However, these methodologies are limited to colorimetric assays with rare reports on other assays such as those based on the fluorescence detection. In this paper, we have investigated for the first time impact of reversible assembly of single strand DNA aptamer on nanoparticles surface chemistry, involving target tunable electrostatic and steric repulsion phenomena for fluorescence based detection of molecular interaction. Recent literature has witnessed immense interest in the exploration of nanomaterials with fluorescence quenching characteristics for various types of applications. One of the attractive areas in this field of research was to integrate fluorescence quenching properties of nanomaterials in designing easy to use and simple aptamer based fluorescence assays to replace the conventional fluorescence detection methodologies. In this context, many nanomaterials have been investigated to develop novel designs of fluorescence aptasensors for various target analytes. However, these literatures reported fluorescence quenching assays mainly rely on the conjugation of aptamer with fluorophore or dye molecules.^{11,12}

The single fluorophore attachment to ss-aptamer/DNA strand decreases the sensitivity of analytical method. A critical assumption is that conformational transition of aptamer from loose random coils to a compact tertiary structure (G-quadruplex ternary complex) might alter the electronic

^aBAE Laboratoire, Université de Perpignan Via Domitia, Bâtiment S, 52 Avenue Paul Alduy, 66860 Perpignan 13 Cedex, France. E-mail: jlmart@univ-perp.fr; Fax: +33 4 68 66 22 23; Tel: +33 4 68 66 22 54

^bBiosensor Lab, Department of Chemistry, BITS, Pilani-K. K. Birla Goa Campus, Zuarinagar 403726, Goa, India

^cInterdisciplinary Research Centre in Biomedical Materials (IRCBM), COMSATS Institute of Information Technology (CIIT), Lahore 54000, Pakistan

^dDepartment of Biosciences and Biotechnology, Banasthali University, Rajasthan, 304022, India

^eDepartment of Chemistry, University of Sargodha, Sargodha 40100, Pakistan

† Electronic supplementary information (ESI) available. See DOI: 10.1039/c6ra10942j



Development of structure switching aptamer assay for detection of aflatoxin M1 in milk sample



Atul Sharma^{a,b}, Gaëlle Catanante^a, Akhtar Hayat^{c,a}, Georges Istamboulie^a,
Ines Ben Rejeb^{d,a}, Sunil Bhand^b, Jean Louis Marty^{a,*}

^a BAE Laboratory, Université de Perpignan Via Domitia, 52 Avenue Paul Alduy, Perpignan 66860, France

^b Biosensor Lab, Department of Chemistry, BITS, Pilani, K. K. Birla Goa Campus, Zuarinagar, Goa 403726, India

^c Interdisciplinary Research Centre in Biomedical Materials (IRCBM), COMSATS Institute of Information Technology (CIIT), Lahore 54000, Pakistan

^d Biocatalysis and Industrial Enzymes Group, Laboratory of Microbial Ecology and Technology, Carthage University, National Institute of Applied Sciences and Technology, BP 676, 1080 Tunis, Tunisia

ARTICLE INFO

Article history:

Received 8 March 2016

Received in revised form

7 May 2016

Accepted 13 May 2016

Available online 14 May 2016

Keywords:

Aptamer

Structure switchable aptamer assay

Aflatoxin M1

Fluorescence quenching

Milk

ABSTRACT

The discovery of *in-vitro* systematic evolution of ligands by exponential enrichment (SELEX) process has considerably broaden the utility of aptamer as bio-recognition element, providing the high binding affinity and specificity against the target analytes. Recent research has focused on the development of structure switching signaling aptamer assay, transducing the aptamer–target recognition event into an easily detectable signal. In this paper, we demonstrate the development of structure switching aptamer assay for determination of aflatoxin M1 (AFM1) employing the quenching–dequenching mechanism. Hybridization of fluorescein labelled anti-AFM1 aptamer (F-aptamer) with TAMRA labelled complementary sequences (Q-aptamer) brings the fluorophore and the quencher into close proximity, which results in maximum fluorescence quenching. On addition of AFM1, the target induced conformational formation of antiparallel G-quadruplex aptamer-AFM1 complex results in fluorescence recovery. Under optimized experimental conditions, the developed method showed the good linearity with limit of detection (LOD) at 5.0 ng kg⁻¹ for AFM1. The specificity of the sensing platform was carefully investigated against aflatoxin B1 (AFB1) and ochratoxin A (OTA). The developed assay platform showed the high specificity towards AFM1. The practical application of the developed aptamer assay was verified for detection of AFM1 in spiked milk samples. Good recoveries were obtained in the range from 94.40% to 95.28% ($n=3$) from AFM1 spiked milk sample.

© 2016 Published by Elsevier B.V.

1. Introduction

Mycotoxin food and feed contamination is a cause of global concern due to associated toxic effects on the human health [1,2]. Aflatoxins (AFs) are naturally occurring secondary metabolite produced by *Aspergillus parasiticus*, *Aspergillus flavus* and *Aspergillus nomius* (rarely) and are often presented in a wide range of food and feed commodities [3]. Among AFs, aflatoxin B1 (AFB1) is the highly toxic contaminant in the feed and subsequent exposure of contaminated feed to lactating mammals leads to the secretion of AFM1 in milk, which is 4-hydroxy metabolite of AFB1 metabolized by liver cytochrome P450 enzyme and known for its carcinogenic side effects [4]. AFM1 is quite stable during the milk pasteurization process, storage as well as processing of dairy products and if present in raw milk may persist to the final stage

for human consumption [5,6]. Although the toxic potency of AFM1 is less than that of its parent compound, it causes DNA intercalation, base impairment, gene mutation and oxidative damage due to intracellular radical generation [7]. International Agency for Research on Cancer (IARC) of the World Health Organization (WHO) has designated the classification of AFM1 from group 2 to group 1 [8]. In order to provide safety for food and human health, regulatory agencies have fixed the maximum residue level (MRL) of AFM1 in milk and milk products, considering milk as the main nutrient to young infants. In the European community, the European Commission Regulation has fixed the much stringent MRL for AFM1 i.e. 50 ng kg⁻¹ or 50 parts per trillion (50 ppt) in milk and milk based products. The maximum permissible limit is even lower for infant milk and baby food i.e. 25 ng kg⁻¹ [9].

Usually, the AFM 1 analysis is performed by the thin layer chromatography (TLC), high-performance liquid chromatography (HPLC) and liquid chromatography coupled with mass spectroscopy (LC-MS) [10–14]. On the other side, the enzyme-linked immunosorbent assays (ELISA) have gained significant attention in

* Corresponding author.

E-mail address: jlmarty@univ-perp.fr (J.L. Marty).



Disposable and portable aptamer functionalized impedimetric sensor for detection of kanamycin residue in milk sample



Atul Sharma^{a,b}, Georges Istamboulie^b, Akhtar Hayat^{b,c}, Gaëlle Catanante^b, Sunil Bhand^{a,*}, Jean Louis Marty^{b,*}

^a Biosensor Lab, Department of Chemistry, BITS, Pilani- K. K. Birla Goa Campus, Zuarinagar, Goa 403726, India

^b BAE Laboratory, Université de Perpignan Via Domitia, 52 Avenue Paul Alduy, Perpignan 66860, France

^c Interdisciplinary Research Centre in Biomedical Materials (IRCBM), COMSATS Institute of Information Technology (CIIT), Lahore 54000, Pakistan

ARTICLE INFO

Article history:

Received 26 September 2016

Received in revised form 23 January 2017

Accepted 1 February 2017

Available online 2 February 2017

Keywords:

Kanamycin

Impedance

Aptasensor

Screen printed carbon electrodes

Milk

Disposable

ABSTRACT

With the increasing incidence and prevalence of antibiotic contamination in animal-derived food and drug resistance around the world, early and specific detection of antibiotic residues has garnered significant attention. Herein, for the first time, we devise a facile, label free and portable aptasensor for quantitative determination of Kanamycin (KANA) by electrochemical impedance spectroscopy (EIS), which accompanying the assembly of *in-vitro* selected single strand DNA (ssDNA) anti-KANA-aptamer functionalized screen printed carbon electrodes (SPCEs) used as transducer. The target detection is based on specific recognition by KANA-aptamer covalently immobilized on SPCEs surface. The surface morphology and electrochemical properties of aptasensor were characterized using Fourier transform infrared spectroscopy (FT-IR), scanning electron microscopy (SEM), atomic force microscopy (AFM), cyclic voltammetry (CV) and EIS. Under optimized experimental conditions, the devised aptasensor exhibited a dynamic range 1.2–600 ng mL⁻¹ with linearity 1.2–75 ng mL⁻¹ and limit of detection (LOD) 0.11 ng mL⁻¹ (S/N = 3) of KANA. The developed aptasensor are endowed with a good selectivity and specificity to KANA without interference from competitive analogues (streptomycin and gentamicin). For practical application, the aptasensor performance was verified in spiked milk samples and the acceptable recovery percentage of 96.88–100.5% (%RSD = 4.56, n = 3) was obtained in milk samples.

© 2017 Elsevier B.V. All rights reserved.

1. Introduction

Antibiotics are the revolutionary medicine, which extensively used in the clinical therapy of many infectious diseases, whereas their abuse results in sustainable side effects to human health and the environment. Owing to the incidences of “suprainfection” caused due to the secondary effects of antibiotics, ensuring their dosage regimen is probably the major health problem [1,2]. Kanamycin (KANA) is an aminoglycoside antibiotic, which perturbs the protein synthesis by misreading the genetic code and inhibiting translation. The extensive use of KANA in modern agriculture, human diseases and domestic animal stockbreeding for prevention and treatment of microbial infections has boosted its consumption with an increase load of microbial resistance [3,4]. The presence of KANA residue in food causes the serious side effects such as hepatotoxicity, nephrotoxicity, ototoxicity in human with an increase in morbidity and mortality rates [5,6]. To ensure the food safety

and quality, monitoring human health and avoiding the evolution of KANA resistance, the maximum stringent limits have been mandated for KANA in food samples such as milk i.e. 150 µg kg⁻¹ (ppb) by European Commission Regulation (EU), considering milk as the main nutrient to young infants [7].

Until now, various analytical methods such as gas chromatography (GC) [8], liquid chromatography coupled with mass spectrometry (LC-MS) [9], high performance liquid chromatography (HPLC) coupled with ultra-violet detection [10], capillary electrophoresis (CE) [11], enzyme-linked immunosorbent assay (ELISA) [12] and immunosensor [13,14] have been reported for the detection of KANA in various food matrices. The reported chromatographic and immunological methods are sensitive and reliable; nevertheless, the inherent imperfectness involved in the above techniques as time consuming process, tedious operation, high consumption of reagents, susceptibility to interferents and *in vivo* antibody production limit their wider application in the analysis of real sample [15]. Therefore, the development of simple, fast, robust, highly selective and specific detection method is particularly important and urgently desired for KANA detection.

* Corresponding authors.

E-mail addresses: sgbhand@gmail.com (S. Bhand), jlmarty@univ-perp.fr (J.L. Marty).

This document is confidential and is proprietary to the American Chemical Society and its authors. Do not copy or disclose without written permission. If you have received this item in error, notify the sender and delete all copies.

Aptamer Integrated Microfluidic Quartz Crystal Biosensing Platform: Application to on-line Determination of Tetracycline in Milk

Journal:	<i>Analytical Chemistry</i>
Manuscript ID	ac-2017-02618p
Manuscript Type:	Article
Date Submitted by the Author:	05-Jul-2017
Complete List of Authors:	Sharma, Atul; BITS, Pilani K.K. Birla Goa Campus, Department of Chemistry Bhand, Sunil; BITS-Pilani, KK Birla Goa Campus, Chemistry

SCHOLARONE™
Manuscripts

1
2
3
4
5
6
7
8
9
10
11
12
13
14
15
16
17
18
19
20
21
22
23
24
25
26
27
28
29
30
31
32
33
34
35
36
37
38
39
40
41
42
43
44
45
46
47
48
49
50
51
52
53
54
55
56
57
58
59
60

Aptamer Integrated Microfluidic Quartz Crystal Biosensing Platform: Application to on-line Determination of Tetracycline in Milk

Atul Sharma and Sunil Bhand*

Biosensor Lab, Department of Chemistry, BITS, Pilani- K. K. Birla Goa Campus, Goa 403726,

India

Atul Sharma

Email: p2012407@goa.bits-pilani.ac.in

*** Corresponding authors**

Prof. Sunil Bhand

Biosensor Lab. Department of Chemistry,

BITS, Pilani– K. K. Birla Goa Campus,

Goa - 403726, INDIA

Ph: +91-832-2580332, Fax: + 91-832-2557030/33

Email: sunilbhand@goa.bits-pilani.ac.in